

**A FLUORESCENT FIBRE SOLAR CONCENTRATOR (FFSC)
DESIGN AND TRIAL RUN**

WANG CHEN

PERPUSTAKAAN ALAM BINA
UNIVERSITI MALAYA

**FACULTY OF BUILT ENVIRONMENT
UNIVERSITY OF MALAYA
KUALA LUMPUR**



SEPTEMBER 2009

UNIVERSITI MALAYA

ORIGINAL LITERARY WORK DECLARATION

**A FLUORESCENT FIBRE SOLAR CONCENTRATOR (FFSC)
DESIGN AND TRIAL RUN**

WANG CHEN

**THESIS SUBMITTED IN FULFILMENT
OF THE REQUIREMENTS
FOR THE DEGREE OF DOCTOR OF PHILOSOPHY**

**FACULTY OF BUILT ENVIRONMENT
UNIVERSITY OF MALAYA
KUALA LUMPUR**

SEPTEMBER 2009

UNIVERSITI MALAYA

ORIGINAL LITERARY WORK DECLARATION

Name of Candidate: WANG CHEN (I/C/Passport No: G19644374)

Registration/Matric No: BHA060006

Name of Degree: PHD in Built Environment

Title of Project Paper/Research Report/Dissertation/Thesis ("this Work"):

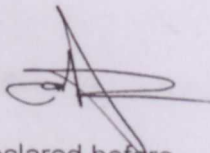
A FLUORESCENT FIBER SOLAR CONCENTRATOR (FFSC) DESIGN AND TRIAL

Field of Study:

I do solemnly and sincerely declare that:

- (1) I am the sole author/writer of this Work;
- (2) This Work is original;
- (3) Any use of any work in which copyright exists was done by way of fair dealing and for permitted purposes and any except or extract from, or reference to or reproduction of any copyright work has been disclosed expressly and sufficiently and the title of the work and its authorship have been acknowledged in this Work;
- (4) I do not have any actual knowledge nor do I ought reasonably to know that the making of this work constitutes an infringement of any copyright work;
- (5) I hereby assign all and every rights in the copyright to this Work to the University of Malaya ("UM"), who henceforth shall be owner of the copyright in this Work and that any reproduction or use in any form or by any means whatsoever is prohibited without the written consent of UM having been first had and obtained;
- (6) I am fully aware that in the course of making this Work I have infringed any copyright whether intentionally or otherwise, I may be subject to legal action or any other action as may be determined by UM.

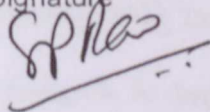
Candidate's Signature



Date 16, Sep 2009

Subscribed and solemnly declared before,

Witness's Signature



Date 16. Sep 2009

Name: S.P. Rao

Designation: Associate Professor

ACKNOWLEDGEMENTS

I am grateful to all the following people who have guided and encouraged me or have given me all kinds of supports during the doctoral journey. This thesis would never have been completed without their contributions.

I would like to acknowledge and thank the following special people who have given me their precious time, wisdom, encouragement and love. The learning process in this research journey is invaluable to me and it was a pleasant and gratifying experience that I would never forget.

Special thanks to Professor Dr. Hamzah Abdul Rahman, my main supervisor, who has given all kinds of support and assistance to me. His guidance and patience was the key to success for the completion of this research. We had many discussions through the research and his wisdom and righteousness shone upon my world. He gave his priceless time in reviewing my work and gave suggestions on my life, and his encouragement was always precious to me. I would like to express my special thanks to him.

Associate Professor S.P. Rao, my second supervisor who has given his full support. I give my deep heartfelt appreciation to him. He gave a lot of his time in reviewing my work and discussing with me, and his specialized knowledge and suggestions were crucial to the research findings. His friendly and warm attitude made this research a pleasant and invaluable process.

Also, I would like to thank En. Yatiman, who is a professional technical staff handling the workshop in Faculty of Built Environment, University of Malaya. He has provided his generous help in fabricating all the needed accessories for the 6-month experimentation in the lab. Many of these accessories were not able to be purchased from markets, and this is crucial to the success of our research. Many thanks to him because all kinds of help he has done for me is unconditional.

Professor Zhou Chenbo, who is a specialist in the field of optical physics in the University of Yantai, China. His professional knowledge in optical physics has brought wonderful inspirations to me so that much time has been saved in looking for necessary literatures.

En. Zailan and En. Ikmal who are technical staff of the Faculty of Built Environment. They have given unconditional assistance to me in providing all the needed equipments, facilities, and manpower. Their help were also encouragements during the research journey.

Thanks also to Assoc. Prof. Dr. Md. Nasir Daud, Dr. Hafez Salleh, Pn. Mazedah, Pn. Norzie, Pn. Rosnah, and Pn. Rosidah, Staffs in the Faculty of Built Environment, University of Malaya, who have eased all the processes in documentation and submission during the research. Their contributions made this work smooth and efficient.

Finally, I would like to thank my parents who have given me earthly life and have given all their love and support to me and the chance to complete this research. The integrity in their individualities is the light of my life.

ABSTRACT

This thesis presents the author's research work on a new concept development in the field of solar energy application for building illumination during his doctoral journey in Malaysia. As a considerable solution to the energy issues, solar energy is made widely available for daylighting and direct production of electricity. Various devices have been developed to collect, concentrate, transport, store, and convert solar irradiation, such as the light pipe, optical fibers, optical solar concentrators, and luminescent solar concentrators (LSC). Many limitations such as the strict dependence on beam irradiation and difficulties for wiring remain in these daylighting devices. This thesis introduces a new concept developed by the author and a new device designed and fabricated based on the concept in mitigating those limitations. The fabricated new device named "Fluorescent Fiber Solar Concentrator" (FFSC) is a 1200mm×1200mm solar concentrator consisting of 150 pieces of three-color 1m long fluorescent fibers with the diameter of 2mm. FFSC is mounted on the roof of a university building, and the concentrated light is transported to a remote dark room through 10m long 2mm diameter clear optical fibers. Outdoor testing for remote indoor daylighting and power production evaluation have been conducted for the fabricated new device FFSC. A 6-month monitored data from 24th May 2008 to 23rd Nov 2008 was analyzed. The radiation-to-radiation efficiency with a mean value of 0.057 and the lighting effect up to 114.1 lumens reveal FFSC a potential in remote indoor daylighting for the application in building integration. The wavelength test and the CIE color analysis present a satisfactory match in color between the FFSC light output and the natural light. Since the sun light is free, even though the luminous efficacy as 0.643lm/W is lower than the normal electrical light sources, FFSC does not consume any electricity when operating.

The light-to-light efficiency falls within the range 0.49% to 0.64% and it is expected to be raised by increasing the diameter of the fluorescent fibers embedded. FFSC systems could probably be applied for the illumination in underground areas of buildings or constructions such as the car park levels in shopping complexes, convention centers, and some office buildings. This system could also be applied to illuminate the inner areas in a building such as meeting rooms and corridors. Since electro circuits are not needed in the FFSC system, potentially FFSC systems are quite suitable for subaqueous and extremely moist operation environments when a durative illumination is needed during the daytime. Further, FFSC systems do not have any risk of fire caused by the electrical current in inflammable gas conditions.

TABLE OF CONTENTS

ACKNOWLEDGEMENTS	- 1 -
ABSTRACT	- 3 -
TABLE OF CONTENTS.....	- 5 -
LIST OF FIGURES.....	- 8 -
LIST OF TABLES.....	- 10 -
LIST OF ABBREVIATIONS.....	- 11 -
LIST OF SYMBOLS	- 12 -
GLOSSARY	- 13 -
 CHAPTER 1	
INTRODUCTION.....	- 15 -
1.1 BACKGROUND OF STUDY	- 15 -
1.2 PROBLEM STATEMENT	- 17 -
1.3 OBJECTIVES AND METHODOLOGY	- 18 -
1.4 SCOPE OF RESEARCH.....	- 19 -
1.5 STRUCTURE OF THE THESIS	- 20 -
 CHAPTER 2	
REVIEW OF DAYLIGHTING RELATED DEVICES	- 22 -
2.1 DAYLIGHT FOR ILLUMINATION	- 23 -
2.1.1 Diffuse light guiding systems.....	- 29 -
2.1.2 Direct light guiding systems.....	- 29 -
2.1.3 Scattering systems.....	- 30 -
2.1.4 Light transport systems.....	- 32 -
2.2 LIGHT PIPES FOR DAYLIGHT TRANSPORTATION	- 39 -
2.2.1 Zenithal systems with active collection	- 44 -
2.2.2 Passive zenithal systems	- 48 -
2.3 OPTICAL FIBER FOR LIGHT TRANSPORTATION	- 50 -
2.4 CONVENTIONAL SOLAR CONCENTRATORS.....	- 56 -
2.5 LUMINESCENT SOLAR CONCENTRATOR (LSC)	- 64 -
2.6 FLUORESCENT FIBER AND ITS USUAL APPLICATIONS.....	- 70 -
2.7 SUMMARY	- 75 -
 CHAPTER 3	
RESEARCH METHODOLOGY	- 77 -
3.1 OVERVIEW OF RESEARCH PROCESS.....	- 77 -
3.2 DETERMINATION OF OBJECTIVES	- 78 -
3.3 QUALITATIVE AND QUANTITATIVE RESEARCH.....	- 80 -
 CHAPTER 4	
DESIGN OF FLUORESCENT FIBER SOLAR CONCENTRATOR (FFSC)	- 84 -
4.1 THE NEED FOR FLUORESCENT FIBER SOLAR CONCENTRATOR (FFSC)	- 84 -
	- 5 -

4.2 DESIGN AND FABRICATION OF FLUORESCENT FIBER SOLAR CONCENTRATOR (FFSC)	- 87 -
4.3 THE PRINCIPLE OF FFSC	- 91 -

CHAPTER 5

EXPERIMENTATION PROCEDURES AND INSTRUMENTATION	- 93 -
5.1 MALAYSIAN CLIMATE AND EXPERIMENTATION DURATION	- 93 -
5.2 EXPERIMENTATION FOR FFSC: DATA COLLECTION	- 95 -
5.3 EXPERIMENTATION FOR FFSC: INSTRUMENTATION	- 96 -
5.3.1 The pyranometers	- 96 -
5.3.2 LUX sensor	- 97 -
5.3.3 Spectrometer	- 99 -
5.3.4 Data logger	- 101 -
5.4 EXPERIMENTATION FOR FFSC: THE BUILDING FOR INSTALLATION	- 107 -
5.5 CRITICAL REVIEW OF EXPERIMENTAL LIMITATIONS	- 110 -
5.6 EXPERIMENTATION FOR FFSC: PARAMETERS ANALYZED	- 111 -

CHAPTER 6

DATA RESTRUCTURING AND INTERPRETATION	- 113 -
6.1 DATA ACQUIRED FROM DATAHOG2	- 113 -
6.2 DATA INTERPRETATION FOR EPP2000 SPECTROMETER	- 118 -
6.3 SUMMARY	- 122 -

CHAPTER 7

RESULTS OF ANALYSIS	- 124 -
7.1 THE SOLAR RADIATION (PY1) AND FFSC OUTPUT (PY2)	- 124 -
7.2 FFSC RADIATION-TO-RADIATION EFFICIENCY	- 128 -
7.2.1 Hourly radiation-to-radiation efficiency	- 129 -
7.2.2 η_r in a 6-month monitoring	- 131 -
7.3 SYSTEM LIGHTING EFFECT	- 132 -
7.3.1 Calculate luminous flux (F) from LUX (Ev)	- 132 -
7.3.2 Comparison of lighting effect between FFSC and incandescent lamps	- 136 -
7.4 ENERGY-TO-ENERGY EFFICIENCY	- 137 -
7.5 LUMINOUS EFFICACY (K) OF FFSC	- 139 -
7.6 LIGHT-TO-LIGHT EFFICIENCY EVALUATION	- 141 -
7.7 THE NEGATIVE TREND BETWEEN RADIATION-TO-RADIATION EFFICIENCY AND SOLAR RADIATION (PY1)	- 143 -
7.8 MATCHING THE NATURAL LIGHT: CIE COLOR ANALYSIS AND WAVELENGTH TEST	- 145 -
7.8.1 CIE color analysis	- 146 -
7.8.2 Wavelength (λ) test	- 151 -
7.9 SUMMARY	- 156 -

CHAPTER 8

CONCLUSIONS AND RECOMMENDATIONS	- 157 -
8.1 CONCLUSIONS	- 157 -
8.2 POTENTIAL APPLICATIONS OF FFSC	- 160 -
8.3 RECOMMENDATIONS FOR FUTURE RESEARCH	- 161 -

REFERENCES	- 163 -
-------------------------	----------------

BIBLIOGRAPHY	- 175 -
---------------------------	----------------

APPENDIX A: WAVELENGTH TESTING DIAGRAM	- 182 -
---	----------------

LIST OF FIGURES

FIGURE 2.1: INTERIOR LIT USING A SQUARE LENS DISCRETE EMITTER	- 32 -
FIGURE 2.2: SCHEMATIC OF A TYPICAL LIGHT PIPE.....	- 40 -
FIGURE 2.3: EXTERNAL VIEWS OF TWO INSTALLATIONS	- 42 -
FIGURE 2.4: INTERNAL VIEWS OF TWO INSTALLATIONS.....	- 43 -
FIGURE 2.5: GENERAL VIEWS OF GUIDES IN ROOF SPACE	- 43 -
FIGURE 2.6 SUN LIGHTING SYSTEM REDIRECTION MIRROR.....	- 45 -
FIGURE 2.7 SUN LIGHTING SYSTEM CONCENTRATORS.....	- 46 -
FIGURE 2.8: ARTHELIO FRESNEL LENS	- 47 -
FIGURE 2.9: EXAMPLE PICTURE OF LIGHT TRANSMITTED THROUGH OPTICAL FIBERS	- 51 -
FIGURE 2.10: ONE EXAMPLE OF THE HELIOSTATS SOLAR CONCENTRATOR AND LIGHT TRANSMISSION THROUGH OPTICAL FIBERS.....	- 57 -
FIGURE 2.11: DEFRAC-SPANISH ACRONYM OF DEVICE FOR THE STUDY OF HIGHLY CONCENTRATED RADIOACTIVE FLUXES.....	- 62 -
FIGURE 2.12: PHOTOGRAPH OF THE POLAR AXIS TRACKING RIDGE CONCENTRATOR WITH 8*55 WP PV PANELS	- 63 -
FIGURE 2.13: PHOTOGRAPH OF A STATIC PRISM-ARRAY CONCENTRATOR MODULE	- 63 -
FIGURE 2.14: SCHEMATIC REPRESENTATION OF LUMINESCENT SOLAR CONCENTRATOR (LSC) ..	- 65 -
FIGURE 2.15: MORE IN DETAILED EXAMPLE OF SCHEMATIC REPRESENTATION OF LUMINESCENT SOLAR CONCENTRATOR (LSC).....	- 65 -
FIGURE 3.1: OVERVIEW OF RESEARCH PROCESS	- 78 -
FIGURE 4.1: FROM ENERGY ISSUES TO SOLAR APPLICATIONS: THE NEEDS FOR FFSC (CONCEPT DEVELOPED BY AUTHOR).....	- 86 -
FIGURE 4.2: AUTO CAD SCHEMA OF FFSC (CONCEPT DEVELOPED BY AUTHOR)	- 88 -
FIGURE 4.2A: DETAIL 1 IN FIGURE 4.2, THE LINK FROM FLUORESCENT FIBER TO CLEAR FIBER.	- 89 -
FIGURE 4.2B: THE SECTIONAL VIEW A-A IN FIGURE 4.2,	- 89 -
FIGURE 4.3: FFSC INSTALLED ON THE BUILDING ROOF (CONCEPT DEVELOPED BY AUTHOR)	- 90 -
FIGURE 4.4: EQUIPMENTS USED FOR TESTING.....	- 91 -
FIGURE 4.5: PRINCIPLE OF WORK FOR FLUORESCENT FIBER (DRAWN BY THE AUTHOR)	- 92 -
FIGURE 4.6: WORKING PRINCIPLE OF FFSC THAT MOUNTED ON THE ROOF.....	- 92 -
FIGURE 5.1: SPECIFICATIONS OF SKS1110 PYRANOMETER.....	- 96 -
FIGURE 5.2: RESPONSE RANGE OF SKS1110 PYRANOMETER.....	- 97 -
FIGURE 5.3: SPECIFICATIONS OF SKL310 LUX SENSOR	- 98 -
FIGURE 5.4: RESPONSE RANGE OF SKL310 LUX SENSOR	- 98 -
FIGURE 5.5: EPP2000 SPECTROMETER CONNECTED WITH LAPTOP AND LIGHT SOURCE	- 100 -
FIGURE 5.6: "COM 1" WAS CONFIGURED TO DATAHOG2.....	- 102 -
FIGURE 5.7: PICTURES AND ANIMATIONS OPTIONS ARE SELECTED.....	- 103 -
FIGURE 5.8: DATA OFFLOADING DIALOGUE BOX IN DATAHOG2	- 104 -
FIGURE 5.9: DATA EXPORT INTO MICROSOFT EXCEL, STEP1 OF 3.....	- 105 -
FIGURE 5.10: DATA EXPORT INTO MICROSOFT EXCEL, STEP2 OF 3.....	- 105 -
FIGURE 5.11: DATA EXPORT INTO MICROSOFT EXCEL, STEP 3 OF 3.....	- 106 -
FIGURE 5.12: DATA EXPORT INTO MICROSOFT EXCEL, THE WORKABLE SPREADSHEET	- 106 -
FIGURE 5.13: BLOCK G22, WHERE FFSC WAS MOUNTED ON.....	- 108 -
FIGURE 5.14: A-A SECTION VIEW FOR BLOCK G22 AND WHERE FFSC INSTALLED	- 108 -
FIGURE 5.15: PHOTO FOR BLOCK G22.....	- 109 -
FIGURE 5.16: THE STAIRCASE THAT CLOSE TO FFSC.....	- 109 -
FIGURE 5.17: LAYOUT OF THE 4 TH FLOOR.....	- 110 -
FIGURE 6.1: MAIN MENU DISPLAYED IN "SKYELYNX STANDARD V2.6"	- 114 -
FIGURE 6.2: DATA OFFLOADING PROCESS DISPLAYED IN MICROSOFT EXCEL.....	- 115 -
FIGURE 6.3: DATA RESTRUCTURE AND PREPARATORY CALCULATION CONDUCTED BY EXCEL.....	- 117 -
FIGURE 6.4: DAILY MEAN VALUE FOR RESTRUCTURED DATA.....	- 118 -
FIGURE 6.5: WAVELENGTH DISPLAY IN "LABVIEW SPECTRAWIZ 6.1 V.1"	- 119 -
FIGURE 6.6: CIE GRAPH DISPLAYED IN "LABVIEW SPECTRAWIZ 6.1 V.1"	- 121 -
FIGURE 6.7: CIE GRAPH MODIFIED BY "ADOBE PHOTOSHOP V7.0"	- 122 -

FIGURE 7.1: HOURLY PY1 FOR A RANDOM WEEK.....	- 125 -
FIGURE 7.2: HOURLY PY2 FOR A RANDOM WEEK.....	- 126 -
FIGURE 7.3: DAILY MEAN VALUE OF PY1 AND 10×PY2 WITHIN A MONTH.....	- 127 -
FIGURE 7.4: THE LINEAR TEST OF PY1 AND PY2.....	- 128 -
FIGURE 7.5: HOURLY CURVE OF RADIATION-TO-RADIATION EFFICIENCY IN A RANDOM WEEK....	- 130 -
FIGURE 7.6: HOURLY CURVE OF RADIATION-TO-RADIATION EFFICIENCY ON 4 TH JUNE 2008....	- 131 -
FIGURE 7.7: HOURLY LUX VALUES IN A RANDOM WEEK.....	- 134 -
FIGURE 7.8: HOURLY LUMINOUS FLUX IN A RANDOM WEEK.....	- 135 -
FIGURE 7.9: NEGATIVE TREND BETWEEN RADIATION EFFICIENCY AND PY1.....	- 144 -
FIGURE 7.10: CIE COLOR ANALYSIS 10CM 12:27, 16OCT2008.....	- 147 -
FIGURE 7.11: CIE COLOR ANALYSIS FOR DIRECT SUN LIGHT 11:33, 12Nov2008.....	- 148 -
FIGURE 7.12: CIE COLOR ANALYSIS 9:50, 16OCT2008 (CLEAR SKY).....	- 149 -
FIGURE 7.13: CIE COLOR ANALYSIS 12:33, 16OCT2008 (SUNNY WITH LITTLE CLOUDS)....	- 149 -
FIGURE 7.14: CIE COLOR ANALYSIS 14:36, 16OCT2008 (OVERCAST).....	- 150 -
FIGURE 7.15: CIE COLOR ANALYSIS NATURAL DAYLIGHT OVERCAST 2ND NOV 2008.....	- 150 -
FIGURE 7.16: WAVELENGTH SCOPE MODE 10CM 12:23, 16OCT2008.....	- 152 -
FIGURE 7.17: WAVELENGTH SCOPE MODE NATURAL LIGHT AT SUNNY CONDITION.....	- 152 -
FIGURE 7.18: WAVELENGTH SCOPE MODE 20CM 9:53, 16OCT2008.....	- 154 -
FIGURE 7.19: WAVELENGTH SCOPE MODE 20CM 12:30, 16OCT2008.....	- 154 -
FIGURE 7.20: WAVELENGTH SCOPE MODE 20CM 14:32, 16OCT2008.....	- 155 -
FIGURE 7.21: SCOPE MODE NATURAL DAYLIGHT OVERCAST 2ND NOV 2008.....	- 155 -
FIGURE A1: WAVELENGTH SCOPE MODE 10CM 12:23 16OCT2008.....	- 182 -
FIGURE A2: WAVELENGTH SCOPE MODE NATURAL LIGHT AT SUNNY CONDITION 11:47, 12Nov2008	- 183 -
FIGURE A3: WAVELENGTH SCOPE MODE 20CM 12:30, 16OCT2008.....	- 183 -
FIGURE A4: WAVELENGTH SCOPE MODE 30CM 12:34, 16OCT2008.....	- 184 -
FIGURE A5: WAVELENGTH SCOPE MODE 40CM 12:37, 16OCT2008.....	- 184 -
FIGURE A6: WAVELENGTH SCOPE MODE 50CM 12:42, 16OCT2008.....	- 185 -
FIGURE A7: WAVELENGTH SCOPE MODE 80CM 12:47, 16OCT2008.....	- 185 -
FIGURE A8: WAVELENGTH SCOPE MODE 100CM 12:51, 16OCT2008.....	- 186 -
FIGURE B1: CIE COLOR ANALYSIS 10CM 12:27, 16OCT2008.....	- 187 -
FIGURE B2: CIE COLOR ANALYSIS FOR DIRECT SUN LIGHT 11:33, 12Nov2008.....	- 188 -
FIGURE B3: CIE COLOR ANALYSIS 20CM 12:33, 16OCT2008.....	- 188 -
FIGURE B4: CIE COLOR ANALYSIS 30CM 12:36, 16OCT2008.....	- 189 -
FIGURE B5: CIE COLOR ANALYSIS 40CM 12:47, 16OCT2008.....	- 189 -
FIGURE B6: CIE COLOR ANALYSIS 50CM 12:47, 16OCT2008.....	- 190 -
FIGURE B7: CIE COLOR ANALYSIS 80CM 12:50, 16OCT2008.....	- 190 -
FIGURE B8: CIE COLOR ANALYSIS 100CM 12:52, 16OCT2008.....	- 191 -

LIST OF TABLES

TABLE 5.1: INFORMATION OF THE SPECTROMETER USED IN EXPERIMENTATION	- 100 -
TABLE 7.1: THE REGRESSION TEST OF PY1 AND PY2.....	- 128 -
TABLE 7.2: 6-MONTH MONTHLY MEAN VALUE OF RADIATION-TO-RADIATION EFFICIENCY	- 131 -
TABLE 7.3: CONVERSION FROM LUX TO LUMINOUS FLUX.....	- 133 -
TABLE 7.4: LUMINOUS FLUX OF FFSC ILLUMINANCE AND EQUIVALENT INCANDESCENT LAMPS .	- 136 -
TABLE 7.5: LINEAR TEST FOR EV AND PY1	- 140 -
TABLE 7.6: THE CORRELATION OF RADIATION EFFICIENCY AND PY1.....	- 145 -

LIST OF ABBREVIATIONS

BIPV	Building Integrated Photovoltaic
CIE	Commission Internationale de l'Eclairage, the International Commission on Color
CTs	Current Transducers
EE	Energy Efficiency
EMI	Electromagnetic Interference
FFSC	Fluorescent Fiber Solar Concentrator
IR	Infra-red
LSC	Luminescent Solar Concentrator
OTDR	Optical Time Domain Reflectometry
PMMA	Poly Methyl Methacrylate
POF	Plastic Optical Fiber
QDs	Quantum Dots
LQE	Luminescence Quantum Efficiency
TDGS	Tubular Daylight Guidance Systems
UV	Ultra-violet
VT	Visible Transmittance

LIST OF SYMBOLS

(Symbols only used in this thesis)

ε	unit for strain resolution
PY1	light radiation monitored by Pyranometer 1 (Watt/m ²)
PY2	light radiation monitored by Pyranometer 2 (Watt/m ²)
η_r	radiation-to-radiation efficiency of FFSC
η_l	light-to-light efficiency of FFSC
K	luminous efficacy of FFSC (lumen/Watt)
K ₀	luminous efficacy of the sunlight (lumen/Watt)
η_{r-avg}	average radiation-to-radiation efficiency of FFSC
η_e	energy-to-energy efficiency of FFSC
η_{e-avg}	average energy-to-energy efficiency of FFSC
F	luminous flux yielding from a FFSC finishing end (lumen)
F ₀	luminous flux dropping on fluorescent fibers (lumen)
E _v	illuminance (LUX)
Shs	the half sphere's surface area radiated by a light source (m ²)
P _{out}	energy output yielding from both finishing ends (Watt)
P _{sun}	solar energy irradiated on the fluorescent fibers (Watt)
S ₀	effective area of the FFSC plate (m ²)
D	diameter of fluorescent fibers (m)
L	length of the fluorescent fibers (m)
n	number of piece for fluorescent fibers
R _f	radius of the finishing end (m)
λ	wave length of light (nm)

GLOSSARY

- CdSe** Cadmium Selenide (CdSe) is a solid, binary compound of cadmium and selenium. Common names for this compound are cadmium (II) selenide, cadmium selenide, and cadmoselite (a very rare mineral). Cadmium selenide is a semiconducting material, but has yet to find many applications in manufacturing. This material is transparent to infra-red (IR) light, and has seen limited use in windows for instruments utilizing IR light. Much current research on cadmium selenide has focused on nanoparticles. Researchers are concentrating on developing controlled syntheses of CdSe nano-particles. In addition to synthesis, scientists are working to understand the properties of cadmium selenide, as well as apply these materials in useful ways (Wikipedia, 2009a).
- CdS** Cadmium Sulfide (CdS) is a chemical compound with the formula CdS. Cadmium sulfide is yellow in colour and is a semiconductor. It exists in nature as two different minerals, hexagonal greenockite and cubic hawleyite. Cadmium sulfide is a direct band gap semiconductor (gap 2.42 eV) and has many applications for example in light detectors. It forms thermally stable pigments and with the addition of e.g. CdTe, HgS colors ranging from deep red to yellow are formed (Wikipedia, 2009a).
- GaAs** Gallium arsenide (GaAs) is a compound of two elements, gallium and arsenic. It is an important semiconductor and is used to make devices such as microwave frequency integrated circuits, infrared light-emitting diodes, laser diodes and solar cells (Wikipedia, 2009a).
- Isotropy** Isotropy is uniformity in all directions. Precise definitions depend on the subject area. The word is made up from Greek ISO (equal) and TROPOS (direction). Exceptions, or inequalities, are frequently indicated by the prefix an, hence anisotropy. Anisotropy is also used to describe situations where properties vary systematically, dependent on direction. Isotropic radiation has the same intensity regardless of the direction of measurement, and an isotropic field exerts the same action regardless of how the test particle is oriented (Wikipedia, 2009a).
- Pointolite** Point light source. A point light source is a single identifiable localized source of light. A point source has negligible extent, distinguishing it from other source geometries. Sources are called point sources because in mathematical modeling, these sources can usually be approximated as a mathematical point to simplify analysis. The actual source need not be physically small, if its size is negligible relative to other length scales in the problem. For example, in astronomy stars are routinely treated as point sources, even though they are in actuality much larger than the Earth (Wikipedia, 2009a).
- Quantum yield** The quantum yield of a radiation-induced process is the number of times that a defined event occurs per photon absorbed by the system. Thus, the quantum yield is a measure of the efficiency with which absorbed light

produces some effect. Quantum yield can be defined by the equation: $Q = \frac{\text{photons emitted}}{\text{photons absorbed}}$. Quantum yield is essentially the emission efficiency of a given fluorochrome. For example, in a chemical photodegradation process, when a molecule falls apart after absorbing a light quantum, the quantum yield is the number of destroyed molecules divided by the number of photons absorbed by the system. Since not all photons are absorbed productively, the typical quantum yield will be less than 1 (Wikipedia, 2009a).

Sagnac interferometer The Sagnac effect (also called Sagnac interference), named after French physicist Georges Sagnac, is a phenomenon encountered in interferometry that is elicited by rotation. The Sagnac effect manifests itself in a setup called ring interferometry. A beam of light is split and the two beams are made to follow a trajectory in opposite directions. To act as a ring the trajectory must enclose an area. On return to the point of entry the light is allowed to exit the apparatus in such a way that an interference pattern is obtained. The position of the interference fringes is dependent on the angular velocity of the setup. This arrangement is also called a Sagnac interferometer (Wikipedia, 2009a).

Snell's law In optics and physics, Snell's law (also known as Descartes' law or the law of refraction), is a formula used to describe the relationship between the angles of incidence and refraction, when referring to light or other waves, passing through a boundary between two different isotropic media, such as water and glass. The law says that the ratio of the sines of the angles of incidence and of refraction is a constant that depends on the media (Wikipedia, 2009a).

Strain resolution Strain is commonly specified in "micro inches per inch" or "micro-strain" which is in "microns per meter". Of course one could specify the length change in percentage if one preferred. The "resolution" to which it can make a measurement is limited by the noise superimposed on the signal. The two basic types of noise are shot noise, which is caused current flow flowing a resistance, and thermal noise, which is a function of the temperature of the input stage of the instrument amplifier, and the bandwidth of the amplifier (Wikipedia, 2009a).

Chapter 1

Introduction

This thesis presents a research work on the solar energy application attempts conducted in Malaysia, where a new concept was developed by the author and a new device named “Fluorescent Fiber Solar Concentrator” (FFSC) was fabricated accordingly. The new device was fabricated, installed and instrumented, and it was monitored for a 6 month period. Testing results reveal FFSC a potential in remote indoor daylighting for the application in building integration.

1.1 Background of study

In the 21st century, the greatest challenge facing the world is the need for workable energy options (Robert & Ernest, 2006). As stated by Robert & Ernest (2006) in one of the Massachusetts Institute of Technology (MIT) energy research council report, researchers must work diligently to reach the need for the new global supplies of the affordable and sustainable energy to power the world. The acuteness of the challenge at this point in time results from the “perfect storm” of supply and demand, security, and environmental concerns, namely: a) a projected doubling of energy use and tripling of

electricity demand within a half century, calling for a substantial increase in fossil fuel supplies or dramatic transformation of the fossil-fuel-based energy infrastructure; b) geological and geopolitical realities concerning the availability of oil and, to some extent, natural gas, specifically the concentration of resources and political instability in the Middle East, underlie major security concerns; and c) greenhouse gas emissions from fossil fuel combustion are increasingly at the center of decisions about how the global energy system evolves, one that carries on in the “business as usual” overwhelming dependence on fossil fuels or one that introduces technologies and policies that greatly improve efficiency, dramatically expand use of less carbon-intensive or “carbon free” energy, and implement large scale carbon dioxide capture and sequestration (Robert & Ernest, 2006).

In most of buildings, the energy consumption for lighting could be reduced by 30% to 50% through the application of renewable energy and better lighting design (EPA, 1999). More than 50% of the existing commercial buildings still use low efficient lighting systems. Efficient lighting designs are used in only a small minority of spaces, and the control systems that maximize the use of daylight are even less common (EPA, 1999).

As a considerable solution to the energy issues, solar energy is made widely available for daylighting and direct production of electricity. Various devices have been developed to collect, concentrate, transport, store, and convert solar irradiation, such as the light pipe, optical fibers, optical solar concentrators, and luminescent solar concentrators (LSC), and so on (Littlefair, 1996; Shao, Riffat, Yohannes, & Elmualim, 1998; Cariou, Martin & Dugas, 1982; Enedir & John, 2006; Ries, Zaibel, Dagan, & Karni, 1995; Beckman, Schlegel, Klein, Wood, & Muhs, 2003; Earp, Geoff, Jim, &

Paul, 2004). However, there are many limitations in such devices, such as the strict dependence on the beam irradiation and the difficulties for wiring (Enedir & John, 2006; Cariou et al., 1982).

1.2 Problem statement

Daylight has a disadvantage that it may not be able to reach many areas such as storerooms, basements, and corridors. It also brings heat gain with the light (Bouchet & Fontoynt, 1996; Shao et al., 1998). Light pipes were designed to transport the daylight to the deeper parts in buildings. However, the light pipes have their difficulties for wiring so that daylight transportation through optical fibers is considered as the best approach so far (Enedir & John, 2006; Cariou et al., 1982). In building integration, one of the most important features of the remote light transportation is the wiring method, and the wiring method is expected to be as simple as that of electrical wires (Kaino, 1992; Nihei, Ishigure, Tanio, & Koike, 1997; Enedir & John, 2006; Cariou et al., 1982). Only optical fibers are suitable for this requirement. However, the optical fiber needs a pointolite for it to transport (Kaino, 1992; Nihei, et al., 1997; Cariou et al., 1982). The proposed design of FFSC is expected to solve this problem.

Solar concentrators have been designed using optical approaches such as using mirrors and/or lens because of the high price for PV cells. Since they are only sensitive for the beam irradiation, they function poorly in the cloudy weather and the diffuse light conditions, and a tracker is always needed (Compagnon, Scartezzini, & Paule, 1993; Page, Kaempf, & Scartezzini, 2003). Luminescent solar concentrators (LSC) and some

static solar concentrators were then designed as the diffuse light solution and the static solution respectively (Weber & Lambe, 1976; Goetzberger & Greubel, 1977; Rapp & Boling, 1978). Static concentrators always come with a poor concentration rate without a tracker, and the light concentrated by normal LSCs could not be transported by optical fibers to a remote place since the light produced by an LSC is not a point source (Compagnon, et al., 1993; Page, et al., 2003; Beckman et al., 2003; Kandilli, Ulgen, & Hepbasli, 2007). The proposed design of FFSC is expected to solve this problem as well.

A more detailed discussion on the working principles and the limitations for the above mentioned kinds of devices as well as the necessities of this study are provided in Chapters 2 and 4. A fluorescent fiber solar concentrator (FFSC) as an alternative solution in mitigating the limitations of present devices is designed by the author for remote indoor daylighting purposes.

1.3 Objectives and methodology

Three main objectives have been developed for this research, namely:

- a) to identify the working principles and to extract the limitations of the present daylighting related devices, and
- b) to develop a new concept to avoid or to mitigate the limitations of the present daylighting related devices and to fabricate a device based on the new concept, and

c) to assess the performance of the fabricated new device for remote indoor daylighting purposes through its trial run.

This research is a combination of the quantitative research and the qualitative research as discussed in Chapter 3. The first objective is achieved through literature reviews as presented in Chapter 2 and through the determination of the need for FFSC as presented in the first part of Chapter 4; the second objective is fulfilled through the concept development and the fabrication process as a qualitative process as described in Chapter 4; the last objective is achieved through the 6-month experimentations as a quantitative process as discussed in Chapters 5, 6, and 7. A conclusion of these objectives' achievements is summarized in Chapter 8. Chapter 8 also provides some potential applications of FFSC and the recommendations for future research.

1.4 Scope of research

In this study, only fluorescent fibers with the diameter of 2mm are embedded in the FFSC plate. This is due to the limitations in the availability of the fluorescent fiber market. There is no fluorescent fiber with larger diameters available with the supplier at that time. Since the reduction of the cross sectional area of the luminescent plate could increase the photon loss according to Richards (2006), Reisfeld (2001), Batchelder, Zewail, & Cole (1979), and Hammam, El-Mansy, El-Bashir, & El-Shaarawy (2007), if fluorescent fibers with a larger diameter could be embedded in FFSC, the performance

parameters of FFSC such as the luminous efficacy and the light-to-light efficiency could be increased. This is recommended for future study.

Experimentations were conducted in a specially prepared dark and windowless storeroom in one of the University buildings. The building is located in Kuala Lumpur, Malaysia, which locates at latitude 3.7° North and longitude 101.33° East in the tropical region (Chia, Hamdan, & Dilshan, 2006). Malaysia has a yearly mean temperature of 26°C to 27°C throughout the year (Sabarinah, 2006). The findings would vary if the device is placed in a different regional or climatic condition, for example somewhere in the temperate zone or in the rigid zone. The radiation of sunshine, the rainfall, and the solar altitude in the temperate region or in the rigid region are different to that in the tropical region, so that the monitored data may vary accordingly. A critical review of the experimental limitations is presented in the latter part of Chapter 5.

1.5 Structure of the thesis

There are totally eight chapters in the thesis. Chapter 1 provides a brief introduction to the thesis, and Chapter 2 introduces the daylighting related devices as well as their principles of work, advantages and disadvantages. The common applications of fluorescent fibers have also been reviewed in Chapter 2. Chapter 3 discusses the research methodology. In the first part of Chapter 4, the author explains the needs for developing the new concept. A detailed description on the new concept development and the design of the new device named “fluorescent fiber solar concentrator” (FFSC) is provided in the latter part of Chapter 4. Chapter 5 discusses the approaches for data

collection and data analysis as well as the experimentation procedures and instrumentation. Raw data restructuring and interpretation processes are explained in Chapter 6. Chapter 7 discussed the analysis results for the FFSC 6-month trial run. Finally, conclusions are drawn in Chapter 8. Some potential applications for FFSC system and the recommendations for future study are also presented in Chapter 8.

Review of Daylighting Related Devices

Besides the rapidly rising price of petroleum, anthropogenic activities, especially the burning of fossil fuels, have released pollutants into the atmosphere increasing global warming and depleting the ozone layer (Hirata & Okamoto, 2022). To improve the situation there appears to be a decrease in energy of which fossil fuel is used. As a result there has been an increased interest in renewable energy such as solar energy is widely widely available for thermal applications, daylighting and direct production of electricity (Mohan, 2019; Reddy, 2019; Laganaga, 1992).

Artificial lighting is one of the major sources of electrical energy consumption in buildings, both directly through lighting energy consumption and indirectly through production of significant heat gain, which increases cooling loads. Lighting energy represents up to 30% of building electricity consumption in commercial buildings (C. Lee, H. H. G. Chan, & McCrann, 1996; Law & Chan, 1996). The recent interest in energy efficiency and sustainability has led to the implementation of design strategies in buildings aimed at the achievement of the optimal utilization of daylight with minimum energy consumption for lighting and cooling (Hirata, 1993).

Chapter 2

Review of Daylighting Related Devices

Besides the rapidly rising price of petroleum, anthropogenic activities, especially the burning of fossil fuels, have released pollutants into the atmosphere increasing global warming and depleting the ozone layer (Mills & Orlando 2002). To improve the situation there needs to be a decrease in energy of which fossil fuel is used. As a result there has been an increased interest in renewable energy systems. Solar energy is made widely available for thermal applications, daylighting, and direct production of electricity (Muhs, 2000; Reisfeld & Jorgensen, 1982).

Artificial lighting is one of the major sources of electrical energy costs in office buildings, both directly through lighting energy consumption and indirectly by production of significant heat gain, which increases cooling loads. Electric lighting represents up to 30% of building electricity consumption in commercial and office buildings (Crisp, Littlefair, Cooper, & McKennan, 1988; Lam & Chan, 1995). The recent interest in energy efficiency and sustainability has led to the implementation of design strategies in buildings aiming at the achievement of the optimal utilization of daylight with minimum energy consumption for lighting and cooling (Hasdemir, 1995).

Sun light as a clean energy source could contribute considerably to a solution of the energy problem if appropriate methods were developed to collect, concentrate, store and convert solar irradiation, which is diffuse and intrinsically intermittent (Reisfeld & Jorgensen, 1982). Daylight is an underused resource that has the potential to improve the quality of indoor lighting, as well as to substantially reduce energy costs.

2.1 Daylight for illumination

Lighting has a profound effect on the lives of people. It facilitates vision, which is the most important source of information on the world, and it affects the basic biological functioning through its effect on human “body clocks” as stated by Webb (2006). Electric lighting is one of the world’s biggest end uses of electricity (Mills & Orlando, 2002). In developed nations, the electricity use for lighting ranges from 5% to 15% of total electrical energy use (Mills & Orlando, 2002). Because the energy for artificial lighting is often supplied by fossil fuel generation, it results in the large scale release of greenhouse gases (GHGs) according to Mills & Orlando (2002). Further, lighting is a major contributor to the peak demand for electrical power, which is often met by the high-GHG generators.

Sunlight is the universal and free sources of renewable energy available throughout the earth. The survival of life and health as well as the conditions of environmental comfort and prosperity are dependent on their effective utilization of sunlight (Muhs, 2000). People can benefit directly from sunlight through active or passive daylighting systems besides the electrical generation and thermal gain from the sunlight. In an

energy-efficient building design, it is always proper to reduce the energy consumption for artificial lighting (Muhs, 2000).

Solar energy utilization and specifically making use of the daylight in the buildings can be a very promising choice among the renewable energy options. Daylight is a kind of light source that most closely matches human visual response so that its quality is as high as to be the best for color rendering (Hasdemir, 1995). The luminous efficacy of sunlight is around 110 lm/W, while the luminous efficacy of fluorescent lamps and incandescent lamps are around 75 lm/W and 20 lm/W, respectively. Further, daylighting generates only 20% to 50% the heating that equivalent electric lighting does, significantly reducing the building cooling load (Hasdemir, 1995). A reduction of 65% of the total lighting energy consumption is achieved by active and passive systems that use daylight and control component (Hasdemir, 1995).

Electric lighting and daylight are compatible and complementary and should be used to bring out the best in the interior environment. Electric lighting can account for 25–40% of a commercial building's energy requirements so that the combined savings from reduced lighting and cooling loads can be substantial (Franzetti, Fraisse, & Achard, 2004). Franzetti et al. (2004) reports that energy saving could be as much as 52% along the window walls. The amount of daylight penetrating a building is mainly through window openings which provide the dual function not only of admitting light for indoor environment with a more attractive and pleasing atmosphere, but also allowing people to maintain visual contact with the outside world. People desire good natural lighting in their living environments (Chel, Tiwari, & Chandra, 2009).

Daylighting is an important issue in modern architecture because it affects the functional arrangement of spaces, visual and thermal comfort of occupants, structure, and energy use in building (Chel, Tiwari, & Chandra, 2009). Danny, Chris, & Joseph (2005) states that illumination levels on a bright sunlight may vary from 50,000 LUX to 100,000 LUX. According to Unver, Ozturk, Adiguzel, & Celik (2003), the first step of designing a building to utilize daylight for illuminating its interior is to acquire information on the amount of daylight available. However, the basic daylight illuminance data are not always readily obtainable in many regions of the world (Unver, et al., 2003).

Daylight has a significant positive impact on the people because it provides a sense of cheerfulness and brightness (Li & Lam, 2001). People spending the day in non-daylit buildings may therefore be in "biological darkness," causing reduced performance (Leslie, 2003). According to Andre (2002), the most powerful impact of daylighting is on the building's occupants even though the potential for reducing energy costs and environmental emissions is substantial. However, the successful integration of such strategies requires data regarding daylight availability and illumination levels for every region in the world.

As reported by Aries & Newsham (2008), lighting has often been the target of energy efficiency initiatives because of its high-energy burden, and one of such initiative is daylight saving time. The principal reason for the application of daylight saving time was to shift human activity patterns to make better use of daylight, and thus reduce the amount of electric lighting necessary to support these activities. Daylight saving time impacts the changes to traffic fatalities and the commercial activities as well (Aries & Newsham, 2008).

The energy consumption of lighting in buildings is a major contributor to carbon emissions and the heat gains produced from such lighting have an important influence upon heating and cooling loads as reported by BRE (1997). With the aim of identifying how technological interventions might reduce emissions by 50% by the year 2030, a program is investigating the carbon emissions of UK buildings as reported by Peacock, Newborough, & Banfill (2005). This program was based on the estimations made with respect to technological and building improvements that, although not necessarily readily available in 2005, should be obtainable within the next 21 years until 2030. Several building categories such as domestic, office and retail are being investigated. Several different types of building are defined that are indicative of that category within each category. For the buildings under investigation in this program, electrical lighting accounts for a substantial proportion of carbon emissions as reported by Peacock et al. (2005).

The reduction of energy consumption is an important agenda in the world. There is an urgent need to search for renewable energy sources and modern technologies. A growing interest of illuminating engineers in the utilization of natural light is well recognized in last decades (Kocifaj, 2009). Paroncini, Calcagni, & Corvaro (2007) have summarized several reasons for preferring the natural light in designing the illumination systems, namely:

- i) solar energy is free,
- ii) the diffuse skylight is available for a whole day (also under overcast conditions),
- iii) direct solar radiation is an extra supply, which increases the efficiency of light-guides dramatically, and,

iv) daylight is considered as the best source of light for good color rendering and it most closely matches human visual response.

Owing to an increasing awareness of the positive effects of daylight on the health and efficiency of humans, a wide range of daylighting systems was developed. Up to the year 2000, around 180 000 m² of daylighting systems were installed in Europe (Koster, 2000).

Boyce (2009) claimed that the value of interior lighting means aesthetic, physiological and economic attributes. The aspect of environmental protection is always understood as a monetary term and analyzed in economics. The values of the aesthetic quality and the human well-being are difficult to quantify and they are only able to be estimated. As reported by Boyce (2009), to improve health and productivity of occupants, energy conservation and wider environmental benefits is the current interest in daylight. The health conditions of working environments can be improved by daylight through physiological responses such as regulation of the diurnal cycle of body activity. Since up to 85% of office costs are staff salaries and in comparison energy costs are tiny, small increases in staff productivity are equivalent to large savings in energy. The visual environment has an affect on wellbeing, personal satisfaction and mood, all of which influence office productivity, but attempts to measure the relationship between productivity and lighting directly have not been successful (Boyce, 2009).

Electricity generation is one of the largest sources of carbon dioxide (CO₂), which comprises a significant amount of greenhouse gas emissions. The amount of CO₂ released into the atmosphere depends on the fuel mix used in generation (Carbon Trust, 2009). A monetary value of £0.0043/kWh may be ascribed to this kind of pollution

using the Climate Change Levy (CCL) and the tax on energy bills (Department of Environment, Farming and Rural Affairs, 2009).

The compliance to be based on a whole-building overall CO₂ emission is implemented in the UK via the energy-related parts of the Building Regulations (2006), and it is required by the European Energy Performance of Buildings Directive. Accordingly, the requirements in building codes have been shifted towards the control of CO₂ emissions (Carter, 2008). The provision of daylight within a building may influence CO₂ emissions if daylight is used as a substitute for electric light. The Building Regulations (2006) define a daylit space as being either within 6m of a window wall, provided that the glazing area is at least 20% of the internal area of the window wall, or below roof-lights or similar provided that the glazing area is at least 10% of the floor area. No distinction is made in the regulations between roof-lights and daylight guidance. For thin roof constructions roof-lights and guides of similar aperture areas will deliver comparable amounts of light into a space, but for deeper roof constructions guides will generally have a superior performance. Smaller areas of external glazing may be needed using guides to produce a given daylight condition (Building Regulations, 2006). This may be beneficial in terms of the overall CO₂ emission (Carter, 2008).

Martin (2002) classified the conventional daylighting systems into shading systems and optical systems. Shading systems have been designed primarily to block direct sun and admit diffuse light, but may address other daylighting issues as well, such as redirection of direct or diffuse sunlight. The use of conventional shading devices to prevent overheating or glare effects also reduces the use of daylight for visual tasks indoors. Shading systems that capable of redirecting diffuse light into the interior by rejecting or diffusing sunlight are developed to increase the use of daylight (Martin, 2002).

According to Martin (2002), optical systems are daylighting systems without shading, they include: diffuse light guiding systems, direct light guiding systems, scattering systems, and light transport systems, as discussed in below:

2.1.1 Diffuse light guiding systems.

The overcast sky is much brighter in the zenithal area than in the horizontal part of the sky (Martin, 2002). The use of light guiding elements that redirect the light from these areas into the depth of the room allows an improved utilization of daylight. The zenith light is normally used near the window opening. Rooms are only well lit nearby the window because the high external obstructions shade the room against the diffuse skylight. This problem can be solved by diffuse light guiding elements, which include light shelf, anidolic integrated systems, anidolic ceiling, fish system, and zenith light guiding elements, and so on (Martin, 2002).

2.1.2 Direct light guiding systems.

The direct light guiding systems include laser cut panel (LCP), prismatic panels, holographic optical elements in the skylight, and light guiding glass, and so on (Martin, 2002). When glare effects and overheating problems are avoided, rooms can be illuminated by direct sun light. Glare reduction needs the even distribution of light in the room without shadows and high contrasts in the working field. The avoidance of cooling loads can be realized by high efficient redirection and distribution of the sun light in a small part of the façade, while the rest of the façade is closed by conventional shading devices (Martin, 2002).

2.1.3 Scattering systems

Scattering systems include light diffusing glass, capillary glass, and frosted glass, and so on (Martin, 2002). Scattering systems are used to realize an even lighting distribution. They are very useful in sky light openings in top-lit rooms. Attached in vertical openings they may produce huge glare problems. Their location has to be considered very carefully or they have to be shielded in some way to prevent glare problems.

The physical and optical properties of daylight emitters are heavily influenced by the transport system to which they are connected. Carter (2004) introduced daylight emitters as combined emitters and discrete emitters. In combined emitters, light is extracted continuously along its length. On the other hand, discrete emitters operate in a manner similar to conventional luminaries. Carter (2004) further classified daylight emitters into hollow prismatic emitters, slit light guides, and discrete emitters.

a) Hollow prismatic emitters

Light transport within hollow prismatic guides is by total internal reflection within the prismatic material (Whitehead, Nodwell, & Curzon, 1982). Imperfections in the prismatic structure and the presence of non-collimated light produce the emission. The loss is approximately two percent per 300mm of pipe length and the effect is to cause the pipe to glow. A number of devices are used to control the light output from the emitter. An extractor, a strip or wedge of diffusing material may be placed inside the guide-causing incident light to be scattered and escape through the walls. A reflective material may cover exterior surfaces of the guide that are not used as an emitter that

redirects light inwards. Control of output along the length is achieved by varying the width and shape of the strip. Prismatic emitters have an appearance similar to large electrically powered diffusing area sources giving light with few shadows and little glare (Carter, 2004).

b) Slit light guides

These are tubes made of elastic polyethlemephate film, which has a high reflectance up to 95% except for a slit running the length of the tube (Carter, 2004). The high reflectance is achieved through the internal coating and the light transmission along the guide is by mirror reflection. The material is fabricated, erected in situ, and air is pumped in under pressure to give the correct shape. However, light can be emitted through the transparent or diffusing slit (Aizenberg, Bukhman, & Pyatigorsky, 1975). The diameters for slit light guides range from 250 to 1200 mm and the angular size of the slit varies from 30 degree to 110 degree subtended by the axis (Aizenberg, et al., 1975).

c) Discrete emitters

In daylight applications, many commercially available discrete emitters are incorporated at the ends of the light guides. The discrete emitters are made of opal or prismatic material of diameters corresponding to the light guides. They are generally circular flush, domed or square. For instance, a 600mm square emitter that fits into suspended ceiling systems is reported by Carter (2004). The square emitter is connected to a 500mm mirrored pipe via a transition box and the light is distributed within the building

interior by either a diffuser or an array of Fresnel lenses as shown in Figure 2.1 (Carter, 2004).

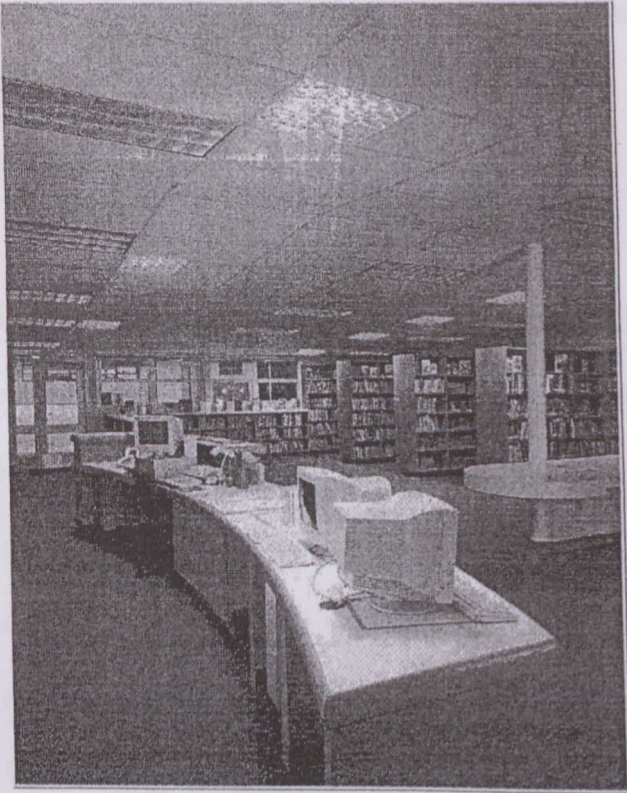


Figure 2.1: interior lit using a square lens discrete emitter (Carter, 2004:223)

2.1.4 Light transport systems

Light transport is the feature that sets light pipes apart from other daylight redirection methods (Martin, 2002). Light transport systems such as light pipes and optical fibers allow daylight to be transported from outside by collating it and guiding it into the depth of the building. Transport elements deliver light from the collector to the point of exit and some devices have their own emitters. Daylight can be transported over long distances into floor areas or rooms without any window opening. At night time, artificial light could also be transported through this kind of systems (Hicks & Wright, 2000).

By considering a major factor of the availability for low-cost light redirection materials, four different transport methods, namely, beam/lens systems, hollow mirrored pipes, hollow prismatic pipes and solid core systems, are examined by Martin (2002).

a) Beam/lens systems

In these systems, light from the collector is collimated by a lens and transported via an arrangement of lenses and mirrors. A physical 'guide' between the lenses is not necessary optically, but may provide protection. These systems have two drawbacks that limit practical application. First, light-redirection equipment such as lenses and mirrors tend to be more expensive than the other methods. Second, there are high levels of light loss in the optical processes. Whilst a clear lens can transmit a maximum of 92% of light, losses increase with dirt deposition on surfaces. Efficiency is also dependent on accurate alignment, so that in systems consisting of several components, losses due to misalignment become significant (Martin, 2002).

The few examples of this type that have been realized are based on the work of Dugay & Edgar (1977). A building at the University of Minnesota, for example, uses heliostats on the roof to capture sunlight that is concentrated and collimated before being beamed through a vertical duct in the building containing lenses and mirrors to a working space 35m below ground. Thirteen optical processes give a maximum system efficiency of 28% in a clean state. The main advantage of this approach is that concentrated sunlight permits the use of smaller ducts than other transport methods delivering the same light flux. However, high capital and maintenance costs combined with low efficiencies

suggest that these methods would almost certainly be uneconomic compared with other transport methods (Dugay & Edgar, 1977).

b) Hollow mirrored guides

These use multiple specula reflections at the inner wall surface to transmit light. Overall light transmission is a function of the surface reflectance, the input angles of the incident light and the proportions of the guide in terms of the ratio of length to diameter. If the light paths are long compared with the axial width of the pipe, the number of reflections is necessarily large (Martin, 2002).

Performance is particularly sensitive to reflectance of the mirror material with variations of as little as 0.1% causing noticeable changes. To attempt to minimize the number of reflections, light must enter the guide as a near collimated axial beam. Efficiency is as a function of both the ratio of effective length to diameter and the angle of incidence of the collimated incoming light. For the best case, efficiency was in excess of 50% for a length/diameter ratio of 40, corresponding to approximately 12m of light travel in a 300-mm diameter guide, but efficiency rapidly diminishes as the alignment of incident rays and guide axis diverges. In practice, dirt and component misalignment will mean that efficiencies are likely to be somewhat lower than those in laboratory measurement are (Hicks & Wright, 2000).

The recent introduction of visible mirror film, a reflecting material based on polymeric multiplayer optical stacks that has a specula reflectance of the order of 99%, in future will increase the economic light transport distance. The efficiency of a 12-m circular

cross-section pipe of 300mm diameter would rise to 70% using this material (Hicks & Wright, 2000).

Aizenberg et al. (1975) described the slit lightguides, essentially a circular cross-section mirrored pipe with a transparent slit throughout its length that serves as a light emitter, in which light is totally reflected internally from a prismatic dielectric surface that traps the light and redirects it down the inside of the guide.

Incident light is totally reflected internally twice at the prismatic surface, thus operating like a mirror for certain angles of incidence. Unlike a mirror, however, the prismatic structure is transparent to light at higher angles of incidence. The main lighting applications use acrylic or polycarbonate materials having a 90-degree prismatic ridge structure on the exterior surface. The devices redirect light down the inside of the guide when the prisms are orientated parallel to the axis provided that the incident light does not exceed 27.5 degree to the axis of the pipe. Overall reflectance is of the order of 98%. In theory, all light would be reflected by this process, but irregularities in the film cause a small proportion of light to exceed the maximum angle and leak out of the pipe (Aizenberg et al., 1975).

c) Solid core systems

The major lighting applications of solid core systems are optical fibers. These consist of two coaxial regions, an inner core that acts as the light transport medium and an outer cladding of lower refractive index that prevents leakage of from the core. The process of total internal reflection in an optical fiber is very efficient and light transport is

essentially a function of length and not of diameter as in the case of mirrored or prismatic transport systems (Martin, 2002).

One of the very few examples of this technology in daylight guidance is the Himawari system as reported by Eben (1993). Sunlight is collected using a tracking Fresnel lens, self-powered by a solar cell, filtered and focused with a concentration of 1:10000 onto the ends of the optical fiber. A single 6 fiber 40mm-long cable (made up of six or nine optical fibers) delivers 1180 lumens from 98000 LUX of direct sunlight over a distance up to 200m from the collector, a distance far beyond the capabilities of the other transport methods. Notwithstanding this, these systems represent an extremely large capital investment that is unlikely to be justified for other than prestige buildings (Eben, 1993).

The huge number of different daylighting systems allows new and optimized ways of daylight utilization. But at least it has to be considered that the different systems have to be used in the right way and that the used system is adjusted to the building and matches the requirements of lighting for this special purpose. Otherwise, problems like overheating of rooms or glare may occur that would lead to refusal of the daylighting system and to stopgap solutions bringing the elements to a standstill to reduce these problems (Martin, 2002).

What makes daylighting a particularly challenging task is the permanent change of availability, brightness and angle of incidence due to weather conditions and the sun path. Other factors also play an important role, e.g. the reflectivity of nearby surfaces, the different levels of brightness due to the latitude, the different composition of direct

and diffuse daylight due to air humidity, and the use of different glazing (Kischkoweit, 1998).

According to Kischkoweit (1998), daylight luminance ranges from 120000 Ev on a sunny day in the tropics to 5000 Ev with overcast sky in temperate climates even at high noon. The necessary average luminance level for most tasks in offices ranges from 500 Ev to 2000 Ev, and these levels are proposed for visually sensitive jobs such as designing. Owing to an ever-increasing amount of computer workplaces, the tolerance for higher or lower luminance, especially in office buildings, is limited. Veiling glare as well as disability glare has to be avoided.

Many options seem revolutionary: zero-energy houses are possible even under poor climate conditions. Energy gains can be obtained with active and passive solar facades. Visual comfort can be increased significantly by daylight guidance systems. Architectural concepts might be affected, e.g. the division of windows into a fanlight, especially equipped with three-dimensional daylight guidance systems for an optimized light distribution without glare and a sun-protected window at eye-level for visual contact with the outside world (Martin, 2002).

According to Laar & Friedrich (2002), an important issue to be considered for daylighting is the user's behavior. Daylighting systems are mainly considered for office buildings. Typically, the full depth of office space is used for working. However, office staffs are generally fully concentrated on their tasks and do not find time to adjust daylighting systems regularly. Therefore, systems with a high demand of user participation may be a problem, for example, once daylighting systems are adjusted to full protection, which means fully closed, they are rarely opened again. Lighting needs

are then fully covered by artificial lighting. However, automatic systems adjust venetian blinds automatically. To avoid being overdriven or turned off by the user, these systems must be highly reliable and robust.

Another important aspect is maintenance. Mechanical systems, especially when applied on the facade, are problematic. While everybody is used to the idea of regular car maintenance, it is not necessarily the same for buildings. The high costs caused by neglecting this item started to lead to a change in this attitude, but it still depends strongly on the individual owner. In addition, a regular cleaning of relatively unprotected systems (outside and inside the building) is necessary to maintain the full efficiency of the applied system. Therefore, systems integrated into the vertical facade, protected by glass on each side, are clearly advantageous. Furthermore, the development of the daylighting systems was generally focused on the temperate climate instead of the tropic climate (Laar & Friedrich, 2002).

Increasing the use of daylighting in buildings can offer significant savings in energy consumption as well as improving the internal environment (Martin, 2002). For example, Bouchet & Fontoynont (1996) suggested that as little as 50 LUX of daylight might provide significant relief from feelings of isolation for people working in underground spaces. However, there can be problems with glare and potential thermal discomfort due to direct solar gain with some daylighting systems. Natural light could be transported by light pipes and optical fibers in a building with little thermal effect (Bouchet & Fontoynont, 1996).

2.2 Light pipes for daylight transportation

Daylight guidance redirects natural light into buildings areas that cannot be lit by conventional glazing. The most commercially successful type is light pipes, also called tubular daylight guidance systems, which comprise a clear polycarbonate domed light collector that accepts sunlight and skylight from the whole sky, a light transport tube lined with highly reflective silvered or prismatic material, and a diffuser commonly made of opal or prismatic material light to distribute light in an interior (Carter, 2004).

The usage of cylindrical tubes for light guiding becomes one of very attractive approaches for delivery the natural light into the interior spaces (Al-Marwaei & Carter, 2006). New technologies support production of light tubes with satisfactory high reflectance of inner surfaces (Elmaualim, Smith, Riffat, & Shao, 1999). This minimizes energy losses during guiding the light.

The development of efficient reflective and refractive optical materials made possible the first light pipes in Australia and the US some two decades ago. The systems were initially aimed at the domestic building market, and subsequently at that for commercial buildings. More recently, light pipes were introduced into the European market where they have been the subject of heavy marketing based around manufacturers' claims of user appreciation of the delivered daylight and of potential energy savings (Carter, 2004).

As illustrated in Figure 2.2, light pipe systems have three components, namely: (i) an outside collector (usually on the roof), generally a clear dome that removes UV radiation and acts as a cap to prevent dust and water from entering the pipe; (ii) the light

pipe itself; (iii) an emitter or luminaries that releases the light into the interior (Oakley, Riffat, & Shao, 2000).

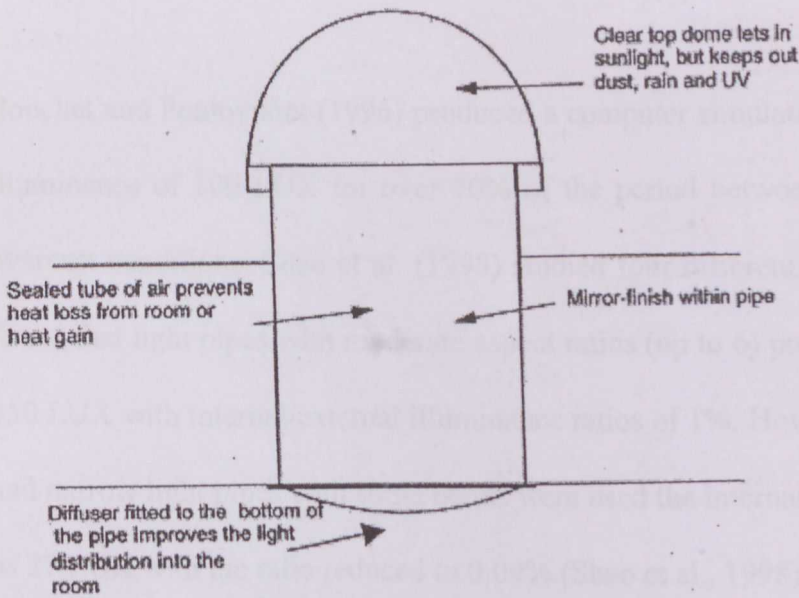


Figure 2.2: schematic of a typical light pipe (Oakley, et al., 2000:91)

The majority of commercially available light pipes are simply empty tubes along which light can travel into the interior of a building or other dark spaces. They are available from a number of manufacturers and are versatile enough to be installed in straight or angled assemblies, enabling them to bring daylight into otherwise inaccessible rooms. The coating on the internal surface of the light pipe is composed of highly reflective materials such as anodized aluminum or coated plastic films such as Alcoa Everbrite and SilverLUX, which have reflectance greater than 95% (Shao et al., 1998).

Light pipes use the principle of high efficiency reflection, and as a result straight light pipes perform better than angled ones as light energy decreases with increased reflections (Sweitzer, 1993). Each light pipe bend may reduce light output by approximately 8% (Monodraught, 1997). The light pipe also transmits less solar heat

than windows, preventing internal heat gains in summer, and heat loss in winter. Finally the diffuser distributes the light more evenly into the space the light pipe is illuminating.

Bouchet and Fontoynont (1996) produced a computer simulation predicting a minimum illuminance of 100 LUX for over 70% of the period between 09:00 and 18:00 under overcast conditions. Shao et al. (1998) studied four different buildings in the UK, and found that light pipes with moderate aspect ratios (up to 6) produced illuminances up to 450 LUX with internal/external illuminance ratios of 1%. However, in cases where long and narrow light pipes with some bends were used the internal illuminance fell to as low as 27 LUX with the ratio reduced to 0.09% (Shao et al., 1998).

Light pipes guide light which enters to the intended exit in the ceiling at the interior of the building. Illuminance from sunlight (and coincidental skylight) through the light pipe can complement that from side lighting especially for the space in the deep interior of a building. Light pipes are effective for a facade which faces the sun all year round and has been presented as an effective means to complement side lighting (Beltran, Lee, & Selkowitz, 1997).

For a tropical location, the sun may traverse in the northern or southern hemisphere depending on the day of the year. It is stated by Surapong, Siriwat, & Liu (2000) that the aperture of light pipes faces either east or west to utilize the sunlight in the morning or in the afternoon. For such a situation, sunlight is utilized only for a few hours for a facade each day, and for the rest of the time electric lighting will be used to supplement side lighting (Surapong et al., 2000).

Carter (2008) presents some photos of the uses of light pipes explored in actual buildings in UK as shown in Figure 2.3, 2.4 and 2.5. Exterior views of two installations are shown in Figure 2.3. Interior views of the same installations illustrated in Figure 2.4 show the circular opal diffuser, or square lens panel output devices. Figure 2.5 provides a general view of guides in roof space.

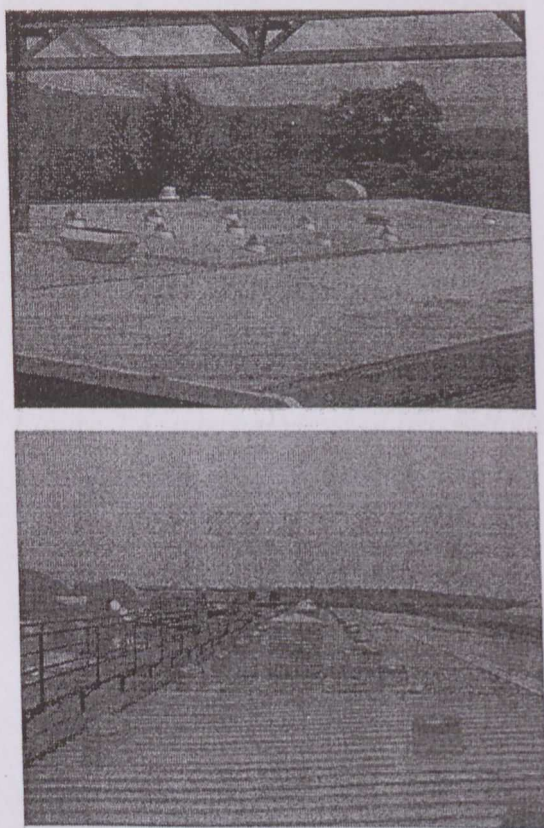


Figure 2.3: external views of two installations (Carter, 2008:526)





Figure 2.4: internal views of two installations (Carter, 2008:526)

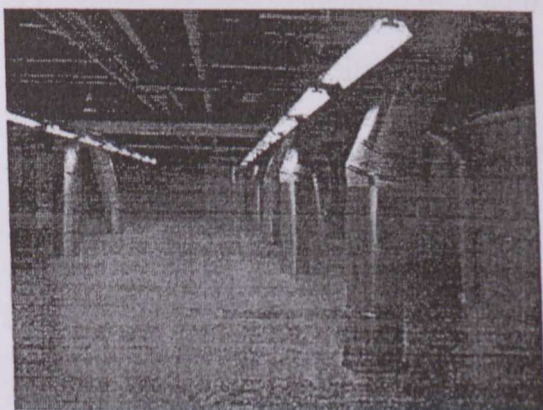
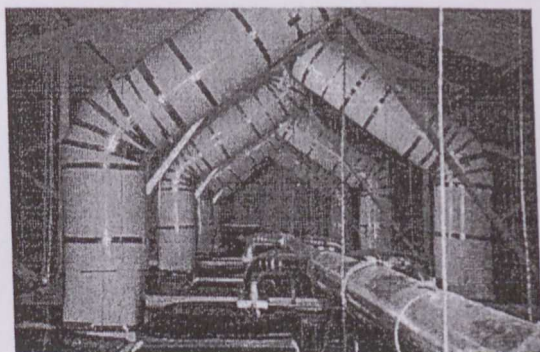


Figure 2.5: general views of guides in roof space (Carter, 2008:526)

Tubular light guidance systems are classified here by their light collection method by Carter (2004). The collector is usually located at roof level to gather light from the zenithal region of the sky and is either mechanical devices that actively focus direct daylight (usually sunlight) or are passive devices that accept sunlight and skylight from part or the whole sky hemisphere (Carter, 2004).

2.2.1 Zenithal systems with active collection

A tracking mirror or Fresnel lens (heliostat) usually on a roof collects concentrates sunlight. A second mirror or lens directs a concentrated beam of sunlight into a light guide. Diffuse daylight is much less suitable as a light source since there are theoretical limits on the concentration achievable (Rabl, 1980). Collimated light is necessary to achieve the necessary concentration for efficient transport. The size of the tracking mirrors or lenses required can be large. It is estimated that a total mirror area of about 40m², or a lens area of half this value, would be required to light a 1000m² office to 500 LUX (Ngai, 1983). Collectors of this size would have high capital cost, require costly control systems and maintenance, and have implications for the external appearance of the building. The majority of light transport systems used for active collector systems are hollow mirrored or hollow prismatic pipes light pipes. Carter (2004) introduced two detailed examples of light pipes, namely: sun lighting system and Arthelio, as described in below:

a) Sun lighting system

An installation in Austria uses sunlight to provide lighting to an underground room with a size of 7.8m length, 4.5m width, and 2.4m height (Pohl & Anselm, 2001). A

sun-tracking heliostat and a redirection mirror redirect light to a concentrator as shown in Figure 2.6.

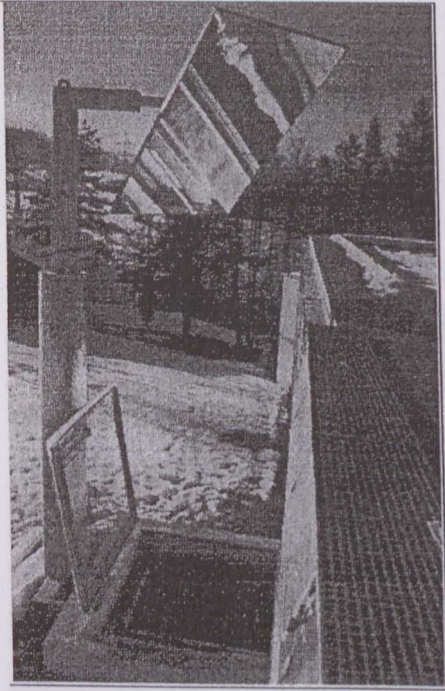


Figure 2.6 sun lighting system redirection mirror (Carter, 2004:224)

Two adjustable Fresnel lenses increase the concentration of incoming sunlight by a factor of 35 for transport in a 300mm diameter tubular prismatic hollow guide (Figure 2.7). The emitter located in a windowless basement consists of two elements. A component similar to a mirrored louvered down light electric luminaires provides glare-free light to a task area. Diffuse ambient light is provided by light from the prismatic walls of the emitter. In addition, users can adjust a mirror to direct sunlight onto the task area thus creating a visual link to outside conditions. Supplementary fluorescent lamps are incorporated in the reflective optical component, which can be dimmed according to outside conditions and provide lighting after dark. The installation delivers glare-free light with working plane luminance between 100 and 1200 LUX given sunny conditions with a 30% overall system efficiency. Energy savings were measured by a combination of continuous monitoring of power consumption and

simulation of the performance of the system located in various parts of Europe. The results indicated power savings of 40–60% compared with a conventional electric lighting system. The quoted capital cost of £225/m² is of the order of ten times that of an electric lighting installation providing comparable lighting conditions. However, this kind of device is highly dependent on the direct sunlight and a tracker is always needed (Pohl & Anselm, 2001).

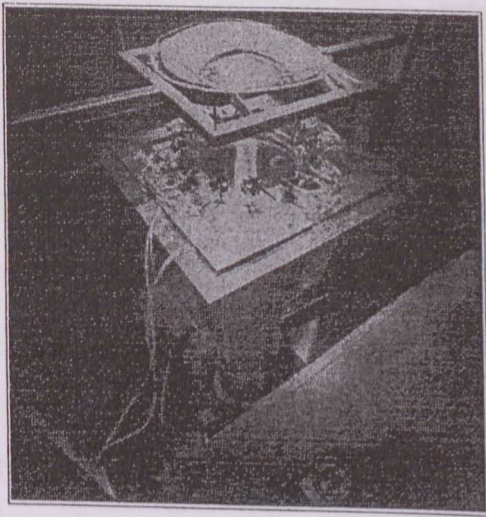


Figure 2.7 sun lighting system concentrators (Carter, 2004:225)

b) Arthelio

The Arthelio study developed systems combining daylight and electric light and culminated in the construction of two large installations: a staircase connecting three floors of an office building in Berlin and a working area of a single-storey warehouse in Milan (Mingozzi, Bottiglioni, & Casalone, 2001). The Berlin installation has a two-axis automatically controlled 6-m² plane mirror directing sunlight horizontally toward four 1*1.4m Fresnel lenses, which concentrate the light by a factor of 100 and hence to a mixing box (Figure 2.8). The mixing box allows introduction of light from 1000W dimmable sulphur lamp to supplement and directs collimated light into two 12m long, 30-cm diameter hollow prismatic light guides with a specula reflectance of 97%. Light

leakage from the guides is regulated by a series of white diffuse hollow tube extractors inside the guide (Mingozzi, et al., 2001).

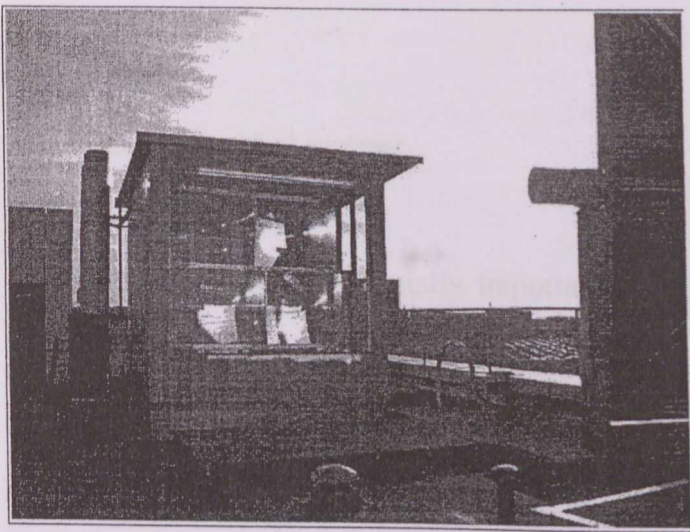


Figure 2.8: ARTHELIO Fresnel lens (Mingozzi et al., 2001:16)

The mixed light supply means that the appearance of the tubes varies with time of day and season. The Milan installation uses a single-axis light-capture head based on a Fresnel lens with an acceptance angle that enables sunlight to be collected from the majority of the sun path at the latitude of the installation. The sunlight is then reflected into a 13m long, 90cm diameter circular guide via an anidolic mirror. The guide is lined with prismatic material with a specula reflectance of 97%. A diffuser unit, shaped like a truncated cone and located at the end of the duct, distributes the light over some 14m² of working area beneath the pipe. Connected to the diffuser unit are two horizontal prismatic light guides powered by 100W dimmable sulphur lamps. These provide a uniform luminance over the working area by a control system that tops up or replaces the daylight as necessary. The system delivers in the order of 200–250 LUX on the working plane and luminance beneath the diffuser is more than 2% of the external luminance from sunlight/ daylight and sunlight. The combination of dimming and the

presence of a detection system give estimated savings of 67% over the fluorescent installation it replaced. No capital costs are quoted for either project (Mingozi, et al., 2001).

2.2.2 Passive zenithal systems

These are the most commercially important form of daylight guidance system. They consist of a light-transport section with, at the upper end, some device for collecting natural light whilst preventing ingress of wind and rain and, at the lower end, a means of distribution of light within the interior. The collector is usually a clear polycarbonate dome that may include a refractive redirection device. Modifications to the basic systems include: cutting the upper end of the tube at an oblique angle inclined toward the equator; laser-cut deflecting panels to redirect light in an axial direction; and reflectors known as 'light scoops' located outside or inside the collector dome to intercept direct sunlight, increasing the fLUX output under a clear sky plus sun, but having a negative effect under overcast conditions. The transport section is a rigid or flexible hollow mirrored or prismatic guide and may include bends or elbows (Carter, 2004).

Studies of achieved conditions and user views in buildings equipped with light pipes suggest that daylight guidance devices are recognized as sources of daylight, but are thought to be generally inferior to windows in the delivery of daylight (Ejhed, 2001; Al-Marwaei & Carter, 2006). Little authoritative work on either energy savings realized, or the general economic viability of light pipes, has been published. Fontoynt (2005) compared theoretical long-term costs of various methods of office lighting and

concluded that whilst the costs of light pipes were similar in magnitude to electric lighting, they were more expensive than conventional windows or roof lights.

Muneer & Jenkins (2004) compared the costs of lighting a number of theoretical small rooms using light pipes. Their results suggested that light pipes may be an economic investment particularly if the economic value of daylight was included, but the limited nature of the study did not permit the viability of actual installations to be investigated.

The innovative nature of light pipes has posed two major problems for designers (Carter, 2008). The first is that there is little accumulated experience of how they are accommodated within a building. As conduits of daylight, light pipes penetrate the exterior envelope of a building but, unlike windows, may also pass through internal structural or construction elements. They thus make demands in terms of structural support and fire protection (fire compartments, fire stopping, and internal and external spread for flame) that other lighting systems do not. In this respect, they are akin to mechanical ventilation systems. In addition, the internal space required to accommodate light pipes components and associated ducts may affect building space planning and cause loss of rentable floor area (Carter, 2008).

The second problem relates to the availability of design guidance and data. Design guidance for conventional glazing sets out desirable window properties, room proportions and surface treatments, and allowable daylight levels and distributions to give satisfactory conditions for users. Similarly, electric lighting codes attempt to create comfortable conditions using recommended planar illuminance levels and limits on surface and source luminance. Little independent specialist design data have been developed for light pipes to date and manufacturers' websites are the main source.

These usually offer little more than output device spacing and installation advice. They are usually based on optimal conditions—the most favorable possible system configuration and assumed daylight resource, which are rarely found in practice. They also use a proliferation of methods of describing system performance, often incomplete, and with little indication of the source of that data. This means that evaluation of the range of alternatives on the market is at best very difficult and in some cases impossible. Indeed, unsubstantiated claims about system performance by a minority of daylight guidance manufacturers threaten to discredit the whole technology. This state of affairs sits uneasily in a lighting industry where standardized methods of design data production and exchange (e.g. utilization factors, luminous intensity tables, daylight factors and glare ratings) have existed for many years (Carter, 2008).

2.3 Optical fiber for light transportation

According to Enedir & John (2006), since the early 1990s, fiber optic cables using an artificial light source have been used in remote-source lighting systems. Using this technology, light travels from its source to one or more remote points through fiber optic cables, one example picture for light transportation through optical fibers is presented in Figure 2.9. The technology has been used in many applications such as museums and retail displays and in architectural applications to emphasize the features of a building or to outline its exterior contours; other applications have involved lighting exit signs and aisles in theatres and aero planes etc. to name but a few.

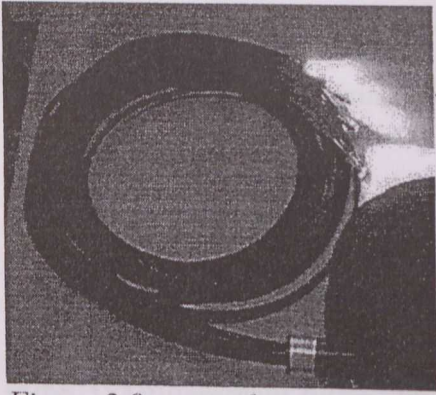


Figure 2.9: example picture of light transmitted through optical fibers (Enedir & John, 2006: 1614)

The idea of concentrated solar energy transport by optical fibers was put forward in 1980 by a group of French investigators (Cariou, Martin & Dugas, 1980). Owing to the unavailability of high quality optical fibers and the high cost of their design, this project limited itself to theoretical analysis only. With the present day availability of fiber-optic techniques, solar energy can be transmitted by high-quality optical fibers of large core diameter and large numerical aperture. With flexible fiber optic solar energy transmission and concentration, a solar laser or any other light powered tool will be able to be moved out of its actual pumping position in the focusing area of the primary parabolic mirror and will find new applications (Cariou, Martin & Dugas, 1980).

Wherever the remote lighting system has been introduced in an architectural project, it was mentioned clearly the practical advantages it breeds. In addition, the main light generators being put away at some distance, in a dry place, gives clear evidence about the safety higher degree of the system. Actually, in important projects where optical fibers take aim to satisfy more complex lighting design purposes, like illumination, safety is appreciated but is not certainly seen as the stimulus of the system choice. Additionally, the practical location of the effective light sources is valued but in terms of lower cost services. In fact, the main advantage aimed for while selecting a remote

lighting system instead of an ordinary one, relates to some extent to the considerable cut down upon the effective running costs (Sala, Milanesi, Ceccherini, & NeW, 1993).

Under such circumstances is the Commercial Fair Tower in Franckfurt. This tall building is crowned by a pyramid previously enhanced by external lighting provided by some 353 fluorescent tubes. These have been now replaced by optical tubes supplied with the necessary light by only 76 metallic vapour lamps (250W). With this new lighting design scheme long term savings are to be realized not only upon the diminution of the effectively operating lamps but also upon the services as the generators are placed within the building (Djamila, 1996).

During the past 30 years a new type of optical fiber has been researched, namely the plastic optical fiber (POF). The situation of this transmission medium had remained rather stagnated for years because of its high attenuation and the lack of demand of specific commercial applications. However, since the development of the graded index plastic optical fibers in 1990 and the later attainment of the low-attenuation per fluorinated fibers in 1996, plastic optical fibers have received a lot of interest, which is expected to give rise to a great deal of applications in the next several years (Joseba & Jon, 2001).

Because of its high frequencies, the optical portion of the electromagnetic spectrum is currently being used by employing optical fibers as transmission media. Specifically, the well-known plastic optical fibers with PMMA core were introduced in the 1960s, although the first optical fibers that were used were made of glass. In the past several decades, concurrent with the successive improvements in glass fibers, POFs have

become increasingly popular, owing to their growing utility (Kaino, 1992; Nihei, et al., 1997).

Although POFs have been available for some time, only quite recently have they found application as a high-capacity transmission medium, thanks to the successive improvements in their transparency and bandwidth (Murofushi, 1996). By the end of 20th century, they are advantageously replacing copper cables in short-haul communications links by offering the advantages intrinsic to any optical fiber in relation to transmission capacity, immunity to interference and small weight. In addition, POFs serve as a complement for glass fibers in short-haul communications links because they are easy to handle, flexible, and economical, although they are not used for very long distances because of their relatively high attenuation. These characteristics make them especially suitable as a means of connection between a large net of glass optical fiber and a residential area, where distances to cover are generally less than 1 km. An example would be Internet access from home or from an office. For this purpose, POFs allowing for increasingly better features regarding distance and transmission speed have been manufactured (Murofushi, 1996)

As that have already mentioned, POFs present some important advantages over their glass counterparts. Specifically, their large diameter typically 0.25-1mm, allows low precision plastic connectors to be used, which reduces the total cost of the system. In addition, POFs stand out for their greater flexibility and resistance to impacts and vibrations, as well as for the greater coupling of light from the light source to the fiber. Because of these merits, varied applications with POFs have been developed and commercialized, from their use as a simple light transmission guide in displays to their utilization (Joseba & Jon, 2001). The following paragraphs introduce a brief view on the

mechanical properties, thermal properties, and chemical resistance for plastic optical fibers:

a) Mechanical properties for plastic optical fibers

Several authors have studied the mechanical properties of POFs. These studies have been focused on the attenuation induced by bends and tensile or torsion stresses (Blyler, 1999; Zubia, Arrue, & Mendioroz, 1997). In contrast to glass fibers, POFs are made of plastic materials. Another difference is that it is nearly two orders of magnitude lower than that of a silica fiber less than 2.1 Gpa for a PMMA POF (Blyler, 1999). For this reason, even a 1 mm diameter POF is sufficiently flexible to be installed according to typical fiber configurations. For the same reason, the minimum bend radius for POFs is smaller, since plastic is more ductile and much less stiff than silica. Similar results have been obtained for polycarbonate POFs, for which POF lies in the range between 1.55 and 2.55 Gpa (Guerrero, Guinea, & Zoido, 1998).

b) Thermal properties for plastic optical fibers

As POFs are made of polymer, they can operate at temperatures up to 80-100°C. Above this limit, POFs begin to lose their rigidity and transparency. The operation temperature can be increased up to 125°C or even to 135°C by using a jacket made of cross-linked polyethylene or of a polyolefine elastomer (Koike, Ishigure, & Nihei, 1995).

On the other hand, the resistance of POFs to high temperatures strongly depends on the degree of moisture. This behavior is due to the strong OH⁻ absorption band in the visible range. Fluorinated fibers do not absorb water, so the attenuation rate through them is not

mechanical properties, thermal properties, and chemical resistance for plastic optical fibers:

a) Mechanical properties for plastic optical fibers

Several authors have studied the mechanical properties of POFs. These studies have been focused on the attenuation induced by bends and tensile or torsion stresses (Blyler, 1999; Zubia, Arrue, & Mendioroz, 1997). In contrast to glass fibers, POFs are made of plastic materials. Another difference is that it is nearly two orders of magnitude lower than that of a silica fiber less than 2.1 Gpa for a PMMA POF (Blyler, 1999). For this reason, even a 1 mm diameter POF is sufficiently flexible to be installed according to typical fiber configurations. For the same reason, the minimum bend radius for POFs is smaller, since plastic is more ductile and much less stiff than silica. Similar results have been obtained for polycarbonate POFs, for which POF lies in the range between 1.55 and 2.55 Gpa (Guerrero, Guinea, & Zoido, 1998).

b) Thermal properties for plastic optical fibers

As POFs are made of polymer, they can operate at temperatures up to 80-100°C. Above this limit, POFs begin to lose their rigidity and transparency. The operation temperature can be increased up to 125°C or even to 135°C by using a jacket made of cross-linked polyethylene or of a polyolefine elastomer (Koike, Ishigure, & Nihei, 1995).

On the other hand, the resistance of POFs to high temperatures strongly depends on the degree of moisture. This behavior is due to the strong OH⁻ absorption band in the visible range. Fluorinated fibers do not absorb water, so the attenuation rate through them is not

altered significantly by the degree of moisture (Naritomi, 1996). High bandwidth POF also has a high thermal stability. No distortion in bandwidth is observed even after more than 10000 h of aging at 85°C (Sato, Ishigure, & Koike, 2000).

c) Chemical Resistance

Most of the work on POFs' chemical resistance deals with the behavior of POFs when they are in contact with those liquids typically found in cars. For example, polycarbonate POFs without jacket only resist 5 minutes immersed in 85-octane petrol. However, these POFs are able to withstand oil and battery liquid for a long time (Guerrero, Zoido, Escudero, & Bernabeu, 1993). The polyethylene jacket of a fiber cord serves to protect the POF when it is dipped into chemical products. When using this jacket, PMMA POFs are protected against liquids such as water, NaOH, sulfuric acid (34.6%), or engine oil. In any of such liquids, the attenuation remains constant when the coated POF is dipped into the liquid at 50°C for 1000 h. Fluorinated POFs (CYTOP), do not show changes in their attenuation when they have been dipped for 1 week into chemical acids such as 50% HF, 44% NaOH, and 98% H₂SO₄ or organic solvents such as benzene, hexane, MEK, and CCL₄ (Daum, Hoffman, & Strecker, 1994).

The continuous lighting industry progress and the perseverance of lighting designers have also allowed relying totally upon the remote lighting system to meet quantitative and qualitative lighting conditions within very spacious environments. A successful experiment has been carried out in the Congress Palace of Madrid (Djamila, 1996). Two auditoria (900 and 2000 seats) are exclusively lit by optical fibers scattered evenly in the ceilings and seeing to the standard of the design objectives required; an illumination level in accordance with the expected comfort lighting norms, a good color rendering, a

uniform lighting and a pleasant luminous internal environment. Furthermore, heat output due to lamps is extracted in the generators and therefore nuisance caused by lighting appliances is not noticeable giving hence additional satisfaction with the adoption of this system (Djamila, 1996).

The use of concentrated solar energy and its transport in optical fibres is studied by Cariou et al. (1982). Transmission properties of fibers as well as geometrical conditions of the association between fibers and concentrator were investigated. It was shown that modules where one fiber is associated with a small parabolic mirror might supply 2W with efficiency greater than 70 percent, whilst the concentration on the exit end of a 10m long fiber may exceed 3000. Such a device has been achieved and the experimental results are in good agreement with the preliminary study (Cariou et al., 1982).

2.4 Conventional solar concentrators

Sunlight holds considerable unrealized potential for application in energy efficient room lighting designs. There are currently few existing systems that efficiently utilize sunlight to provide sufficient room lighting to remote non-daylit rooms. Anidolic optics can be used for lighting of a room with an immediate daylighting aperture (Compagnon, et al., 1993; Page, et al., 2003). Recently, systems involving concentrating collectors (Beckman et al., 2003), heliostats (Pohl & Anslem, 2002), or mirror light pipes (Garcia-Hansen & Edmonds, 2003) have been developed for illumination of remote rooms. A fatal disadvantage of conventional solar concentrators is while systems using mirrors or lens may be advantageous for large-scale room lighting, they chiefly rely on

beam solar irradiation and require tracking mechanisms to avoid astigmatism and other light losses experienced during collection of solar energy so that they lose their functions in cloudy and diffuse conditions (Ries et al., 1995). Figure 2.10 presents an example of the heliostats solar concentrator and light transmission through optical fibers developed by Kandilli, et al. (2007).



Figure 2.10: one example of the heliostats solar concentrator and light transmission through optical fibers (Kandilli, et al., 2007:23)

Solar concentrators were early brought into consideration as alternative ways to reduce the cost of photovoltaic electricity and solar heat due to the relatively high material and production costs of solar cells and solar thermal absorbers. One approach is to use concentrators that increase the irradiance on the modules or absorbers and thus the electricity or heat production per unit receiver area, which in turn reduces the area needed for a given output (Maria, Anna, Bjorn, Johan, & Arne, 2004).

Concentrating systems use lenses or reflectors to focus sunlight onto the solar cells or solar thermal absorbers. High concentration of solar radiation requires tracking of the sun around one axis or two axes, depending on the geometry of the system. The higher the concentration, the more concentrator material per unit area of solar cell or thermal absorber area is generally needed. It is therefore more appropriate to use lenses than

reflectors in highly concentrating systems, because of their lower weight and material costs. Lenses, typically point-focus or linear-focus Fresnel lenses with concentration ratios of 10 – 500 are most often manufactured out of inexpensive plastic material with refracting features that direct light onto a small or narrow area of photovoltaic cells or on a linear thermal absorber. The cells are usually silicon cells. Single or mono-crystalline silicon approaches accounted for 93% of the annual cell production in 2002 (Schmela, 2003). Cells of GaAs and other compound materials have higher conversion efficiencies than silicon, and can operate at higher temperatures, but they are often substantially more expensive (Swanson, 2000). Concentrator module efficiencies range from 17% and upwards and concentrator cells have been designed with conversion efficiencies in excess of 30% (Yamaguchi & Luque, 1999; Fraas, Sundaram, Dinh, Davenport, & Yerkes, 1990). However, concentrator systems that utilize lenses are unable to focus scattered light, limiting their use to areas with mostly clear weather (Yamaguchi & Luque, 1999).

In areas with a lot of diffuse irradiation, as well as for moderate ($5 - 20\times$) and low (less than $5\times$) concentration ratios, reflectors are often more cost-effective than lenses and therefore the most common type of concentrator. Below $5\times$ concentration, it is possible to construct cost-effective static concentrators, both for photovoltaic and solar thermal systems (Whitfield, Bentley, & Burton, 1995; Hellstrom, Adsten, Nostell, Karlsson, & Wackelgard, 2003). These are mostly two-dimensional parabolic troughs or plane booster reflectors. Plane mirrors in front of the collector area increase the collected energy with 20 – 50% and reduce some of the diurnal variation (McDaniels, Lowndes, Mathew, Reynolds, & Gray, 1975). Reflectors for solar energy applications should fulfill a number of requirements (Maria et al., 2004):

- * They should reflect as much as possible of the useful incident solar radiation onto the absorbers.
- * The reflector material and its support structure should be inexpensive compared to the solar cells or thermal absorbers onto which the reflector concentrates radiation.
- * The high reflectance should be maintained during the entire lifetime of the solar collector or photovoltaic module, which is often longer than 20 years.
- * If cleaning is necessary, the surface should be easily cleaned without damaging its optical properties and the maintenance should not be expensive.
- * The construction must be mechanically strong to resist hard winds, snow loads, vibrations, etc.
- * The reflector should preferably be lightweight and easy to mount.
- * The reflector material should be environmentally benign and should not contain any hazardous compounds.
- * The visual appearance of the reflector should be aesthetical, since solar concentrators often are large and must be placed fully visible on open spaces so that the concentrator aperture is not shaded by objects in the surroundings.

The optical requirement that must be fulfilled for reflector materials in solar thermal applications is a high reflectance in the entire wavelength range of the solar spectrum (300 - 2500 nm). In lighting and photovoltaic applications, photons with lower energy than the band gap of the solar cell, which corresponds to wavelengths longer than about 1100 nm for a silicon cell, do not contribute to the photoelectric conversion but only to overheating. Hence, metals that are free electron-like are suitable as reflectors for solar thermal applications, but not optimal for lighting and photovoltaic applications. There are no known metals that combine a low reflectance in the near-infrared with a high reflectance in the ultraviolet and in the visible (Mwamburi & Roos, 2000).

Among the Drude metals, silver and aluminum are the best solar reflectors with a solar hemispherical reflectance of approximately 97% and 92%, respectively (Granqvist, 2003). Due to its lower cost, the material, which is most often used for solar reflectors today, is anodized aluminum. However, if the anodized aluminum is not protected, for example by a glazing, a plastic foil, or a lacquer, its optical performance degrades severely in only a couple of months (Bouquet, Helms, & Maag, 1987). The degradation of silver is essentially as rapid as that of aluminum (Czanderna, 1981). Due to the limited corrosion resistance of the free electron-like metals, they are often used in back surface mirrors, evaporated on the back of a glass or polymer substrate that protects the metal from oxidation. Among the state-of-the art in solar reflector materials are polymethylmethacrylate (PMMA) or back-surface-silvered low-iron glass (Schissel, Jorgensen, Kennedy, & Goggin, 1994). However, glass mirrors tend to be brittle and heavy. Front surface mirrors, on the other hand, are often bendable and of lightweight, but more susceptible to chemical attack (Roos, Ribbing, & Karlsson, 1989).

A solar reflector is not subject to the same high temperatures and thermal cycling as a solar absorber. Nevertheless, environmental conditions impose stringent demands on the material, whose surface will deteriorate more or less upon exposure to the environment. Loss of solar reflectivity can result from erosion or oxidation of the surface, dirt accumulation on the reflector, and action of cleaning agents (Duffie, 1962).

While degradation caused by accumulation of dust on the reflecting surface is essentially reversible, surface oxidation is not. The optical performance of solar reflectors thus depends on the mechanical and chemical properties of the surface and the protective coating, if such is present. For flexible reflective foils, a support of sheet

metal may be necessary, while only a simple frame construction is needed if the reflector is self-supporting, which is the case for corrugated sheets. When installing booster reflectors, the cost of the reflector material, the frame and support construction, as well as mounting and installation of the reflector must be taken into account. Maintenance should also be included in lifecycle cost (Morris, 1980).

Mora, Jaramillo, Navaa, Taguena-Martinez, & Rio (2009) reported using porous silicon photonic mirrors (PSPM) as secondary reflectors in solar concentration systems. The PSPM were fabricated with nanostructured porous silicon to reflect light from the visible range to the near-infrared region (500–2500nm), although this range could be tuned for specific wavelength applications. The PSPM are multilayer of two alternated refractive indexes (1.5 and 2.0), where the condition of a quarter wavelengths in the optical path was imposed. The PSPM were exposed to high radiation in solar concentrator equipment as shown in Figure 2.11. As a result, it observed a significant degradation of the mirrors at an approximated temperature of 900°C. In order to analyze the origin of the degradation of PSPM, it was modeled the samples with a non-linear optical approach and study the effect of a temperature increase. It concluded that the main phenomenon involved in the breakdown of the photonic mirrors is of thermal origin, produced by heterogeneous expansion of each layer (Mora, et al., 2009).

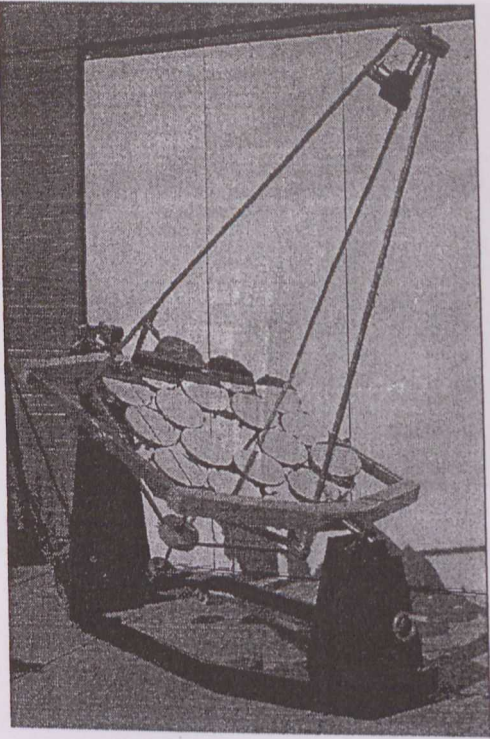


Figure 2.11: DEFAC-Spanish acronym of device for the study of highly concentrated radioactive fluxes (Éstrada, Jaramillo, & Acosta, 2007: 1308)

Poulek & Libra (2000) developed a tracking ridge concentrator using proven tracker hardware. This system combines simple low-cost tracker with flat booster mirrors but unlike V-trough concentrator (Klotz, 1995; Nann, 1991) by the new ridge concentrator the mirror has been eliminated as shown in Figure 2.12. On single axis trackers, both horizontal and polar, the mirrors have to be extended beyond PV panels to ensure uniform illumination of panels at seasonally variable elevation of the sun. On polar axis trackers with seasonally adjustable slope of the axle the extended mirror is not needed. Unlike V-trough concentrators, no additional mirror supporting structures are needed. However, it could only double solar energy gain of PV panels in comparison with fixed ones (Poulek & Libra, 2000).

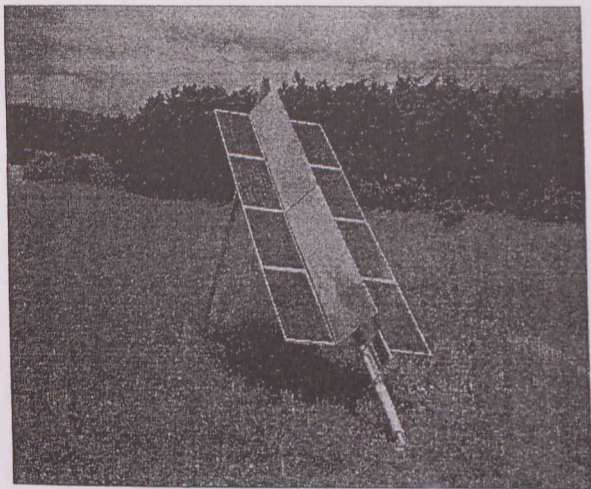


Figure 2.12: photograph of the polar axis tracking ridge concentrator with 8*55 Wp PV panels (Poulek & Libra, 2000:201)

To obtain cost-effective photovoltaic modules, Uematsu et al. (2001) have developed static prism-array concentrator modules consisting of prism concentrators about 4mm thick assembled unidirectional under a 3.2-mm-thick cover glass as shown in Figure 2.13. Calculating the optical collection efficiency for the annual solar irradiation in Tokyo, it found that the theoretical efficiency of the modules is 94.4% when the geometrical concentration ratio is 1.88 and that it is 89.1% when that ratio is 2.66, respectively. Fabricating prism-array-concentrator modules with a geometrical concentration ratio of 2.66, it only obtained a maximum optical collection efficiency of 82% with a flat reflector and 81.7% with a V-grooved reflector (Uematsu et al., 2001).

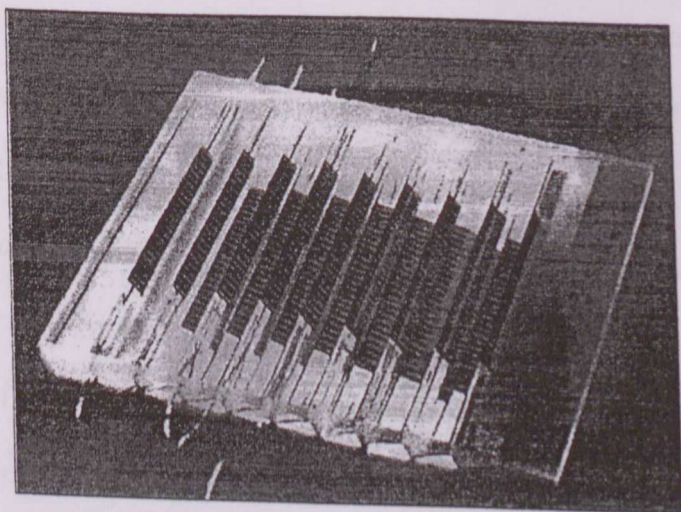


Figure 2.13: photograph of a static prism-array concentrator module (Uematsu et al., 2001:420)

on the following principle. One or more high quantum yield species are dissolved in a

In order to remove the trackers, a static solar concentrator is proposed by Masato & Toshiro (2005) to match the aesthetic features of towns. The concentrator consists of vertical plate solar cells and white/transparent switchable bottom plate, which is operated with external power. The bottom is switched to be a diffuse reflection white surface when the cell generates electric power, and switched to be a light transmissible transparent surface when the cell does not deliver power. The light collection of this concentrator was analyzed by using multiple total internal reflection model and ray tracing simulation. However, the results are not significantly satisfying for a static solution for solar concentration (Masato & Toshiro, 2005).

2.5 Luminescent solar concentrator (LSC)

The luminescent planar solar concentrator was proposed in the late 1970s (Weber & Lambe, 1976; Goetzberger & Greubel, 1977; Rapp & Boling, 1978) consisting of a transparent plastic sheet doped with organic dyes. Sunlight is absorbed by the dye and then re-radiated isotropically, ideally with high quantum efficiency, and trapped in the sheet by internal reflection. A stack of sheets doped with different dyes can separate the light. Solar cells can be chosen to match the different luminescent wavelengths to convert the trapped light at the edge of the sheet (Goetzberger & Greubel, 1977).

Luminescent solar concentrators (LSCs) have attracted the attention of a large number of scientists and engineers since the first proposal by Weber and Lambe (1976). The operation of the LSC, which can be considered as a peculiar kind of light guide, is based

on the following principles. One or more high quantum yield species are dissolved in a rigid highly transparent medium of high refractive index. Solar photons entering the plate are absorbed by the luminescent species and reemitted in random directions. Following Snell's law, a large fraction of the emitted photons will be trapped within the plate and transported by total internal reflections to the edge of the plate, as illustrated in Figure 2.14 and Figure 2.15, where they will be converted by appropriate photovoltaic cells (Richards, 2006; Reisfeld, 2001; Batchelder et al., 1979; Hammam et al., 2007)

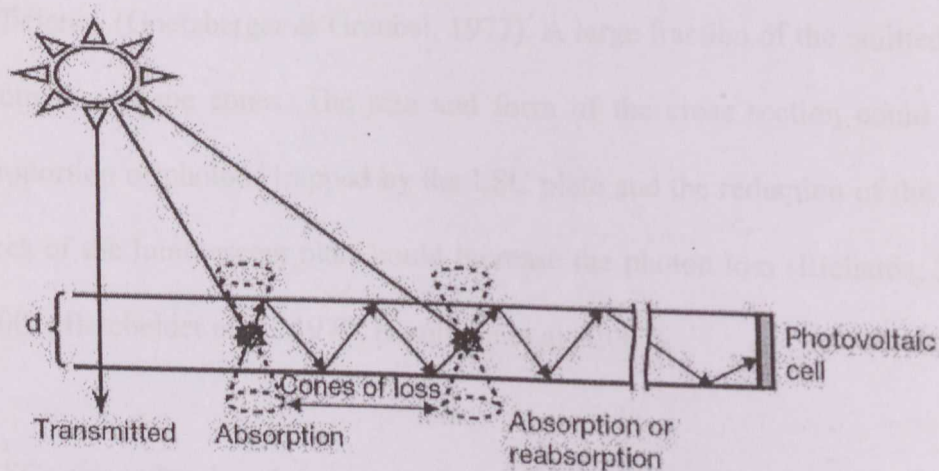


Figure 2.14: schematic representation of luminescent solar concentrator (LSC) (Hammam et al., 2007:245)

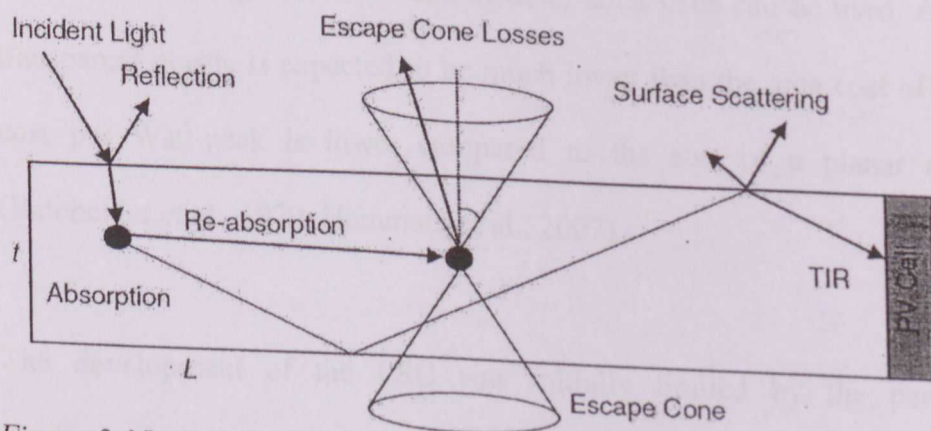


Figure 2.15: more in detailed example of schematic representation of luminescent solar concentrator (LSC) (Richards, 2006:2335)

Conversion of the incident solar spectrum to monochromatic light would greatly increase the efficiency of solar cells. Since LSC were proposed in 1970s, solar cells were attached to it. LSCs consist of a highly transparent plastic, in which luminescent species, originally organic dye molecules, are dispersed. These dyes absorb incident light and isotropically emit it at a red-shifted wavelength, with high quantum efficiency. Internal reflection ensures collection of part of the emitted light in the solar cells at the sides of the plastic body. The energy of the emitted photons ideally is only somewhat larger than the band gap of the attached solar cells, to ensure near-unity conversion efficiency (Goetzberger & Greubel, 1977). A large fraction of the emitted photons loses from the escape cones. The size and form of the cross section could impact on the proportion of photons trapped by the LSC plate and the reduction of the cross sectional area of the luminescent plate could increase the photon loss (Richards, 2006; Reisfeld, 2001; Batchelder et al., 1979; Hammam et al., 2007).

LSCs were developed as an alternative approach to lower the costs of PV. As both direct and diffuse light is concentrated by a factor of 5-10, without the need for expensive tracking, smaller silicon or other solar cells can be used. As the cost of the transparent plastic is expected to be much lower than the area cost of the solar cell the cost per Watt-peak is lower compared to the cost of a planar silicon solar cell (Batchelder et al., 1979; Hammam et al., 2007).

The development of the LSC was initially limited by the performance of the luminescent dyes available some decades ago. Nevertheless, efficiencies of up to 4% have been reported for a stack of two plates ($40\text{cm} \times 40\text{cm} \times 0.3\text{cm}$), one being coupled to a GaAs solar cell, and the other to a Si solar cell (Wittwer, Stahl, & Goetzberger, 1984). Particular problems were the poor stability of the dyes under solar irradiation and

the large re-absorption losses owing to significant overlap of the absorption and emission. Within the fullspectrum project (Luque et al., 2005) the performance of both quantum dots and organic dyes are being evaluated as the luminescent species in the LSC. The important characteristics of organic dyes are that they: (i) can provide extremely high luminescence quantum efficiency (near unity), (ii) are available in a wide range of colours and, (iii) new molecular species are now available with better re-absorption properties that may also provide the necessary UV stability. quantum dots have advantages over dyes in that: (i) their absorption spectra are far broader, extending into the UV, (ii), their absorption properties may be tuned simply by the choice of nanocrystal size, and (iii) they are inherently more stable than organic dyes. Moreover, (iv) there is a further advantage in that the red-shift between absorption and luminescence is quantitatively related to the spread of quantum dot sizes, which may be determined during the growth process, providing an additional strategy for minimizing losses due to re-absorption (Barnham, Marques, Hassard, & Brien, 2000). However, as yet quantum dots can only provide reasonable luminescence quantum efficiency: luminescence quantum efficiency more than 0.8 has been reported for core-shell quantum dots (Peng, Schlamp, Kadavanich, & Alivisatos, 1997).

Advantages over geometric luminescent concentrators include that solar tracking is unnecessary and that both direct and diffuse radiation can be collected and, in addition, the sheets are inexpensive. However, the development of this promising concentrator was limited by the stringent requirements on the luminescent dyes, namely high quantum efficiency, suitable absorption spectra and red shifts and stability under illumination (Goetzberger, Stahl, & Wittwer, 1985; Wittwer, Goetzberger, Heidler, & Zastrow, 1981). Concentration ratios of $10\times$ were achieved (Goetzberger et al., 1985; Wittwer et al., 1981). A typical measured electrical efficiency with a two-stack

concentrator with GaAs solar cells was 4% (Goetzberger et al., 1985; Wittwer et al., 1981), whereas the original predictions were in the range 13 – 23% (Goetzberger & Greubel, 1977).

Barnham et al. (2000) have proposed a novel concentrator in which the dyes are replaced by quantum dots. The first advantage of the quantum dots over dyes is the ability to tune the absorption threshold simply by choice of dot diameter. For example, colloidal InP quantum dots, separated by dot size, have thresholds, which span the optical spectrum (Micic et al., 1997). Secondly, high luminescence quantum efficiency has been observed. CdSe/CdS hetero-structure dots have demonstrated luminescence quantum yields of above 80% at room temperature. Thirdly, since they are composed of crystalline semiconductor, the dots should be inherently more stable than dyes (Chattena, Barnhama, Buxtonb, Ekins-Daukesa, & Malik, 2003).

The disappointing results obtained with dye concentrators were probably mainly because of re-absorption, which was considered, but not modeled at the time of the original calculations (Goetzberger & Greubel, 1977). Barnham et al. (2000) have argued that there is a further advantage in that the red shift between absorption and luminescence is quantitatively related by the thermodynamic model to the spread of quantum dot sizes, which can be determined during the growth process. The ability to limit the overlap between the luminescence and absorption by the choice of quantum dot size distribution is a significant improvement compared to dye concentrators (Micic, Curtis, Jones, Nozik, & Sprague, 1994).

Goldschmidt et al. (2009) demonstrated how the collection efficiency of fluorescent concentrator systems is increased by two independent measures. One approach is to

combine different dyes to enlarge the used spectral range. A system using the combination of two materials had an efficiency of 6.7%. The other approach is to increase the collection efficiency by the application of a photonic structure, which acts as a band stop reflection filter in the emission range of the dye. A relative efficiency increase of 20% with a commercially available filter was achieved. With the achieved efficiency of 3.1% and concentration ratio of 20, the realized fluorescent concentrator produces about 3.7 times more energy than that of the used GaInP solar cell produced on its own. Photonic structures are especially beneficial for larger systems. Goldschmidt et al. (2009) clarified the role of a white bottom reflector and its interaction with the photonic structure. The white bottom reflector increases the efficiency by two mechanisms. It increases the absorption of light in the fluorescent concentrator as it reflects non-absorbed light back into the fluorescent concentrator and it directly reflects light towards the solar cells. The second mechanism is especially important for small distances from the solar cell (Goldschmidt et al., 2009).

An LSC daylighting system has been produced by Earp, et al. (2004), which transports sunlight to remote areas of a building using a stack of pink, green and violet LSCs and clear PMMA (poly methyl methacrylate) light guides. In direct sun of intensity 100,000 LUX, prototypes with collector area of $1.2\text{m} \times 0.135\text{m} \times 0.002\text{m}$ deliver 1000 lumen of near-white light with a luminous efficacy of 311 lm/W and a light-to-light efficiency up to 6%. The light-to-light efficiency of the violet sheet is 0.29% and that of the green sheet is 5.8%. The light-to-light efficiency of the pink sheet is 1.5%. Surface effects such as excess adhesive and variations in flatness are thought to be causing unnecessary light loss, which can be avoided by careful LSC production (Earp, et al., 2004). A limitation in the wiring for long distance light transportation has emerged in this LSC system.

2.6 Fluorescent fiber and its usual applications

Although the fluorescent fiber have not experienced the dramatic commercial success for communications and lighting purposes, they have been continuously and enthusiastically studied. (Udd, 2002; Beller, 1998; Sorin, 1998). Fluorescent fibers are often used in radiation protection and measuring devices. Their working principle is similar as luminescent fibers. The fluorescent material absorbs high-energy alpha, beta and gamma radiation and converts that energy into forms that can be measured by conventional visible light detectors. Optical fiber sensors have unique advantages such as high sensitivity, immunity to electromagnetic interference (EMI), small size, lightweight, robustness, and the ability to provide multiplexed or distributed sensing (Peng & Chu, 2002). Since fluorescent fibers have not achieved a success in commercialization, there was hardly found any record for fluorescent fibers' application in remote indoor day-lighting purpose.

It has been reported that thin luminescent concentrator films could be implemented in the form of integrated devices or as sensitive elements in the traditional four-detector differential position sensors (Evenson & Rawicz 1995; Melnik & Rawicz, 1997).

Various ideas have been developed for applications (Yu & Yin, 2002; Grattan & Meggitt, 1998; Grattan & Meggitt, 1999; Othonos & Kalli, 1999; Marazuela & Moreno-Bondi, 2002). To date, some types of optical fiber sensors have been commercialized, but it is also true that, among the various techniques that have been

studied, only a limited number of techniques and applications have been commercially successful. Optical fiber sensors have advantages such as immunity to EMI, lightweight, small size, high sensitivity, large bandwidth, and ease in signal light transmission. However, in many fields of application, optical fiber sensors should compete with other rather mature technologies such as electronic measurements. To appeal to users already accustomed to other mature technologies, the superiority of optical fiber sensors over other techniques needs to be clearly demonstrated. Typical users are not interested in specific techniques involved in measurement. They simply desire sensor systems having good performances with reasonable price except for very special uses. Hence, optical fiber sensor systems should be available in the form of complete systems including detecting and signal-processing electronics. In some cases such as electric protection relaying systems, the sensor systems are simply subsystems of rather larger systems. In some cases such as optical gyroscopes and optical current sensors, the optical fiber sensors should compete with other optical bulk sensors as well. Even with these difficulties, considerable efforts have been made to study of optical fiber sensors, and some of them are now nearing maturity (Yu & Yin, 2002; Grattan & Meggitt, 1998; Grattan & Meggitt, 1999; Othonos & Kalli, 1999; Marazuela & Moreno-Bondi, 2002). Some applications of optical fibers as fiber grating sensor, fiber-optic gyroscopes (FOGs), fiber-optic current sensors, and other sensors are briefly discussed below:

a) Fiber grating sensors

Although the formation of fiber gratings had been reported in 1978 (Hill, Fujii, Johnson, & Kawasaki, 1978), intensive study on fiber gratings began after a controllable and effective method for their fabrication was devised in 1989 (Meltz, Morey, & Glenn, 1989). Fiber gratings have been applied to add/drop filters, amplifier gain flattening filters, dispersion compensators, and fiber lasers and so on for optical communications.

studied, only a limited number of techniques and applications have been commercially successful. Optical fiber sensors have advantages such as immunity to EMI, lightweight, small size, high sensitivity, large bandwidth, and ease in signal light transmission. However, in many fields of application, optical fiber sensors should compete with other rather mature technologies such as electronic measurements. To appeal to users already accustomed to other mature technologies, the superiority of optical fiber sensors over other techniques needs to be clearly demonstrated. Typical users are not interested in specific techniques involved in measurement. They simply desire sensor systems having good performances with reasonable price except for very special uses. Hence, optical fiber sensor systems should be available in the form of complete systems including detecting and signal-processing electronics. In some cases such as electric protection relaying systems, the sensor systems are simply subsystems of rather larger systems. In some cases such as optical gyroscopes and optical current sensors, the optical fiber sensors should compete with other optical bulk sensors as well. Even with these difficulties, considerable efforts have been made to study of optical fiber sensors, and some of them are now nearing maturity (Yu & Yin, 2002; Grattan & Meggitt, 1998; Grattan & Meggitt, 1999; Othonos & Kalli, 1999; Marazuela & Moreno-Bondi, 2002). Some applications of optical fibers as fiber grating sensor, fiber-optic gyroscopes (FOGs), fiber-optic current sensors, and other sensors are briefly discussed below:

a) Fiber grating sensors

Although the formation of fiber gratings had been reported in 1978 (Hill, Fujii, Johnson, & Kawasaki, 1978), intensive study on fiber gratings began after a controllable and effective method for their fabrication was devised in 1989 (Meltz, Morey, & Glenn, 1989). Fiber gratings have been applied to add/drop filters, amplifier gain flattening filters, dispersion compensators, and fiber lasers and so on for optical communications.

Extensive studies have also been performed on fiber grating sensors and some of which have now reached commercialization stages (Othonos & Kalli, 1999).

b) Fiber-optic gyroscopes

It is generally recognized that the first demonstration of the FOG was achieved 33 years ago by Vali & Shorthill (1976), though there had been a few previous studies. The basic concept is based on the Sagnac interferometer and is quite simple. It is a good example of an application of special relativity. For a rotating optical fiber coil, two lights traveling in opposite directions in the coil experience different lengths, which results in different travel times and a phase difference in the two optical waves (Vali & Shorthill, 1976).

c) Fiber-optic current sensors

With the growth in the capacity of electric power systems, the role of protection relaying systems is becoming more important. Such a system can immediately recognize any sudden failures, such as a surge, and separate the failure parts from the power systems. These relaying systems require current sensors, referred to as current transformers or current transducers. Most current transducers currently in use are electromagnetic devices that suffer from magnetic saturation effects and residual field effects. Moreover, with the super increase in voltages (several hundred kV) in power distribution systems, the insulation of the current transducers becomes more difficult and expensive. Hence, optical current sensors that do not suffer from electromagnetic interference are good substitutes for conventional current transducers. In addition to protection relaying systems, the deregulation and growth of independent power producers and regional transmission companies have created a need for many new high voltage revenue-metering points (Sanders, Blake, Rose, Rahmatian, & Herdman, 2002).

In the transfer of power from a generation company to a regional transmission company, a 0.5% uncertainty in metering may result in an uncertainty of millions of dollars per year at a high power metering location. Hence the potential use of optical current transducers that provide high accuracy is promising (Sanders et al., 2002).

d) Others

Some other types of optical fiber sensors based on very simple concepts have been commercialized. Some examples include the displacement or pressure sensor based on the light coupling of two fibers, the liquid-level sensor based on frustrated total internal reflection, the pressure sensor using a wiggled (periodically bent) fiber, and the temperature sensor based on the detection of radiation from a heated sensor head (blackbody cavity) (Udd, 2002).

One of the most well-developed and commercialized in-line fiber sensors or diagnostic tools is Optical Time Domain Reflectometry (OTDR), which is based on the monitoring of the backscattering along the fiber. The concept is also quite old (Barnoski & Jensen, 1976) and the OTDR has become a standard technique for testing optical fiber links (Beller, 1998). It typically provides sub-meter spatial resolution but improved techniques can provide mm-order resolution. More complicated methods such as optical frequency domain reflectometry have been studied to achieve or sub-millimeter ($\sim 10 \mu\text{m}$) spatial resolution (Sorin, 1998).

While OTDRs are generally aimed at monitoring optical fiber communication links, active research has also been done on distributed sensors for civil structure monitoring. One example is a distributed temperature sensor for monitoring concrete setting temperatures of a large dam (Thevenaz et al., 1999). The principle is based on the

stimulated Brillouin scattering. An acoustic wave couples two counter-propagating beams, which are frequency-shifted by an amount that is dependent on temperature or strain. A commercialized distributed temperature and strain monitoring system shows the measurement range of up to 20 km with a spatial resolution of 0.8 m over 1 km (2–5 m at 10 km and 5–15 m at 20 km), a strain resolution of $20 \mu \epsilon$ (measurement range of up to $25 m \epsilon$) and a temperature resolution of 1°C (Thevenaz et al., 1999).

Optical fiber acoustic sensors or optical fiber hydrophone systems have also been intensively studied and tested for marine or submarine applications (Peng & Chu, 2002). Fiber-optic low coherence interferometer has also been commercialized for civil applications (Inaudi & Casanova, 2002). The dynamic range of the commercialized deformation sensor using the method is of the order of a few tens of $m \epsilon$ for elongation ($\sim 5 m \epsilon$ for shortening) (Thevenaz et al., 1999).

Cryogenic temperature sensing is also an attractive field for fiber-optic sensors (Lee & Lee, 2002). Fiber-optic chemical sensors or biosensors have been continuously studied. The principles are based on the monitoring of absorbance, reflectance, luminescence, reflective index change, or light scattering and aimed at the measurement of oxygen, pH, carbon dioxide, ammonia, detergents, biochemical oxygen demand, pesticides, and humidity (Marazuela & Moreno-Bondi, 2002; Orellana & Moreno-Bondi, 2002). In many cases optical fibers are simply used to guide light to the measurement point in the specimen. In some cases optical fibers are monitoring the response of a material deposited on the end of the fiber (Arregui, Galbarra, Matias, Cooper, & Claus, 2002). In some other cases well-developed sensor technologies such as FBG temperature sensors have been used for biological tests (Webb et al., 2000).

A good example of optical fiber chemical sensors in which the fiber itself plays a key role in the measurement is the use of LPGs (James, Rees, Tatam, & Ashwell, 2002; Allsop, Webb, & Bennion, 2002). An LPG can couple the core mode to a cladding mode. If the coating or jacket is removed from the optical fiber, the evanescent field of the cladding mode that exists outside the cladding experiences the refractive index change of the outside material. The sensitivity can be adjusted by fiber etching (Kim, Jeong, Kim, Kwon, Park, & Lee, 2000).

2.7 Summary

This chapter has introduced the daylighting related devices such as light pipes (or tubular daylight guidance systems), optical fibers for light transport, conventional solar concentrators, and luminescent solar concentrators (LSC). The common applications of fluorescent fibers have also been reviewed in this chapter since their application for remote indoor daylighting purpose has not been found in literatures. The principles of work, advantages and disadvantages for application of these daylighting related devices have been explained. Daylight has a disadvantage of not being able to reach deeper areas in a building such as storerooms, basements, and corridors, and it also brings the heat gain with the light. Light pipes and optical fibers were expected to transfer daylight to unreached areas, but light pipes have their difficulties in wiring and the optical fiber needs a pointolite for the light transportation. Solar concentrators are only sensitive for the beam radiation and they function poorly in overcast sky conditions. Even under a clear sky condition, trackers are always needed for conventional solar concentrators. Static concentrators always come with a poor concentration rate without a tracker, and

the light concentrated by normal luminescent solar concentrators could not be transported by optical fibers to a remote place since the light produced by LSCs is not a pointolite.

Chapter 3

The objectives of this research are determined based on the problems identified during the literature review as discussed in Chapter 3. The explanation on the need for FFSC as presented in Chapter 4 is based on the limitations of daylighting related devices as identified through the literature review. The next chapter, Chapter 3, provides a discussion on the research methodology of this study.

Chapter 3

Research Methodology

3.1 Overview of research process

In this chapter, the research methodology is discussed. This research starts with a literature review on daylighting related devices. The principles of work, advantages and disadvantages for application of these daylighting related devices have been studied. To seek for an alternative way in mitigating the limitations relevant in the studied devices, a new concept, which is to use fluorescent fibers for solar concentration and to use clear optical fiber bundles to transport the absorbed daylight into a target area for remote indoor daylighting purpose, is proposed and developed by the author. Accordingly, a new device named “fluorescent fiber solar concentrator” (FFSC) is designed and fabricated in this study based on the concept. The details about the design are explained in Chapter 4. To assess the performance of the fabricated new device for remote indoor daylighting purposes, the FFSC was mounted on a University building and a 6-month trial run was conducted for it. The detailed experimentation procedures and instrumentation are discussed in Chapter 5. Figure 3.1 illustrates the steps that have been made in the research.

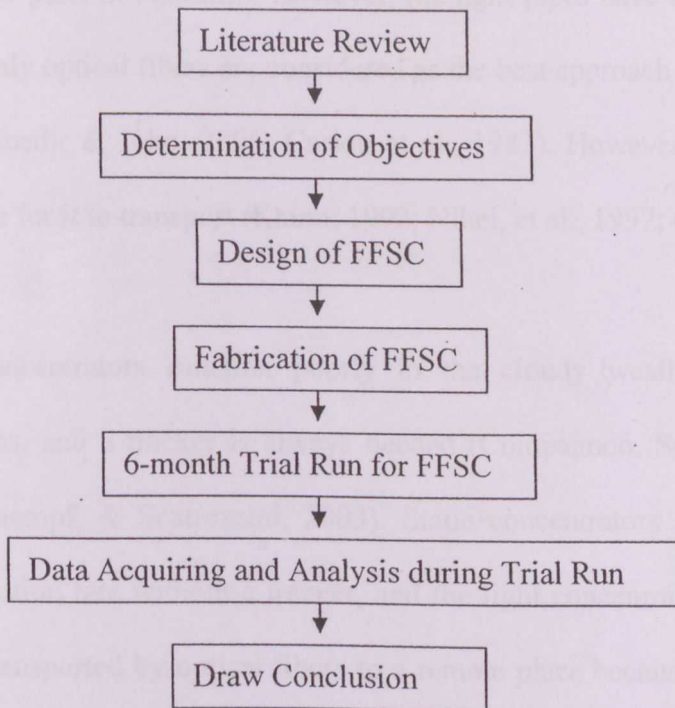


Figure 3.1: overview of research process

3.2 Determination of objectives

Objectives are the breakdown of the aim, which focuses on searching out or establishing certain issues, which will directly achieve the aim in the ultimate stage (Creswell, 1994; Fellows & Liu, 2003). Objectives of this research are raised based on the problems identified during the literature review. In solar energy applications, various methods have been developed to collect, concentrate, transport, store, and convert solar irradiation. However, there are many limitations relevant in such devices, such as the strict dependence on beam irradiation and the difficulties for wiring (Enedir & John, 2006; Cariou et al., 1982). Daylight may not be able to reach many areas such as store rooms, basements, and corridors. It also brings heat gain with the light (Bouchet &

Fontoynt, 1996; Shao et al., 1998). Light pipes were designed to transport daylight to the deeper parts in buildings. However, the light pipes have their difficulties for wiring so that only optical fibers are considered as the best approach for daylight transportation so far (Enedir & John, 2006; Cariou et al., 1982). However, an optical fiber needs a pointolite for it to transport (Kaino, 1992; Nihei, et al., 1997; Cariou et al., 1982).

Solar concentrators function poorly in the cloudy weather and the diffuse light conditions, and a tracker is always needed (Compagnon, Scartezzini, & Paule, 1993; Page, Kaempf, & Scartezzini, 2003). Static concentrators always come with a poor concentration rate without a tracker, and the light concentrated by normal LSCs could not be transported by optical fibers to a remote place because the light produced by an LSC is not a pointolite (Compagnon, et al., 1993; Page, et al., 2003; Beckman et al., 2003; Kandilli, Ulgen, & Hepbasli, 2007). An alternative way to mitigate the limitations inherited in the present daylighting related devices is needed to be proposed. Accordingly, the author proposed a new concept, which is to use fluorescent fibers for solar concentration and to use clear optical fiber bundles to transport the concentrated daylight into a target area for the remote indoor daylighting purpose. The objectives of this research are therefore determined as follows:

- a) to identify the working principles and to extract the limitations of the present daylighting related devices, and
- b) to develop a new concept to avoid or to mitigate the limitations of the present daylighting related devices and to fabricate a device based on the new concept, and

c) to assess the performance of the fabricated new device for remote indoor daylighting purposes through its trial run.

3.3 Qualitative and quantitative research

It is appropriate to define the classification of the approaches for obtaining data. Some commonly applied research strategies are proposed by Denscombe (1998), namely: survey, case study, experiment, and action research. The above-mentioned research strategies can be classified as the quantitative research and the qualitative research (Denscombe, 1998). Quantitative research has an enquiry arising based on the hypothesis tested or a theory variable. It is a measurable statistical approach to determine whether or not the particular theory holds true (Creswell, 1994; Melville, 1996). Creswell (1994) describes that the quantitative research deals with countable, tangible and solid data that can be recorded easily as documentation. In a quantitative research, the measurement must be objective, quantitative, and statistically valid, and it is about numbers and objective hard data (Creswell, 1994; Bouma, Atkinson & Dixon, 1995).

Likewise, qualitative research focuses more on one's professionalisms, knowledge, experiences and it is subjective in nature (Melville, 1996; Creswell, 1994). It requires a wide range of explanatory format of discussion in obtaining the descriptive data. Qualitative research is collecting, analyzing, and interpreting data by observing what people do and say. Whereas, quantitative research refers to counts and measures of things, but qualitative research refers to the meanings, concepts, definitions, characteristics, metaphors, symbols, and descriptions of things (Creswell, 1994).

Qualitative research is much more subjective than quantitative research and it uses very different methods of collecting information. The nature of this type of research is exploratory and open-ended (Melville, 1996; Neuman, 2003; Bouma et al., 1995).

Basically, quantitative research is objective and qualitative research is subjective. Quantitative research seeks explanatory laws; qualitative research aims at in-depth description. Qualitative research measures what it assumes to be a static reality in hopes of developing universal laws. Qualitative research is an exploration of what is assumed to be a dynamic reality. It does not claim that what is discovered in the process is universal, and thus, replicable (Creswell, 1994; Melville, 1996; Bouma et al., 1995).

In this research, both the qualitative approach and the quantitative approach are employed. The new concept development process is based on the author's professionalisms, knowledge, and experiences and it is subjective, exploratory and open-ended in nature. According to Creswell (1994) and Melville (1996), the new concept development is a process of qualitative research. The detailed description of the new concept development and the new device design is provided in Chapter 4.

After the new concept is developed, a device named FFSC is fabricated accordingly. A 6-month trial run is conducted to assess the performance of the fabricated device for remote indoor daylighting purposes. The data acquired during this process is countable, tangible and solid that can be recorded easily as documentation. According to Creswell (1994) and Melville (1996), the process of FFSC trial run is classified as quantitative research. Therefore, the research conducted by the author is a combination of the qualitative research and the quantitative research. The detailed explanation on the experimentation procedures and instrumentation is presented in Chapter 5.

(d) Instrumental Research

There are four types of quantitative research classified by the goals, namely: the exploratory research, the descriptive research, explanatory research, and instrumental research (Eng, 2007; Neuman, 2003; Fellows & Liu, 2003). The definitions of these types were explained in below:

a) Exploratory Research

Become familiar with the basic facts, setting and concerns. Create a general mental picture of conditions. Formulate and focus questions for future research. Generate new ideas, conjectures, or hypotheses. Determine the feasibility of conducting research. Develop techniques for measuring and locating future data (Neuman, 2003:29).

b) Descriptive Research

Provide the detailed, highly accurate picture. Locate new data that contradict past data. Create a set of categories or classify types. Clarify a sequence of steps or stages. Document a causal process or mechanism. Report on the background or context of a situation (Neuman, 2003:29).

c) Explanatory Research

Test a theory's predictions or principle. Elaborate and enrich a theory's explanation. Extend a theory to new issues or topics. Support or refute and explanation or prediction. Link issues or topics with a general principle. Determine which of several explanations is best (Neuman, 2003:29).

d) Instrumental Research

Construct/Calibrate research instruments, whether physical measuring equipment or as tests/data collection. In such situations the construction of instruments and data measurement in terms of meaning which renders the activity of scientific research. The evaluation will be based on theory (Fellows & Liu, 2003:11).

The quantitative process conducted by the author in the research is a combination of the types (c) and (d). After the new concept is generated and a device named FFSC is fabricated based on the concept, a 6-month trial run is conducted to test the performance of the fabricated new device. Many instruments such as the pyranometers, the LUX sensor, the spectrometer, and the data logger are calibrated and employed during the trial run. According to Neuman (2003) and Fellows & Liu (2003), this is classified as both (c) explanatory research and (d) instrumental research.

According to Neuman (2003), the process of the 6-month trial run is neither an exploratory research nor descriptive research because there is no general mental picture of conditions created during the trial run, there is no new data located to contradict past data, and there are no categories created or new types classified. There is no sequence of steps or stages clarified. No causal process or mechanism is documented. No background or context of a situation is reported.

In sum, the research conducted by the author is a combination of the qualitative research and the quantitative research. During the quantitative process, it combines the explanatory research and the instrumental research.

Chapter 4

Design of Fluorescent Fiber Solar Concentrator (FFSC)

4.1 The need for fluorescent fiber solar concentrator (FFSC)

In building integration, one of the important features of remote light transportation is the wiring method, and the wiring method is expected to be as simple as that of electrical wires (Enedir & John, 2006; Cariou et al., 1982). As discussed in Chapter 2, only optical fibers are competent for this requirement. For instance, an LSC developed by Earp, et al. (2004) is transported by polymer sheets instead of the optical fibers because the light produced by the LSC is not a pointolite. The polymer sheets have a disadvantage in wiring, which brings difficulties in building integration. It is also not energy-efficient to further concentrate the rectangular light produced by the LSC into a pointolite for the transportation through optical fibers to a remote place in a building. Such a problem is expected to be solved by an alternative method, such as the developed FFSC system.

Figure 4.1 illustrates the needs to develop FFSC. In Figure 4.1, there are two groups of solutions that are practised in the building sector for general energy issues, namely: the building energy saving approaches and the renewable energy application approaches, which are presented in the left branch and the right branch, respectively.

According to the left branch shown in Figure 4.1, as an approach for energy saving, daylight has a disadvantage of not being able to reach many areas of a building such as store rooms, basements, and corridors, and it also brings heat gain with the light (Bouchet & Fontoynt, 1996; Shao et al., 1998). Light pipes were designed to transport daylight to unreached areas, but light pipes have their difficulties for wiring, so that optical fibers are considered as the best approach for the daylight transportation so far. However, the optical fiber needs a pointolite for the light transportation. An alternative device, such as the FFSC is designed to fulfill this requirement.

The right branch in Figure 4.1 shows various solar concentrators that were designed using optical approaches such as using mirrors or lens for the solar energy concentration. Since they are only sensitive for the beam irradiation, they function poorly in the cloudy weather and the diffuse light conditions, and even if they are under a clear sky condition, trackers are always needed. Luminescent solar concentrators (LSC) and some static solar concentrators were then designed as the diffuse light solution and the static solution, respectively. Static concentrators always come with a low concentration rate without a tracker, and the light concentrated by normal LSCs could not be transported by optical fibers to a remote place since the light produced by an LSC is not a pointolite. The FFSC is expected to solve this problem as well.

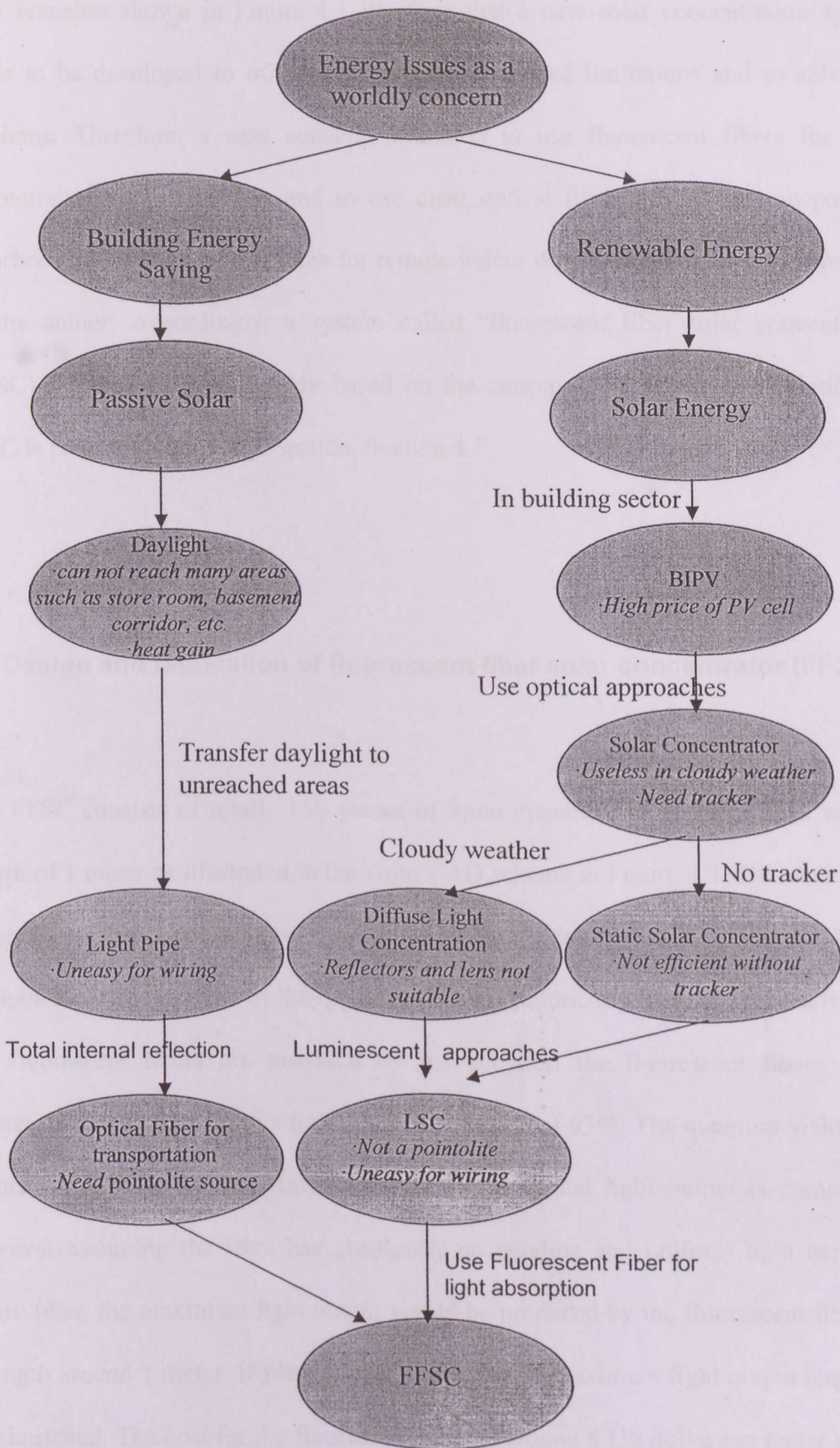


Figure 4.1: from energy issues to solar applications: the needs for FFSC (concept developed by author)

Both branches shown in Figure 4.1 illustrate that a new solar concentration system needs to be developed to mitigate the above-mentioned limitations and to solve the problems. Therefore, a new concept, which is to use fluorescent fibers for solar concentration and absorption and to use clear optical fiber bundles to transport the absorbed daylight into a target area for remote indoor daylighting purpose, is developed by the author. Accordingly, a system called “fluorescent fiber solar concentrator” (FFSC) is designed in this study based on the concept. The detailed description for FFSC is presented in the next section, Section 4.2.

4.2 Design and fabrication of fluorescent fiber solar concentrator (FFSC)

The FFSC consists of totally 150 pieces of 2mm diameter fluorescent fibers with the length of 1 meter as illustrated in the Auto CAD schema in Figure 4.2. The material for these fluorescent fibers is acrylic with quantum dots seeded in them. Detailed composition and structure of the quantum dots are proprietary, but the characteristics of the fluorescent fibers are provided by the supplier: the fluorescent fibers have a refractive index of 1.49 and a light transmission rate of 93%. The quantum yields of all colors range from 0.8-1.0. Relation between length and light output is complicated, however assuming the fiber has absolutely no bending and uniform light across the entire fiber, the maximum light output would be produced by the fluorescent fiber with a length around 1 meter. If fiber is coiled or bent, the maximum light output length will be shortened. The cost for the fluorescent fiber is around 6 US dollar per meter in 2007. The cost for the clear fiber is around 1 US dollar per meter in 2007.

The 150 pieces of fluorescent fibers consist of three colors (green, red, and yellow) as shown in Figure 4.3. There are 50 pieces for each color. The total 150 pieces of fluorescent fibers are symmetrically embedded in a 1200mm×1200mm Poly Methyl Methacrylate (PMMA) plate with a space of 2mm between each two pieces of fibers. The Auto CAD schema of FFSC is provided in Figure 4.2. The detail drawing of “Detail 1” in Figure 4.2 is illustrated in Figure 4.2a. The section view of “A-A” is shown in Figure 4.2b. The scaled drawings of FFSC are provided in APPENDIX C.

At both edges of the FFSC plate, each fluorescent fiber is connected with a 10m long 2mm diameter PMMA clear optical fiber by an aluminum bushing and fixed by a type of UV glue as shown in Figure 4.2a. The light absorbed by the fluorescent fibers is therefore transported by these clear fibers to a remote place for lighting or power production purposes.

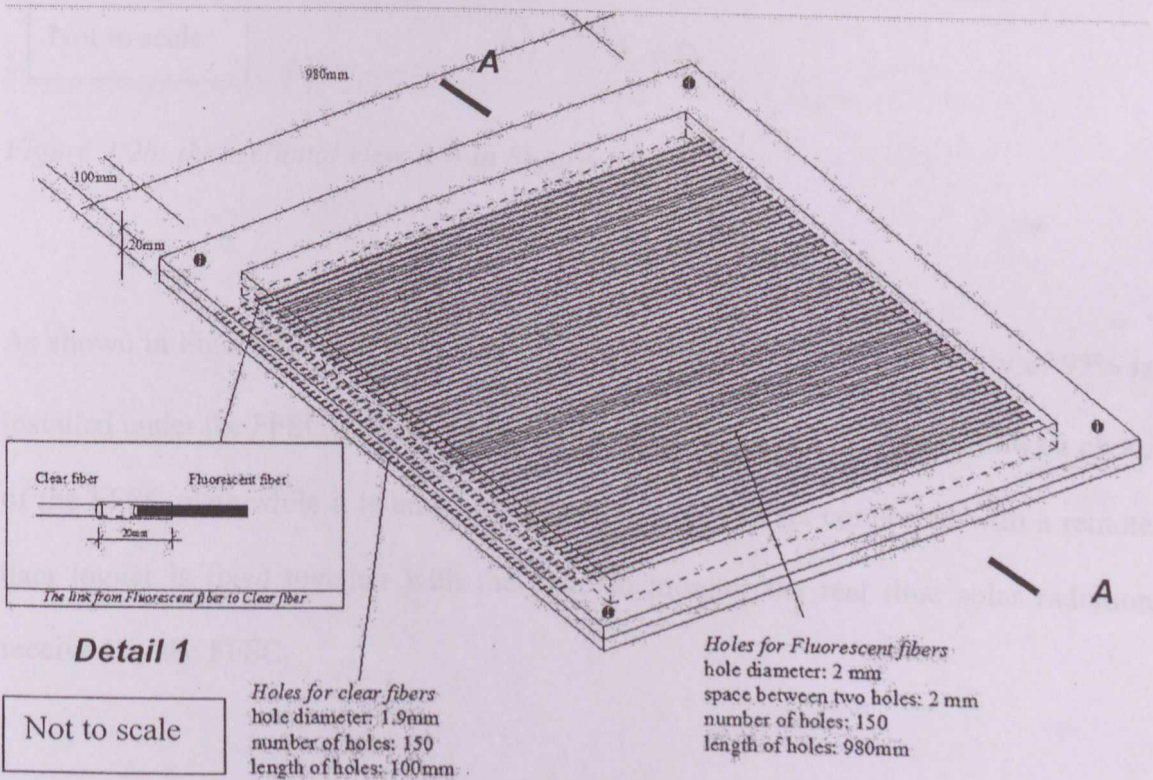


Figure 4.2: Auto CAD schema of FFSC (concept developed by author)

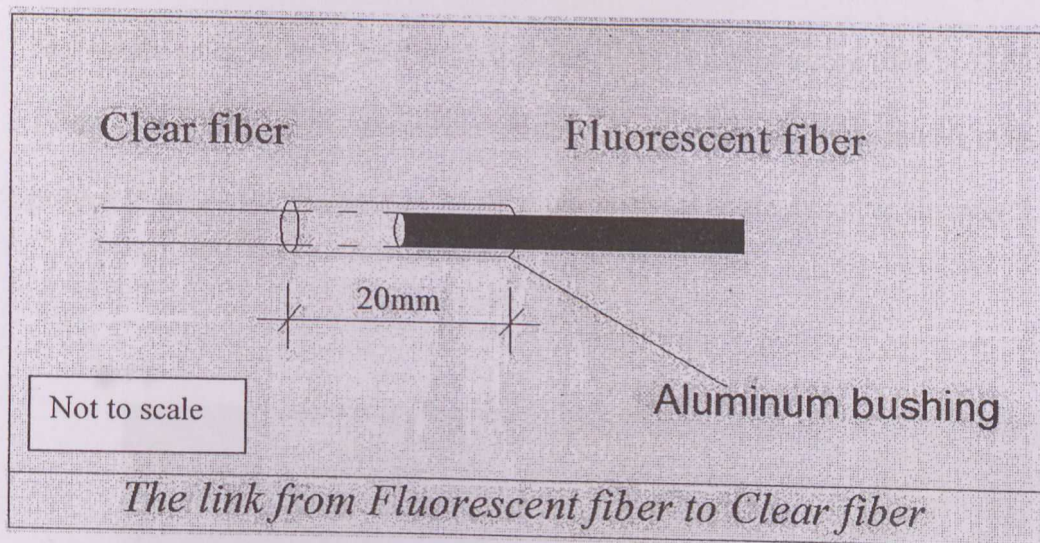


Figure 4.2a: Detail 1 in Figure 4.2, the link from fluorescent fiber to clear fiber

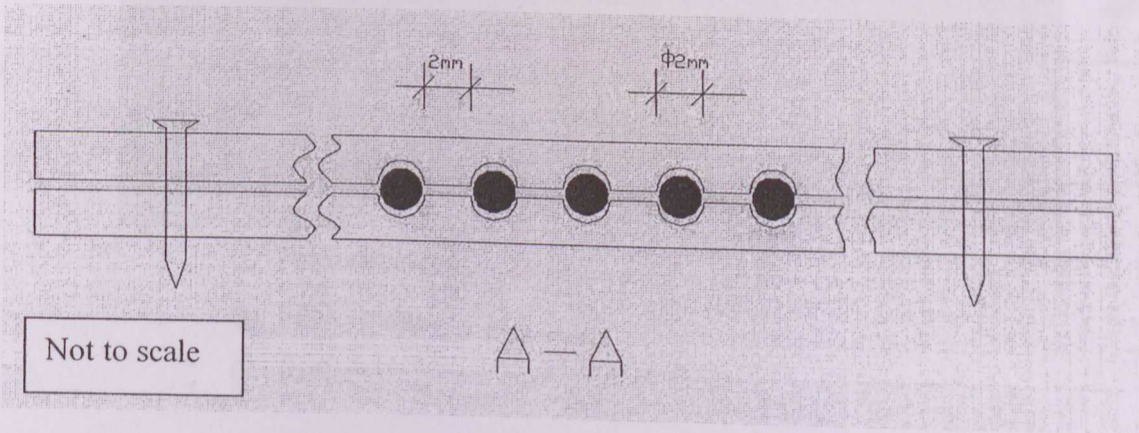


Figure 4.2b: the sectional view A-A in Figure 4.2,

As shown in Figure 4.3, a $1.3\text{m} \times 1.3\text{m}$ silver-gilt reflector with a reflectivity of 95% is installed under the FFSC plate to increase the light absorption. Figure 4.3 shows a photo of the FFSC plate while it is under operation. A pyranometer connected with a remote data logger is fixed together with the plate to monitor the real time solar radiation received by the FFSC.

One reason for using fibers in three colors is trying to cover the full spectrum band (Earp, et al., 2004). Another reason for using three color fibers is because the

transported light coming out of the finishing end could considerably mix into a near-white color light by self-scattering for illumination purpose (Yoshi, 2000; Schiler, 1992). The mixed light was observed as yellow-white light by naked eyes and was proved to match the daylight by a CIE color analysis as discussed in Chapter 7.

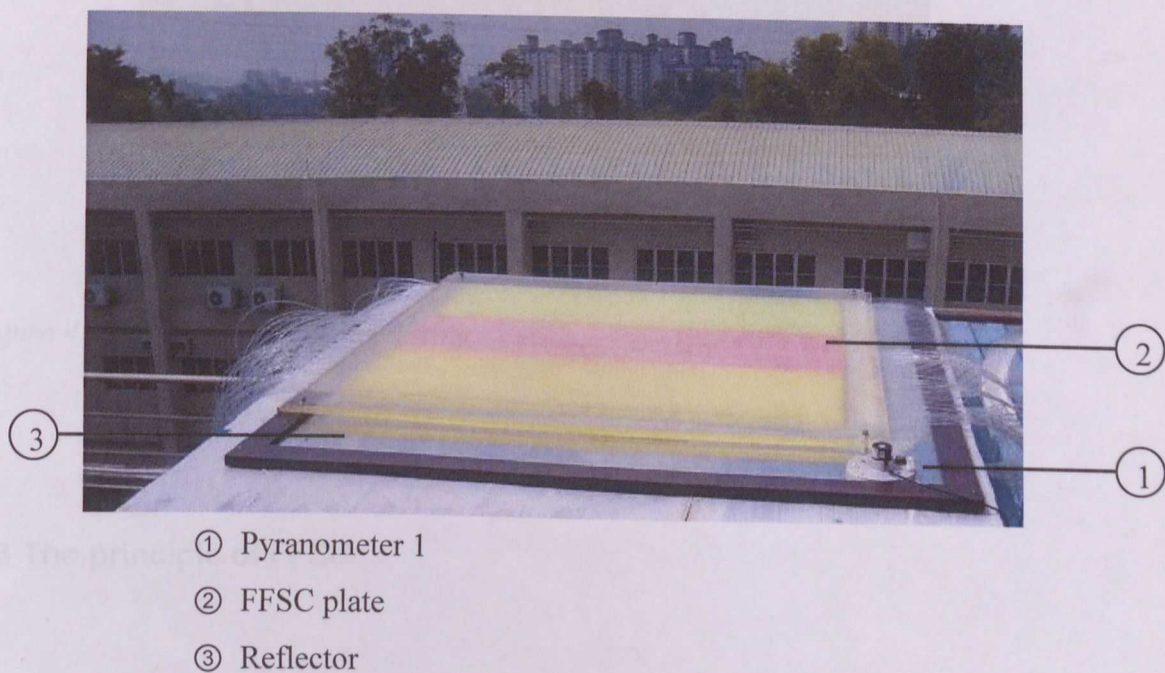
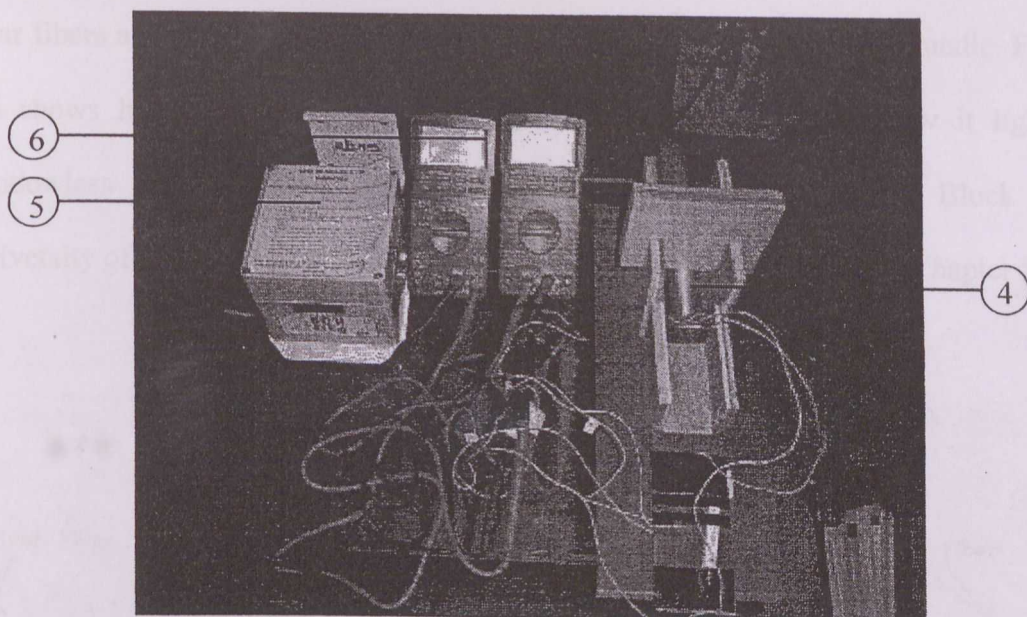


Figure 4.3: FFSC installed on the building roof (concept developed by author)

The light concentrated by FFSC is transported by two clear fiber bundles with a diameter of 30mm for each, which is reasonably easy for wiring in the building integration. Each finishing end of the fiber bundles has an diameter of only 30mm, as shown in Figure 4.4 marked by serial number ④.



- ④Finishing end
- ⑤Data logger
- ⑥Multimeters

Figure 4.4: equipments used for testing

4.3 The principle of FFSC

The FFSC designed in this study consists of transparent acrylic fibers doped with appropriate quantum dyes. In brief, sunlight is absorbed by the fibers and then re-radiated isotropically by the quantum dots, ideally with high quantum efficiency, and trapped in the fibers by internal reflection. The micro operation of the FFSC is similar as that for luminescent solar concentrators that has been discussed by Weber & Lambe (1976), Goetzberger & Greubel (1977), and Rapp & Boling (1978). As elaborated in Figure 4.5, quantum yield species are dissolved in rigid highly transparent acrylic fibers of high refractive index. Solar photons entering the FFSC plate are absorbed by the luminescent species and reemitted in random directions. Following Snell's law, a large fraction of the emitted photons are trapped within the fibers and transported by total internal reflections to the edge of the fluorescent fibers, where they enter the edge of the

Chapter 5

Experimentation Procedures and Instrumentation

This chapter describes the procedures and instrumentation of the experimentation, starting with a discussion on the Malaysian climate and the experimentation duration and followed by the explanation on the data collection approaches, apparatus, building context of the experimentations, data analysis approaches, and a critical discussion on experimentation limitations.

5.1 Malaysian climate and experimentation duration

The building used for the experimentation is located in the city of Kuala Lumpur, latitude 3.7° North and longitude 101.33° East in the tropical region (Chia, et al., 2006). Malaysia has a yearly mean temperature of 26°C to 27°C and relative humidity (RH) of 70% to 90% throughout the year (Sabarinah, 2006). Records of hourly solar radiation data for latitude 3.7° North and longitude 101.33° East (Subang Jaya Meteorological Station, Malaysia) received an annual maximum of more than $1000\text{W}/\text{m}^2$ on horizontal surface and about $850\text{W}/\text{m}^2$ on vertical surface for east and west facing surfaces. This is

about 75% to 80% of the solar radiation outside the earth's atmosphere. (Dilshan, Hamdan, & Nor, 2006).

Malaysia is located in the tropical region. The climate is governed by the regime of the North-east and South-West monsoons, which blows alternatively during the course of the year. The north-west monsoon blows from approximately October until March, and the south-west monsoon blows between May and September. The period of change between the two monsoons is being marked by heavy rainfall. The period of south-west monsoon is a drier period. Hence, heavy rainfall, constantly high temperature and relative humidity characterize the Malaysia climate. Much of the precipitation occurs as thunderstorms and the normal pattern is one of heavy falls within a short period. Generally, chances of rain falling in the afternoon or early evening are high compared with that in the morning (Kamaruzzaman, 2006). The country experiences more than 170 rainy days per year; however, an area may have a greater number of rainy days and yet receive a lesser amount of rain in a year than another area with smaller number of rainy days but receiving its rain in heavy spells. Ambient temperature remains uniformly high over the country throughout the year.

The intensity of solar radiation in hot humid climates such as Malaysia is generally high and uniform throughout the year (Dilshan et al., 2006). Therefore, the duration from 24th May 2008 to 23rd November 2008, all together 6 months, which covers both the north-east monsoon and south monsoons, has been chosen for data monitoring. Since the daily intensity of sunshine in Malaysia is remarkably stable through a year according to Kamaruzzaman (2006) and Dilshan et al. (2006), the data in a random week from 2nd June 2008 to 8th June 2008 (Monday to Sunday) has been chosen for the hourly data analysis.

5.2 Experimentation for FFSC: data collection

The fabricated new device called Fluorescent Fiber Solar Concentrator (FFSC) is mounted horizontally (with a low gradient of around 3° to the horizontal to lead the rainwater out of the surface, the effect caused by the small gradient was not considered in the analysis) on the roof of a building roof and the concentrated light is transported by two 10m long clear fiber bundles into a remote windowless dark room. One pyranometer, which is denoted as Pyranometer 1 in the thesis, is installed with the FFSC plate to detect the solar radiation. The light radiation yielding out of a finishing end is measured by another pyranometer denoted as Pyranometer 2. The values measured by the Pyranometer 1 and Pyranometer 2 are marked as PY1 and PY2 respectively, and are recorded by a remote data logger at an interval of 10 minutes for 24 hours a day. The units for both PY1 and PY2 are W/m².

Another finishing end is installed upon a LUX sensor at a distance of 100mm. The values measured by the LUX sensor are marked as Ev and they are recorded by the remote data logger at an interval of 10 minutes for 24 hours a day. The unit for Ev is LUX. In addition, it should be noted that the direct display from the LUX sensor uses a unit of kLUX. In the analysis, the unit of Ev is converted from kLUX to LUX to be inline with the international common practice.

PY1 and PY2 were recorded from 24th May 2008 to 23rd November 2008, all together 6 months. Ev was recorded from 24th May 2008 to 12th June 2008, all together 20 days,

because the finishing end used for the LUX sensor since 13th June 2008 had been used for other testing purposes until 23rd November, say, for wavelength monitoring and CIE (Commission Internationale de l'Eclairage, the International Commission on Color) color analysis.

5.3 Experimentation for FFSC: instrumentation

5.3.1 The pyranometers

The SKS1110 Pyranometer sensor has been chosen in the experimentation because it is the widest selling unit in the Skye instruments' range of sensors. It gives much greater output than thermopile instruments, which, with its better temperature stability, makes it easier to use. The sensors are calibrated against precision reference thermopile pyranometers in natural light conditions. The specifications of SKS1110 pyranometer are shown in Figure 5.1 and its responding range is from 400nm to 1100nm as shown in Figure 5.2. The calibration files are enclosed in APPENDIX E.


Dimensions	Weight	Construction	Cable	Sensor	Detector	Filters	Sensitivity -current (1)	Sensitivity -voltage	Working range (2)
	130g (with 3m cable)	Material DuPont 'Delrin' fully sealed to IP68	2 core screened DEF std 61-12/4.5	Cosine corrected head	Silicon photocell	N/A	5µA/100 W/m ²	1mV/ 100W/m ²	0-5000 Wm ²
Linearity error	Absolute calibration error (3)	Cosine error (4)	Azimuth error (5)	Temperature coefficient	Longterm stability (6)	Response time (7) - voltage output	Internal resistance - voltage output	Temperature range	Humidity range
<0.2%	typ. <3% 5% max.	3%	<1%	+0.2%/°C	+2%	10ns	c 200 ohms	-30 to + 75°C	0-100% RH

Figure 5.1: specifications of SKS1110 pyranometer (provided by supplier)

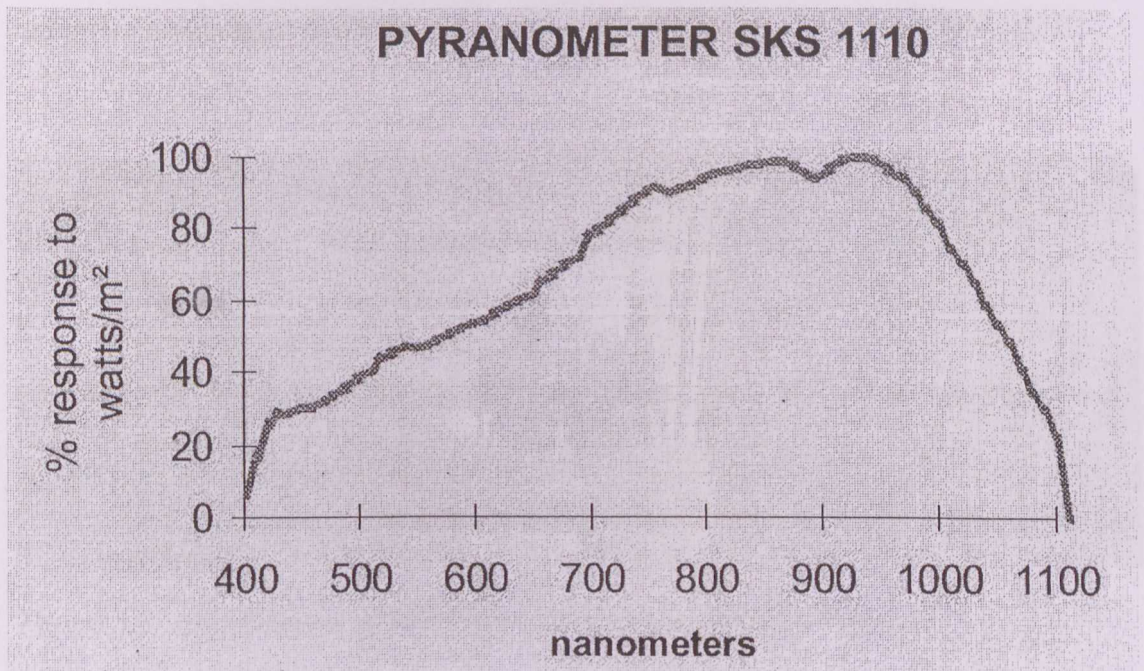


Figure 5.2: response range of SKS1110 pyranometer (provided by supplier)

5.3.2 LUX sensor

The LUX sensor SKL 310 was chosen since its responding range from 350nm to 750nm is sufficient for the experimentation. Its specification is shown in Figure 5.3 and its responding range graph is shown in Figure 5.4. Visible light can be defined as the part of the wavelength spectrum perceived by the human vision in a manner similar to the eyes. This response to the human eyes to light can be expressed as a spectral response curve which has the form shown on reverse. There is a peak sensitivity at 555nm for the light adapted eye. This curve is known as the photopic curve or CIE Standard Observer Curve. The response curve for this filtered sensor is almost indistinguishable from the photopic curve shown on the reverse. Light falling within the curve is measured in LUX sensors. Appropriate levels of light measured in LUX are important in many areas of

human activity such as close fieldwork, general reading, and relaxation and can have important psychological effects. The calibration files are enclosed in APPENDIX E.


Dimensions	Weight	Construction	Cable	Sensor	Detector	Filters	Sensitivity -current (1)	Sensitivity -voltage	Working range (2)
	130g. (with 3m cable)	Material Dupont 'Delrin' fully sealed to IP68	2 core screened DEF std 61-12/4.5	Cosine corrected head	Silicon photo cell Low fatigue characteristics	Multi-Element with 555nm peak	1.6µA/ 10kLux	1mV/ 10kLux	0-500 kLux
Linearity error-to above level	Absolute calibration error (3)	Cosine error (4)	Azimuth error (5)	Temperature coefficient	Longterm stability (6)	Response time (7) - voltage output	Internal resistance - voltage output	Operating range	Humidity range
<0.2%	typ. <3% 5% max.	3%	<1%	±0.1%/°C	±2%	10ns	c.650 ohms	-35 to +75°C	0-100% RH

Figure 5.3: specifications of SKL310 LUX sensor (provided by supplier)

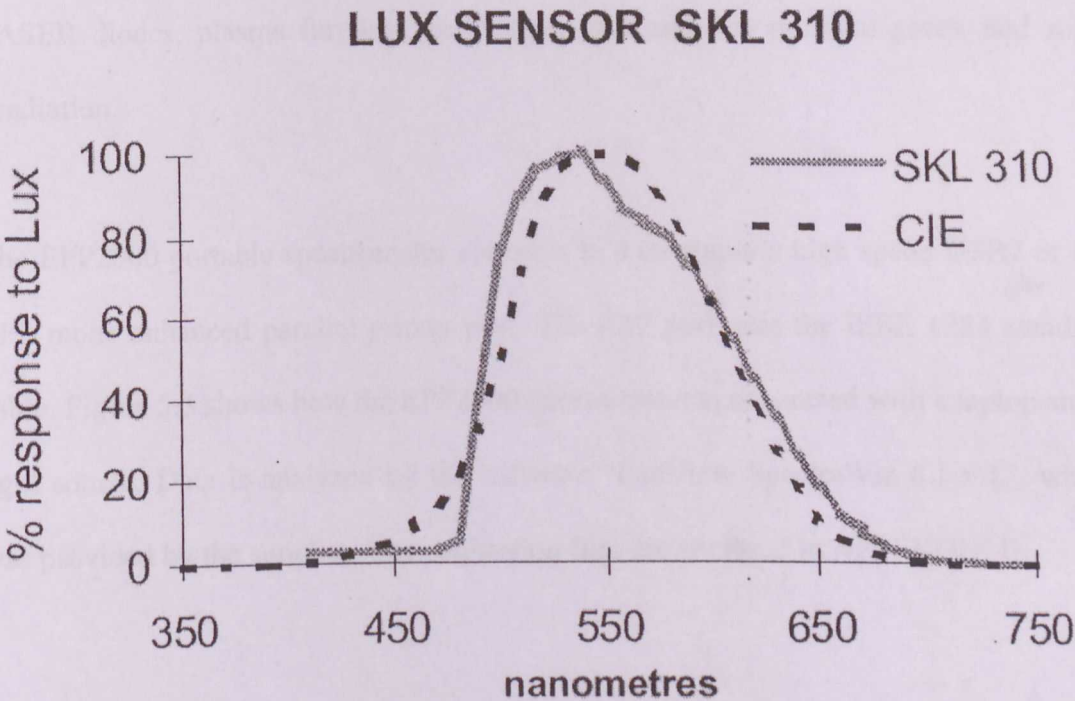


Figure 5.4: response range of SKL310 LUX sensor (provided by supplier)

5.3.3 Spectrometer

The EPP2000 (portable) spectrometer is employed in the 6-month experimentation for the wavelength testing and the CIE color analysis. Table 5.1 briefs some information about this model. The EPP2000 spectrometer is a compact, fiber optic spectrometer instrument. It is used to make various types of spectral measurements in the UV-VIS-NIR ranges from 190-2200nm. When it is used for spectroscopy applications, the instrument provides wavelength information for compute sample absorbance, transmittance, reflectance and emittance (such as fluorescence, plasma, laser induced breakdown and Raman spectroscopy). The spectrometer could be used to measure spectral emissions from various light sources such as LED's (Light Emitting Diodes), LASER diodes, plasma furnaces, arc lamps, high and low pressure gases, and solar irradiation.

The EPP2000 portable spectrometer connects to a computer's high speed USB2 or the EPP mode enhanced parallel printer port. The EPP port uses the IEEE 1284 standard cable. Figure 5.5 shows how the EPP2000 spectrometer is connected with a laptop and a light source. Data is analyzed by the software "LabView SpectraWiz 6.1 v.1", which was provided by the supplier. The calibration files are enclosed in APPENDIX E.

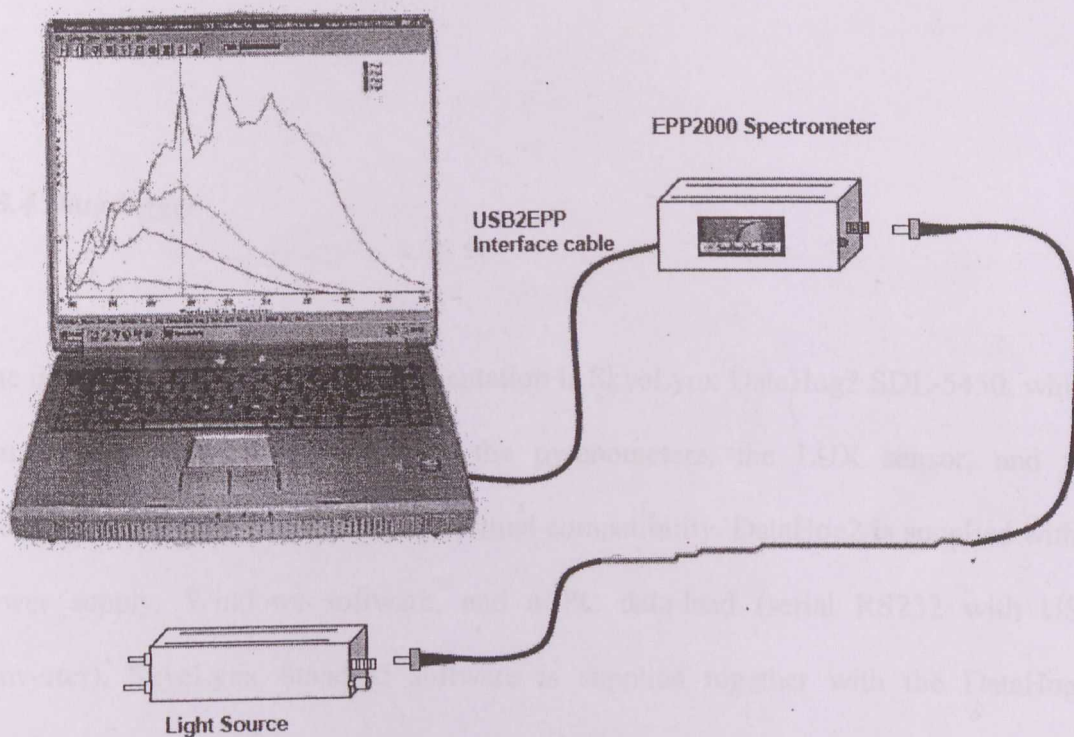


Figure 5.5: EPP2000 Spectrometer connected with laptop and light source

Table 5.1: information of the spectrometer used in experimentation (provided by supplier)

Product name:	Miniature Fiber Optic Spectrometer
Product type:	Spectrum Analyzer
Product models:	EPP2000
Safety:	EN61010-1, EN61010-2-031, IEC61010-3-1
EMC:	EN61326 + A1
Supplementary information:	The product complies with the requirements of the Low Voltage Directive 73/23/EEC-93/68/EEC, and the EMC Directive 89/336/EEC-92/31/EEC and 93/68/EEC.

5.3.4 Data logger

The data logger used in this experimentation is SkyeLynx DataHog2 SDL-5450, which comes from the same supplier of the pyranometers, the LUX sensor, and the spectrometer, for the purpose of the optimal compatibility. DataHog2 is supplied with a power supply, Windows software, and a PC data-lead (serial RS232 with USB converter). SkyeLynx Standard software is supplied together with the DataHog2. SkyeLynx Standard allows the setup and the configuration of the logger or meter, plus the downloading of the data stored in the instrument's memory. Data can be transferred to a PC hard drive in an ASCII numerical format compatible with the word processors and spreadsheets such as Microsoft Word and EXCEL. The software version "SkyeLynx Standard v2.6" provided by the supplier is used for the data analysis during the FFSC trial run.

Measurements direct from the DataHog2 and sensors can be viewed using the SkyeLynx Standard software. These measurements are stored using the "Log on Demand" function. A system check of the logger battery and memory status can be performed on screen. All these functions are accessed via the logging meter's own display.

All files are created in ASCII space delimited format. Each file contains an instrument identifier. Each measurement has a real time and date stamp. DataHog2 uses the

“Off-Load” button for automatic fast data downloading or use the software main menu “Offload data” option and “Capture File” feature.

When the program SkyeLynx Standard starts to run, firstly the choice of Com Ports are made. The “Com 1” of the computer is selected as the required port for this experimentation, as shown in Figure 5.6.

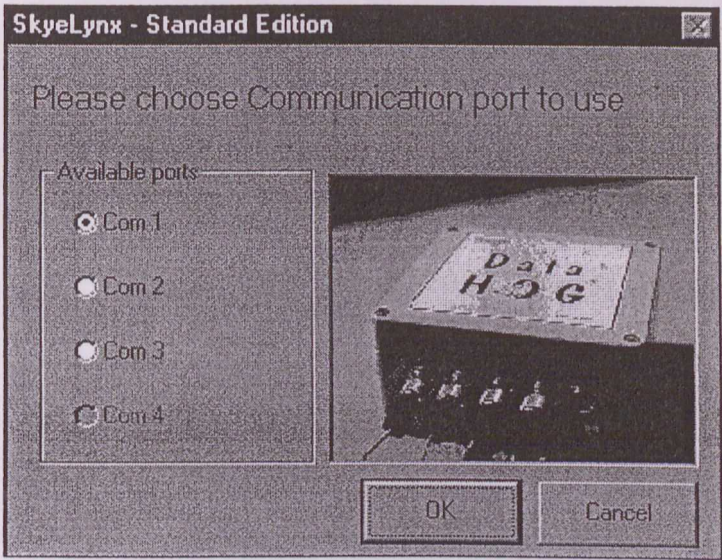


Figure 5.6: “Com 1” was configured to DataHog2

After that, the screen colors, and the options to see pictures and animations in the program are also specified as shown in Figure 5.7.

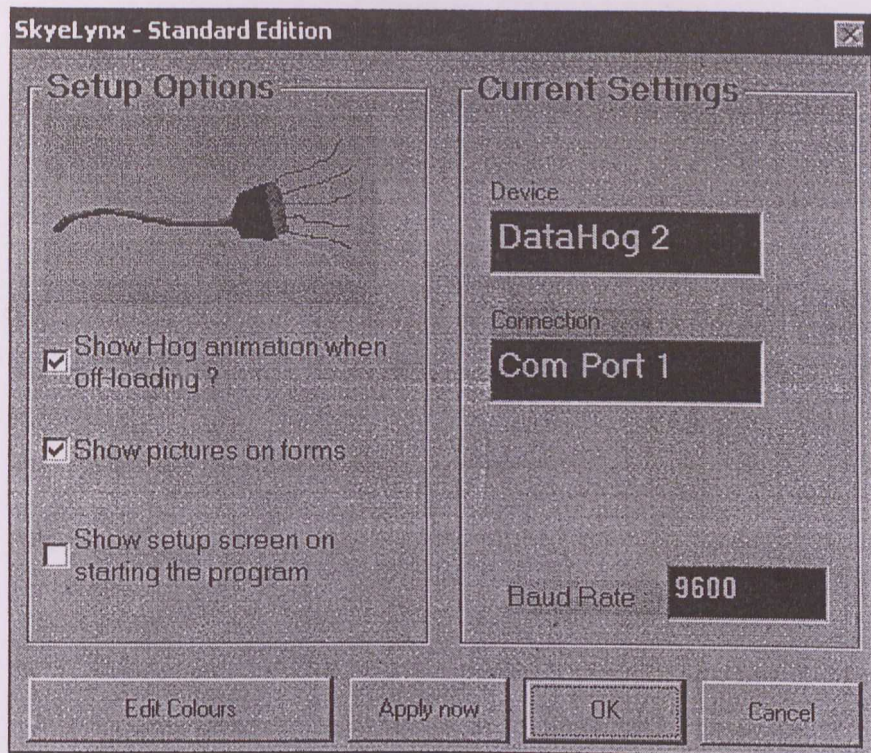


Figure 5.7: pictures and animations options are selected

The settings for channel configurations and logging intervals are done before it starts working. The Channel 1 is configured for Pyranometer1 and the Channel 2 for Pyranometer2. The Channel 3 is configured for the LUX sensor. All intervals are set into 10 minutes.

In the 6-month experimentation for FFSC, data are captured and stored directly in Microsoft EXCEL files for analysis. The function of “Capture File” is often used. Everything displayed in the main screen after the file is opened are written into the file. This is a useful way of recording details from the logger. For instance, if a capture file is opened, then through various menus on the SkyeLynx Standard program, all sorts of details for later viewing are record. This method is used for off-loading data. The capture file is closed before anything else in the program could be done. If the file already exists, it will be asked if it wish to append to the end of the existing file, or to

overwrite it. During the experimentation, the options “append” are always selected so that any new data off-loaded are added to the end of the existing file. Sometimes the data file is getting very big so that the computer process may take a long time because of the groups of new data inserted. Therefore, a new capture file is always created for each 4 or 5 days’ period.

Data off-loading allows DataHog2 to download the data into a file on a PC. A fast Off-Load response box is shown in Figure 5.8. This is where the data is read from the logger in the binary mode, and then decoded on a PC.

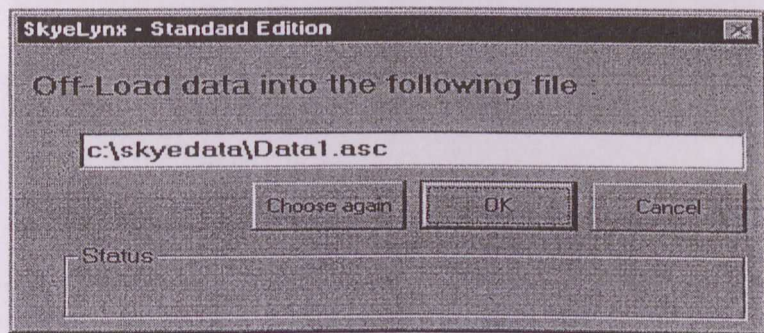


Figure 5.8: data offloading dialogue box in DataHog2

After each time data off-loading, the DataHog2 is returned to the logging mode manually. This allows the device to return to its logging state, where it is recording data. The logger is always left in this mode; otherwise, it will not record any new information.

The off-loaded data from the DataHog2 are imported into Microsoft EXCEL for manipulating. Firstly, the offloaded ASCII data file are captured in EXCEL as a space delimited file and then are transferred manually into a workable format through 3 steps as demonstrated in Figure 5.9, Figure 5.10, and Figure 5.11. This brings the data into a

spreadsheet as shown in Figure 5.12. Data in this format are then workable for the analysis purpose.

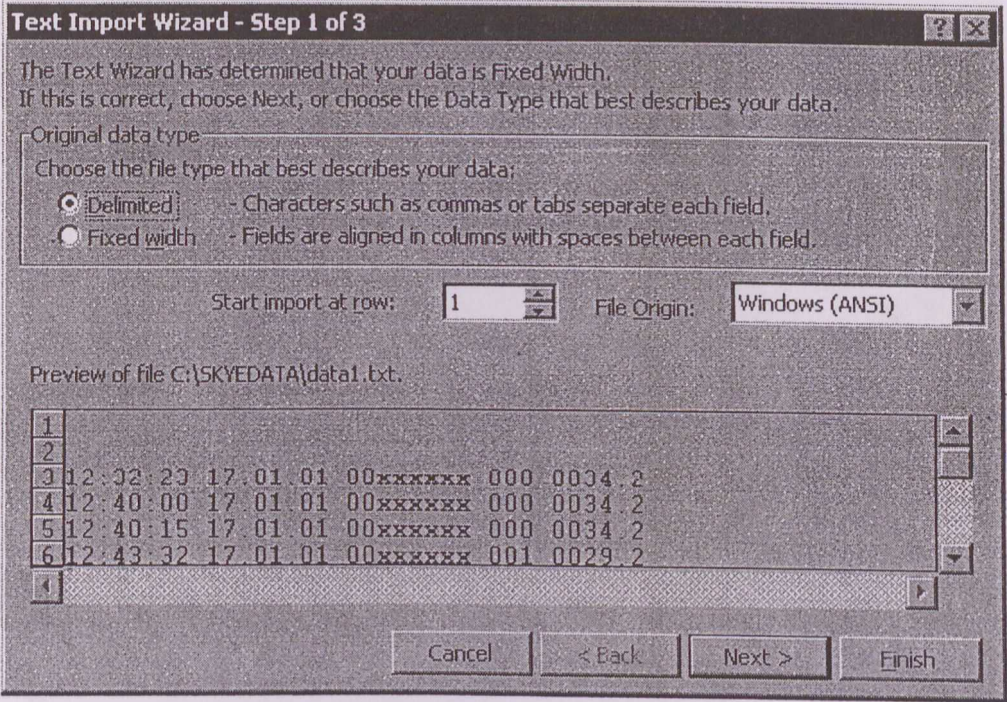


Figure 5.9: data export into Microsoft EXCEL, Step1 of 3 (displayed data only for demonstration)

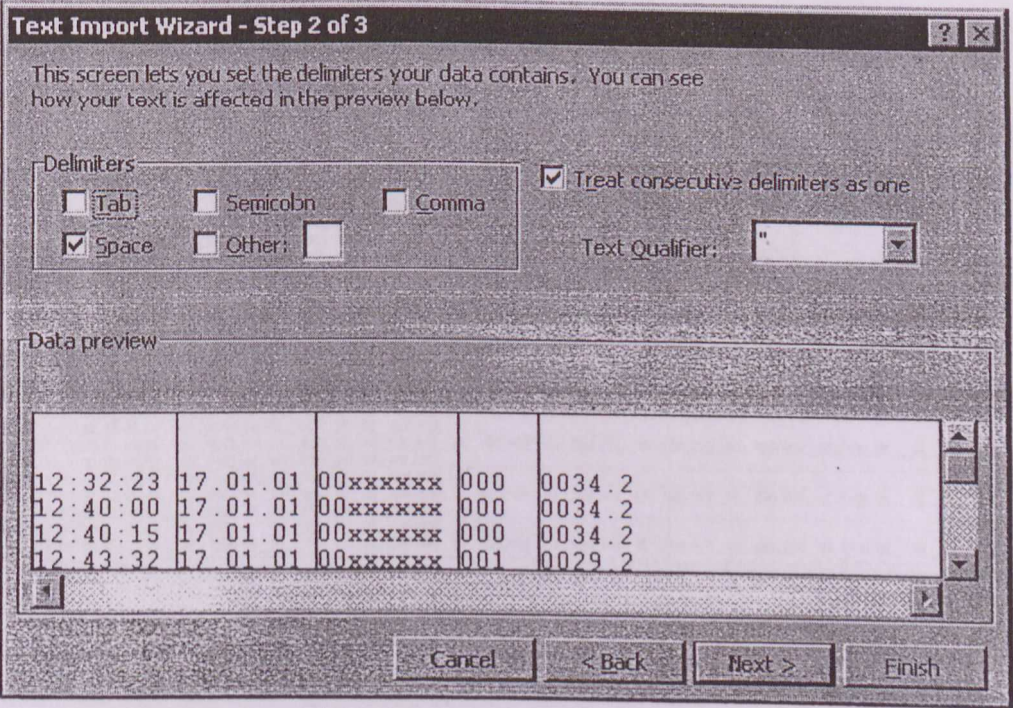


Figure 5.10: data export into Microsoft EXCEL, Step2 of 3 (displayed data only for demonstration)

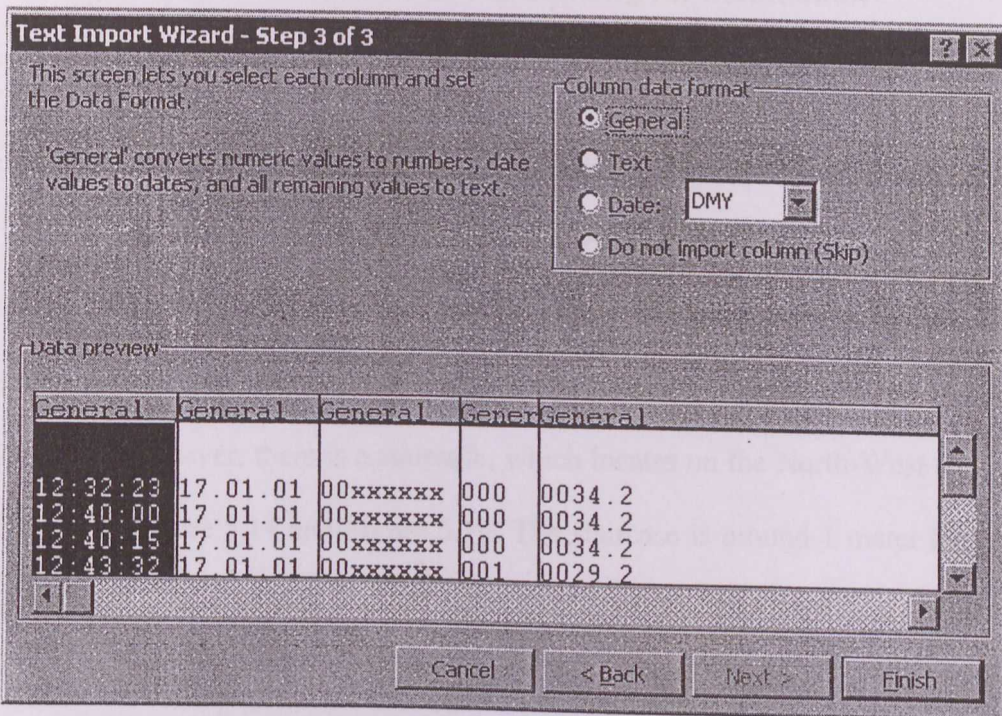


Figure 5.11: data export into Microsoft EXCEL, Step 3 of 3 (displayed data only for demonstration)

	A	B	C	D	E	F	G	H	I	J	K	L	M	N	O	P	Q	
62	14:30:00	23.05.08	00	0879.83	01	0048.86	02	000.192	03	023.926	04	028.905	05	000.000	06	000.000	07	<-20 UR
63	14:40:00	23.05.08	00	1041.99	01	0053.85	02	000.205										
64	14:50:00	23.05.08	00	1061.12	01	0054.78	02	000.218										
55	15:00:00	23.05.08	00	0769.85	01	0038.12	02	000.154	03	019.315	04	023.336	05	000.000	06	000.000	07	<-20 UR
56	15:10:00	23.05.08	00	0278.79	01	0018.32	02	000.000										
57	15:20:00	23.05.08	00	0320.79	01	0021.65	02	000.012										
58	15:30:00	23.05.08	00	0635.55	01	0032.94	02	000.000	03	018.768	04	021.357	05	000.000	06	000.000	07	<-20 UR
59	15:40:00	23.05.08	00	0166.94	01	0011.84	02	000.000										
60	15:50:00	23.05.08	00	0042.82	01	0003.70	02	000.000										
61	16:00:00	23.05.08	00	0038.12	01	0006.47	02	000.012	03	018.652	04	020.957	05	000.000	06	000.000	07	<-20 UR
62	16:10:00	23.05.08	00	0225.15	01	0013.51	02	000.012										
63	16:20:00	23.05.08	00	0194.17	01	0012.77	02	000.012										
64	16:30:00	23.05.08	00	0057.17	01	0004.62	02	000.012	03	018.778	04	021.389	05	000.000	06	000.000	07	<-20 UR
65	16:40:00	23.05.08	00	0054.67	01	0004.44	02	000.000										
66	17:00:00	23.05.08	00	0102.49	01	0007.21	02	001.965	03	018.673	04	021.073	05	000.000	06	000.000	07	<-20 UR
67	17:10:00	23.05.08	00	0118.29	01	0007.53	02	000.295										
68	17:20:00	23.05.08	00	0142.20	01	0009.06	02	002.633										
69	17:30:00	23.05.08	00	0110.81	01	0007.03	02	002.094	03	018.463	04	020.410	05	000.000	06	000.000	07	<-20 UR
70	17:40:00	23.05.08	00	0100.41	01	0006.29	02	001.862										
71	17:50:00	23.05.08	00	0169.64	01	0010.17	02	002.993										
72	18:00:00	23.05.08	00	0179.83	01	0010.36	02	002.993	03	018.452	04	020.284	05	000.000	06	000.000	07	<-20 UR
73	18:10:00	23.05.08	00	0055.48	01	0004.44	02	001.233										
74	18:20:00	23.05.08	00	0041.99	01	0002.96	02	000.835										
75	18:30:00	23.05.08	00	0044.07	01	0002.96	02	000.809	03	018.584	04	020.947	05	000.000	06	000.000	07	<-20 UR
76	18:40:00	23.05.08	00	0020.79	01	0000.00	02	000.000										
77	18:50:00	23.05.08	00	0004.57	01	0000.00	02	000.000										
78	19:00:00	23.05.08	00	0000.00	01	0000.00	02	000.000	03	018.694	04	020.894	05	000.000	06	000.000	07	<-20 UR

Figure 5.12: data export into Microsoft EXCEL, the workable spreadsheet (displayed data only for demonstration)

5.4 Experimentation for FFSC: the building for installation

The University building, Block G22, was chosen as the building for FFSC's installation because its roof and the roof of its next building, Block G21, have the same height of 23.1m, and they are the tallest building roofs amongst the surrounding 500 square meters. There is no any other building or tree causing shading on the FFSC plate during daytime. However, there is a staircase, which locates on the North-West to the FFSC as shown in Figure 5.14 and Figure 5.16. The staircase is around 1 meter higher than the FFSC plate. Even though, according to Dilshan et al. (2006) and Kamaruzzaman et al. (2006), since Kuala Lumpur is located in the northern hemisphere and the beam solar irradiation comes only from the South and Top, the staircase does not cause any shading for beam solar irradiation but probably some negligible diffuse irradiation on FFSC. However, the light reflected from the staircase's South-East surface may considerably counteract the blocked diffuse irradiation. This is discussed in Section 5.5. Figure 5.13 shows the orientation of this building and it also shows where FFSC was mounted on. The A-A section view is provided in Figure 5.14, in which the FFSC's location is illustrated. A photo for Block 22 has been taken towards the North-West facade as shown in Figure 5.15, where the staircase appears in the middle. After the FFSC is mounted on the roof, the concentrated light is transported through 10m long clear fiber bundles to a dark room located on the 4th floor of the building for monitoring. The dark room (width 3.15m \times length 6.50m \times height 3.30m) was a store room before it was employed for this experimentation. The layout of the 4th floor is presented in Figure 5.17.

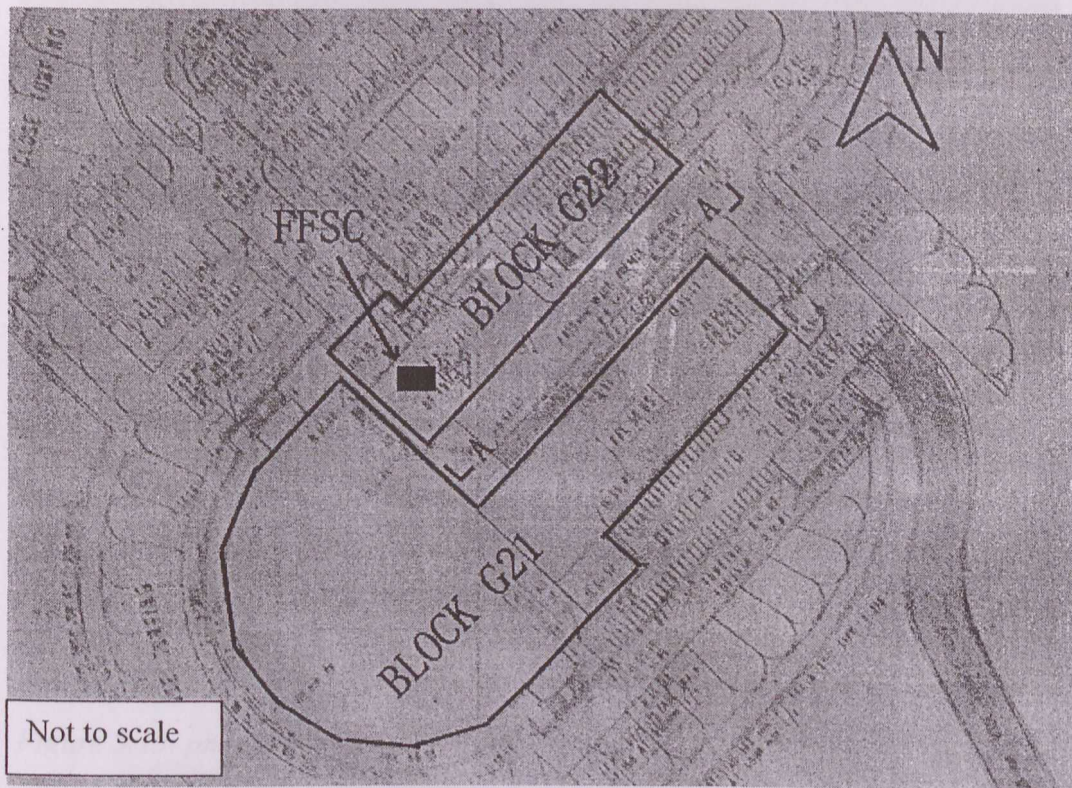


Figure 5.13: Block G22, where FFSC was mounted on

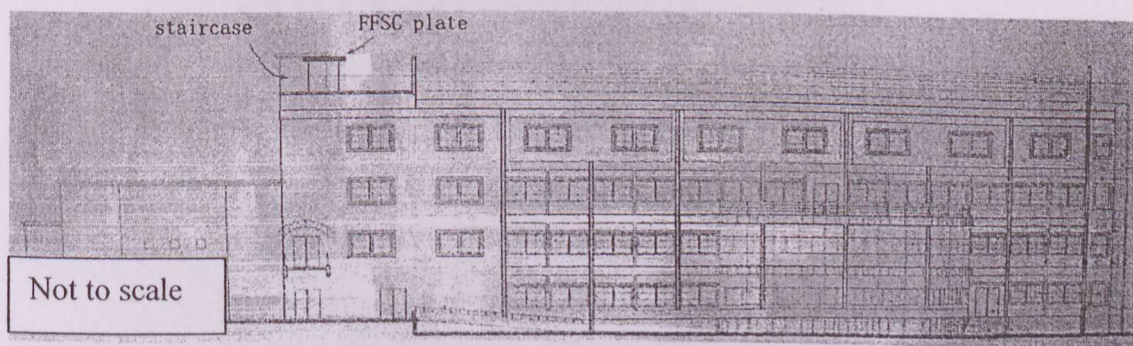


Figure 5.14: A-A section view for Block G22 and where FFSC installed



Figure 5.15: photo for Block G22

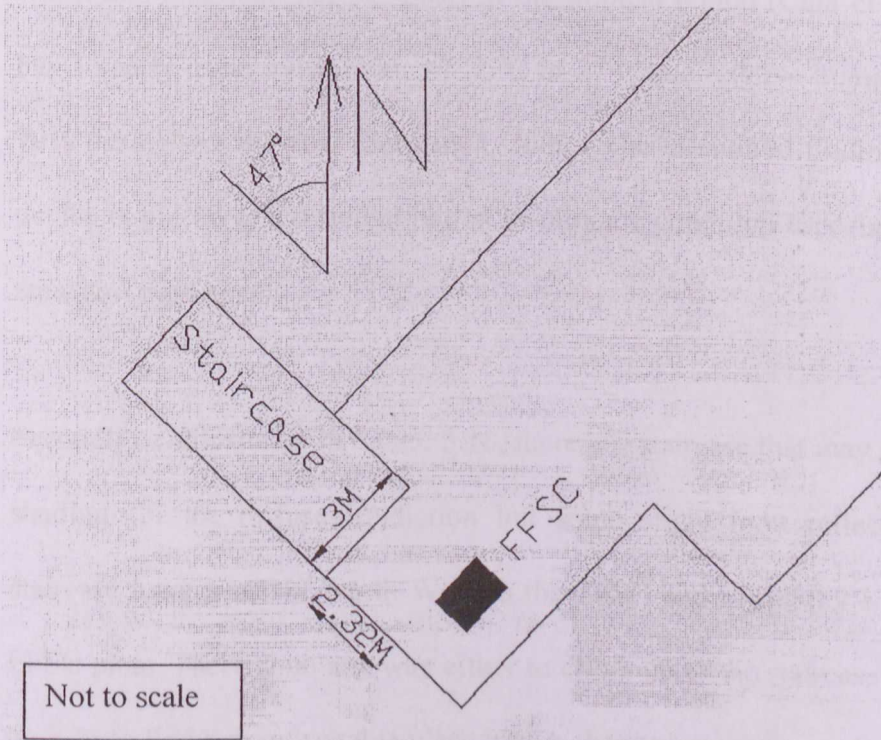


Figure 5.16: the staircase that close to FFSC

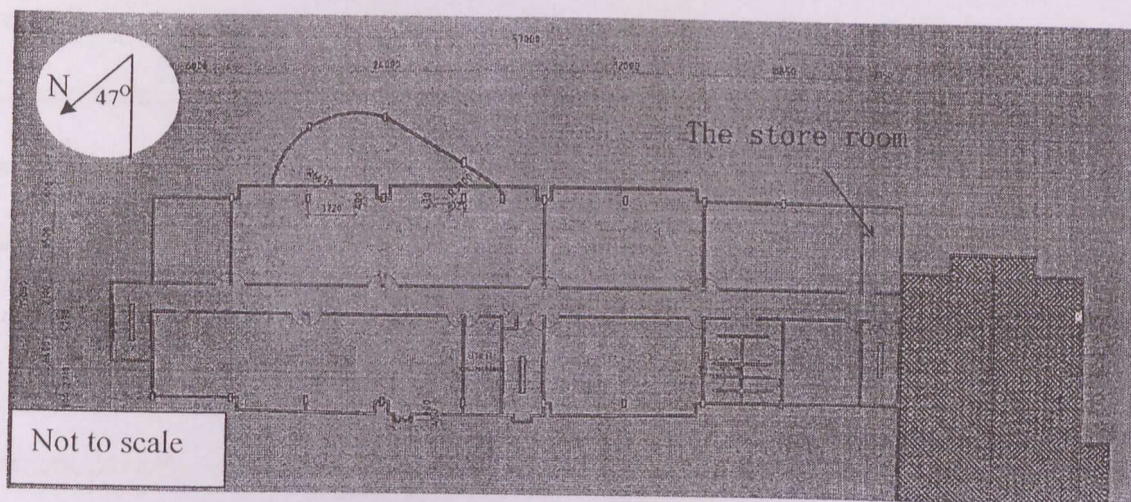


Figure 5.17: layout of the 4th floor

5.5 Critical review of experimental limitations

In general, experimentations were conducted in Kuala Lumpur, Malaysia (latitude 3.7° North and longitude 101.33° East) in the tropical region (Chia et al., 2006). Malaysia has a yearly mean temperature of 26°C to 27°C and relative humidity (RH) of 70% to 90% throughout the year (Sabarinah, 2006). The monitored findings would vary if the device is placed in a different region or climatic condition especially for the temperate zone and rigid zone.

Secondly, as illustrated in Figure 5.16, there is a staircase that may probably cause some shading for the diffuse irradiation but some slight light reflection on FFSC. The staircase locates on the North-West to the FFSC and is about 1 meter higher than the FFSC plate. There is no any way either to climb up to the staircase roof to install FFSC on it or to find a more suitable place higher than the staircase roof according to the field limitation. However, the staircase does not cause any shading for beam solar irradiation since that Kuala Lumpur is located in the northern hemisphere and the beam solar

irradiation only comes from the South and Top according to Dilshan et al. (2006) and Kamaruzzaman et al. (2006). Therefore, the impact caused by the staircase was not experimentally studied because it was considered as insignificant and negligible as mentioned above.

Finally, the limitations in the availability of the fluorescent fiber market also bring limitations to the study. In this research, only fluorescent fibers with a diameter of 2mm are supplied. There is no fluorescent fiber with a larger diameter available with the supplier at that time. According to Richards (2006), Reisfeld (2001), Batchelder et al. (1979) and Hammam et al. (2007), the size and the form of the cross sectional area could impact on the proportion of photons trapped by the luminescent plate and the reduction of the cross sectional area of the luminescent plate could remarkably increase the photon loss. Accordingly, if fluorescent fibers with a larger diameter could be embedded in FFSC, say 10mm diameter, the performance parameters of FFSC such as the luminous efficacy and the light-to-light efficiency could increase. Experimentation for fluorescent fibers with larger diameters is recommended in future study as mentioned in Chapter 8.

5.6 Experimentation for FFSC: parameters analyzed

The time system used in this research is the 24-hour system. The daily data recorded for FFSC from 6:00 to 20:00 were selected for every day, because there was no any significant response from all the light meters during the rest hours of a day when it was during nighttime. The following analysis has been conducted for the FFSC system,

namely: radiation-to-radiation efficiency (η_r), lighting effect, energy-to-energy efficiency (η_e), luminous efficacy (K), light-to-light efficiency (η_l), wavelength test, CIE color analysis, and the negative trend between radiation-to-radiation efficiency (η_r) and solar radiation (PY1), and so on, which are discussed in Chapter 6 and Chapter 7. The statistic methods such as correlation and linear test are employed. The program “Statistical Package for Social Science (SPSS) program for Windows98/XP” is employed for the statistic analysis.

Chapter 6

Data Restructuring and Interpretation

Data used for the analysis were mainly acquired through the DataHog2 and the EPP2000 spectrometer. The DataHog2 was linked with the Pyranometer1, the Pyranometer2, and the LUX sensor, and it transferred the data measured from all these meters to a computer for the recording and the analysis purposes. The EPP2000 spectrometer has its own built-in data logger and it was linked to the computer directly without connecting to the DataHog2. The following sections explain how the data measured by various meters were restructured and interpreted into an analyzable format.

6.1 Data acquired from DataHog2

The DataHog2 is able to record data using its built-in memory for around 1 week without off-loading to a computer hard disk until its built-in memory is full. The program “SkyeLynx Standard v2.6” is used for data acquiring for DataHog2. The following main menu is displayed on the screen for operation as shown in Figure 6.1. The calibration results for DataHog2 are attached in APPENDIX E.

By selecting the option “SET CHANNEL CONFIGUR’NS” as shown in Figure 6.1, all together 8 channels in the DataHog2 are configured to various meters. In this experimentation, there are three channels configured for light meters. Channel 1 is configured to Pyranometer1, and Channel 2 is configured to Pyranometer2. Channel 3 is for the LUX sensor. Channels 4 to Channel 8 are not configured and they are not used in the experimentation, so that the values appeared under these channels do not make any sense and they are not analyzed.

By selecting the option “SET CHANNEL SAMPLE & LOG INTERVALS”, Channel 1 is coded as “00”; Channel 2 is coded as “01”, and Channel 3 is coded as “02”. For the intervals, there are two types of intervals to be set, namely: sampling intervals and logging intervals. The sampling interval is where a reading is taken from the associated channel and stored in the temporary memory. On the other hand, at the chosen logging interval, the sampled readings are divided by the number of samples and the single averaged measurement stored in memory with the appropriate time and date. If the sample time and the log times are equal, the averaging process is irrelevant, and readings are stored directly. During the 6-month monitoring, both the sampling interval and logging interval are set at 10 minutes as decided by the research group.

K9										
	A	B	C	D	E	F	G	H	I	J
19	SEND CHARACTER SHOWN TO SELECT ITEM									
20	<ESC> RETURNS TO LOGGING									
21										
22	- MAIN MENU -									
23	0) DISPLAY READINGS FROM ALL ACTIVE CHANNELS									
24	1) DISPLAY CURRENT SETUP									
25	2) DISPLAY SOFTWARE VERSION									
26	3) OFFLOAD 24HOUR DATA SUMMARY									
27	4) OFFLOAD DATA									
28	5) RESET MEMORY									
29	6) SET CLOCK									
30	7) SET DATAFILE I/D. PLUS MEM OVERWRITE & TIMED LOGGING MODES									
31	8) SET CHANNEL SAMPLE & LOG INTERVALS									
32	9) SET AX+B CALIBRATION FACTORS									
33	A) SET CHANNEL CONFIGUR'NS									
34	B) SET INT'NL RH% SENSOR CALIB'N									
35	C) SET ALARM RELAY(S)									
36	D) SET CHANNELS FOR NONZERO THRESHOLD LOG MODES									
37	E) ENTER * LOG ON DEMAND' MODE									
38										
39	4									
40	*****									
41										
42	OFFLOAD FROM START OF MEMORY TO LATEST RECORD									
43										

Figure 6.1: main menu displayed in “SkyeLynx Standard v2.6”

A Microsoft EXCEL file is opened for the data capturing and recording before the data is off-loaded. By selecting the option “OFFLOAD DATA”, data are displayed in the Microsoft EXCEL spreadsheet as shown in Figure 6.2.

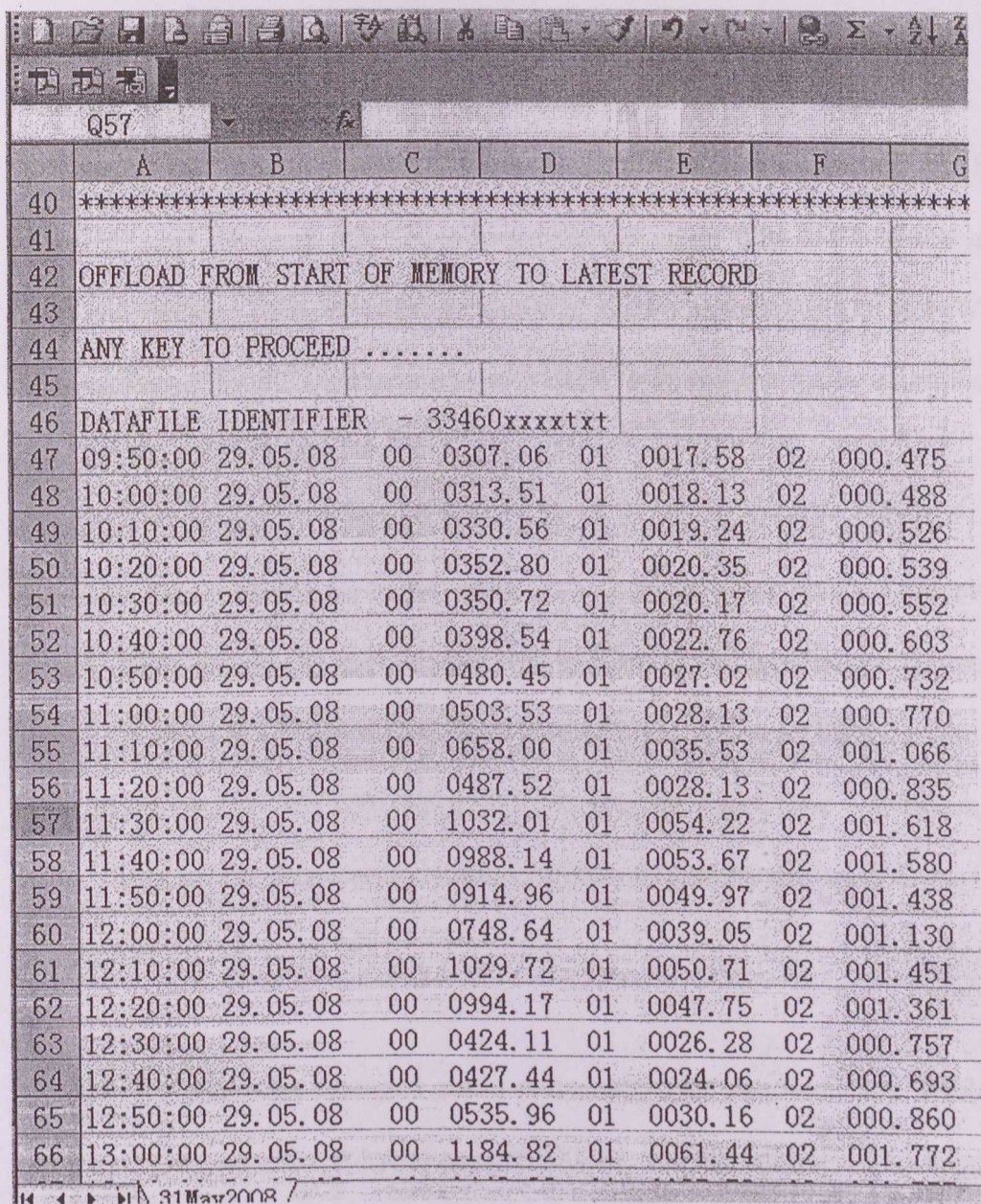


Figure 6.2: data offloading process displayed in Microsoft EXCEL

In Figure 6.2, each row displays a group of data acquired from different meters at a same moment. In the column “A” it displays the time when the data are read from the meters and in the column “B” it displays the date. For instance, in the row number “57”,

the time “11:30:00” is shown in column “A” and the date “29.05.08” is shown in column “B”, which means the data in the whole row number “57” were measured at 11:30 on 29th May 2008.

The mark “00” displayed in column “C” is the code for Pyranometer1, followed by the value measured by the Pyranometer1. The mark “01” is for Pyranometer2 and “02” for the LUX sensor. For the same instance in the row number “57”, the mark “00” is followed by the value “1032.01”; the mark “01” in this row is followed by the value “0054.22”, and the mark “02” is followed by the value “001.618”, which means at 11:30 on 29th May 2008, the value measured by the Pyranometer1 is 1032.01W/m2, the value measured by the Pyranometer2 is 54.22W/m2, and the value measured by the LUX sensor is 1.618 kLUX.

The daily data recorded for FFSC from 6:00 to 20:00 were selected for every day, because there was no any significant response from all the light meters during the rest hours of a day when it was during night time. All the measured values in the duration from 20:00 to 6:00 are zero since it is during the night time. Therefore, in data restructuring, all the data captured during 20:00 to 6:00 every day were deleted from the spreadsheet.

The selected data were arranged and a preparatory calculation such as PY2/PY1 and LUX/PY2 were conducted by Microsoft EXCEL for the analysis. The interval of 10 minutes remains. The light radiation monitored by Pyranometer1 that installed on the building roof is denoted as PY1, and the light radiation monitored by Pyranometer2 that installed with the finishing end is denoted as PY2. Figure 6.3 demonstrates one of the screens for data restructuring and the preparatory calculation conducted by Microsoft

EXCEL, where data were sorted by “Pyranol”, “Pyrano2”, “LUX”, “P2/P1”, and “LUX/PY2” in various columns. “Pyranol” or “P1” presents the values for Pyranometer1 and they are equal as PY1. “Pyrano2” or “P2” presents the values for Pyranometer2 and they are equal as PY2. However, these different symbols were only employed to ease the data restructuring process. Therefore, in the discussion of the analysis results as presented in Chapter 7, only the symbols as PY1 and PY2 are employed to indicate the values measured by the pyranometers.

	A	B	C	D	E	F	G	H	I	J	K	L	M	N	O	P	Q	R	S
37	11:50:00	24.05.08	Pyranol	960.7		Pyranol2	50.52		kLux	1.464		P2/P1	0.062507		Lux	1464		Lux/PY2	28.97862
38	12:00:00	24.05.08	Pyranol	939.91		Pyranol2	48.67		kLux	1.413		P2/P1	0.061762		Lux	1413		Lux/PY2	29.03225
39	12:10:00	24.05.08	Pyranol	995.63		Pyranol2	48.12		kLux	1.387		P2/P1	0.062331		Lux	1387		Lux/PY2	28.82377
40	12:20:00	24.05.08	Pyranol	1043.03		Pyranol2	49.97		kLux	1.464		P2/P1	0.061906		Lux	1464		Lux/PY2	29.29758
41	12:30:00	24.05.08	Pyranol	1036.79		Pyranol2	50.71		kLux	1.464		P2/P1	0.061911		Lux	1464		Lux/PY2	28.87005
42	12:40:00	24.05.08	Pyranol	997.92		Pyranol2	50.52		kLux	1.451		P2/P1	0.060625		Lux	1451		Lux/PY2	28.72113
43	12:50:00	24.05.08	Pyranol	1080.66		Pyranol2	54.96		kLux	1.567		P2/P1	0.060383		Lux	1567		Lux/PY2	28.51164
44	13:00:00	24.05.08	Pyranol	1066.73		Pyranol2	56.25		kLux	1.618		P2/P1	0.062741		Lux	1618		Lux/PY2	28.75933
45	13:10:00	24.05.08	Pyranol	1151.76		Pyranol2	60.89		kLux	1.798		P2/P1	0.062867		Lux	1798		Lux/PY2	29.52866
46	13:20:00	24.05.08	Pyranol	1151.76		Pyranol2	57.37		kLux	1.682		P2/P1	0.060941		Lux	1682		Lux/PY2	29.31846
47	13:30:00	24.05.08	Pyranol	187.11		Pyranol2	19.73		kLux	0.308		P2/P1	0.061746		Lux	308		Lux/PY2	28.70457
48	13:40:00	24.05.08	Pyranol	1006.56		Pyranol2	46.08		kLux	1.31		P2/P1	0.061664		Lux	1310		Lux/PY2	28.42882
49	13:50:00	24.05.08	Pyranol	989.02		Pyranol2	22.98		kLux	0.655		P2/P1	0.061199		Lux	655		Lux/PY2	29.00797
50	14:00:00	24.05.08	Pyranol	849.87		Pyranol2	43.12		kLux	1.181		P2/P1	0.060147		Lux	1181		Lux/PY2	27.38668
51	14:10:00	24.05.08	Pyranol	1000.83		Pyranol2	52		kLux	1.413		P2/P1	0.061657		Lux	1413		Lux/PY2	27.17308
52	14:20:00	24.05.08	Pyranol	861.95		Pyranol2	44.6		kLux	1.233		P2/P1	0.061743		Lux	1233		Lux/PY2	27.64574
53	14:30:00	24.05.08	Pyranol	359.25		Pyranol2	21.09		kLux	0.59		P2/P1	0.062766		Lux	590		Lux/PY2	27.97534
54	14:40:00	24.05.08	Pyranol	188.58		Pyranol2	10.54		kLux	0.308		P2/P1	0.062773		Lux	308		Lux/PY2	29.22201
55	14:50:00	24.05.08	Pyranol	213.09		Pyranol2	12.03		kLux	0.346		P2/P1	0.062485		Lux	346		Lux/PY2	28.76143
56	15:00:00	24.05.08	Pyranol	424.53		Pyranol2	24.98		kLux	0.693		P2/P1	0.062842		Lux	693		Lux/PY2	27.74219
57	15:10:00	24.05.08	Pyranol	468.19		Pyranol2	26.83		kLux	0.745		P2/P1	0.062300		Lux	745		Lux/PY2	27.76742
58	15:20:00	24.05.08	Pyranol	428.89		Pyranol2	25.17		kLux	0.693		P2/P1	0.062468		Lux	693		Lux/PY2	27.53278
59	15:30:00	24.05.08	Pyranol	729.1		Pyranol2	37.57		kLux	1.002		P2/P1	0.061822		Lux	1002		Lux/PY2	26.67022
60	15:40:00	24.05.08	Pyranol	393.36		Pyranol2	22.39		kLux	0.616		P2/P1	0.062415		Lux	616		Lux/PY2	27.51228
61	15:50:00	24.05.08	Pyranol	464.44		Pyranol2	26.09		kLux	0.706		P2/P1	0.062759		Lux	706		Lux/PY2	27.06018
62	16:00:00	24.05.08	Pyranol	386.9		Pyranol2	22.2		kLux	0.578		P2/P1	0.062422		Lux	578		Lux/PY2	26.03604
63	16:10:00	24.05.08	Pyranol	587.52		Pyranol2	27.57		kLux	0.693		P2/P1	0.062494		Lux	693		Lux/PY2	25.13602
64	16:20:00	24.05.08	Pyranol	210.6		Pyranol2	12.95		kLux	0.372		P2/P1	0.061348		Lux	372		Lux/PY2	28.72587
65	16:30:00	24.05.08	Pyranol	161.96		Pyranol2	9.99		kLux	0.295		P2/P1	0.061348		Lux	295		Lux/PY2	29.52953
66	16:40:00	24.05.08	Pyranol	150.31		Pyranol2	9.06		kLux	0.269		P2/P1	0.060276		Lux	269		Lux/PY2	29.69095
67	16:50:00	24.05.08	Pyranol	30.06		Pyranol2	4.44		kLux	0		P2/P1	0.060276		Lux	0		Lux/PY2	

Figure 6.3: data restructure and preparatory calculation conducted by EXCEL

Daily mean values for “Pyranol”, “Pyrano2”, “LUX”, “P2/P1”, and “LUX/PY2” were also calculated by Microsoft EXCEL as demonstrated in Figure 6.4. Advanced analysis such as the linear test and the correlation test in radiation-to-radiation efficiency (η_r), lighting effect, energy-to-energy efficiency (η_e), luminous efficacy (K), and the negative trend between radiation-to-radiation efficiency (η_r) and solar radiation (PY1) were conducted in the “Statistical Package for Social Science (SPSS) program for Windows98/XP” as discussed in Chapter 7.

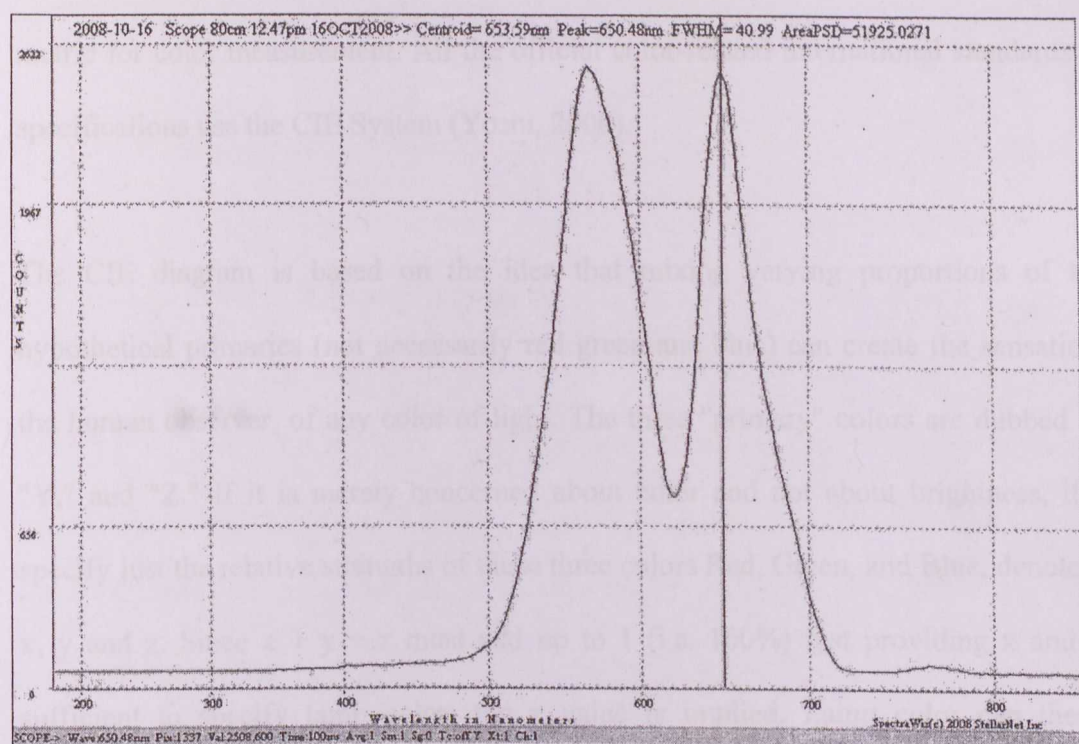


Figure 6.5: wavelength display in “LabView SpectraWiz 6.1 v.1”

In order to analyze the color of the FFSC light output, a CIE (Commission Internationale de l'Eclairage, the International Commission on Color) color analysis is conducted under the irradiant mode. The term “color” is used with different meanings in different technologies. To lamp engineers, color refers to a property of light sources. To graphics art engineers, color is a property of an object’s surface (under a given illumination). In each case, color must be physically measured in order to record it and reproduce the same color. The perception of color is a psychophysical phenomenon, and the measurement of color must be defined in such a way that the results correlate accurately with what the visual sensation of color is to a normal human observer (Wyszecki & Stiles, 1982). Colorimetry is the science and technology used to quantify and describe physically the human color perception. The basis for colorimetry was established by CIE in 1931 based on visual experiments. Even though limitations are well recognized, the CIE system of colorimetry remains the only internationally agreed

metric for color measurement. All the official color-related international standards and specifications use the CIE System (Yoshi, 2000).

The CIE diagram is based on the idea that mixing varying proportions of three hypothetical primaries (not necessarily red green and blue) can create the sensation in the human observer, of any color of light. The three "primary" colors are dubbed "X," "Y," and "Z." If it is merely concerned about color and not about brightness, it can specify just the relative strengths of these three colors Red, Green, and Blue, denoted by x , y and z . Since $x + y + z$ must add up to 1 (i.e. 100%) just providing x and y is sufficient to specify lamp color; the z value is implied. Lamp color can then be represented on a two-dimensional plot of x and y . All possible colors then fall under a "guitar-pick" shaped triangle in which the perimeter encompasses spectrally pure colors (seen in nature only in rainbows and prisms) ranging from red to blue. Moving toward the center "dilutes" the color until it ultimately becomes "white". Specifying the x, y coordinates locates a color on the color triangle (ISO/CIE10526, 1991).

The color points traversed by an incandescent object as its temperature is raised can be plotted on the CIE Chromaticity diagram as the "Blackbody curve" and occupies the central white region. Two lamps whose x, y co-ordinates fall one above the Blackbody curve and one below could have the same correlated color temperature (CCT). However, the one above will appear slightly greener, and the one below slightly pinker. This is why two lamps having the same color temperature can still show differences in color as seen by the human eye. Color is complex; attempting to describe the lamp color with just one number (or even with two numbers) does not provide total information on how different materials will appear under that light (CIE Publication, 1986).

The CIE graph in the program “LabView SpectraWiz 6.1 v.1” is displayed in color screen with a black background as shown in Figure 6.6, which is not suitable for the monochrome printing purpose since the colors are not able to be recognized in the black and white mode. All the CIE graphs captured from the program “LabView SpectraWiz 6.1 v.1” were transformed into grayscale mode using the program “Adobe Photoshop v7.0”. Annotations such as “Green”, “Yellow”, “Orange”, “Red”, “Violet”, and “Blue” were added in the modified CIE graphs and the dimensional values of “x” and “y” were also annotated below the graphs as demonstrated in Figure 6.7.

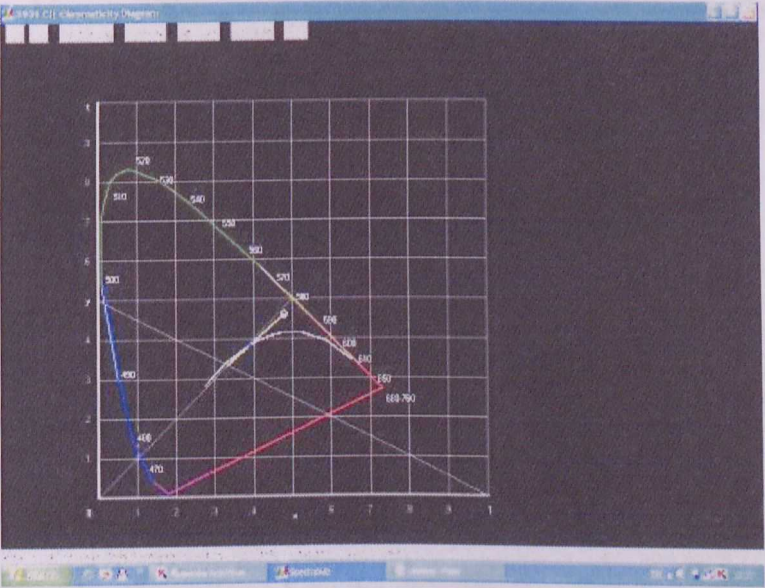
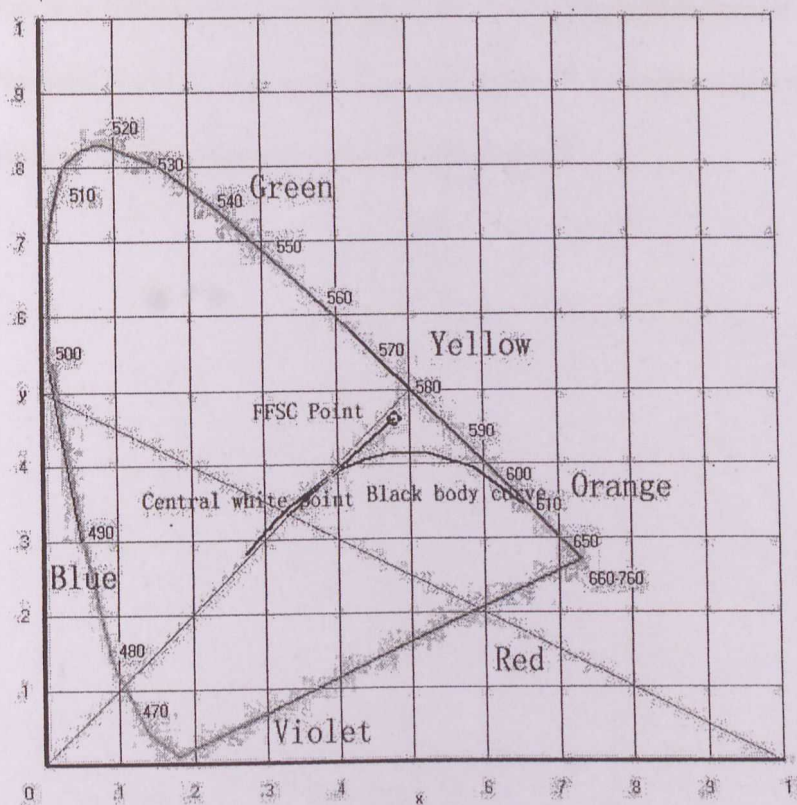


Figure 6.6: CIE graph displayed in “LabView SpectraWiz 6.1 v.1”



Note: $x=0.479$ and $y=0.460$

Figure 6.7: CIE graph modified by "Adobe Photoshop v7.0"

6.3 Summary

This chapter explains how the raw data acquired from the DataHog2 and the EPP2000 spectrometer were restructured and interpreted. Some captured screen and data segments are presented for the explanation. The programs "SkyeLynx Standard v2.6", "Microsoft EXCEL", and "Statistical Package for Social Science (SPSS)" were used in analyzing the data acquired from the DataHog2. Data acquired from the EPP2000 spectrometer was analyzed using the program "LabView SpectraWiz 6.1 v.1" provided by the same supplier. This chapter has interpreted the wavelength graphs and the CIE

graphs displayed in the program “LabView SpectraWiz 6.1 v.1”, and it has introduced that how the graphs were restructured into a presentable format by the program “Adobe Photoshop v7.0”. The next chapter, Chapter 7, provides a detailed discussion about the research findings through the in-depth analysis.

*** Historical Analysis ***

7.1 The solar radiation (PV1) and PV2 output (PV2)

As mentioned in Chapter 5, the radiation measured by Pyranometer 1 (the standard) at the building roof is called as PV1 (W/m²), and the radiation measured by Pyranometer 2 that installed with the thin layer coating on a panel is PV2 (W/m²).

The mean value for PV1 and PV2 in June 6 is shown in Figure 7.1 and 7.2 respectively. The radiation values for PV1 and PV2 in June 6 are 11.05 or 14.54 W/m² and 11.05 or 14.54 W/m² respectively. The hourly diagram of PV1 and PV2 in June 6 is shown in Figure 7.1 and 7.2 respectively. The mean value of PV1 and PV2 in June 6 is shown in Figure 7.1 and 7.2 respectively. The mean value of PV1 and PV2 in June 6 is shown in Figure 7.1 and 7.2 respectively.

APPENDIX 12

Chapter 7

Results of Analysis

7.1 The solar radiation (PY1) and FFSC output (PY2)

As mentioned in Chapter 5, the radiation monitored by Pyranometer 1 that installed on the building roof is denoted as PY1 (W/m^2), and the radiation monitored by Pyranometer 2 that installed with the fiber bundle finishing end is denoted as PY2 (W/m^2).

The mean values for PY1 and PY2 in these 6 months are 307.73 W/m^2 and 17.02 W/m^2 , respectively. The maximum values for PY1 and PY2 in these 6 months are both at 13:00 on 14th June 2008, which are 1308.31 W/m^2 and 64.77 W/m^2 , respectively. The hourly diagram of PY1 and PY2 for seven days in a random week from 2nd June 2008 to 8th June 2008 is presented in Figure 7.1 and Figure 7.2, respectively. The precise values of PY1 and PY2 for these seven days at an interval of 10 minutes are provided in APPENDIX D.

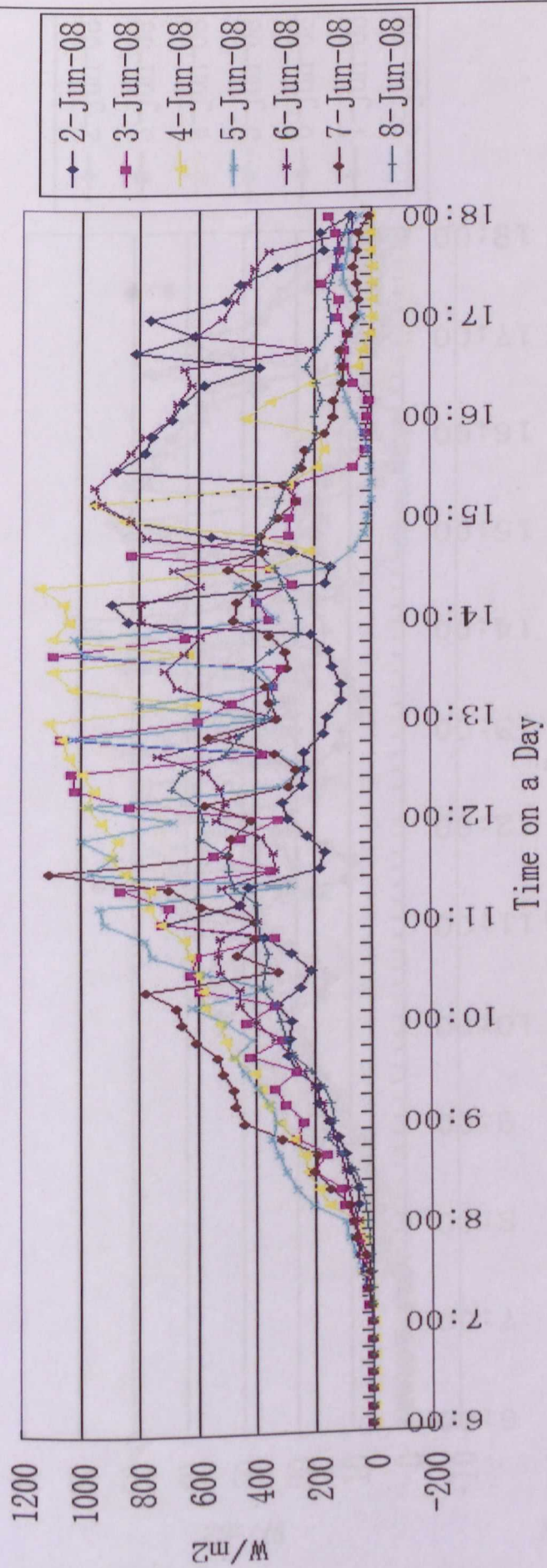


Figure 7.1: hourly PYI for a random week

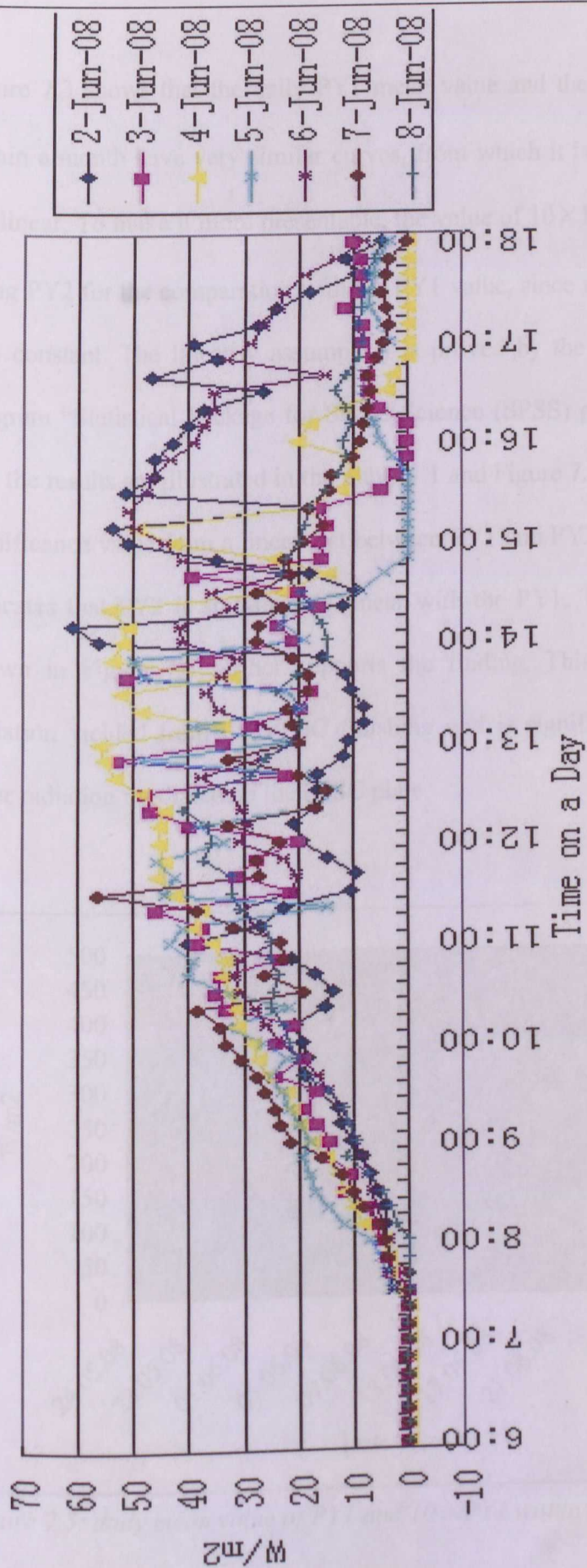


Figure 7.2: hourly PY2 for a random week

Figure 7.3 shows that the daily PY1 mean value and the daily $10 \times \text{PY2}$ mean value within a month have very similar curves, from which it is assumed that PY1 and PY2 are linear. To make it more presentable, the value of $10 \times \text{PY2}$ is plotted here instead of using PY2 for the comparison with the PY1 value, since the magnifying coefficient 10 is a constant. The linearity assumption is proved by the linear test conducted in the program “Statistical Package for Social Science (SPSS) program for Windows98/XP” and the results are illustrated in the Table 7.1 and Figure 7.4. As shown in Table 7.1, the significance value from a linear test between PY1 and PY2 is under a 0.05 level, which indicates that PY2 is significantly linear with the PY1. The linearity-testing graph as shown in Figure 7.4 further supports the finding. This finding concludes that the radiation yielded from the FFSC finishing end is significantly proportional with the solar radiation irradiated on the FFSC plate.

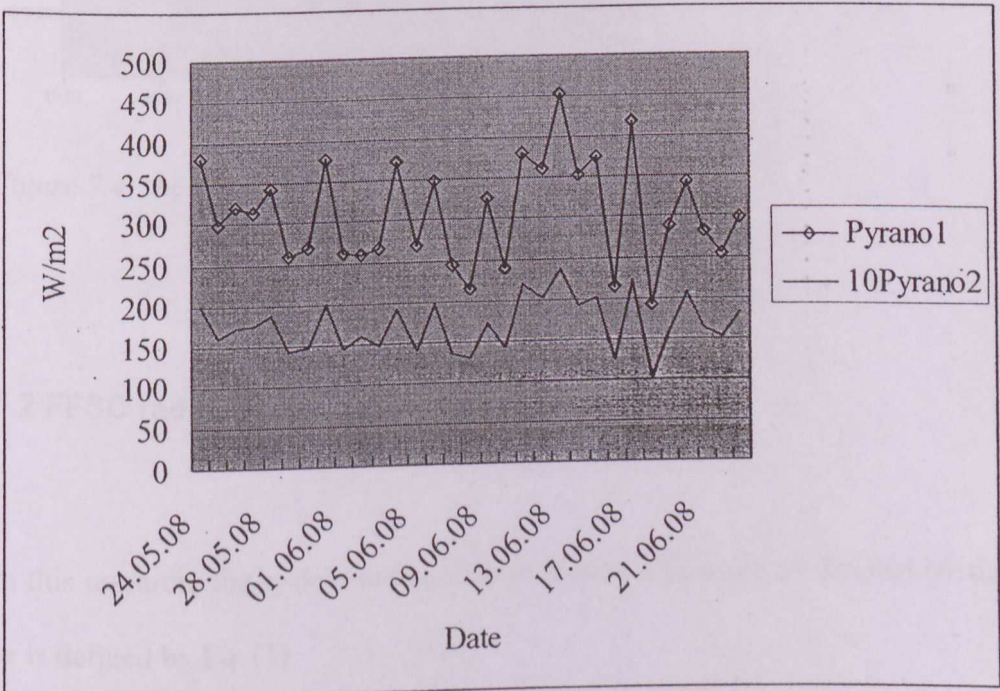


Figure 7.3: daily mean value of PY1 and $10 \times \text{PY2}$ within a month

Table 7.1: the regression test of PY1 and PY2

ANOVA ^b						
Model		Sum of Squares	df	Mean Square	F	Sig.
1	Regression	291.779	1	291.779	458.973	.000 ^a
	Residual	18.436	29	.636		
	Total	310.215	30			

a. Predictors: (Constant), Pyranometer1

b. Dependent Variable: Pyranometer2

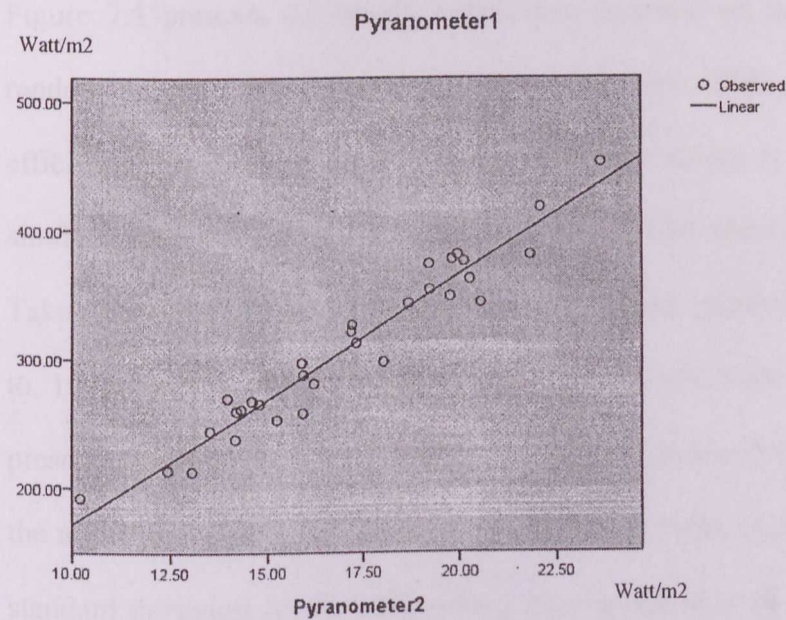


Figure 7.4: the linear test of PY1 and PY2

7.2 FFSC radiation-to-radiation efficiency (η_r)

In this research, the system radiation-to-radiation efficiency as denoted by the variable η_r is defined by Eq. (1).

$$\eta_r = \text{PY2/PY1} \tag{1}$$

Where PY1 is the light radiation monitored by Pyranometer 1 and PY2 is the light radiation monitored by Pyranometer 2. This section presents the FFSC radiation-to-radiation efficiency (η_r) and discusses the hourly and monthly stability of η_r .

7.2.1 Hourly radiation-to-radiation efficiency

Figure 7.5 presents the hourly radiation-to-radiation efficiency for seven days in a random week, from 2nd June 2008 to 8th June 2008. The radiation-to-radiation efficiency from 9:00 to 16:00 appears stable. The curves of these seven days appear a similar trend. The peak values appear at around 7:30 when the sun light is very weak. Taken from Figure 7.5, the curve of the radiation-to-radiation efficiency (η_r) from 7:00 to 17:00 on a random day 4th June 2008 is illustrated in Figure 7.6 for better presentation. On the day 4th June 2008, the maximum value of η_r is 0.11 (at 7:50) and the minimum value is 0.046 (at 17:00). The mean value of η_r on that day is 0.056. The standard deviation for the values on a 10 minutes interval is 0.012, which is under a 0.05 level, so that the radiation-to-radiation efficiency mean value of 0.056 is significantly representative for that day.

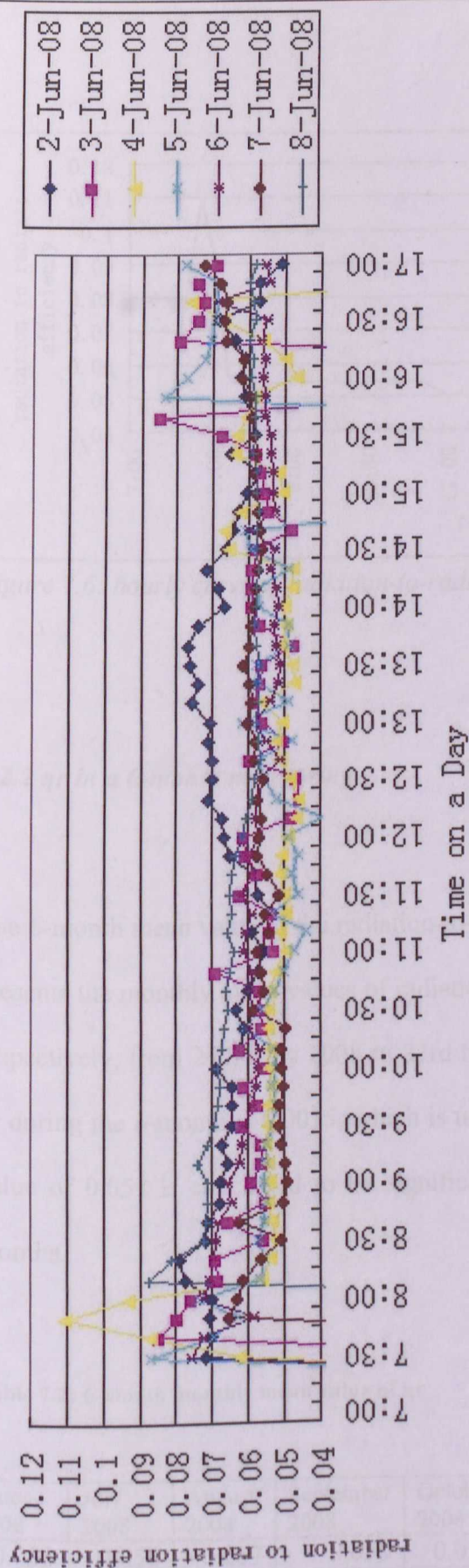


Figure 7.5: hourly curve of radiation-to-radiation efficiency (η_r) in a random week

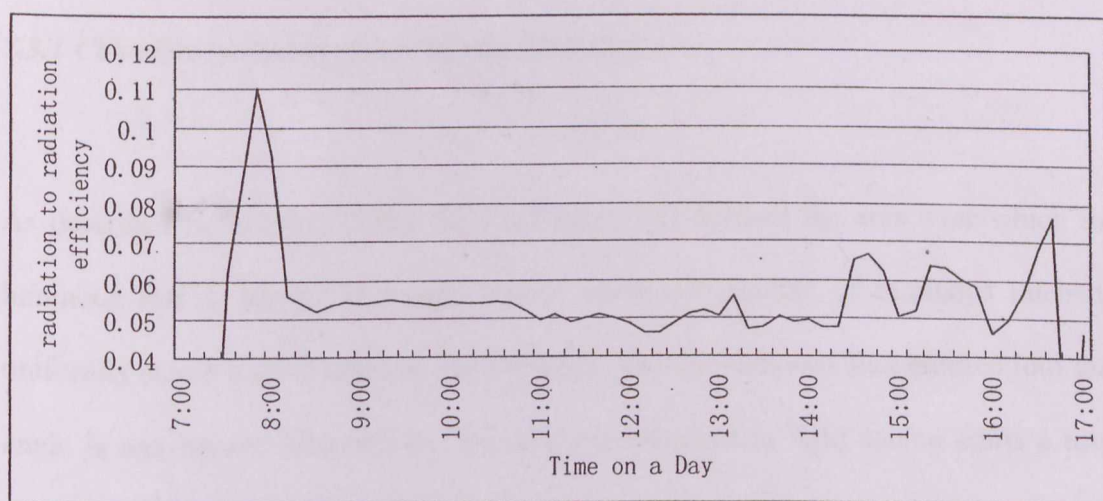


Figure 7.6: hourly curve of radiation-to-radiation efficiency (η_r) on 4th June 2008

7.2.2 η_r in a 6-month monitoring

The 6-month mean value of the radiation-to-radiation efficiency (η_r) is 0.057. Table 7.2 presents the monthly mean values of radiation-to-radiation efficiency in these 6 months respectively, from 24th May 2008 to 23rd November 2008. The standard deviation for η_r during the 6-month is 0.0015, which is under a 0.01 level, so that the monthly mean value of 0.057 is concluded to be significantly stable and representative for these 6 months.

Table 7.2: 6-month monthly mean value of η_r

June 2008	July 2008	August 2008	September 2008	October 2008	November 2008
0.056	0.058	0.057	0.059	0.055	0.056

7.3 System lighting effect

7.3.1 Calculate luminous flux (F) from LUX (E_v)

As described by Schiler (1992), the LUX takes into account the area over which the luminous flux is spread. If a light source emits one candela of luminous intensity uniformly across a solid angle of one steradian, its total luminous flux emitted into that angle is one lumen. Alternatively, an isotropic one-candela light source emits a total luminous flux of exactly 4π lumens. If the source were partially covered by an ideal absorbing hemisphere, that system would radiate half as much luminous flux, which is only 2π lumens. The luminous intensity would still be one candela in those directions that are not obscured (Schiler, 1992). The luminous flux (F) for one FFSC finishing end in this research is therefore calculated in Eq. (2):

$$F = E_v \times S_{hs} \quad (2)$$

Where the E_v is the values detected by the LUX sensor and the S_{hs} is the half sphere's surface area radiated by the light source, the FFSC finishing end. The distance between the finishing end and the LUX sensor as denoted by R_l is 0.1m. So that the radiated half sphere's surface area is calculated in Eq. (3) as below:

$$S_{hs} = 2\pi R_l \times R_l = 2 \times 3.14 \times 0.1 \times 0.1 = 0.063\text{m}^2 \quad (3)$$

Therefore, the luminous flux (F) of one finishing end is calculated as shown in Eq. (4):

$$F=E_v \times Sh_s=0.063E_v$$
(4)

Where E_v is the illuminance values detected by the LUX sensor.

Eq. (4) indicates that the luminous flux (F) of one FFSC finishing end is proportional to the illuminance values. By using Eq. (4), the luminous flux (F) of one FFSC finishing end is calculated in Table 7.3.

Table 7.3: conversion from LUX to luminous flux

Illuminance (LUX)	luminous flux (<i>lumen</i>)
400	25.2
600	37.8
800	50.4
1000	63.0
1200	75.6
1400	88.2
1600	100.8
1800	113.4
2000	126.0

Figure 7.7 presents the hourly illuminance (LUX) for seven days in a random week, from 2nd June 2008 to 8th June 2008 (Monday to Sunday). The precise values of the illuminance (LUX) for these seven days at an interval of 10 minutes are provided in APPENDIX D. As shown in Figure 7.7, for most of the time in the duration from 9:00 to 16:00, which almost covers the main office hours on a day, the lighting effect provided by one of the FFSC finishing end is above 400 LUX (equals to a luminous flux of 25.2 lumens). By using Eq. (4) and Table 7.3, the seven-day hourly luminous flux of one FFSC finishing end is calculated and illustrated in Figure 7.8. As presented in Figure 7.8, one FFSC finishing end could provide a luminous flux of from 20 lumens to 110 lumens during the office hour from 9:00 to 17:00.

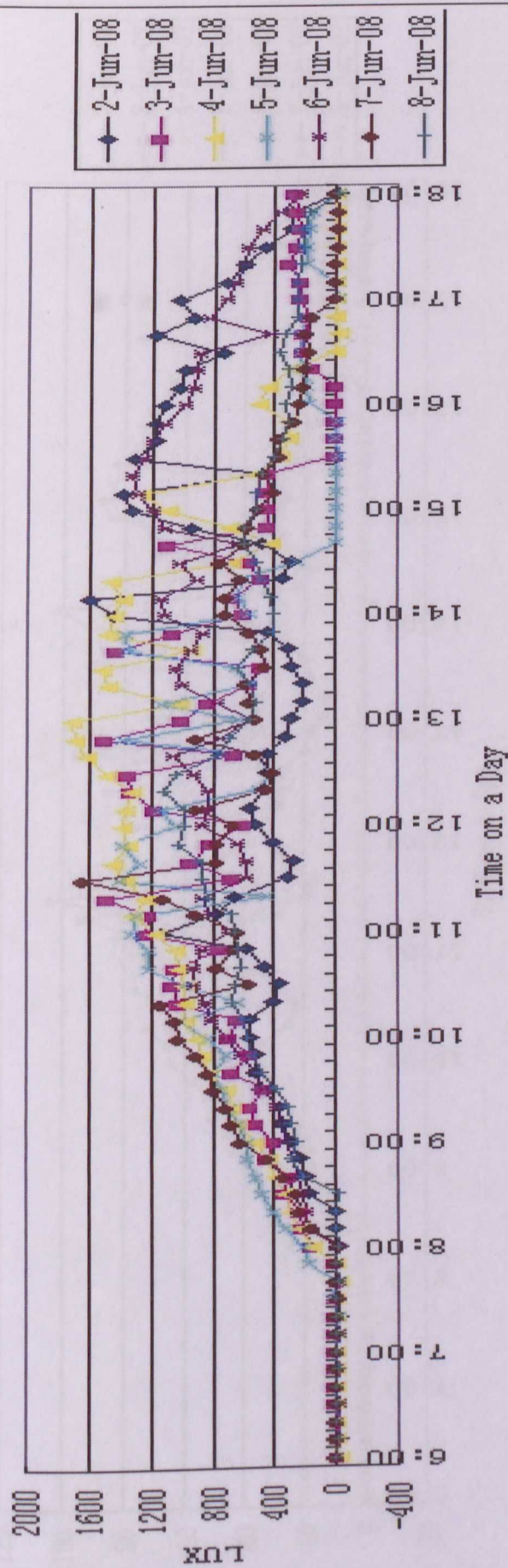


Figure 7.7: hourly LUX values in a random week

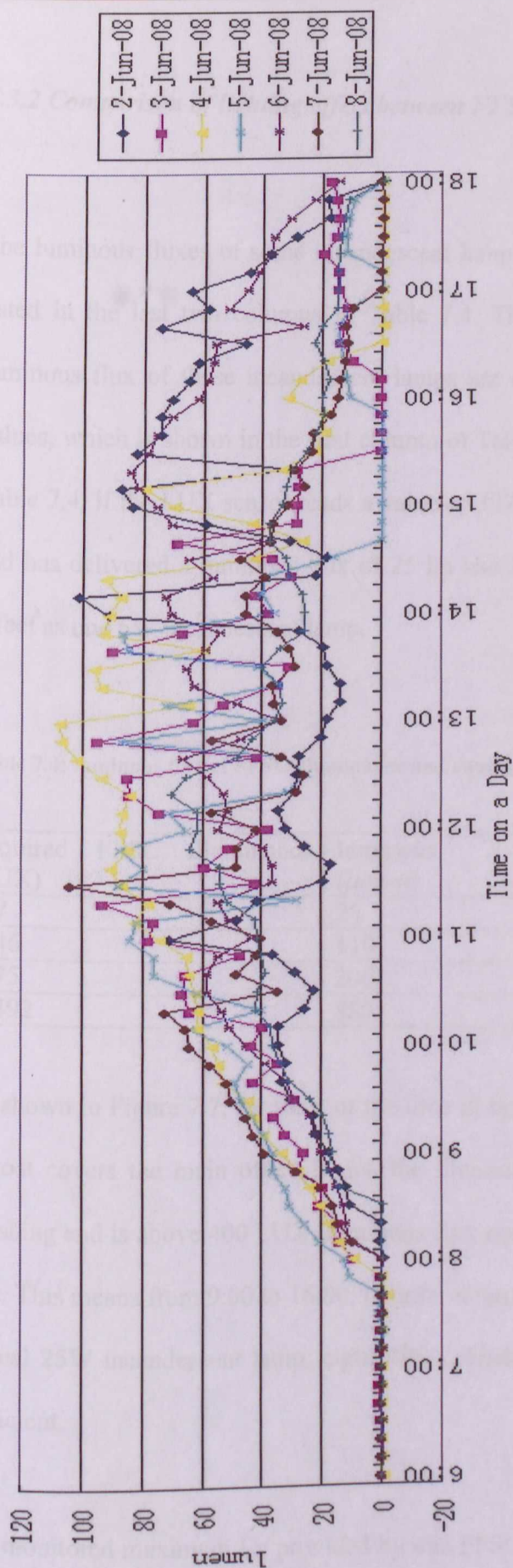


Figure 7.8: hourly luminous flux in a random week

7.3.2 Comparison of lighting effect between FFSC and incandescent lamps

The luminous fluxes of some incandescent lamps (Egan, 1983; Wikipedia, 2009b) are listed in the last two columns in Table 7.4. Through calculation using Eq. (4), the luminous flux of these incandescent lamps are converted into the FFSC illuminance values, which is shown in the first column of Table 7.4. For instance in the first row in Table 7.4, if the LUX sensor reads a value of 397 LUX, that means the FFSC finishing end has delivered a luminous flux of 25 lm and it has achieved an equivalent lighting effect as one 5W incandescent lamp.

Table 7.4: luminous flux of FFSC illuminance and equivalent incandescent lamps

Required FFSC illuminance (LUX)	luminous flux (lumen)	Watt of equivalent Lamps
397	25	5W
1746	110	15W
3175	200	25W
13492	850	60W

As shown in Figure 7.7, for most of the time in the duration from 9:00 to 16:00, which almost covers the main office hours, the illuminance provided by one of the FFSC finishing end is above 400 LUX (luminous flux equals to 25 lumens according to Table 7.4). This means from 9:00 to 16:00, in order to provide 200 lumens that equivalent to a typical 25W incandescent lamp, eight FFSC finishing ends or four FFSC systems are sufficient.

The monitored maximum E_v provided by one FFSC finishing end in these 20 days was 1811 LUX, which appeared at 13:00 on 31 of May 2008, when the solar radiation PYI

was 1156.13W/m². The luminous flux (F) of a finishing end at that time equals to 114.1 lumens as calculated by Eq. (4). It is higher than that of a 15W incandescent lamp (110 lumens) according to Table 7.4. However, a typical room normally requires a 60W bulb (850 lumens), which means totally eight FFSC finishing ends or four FFSC systems are required to deliver a equivalent lighting effect.

7.4 Energy-to-energy efficiency (η_e)

The energy-to-energy efficiency denoted by η_e in this research is defined as the ratio of total energy output yielding from both finishing ends divided by the solar energy irradiated on the fluorescent fibers, which is illustrated by Eq. (5):

$$\eta_e = P_{out}/P_{sun} \quad (5)$$

Where P_{out} is the total energy output yielding from both finishing ends and P_{sun} is the solar energy irradiated on the fluorescent fibers. The effective area of the FFSC plate is calculated in Eq. (6) as follows:

$$S_0 = D \times L \times n = 0.002 \times 1 \times 150 = 0.3 \text{ m}^2 \quad (6)$$

Where D and L are the diameter and the length of the fluorescent fibers respectively. The variable n is the number of piece for the fluorescent fibers, which is 150. The effective area of one finishing end is calculated as shown in Eq. (7):

$$S_f = \pi \times R_f \times R_f = 3.14 \times 0.015 \times 0.015 = 0.0007 \text{ m}^2 \quad (7)$$

Where R_f is the radius of the finishing end.

Therefore, the energy-to-energy efficiency η_e is calculated as shown in Eq. (8):

$$\begin{aligned}\eta_e &= P_{out}/P_{sun} \\ &= 2 \times PY_2 \times S_f / (PY_1 \times S_0) \\ &= (2 \times 0.0007 / 0.3) PY_2 / PY_1 = 0.0047 PY_2 / PY_1\end{aligned}\tag{8}$$

Where $PY_2/PY_1 = \eta_r$ as defined by Eq. (1),

Therefore,

$$\eta_e = 0.0047 \eta_r\tag{9}$$

The average radiation-to-radiation efficiency denoted by η_r -avg in these 6 months is 0.057 as mentioned in Section 7.2.2, which is shown in Eq. (10):

$$\eta_r\text{-avg} = 0.057\tag{10}$$

So that the average energy-to-energy efficiency in these 6 months is calculated in Eq.

$$\begin{aligned}(11): \\ \eta_e\text{-avg} &= 0.0047 \times \eta_r\text{-avg} = 0.0047 \times 0.057 = 0.000268\end{aligned}\tag{11}$$

The mean value of energy-to-energy efficiency is low at 0.000268. This reveals that FFSC currently is not suitable to replace the conventional PV cells for power production as present.

7.5 Luminous efficacy (K) of FFSC

Luminous efficacy is a figure of merit for light sources. It is the ratio of luminous flux (in lumens) to power (usually measured in watts). As most commonly used, it is the ratio of luminous flux emitted from a light source to the power consumed by the source, and thus describes how well the source provides visible light from a given amount of energy (Yoshi, 2004). Accordingly, the luminous efficacy (K) for FFSC is defined by Eq. (12):

$$K=2F/P_{\text{sun}} \quad (12)$$

Where F is the luminous flux produced by one finishing end, and P_{sun} is the solar energy irradiated on the fluorescent fibers. Since there are two finishing ends equally sharing the irradiation from the fluorescent fibers, the coefficient “2” is used here in Eq. (12). Therefore, the luminous efficacy (K) is calculated as shown in Eq. (13):

$$K=2F/P_{\text{sun}}=2 \times 0.063\text{Ev}/(\text{PY1} \times S_0)=2 \times 0.063\text{Ev}/(\text{PY1} \times 0.3)=0.42\text{Ev}/\text{PY1} \quad (13)$$

A significant value of 0.01 as shown in Table 7.5 in the linear test conducted for Ev and PY1 indicates that the values of Ev and PY1 are linear so that Ev/PY1 is considered

here as a comparatively stable value. Hence, an average ratio of Ev/PY1 could be used in the above equation as a constant in general. From the monitored data, the monthly mean value of Ev/PY1 is calculated as 1.53. Therefore, the luminous efficacy (K) of the FFSC finishing end is shown in Eq. (14):

$$K=0.42\times Ev/PY1=0.42\times 1.53=0.643lm/W \tag{14}$$

Table 7.5: linear test for Ev and PY1

Coefficients(a)					
Model	Unstandardized Coefficients		Standardized Coefficients	t	Sig.
	B	Std. Error	Beta		
1 (Constant)	-8.389	3.234		-2.594	.010
LUX	.657	.005	.987	136.389	.000

a Dependent Variable: PY1

The value of FFSC luminous efficacy is below that of the natural daylight, which generally falls within the range 100lm/W to 130lm/W (Lam & Li, 1996). When compared to standard artificial light sources (Lam & Li, 1996) such as incandescent light bulbs (16 - 40 lm/W) and fluorescent lamps (50 - 80 lm/W), the FFSC luminous efficacy as 0.643lm/W is considered low. However, it is higher than the luminous efficacy of a combusting candle at 0.3 lm/W according to Wapedia (2009). Furthermore, since the sun light is free, different from all the electrical light sources, the low luminous efficacy of FFSC does not mean any electricity consumption when it is under operation.

7.6 Light-to-light efficiency (η_l) evaluation

Light-to-light efficiency is the ratio of output luminous flux to the input luminous flux (Earp et al., 2004; Yoshi, 2004). Evaluation is conducted to calculate the ratio of the luminous flux yielding from the two FFSC finishing ends to the luminous flux dropping on the fluorescent fibers and it is defined here as the light-to-light efficiency (η_l). The luminous flux yielding from a FFSC finishing end is denoted as F , and it has been calculated in Eq. (4). The luminous flux dropping on the fluorescent fibers is denoted as $F0$, and the luminous flux is from the solar irradiation. Accordingly, the light-to-light efficiency (η_l) is defined by Eq. (15):

$$\eta_l = 2F/F0 \quad (15)$$

The value of $F0$ could be calculated from either the illuminance (LUX) or the radiation (W/m^2) (Yoshi, 2004; Schiler, 1992). Since in this experimentation only a Pyranometer instead of a LUX sensor is installed to measure the solar irradiation, the values of $F0$ are calculated from the solar radiation PY1 (W/m^2). The luminous flux is the product of the irradiation energy and the luminous efficacy of the irradiation (Yoshi, 2004; Schiler, 1992). Therefore, the luminous flux dropping on the fluorescent fibers is calculated in Eq. (16):

$$F0 = (PY1 \times S0) \times K0 \quad (16)$$

Where $S0$ is the total effective area of the fluorescent fibers on the FFSC plate and it is calculated as 0.3 m^2 by Eq. (6). $K0$ is the luminous efficacy of the sunlight. According

to Lam & Li (1996), the luminous efficacy of the sunlight K0 is remarkably stable and it generally falls within the range 100lm/W to 130lm/W.

By synthesizing Eq. (4), Eq. (15) and Eq. (16), the FFSC light-to-light efficiency (η_l) is calculated as shown in Eq. (17):

$$\eta_l = 2F/F0 = 2 \times 0.063E_v / (PY1 \times 0.3 \times K0) = (0.42/K0) \times (E_v/PY1) \quad (17)$$

From the monitored data, the monthly mean value of $E_v/PY1$ is stable and is calculated as 1.53 as mentioned in Section 7.5. The Eq. (17) is therefore transformed into Eq. (18):

$$\eta_l = (0.42/K0) \times (E_v/PY1) = (0.42/K0) \times 1.53 = 0.64/K0 \quad (18)$$

According to Lam & Li (1996), the luminous efficacy of the sunlight K0 generally falls within the range 100lm/W to 130lm/W. By substituting this range into Eq. (18), the evaluated FFSC light-to-light efficiency (η_l) falls within the range 0.49% to 0.64%.

Comparing to the light-to-light efficiency of the LSC produced by Earp et al. (2004) as 6%, the FFSC light-to-light efficiency is low. This is because of the small cross sectional area of the fluorescent fibers in FFSC. However, there is no comparability between FFSC and Earp et al.'s LSC because the size and the form of these two types of cross sections are greatly different. The cross sectional area of the fluorescent fiber in FFSC is only 12.56 mm² but the cross sectional area of the Earp et al.'s (2004) LSC is 270mm². The cross section of the LSC produced by Earp et al. (2004) is a 2mm × 135mm rectangular section. Since solar photons entering the FFSC plate are absorbed by the luminescent species and reemitted in random directions, a large fraction of the

emitted photons lose from the escape cones. The size and the form of the cross section could impact on the proportion of photons trapped by the LSC plate and the reduction of the cross sectional area of the luminescent plate could increase the photon loss (Richards, 2006; Reisfeld, 2001; Batchelder et al., 1979; Hammam et al., 2007). Accordingly, the light-to-light efficiency of the FFSC could be raised by increasing the diameter of the fluorescent fibers embedded. Therefore, in future study, the fluorescent fibers with a large diameter, say 10mm diameter, is recommended for the testing in FFSC system. This is expected to increase the light-to-light efficiency of FFSC and it will not bring extra difficulties for wiring. Moreover, a study on the relationship between the diameter and the light-to-light efficiency for fluorescent fibers is also recommended. Even though the light-to-light efficiency of FFSC appears lower than the LSC produced by Earp et al. (2004), FFSC has a greater advantage in wiring as it is designed to be, because the light transportation media of FFSC are optical fibers but this is difficult for the LSC produced by Earp et al. (2004) to achieve.

7.7 The negative trend between radiation-to-radiation efficiency (η_r) and solar radiation (PY1)

Based on the monitored 10167 sets of effective data in the 6 months from 6:00 to 20:00 at an interval of 10 minutes, the system radiation-to-radiation efficiency (η_r) presents a holistic negative trend with the solar radiation PY1. As shown in Figure 7.9, all these 10167 sets of data are symmetrically sorted by the radiation-to-radiation efficiency (η_r) in an ascending order while the corresponding values of the solar radiation (PY1) present a descending trend.

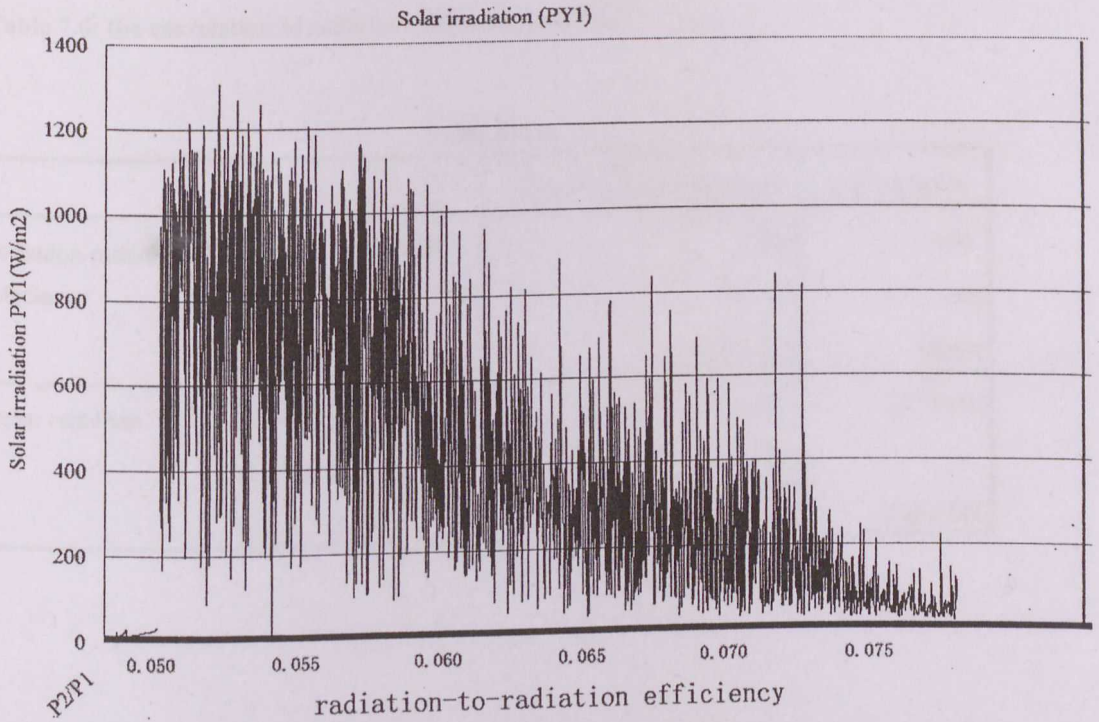


Figure 7.9: negative trend between radiation efficiency and PY1

There is a negative correlation coefficient (-0.643) in Table 7.6 between the radiation-to-radiation efficiency and the solar radiation, indicating that the relationship between these two variables is that the values of one variable decrease as the other increases. However, this kind of negative trend does not indicate a strictly negative association, for the negative correlation coefficient (-0.643) is not significantly under a 0.01 level. The reason for the negative trend between the radiation-to-radiation efficiency (η_r) and the solar radiation (PY1) is not discussed here because it may be beyond the researchers' specialized knowledge and it is recommended in the future study.

Table 7.6: the correlation of radiation efficiency and PY1

Correlations			
		radiation-radiation efficiency	solar radiation
radiation-radiation efficiency	Pearson Correlation	1.000	-.643**
	Sig. (2-tailed)		.000
	N	10167.000	10167
solar radiation	Pearson Correlation	-.643**	1.000
	Sig. (2-tailed)	.000	
	N	10167	10167.000

7.8 Matching the natural light: CIE color analysis and wavelength (λ) test

The CIE color analysis and wavelength test for the artificial light produced by the FFSC were conducted on a random day 16th Oct 2008 from 9:00 to 15:00. The weather on that day was sunny with a clear sky from 9:00 to 11:00, while from 11:30 to 13:30 it was sunny with little clouds. Since 14:00, it was overcast and raining until the evening.

The device used for the CIE color analysis and the wavelength test is the EPP2000&ISA2000 spectrometer as introduced in Chapter 5, the responding range for which is from 190nm to 2200nm. Since the visible light waveband drops between 400nm to 700nm (Geoffrey, 2004), and according to Geoffrey (2004) and Earp et al. (2004), the average wavelength for the white light is around 555nm, therefore, this device is suitable for the test described in this section.

The detector of the spectrometer was placed towards the FFSC finishing end at the distances of 10cm, 20cm, 30cm, 40cm, 50cm, 80cm, and 100cm, respectively. The reason for using these various distances is to prove that the light yielding out of the finishing end could considerably mix into a white color light through a short distance by self-scattering.

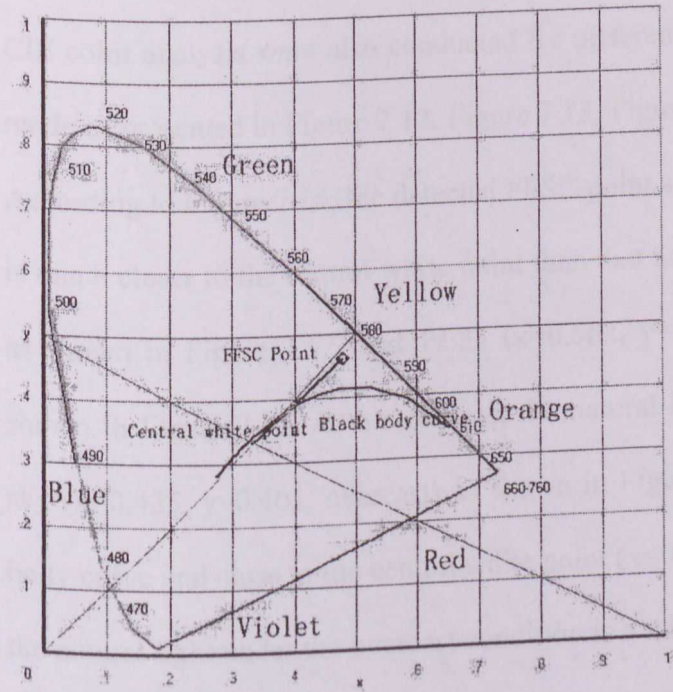
In order to find out the relationship between the output color and the various sky conditions, a same group of tests was repeated three times on 16th Oct 2008. The first group of tests was conducted at around 10:00 (clear sky), and it was repeated at around 12:30 (sunny with little clouds). The last group of tests was conducted at around 14:30 (overcast).

7.8.1 CIE color analysis

A CIE color analysis was conducted under the irradiant mode at around 12:30 (sunny with little clouds) on a random day on 16th Oct 2008. Figure 7.10 presents the screen of the detected data. As indicated in Figure 7.10, the solid curve in the right of the diagram is the black body curve. There are two diagonals forming a cross in the central area and the cross point is indicated as “central white point” in the diagram, where $x=0.333$, $y=0.333$. Any detected point drops on or near this central white point is considered as white color (Yoshi, 2000). The FFSC point in the diagram drops between the central white point and the yellow area, where $x=0.479$ and $y=0.460$, indicating that the FFSC light output at a 10cm distance to the light detector leans a bit towards the yellow area comparing to the absolutely white light. Referring to the CIE diagram for the direct sun

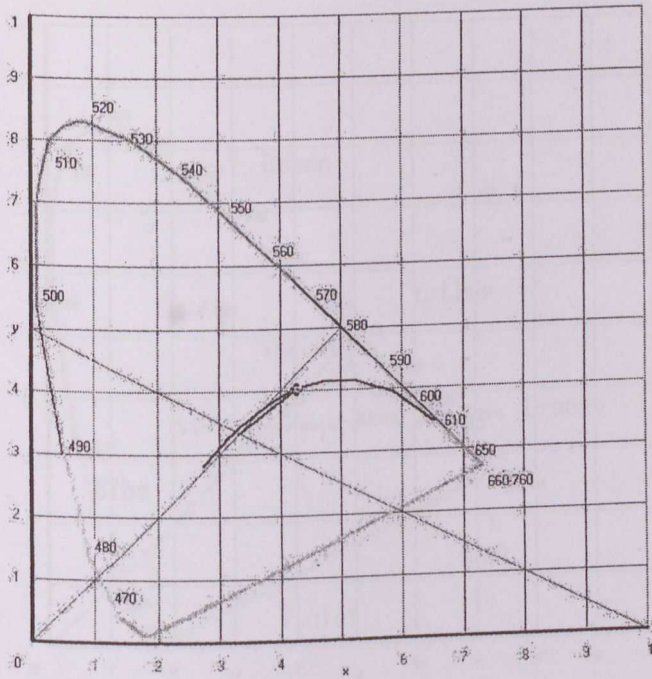
light ($x=0.427, y=0.401$) shown in Figure 7.11, the FFSC point ($x=0.479$ and $y=0.460$) appears a great match to the direct sun light. Therefore, it concludes that the FFSC light output under a sunny sky is a kind of yellow-white color light and its color has a good match to that of the direct sunlight. According to Yoshi (2000) and Schiler (1992), a yellow-white color light is comforting to human eyes.

It is noticed that as the distance between the detector and the finishing end increases from 10cm to 100cm, the FFSC points in CIE diagrams are getting closer to the yellow area and getter apart from the white color region around the cross point (central white point) in the middle of the diagram, as indicated in from Figure B1 to Figure B8 as enclosed in APPENDIX B.



Note: $x=0.479, y=0.460$

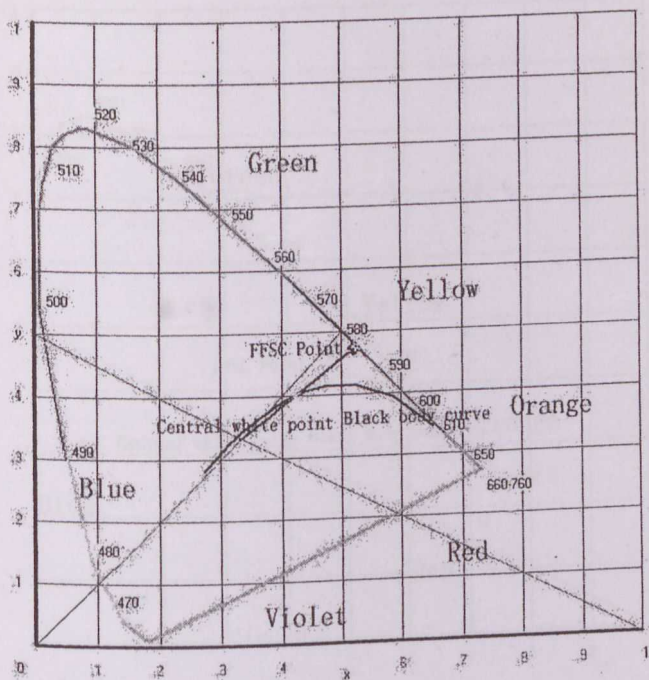
Figure 7.10: CIE color analysis 10cm 12:27, 16OCT2008



Note: $x=0.427$, $y=0.401$

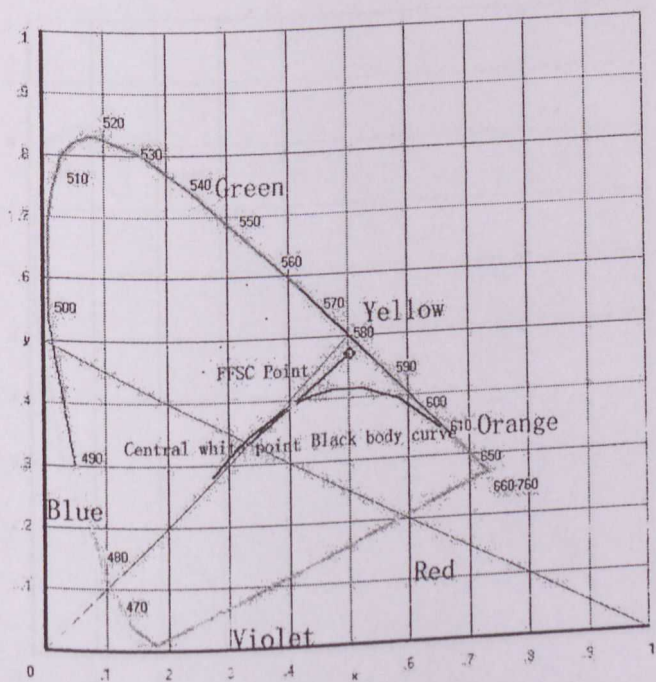
Figure 7.11: CIE color analysis for direct sun light 11:33, 12Nov2008

CIE color analysis were also conducted for different sky conditions under the irradiant mode as presented in Figure 7.12, Figure 7.13, Figure 7.14, and Figure 15, respectively. According to Figure 7.14, the detected FFSC point at 14:36 ($x=0.481$, $y=0.449$, overcast) is much closer to the central white point than that at 9:50 ($x=0.520$, $y=0.471$, clear sky) as shown in Figure 7.12, and 12:33 ($x=0.502$, $y=0.470$, sunny with little clouds) as shown in Figure 7.13. As a reference, the natural light color point under the overcast sky ($x=0.425$, $y=0.403$, overcast) as shown in Figure 7.15 is just located on the black body curve and close to the central white point ($x=0.333$, $y=0.333$), which indicates that the natural light under the overcast condition is a white light. Therefore, the light output of FFSC in all the sky conditions is proved to be a kind of yellow-white color light. In addition, under the overcast sky, the FFSC light color is whiter than that under the clear sky condition.



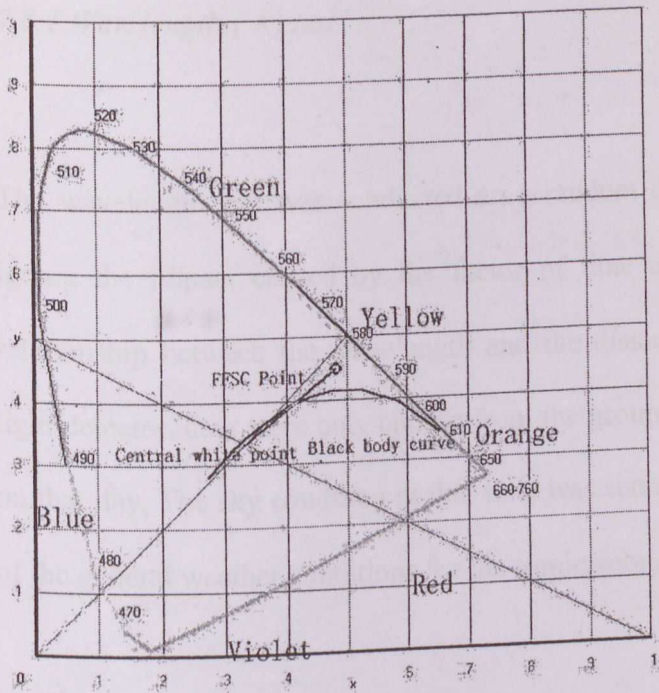
Note: $x=0.520$, $y=0.471$

Figure 7.12: CIE color analysis 9:50, 16OCT2008 (clear sky)



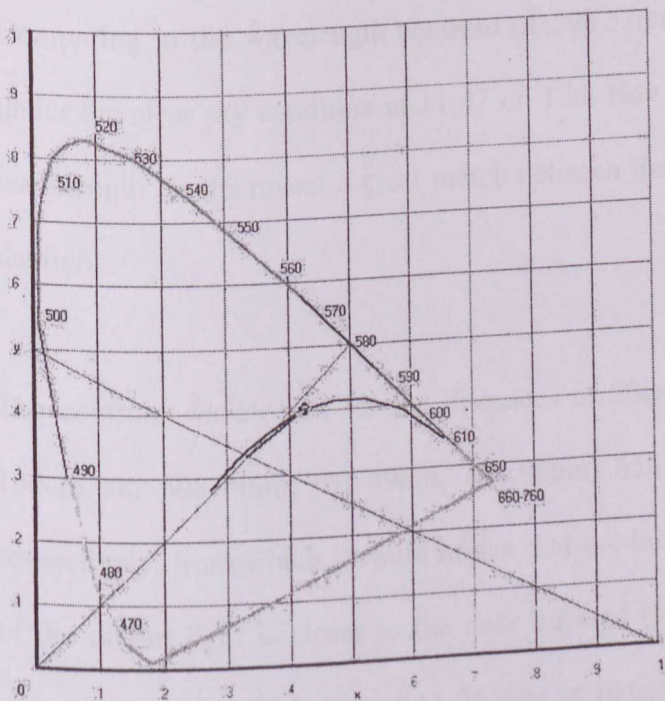
Note: $x=0.502$, $y=0.470$

Figure 7.13: CIE color analysis 12:33, 16OCT2008 (sunny with little clouds)



Note: $x=0.481$, $y=0.449$

Figure 7.14: CIE color analysis 14:36, 16OCT2008 (overcast)



Note: $x=0.425$, $y=0.403$

Figure 7.15: CIE color analysis natural daylight overcast 2nd Nov 2008

7.8.2 Wavelength (λ) test

The wavelength test was conducted on a random day on 16th Oct 2008. In order to ignore the impact caused by the factor of time and the weather, in analyzing the relationship between the wavelength and the distances from the finishing end to the light detector, data were only chosen from the group of tests conducted at around 12:30 on that day. The sky condition at that time was sunny with little clouds, which was one of the general weather conditions for the tropic zone.

Figure 7.16 presents a wavelength screen in the scope mode at 12:23 on 16th Oct 2008 at a distance of 10cm from the FFSC finishing end to the detector, from which it indicates on the top of the screen that the centroid is 607.31nm. The wave band as 607.31nm is not far from the average band for the white light, which is 555nm. Comparing to the wavelength centroid of 598.57nm captured for the natural daylight under the clear sky condition at 11:47 on 12th Nov 2008 as shown in Figure 7.17, the wavelength results reveal a great match between the FFSC light output and the natural daylight.

The centroid wavelength for the distances at 20cm, 30cm, 40cm, 50cm, 80cm, and 100cm are 608.74nm, 610.49nm, 610.00nm, 654.29nm, 653.59nm, and 653.52nm, respectively, from which it could notice that the longer the distance is, the wavelength of the output light is closer to the near infrared (NIR) area and more apart from the white light band which is around 555nm as indicated in Figure A1 to Figure A8 in APPENDIX A as enclosed.

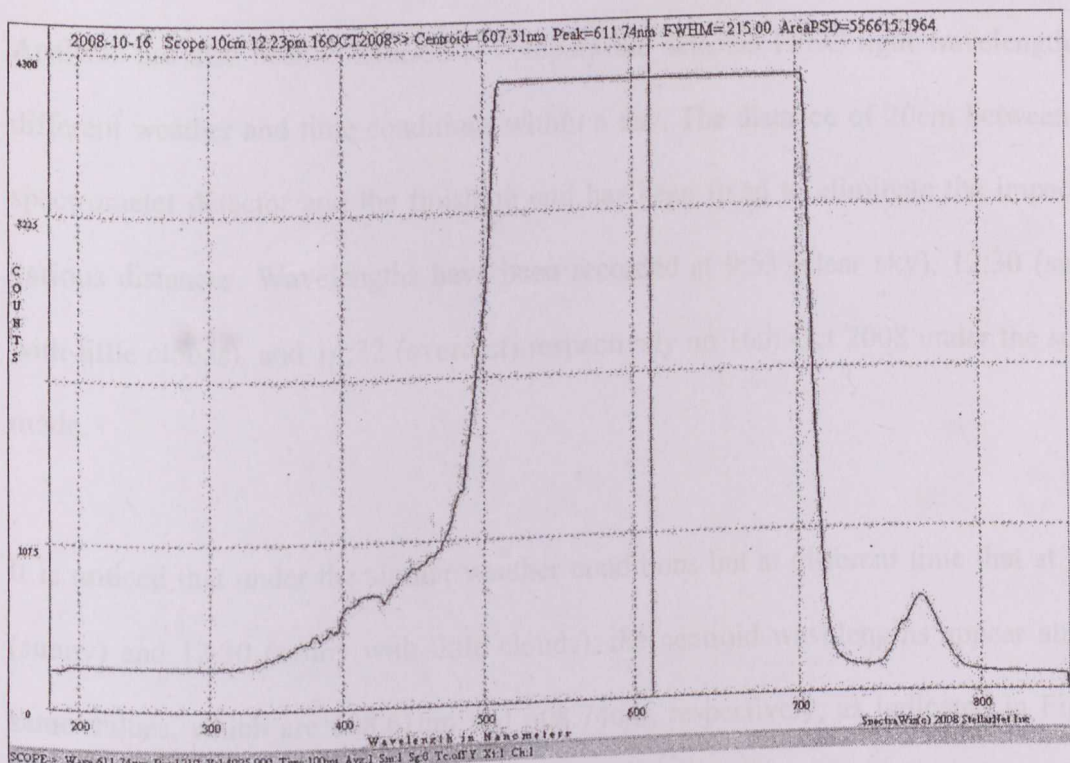


Figure 7.16: wavelength Scope mode 10cm 12:23, 16OCT2008

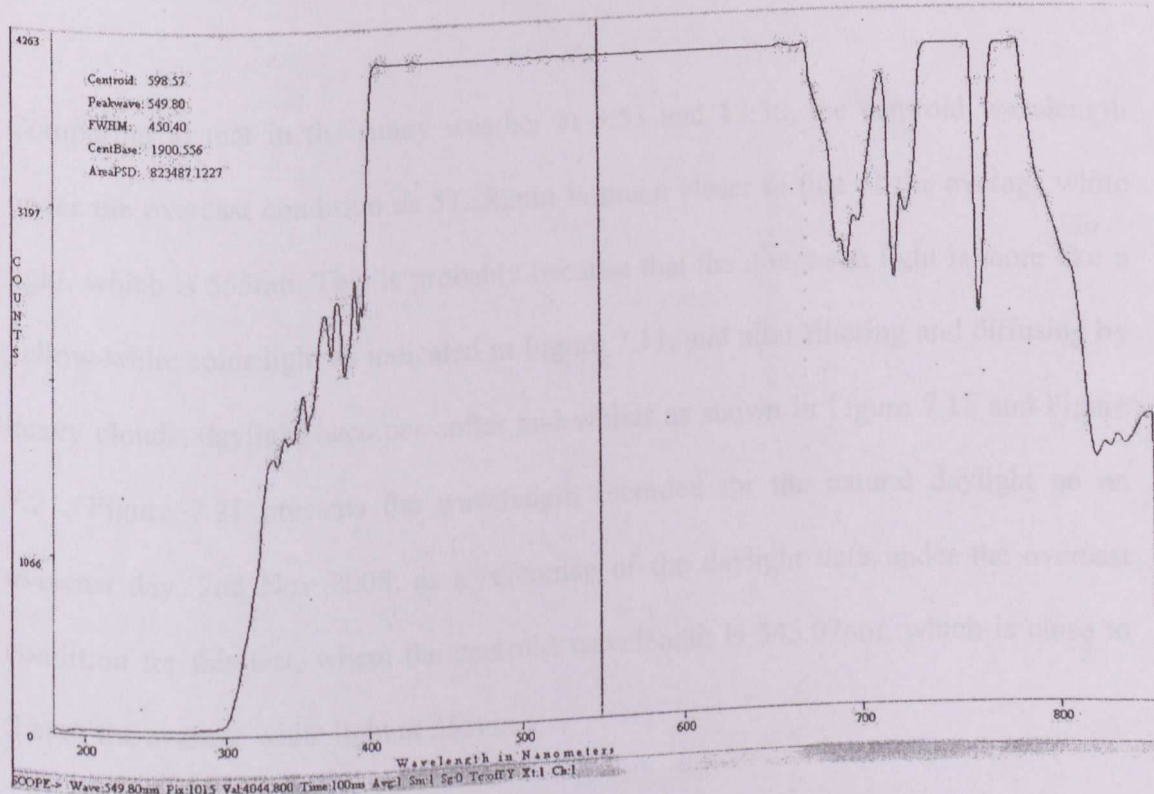


Figure 7.17: wavelength Scope mode natural light at sunny condition 11:47, 12Nov2008

Analysis has also been conducted to compare the detected FFSC light wavelengths in different weather and time conditions within a day. The distance of 20cm between the spectrometer detector and the finishing end has been fixed to eliminate the impact of various distances. Wavelengths have been recorded at 9:53 (clear sky), 12:30 (sunny with little clouds), and 14:32 (overcast) respectively on 16th Oct 2008 under the scope mode.

It is noticed that under the similar weather conditions but at different time that at 9:53 (sunny) and 12:30 (sunny with little clouds), the centroid wavelengths appear almost same values, which are 608.61nm and 608.74nm, respectively, as indicated in Figure 7.18 and Figure 7.19. However, differences has emerged when the weather rapidly changed into the overcast condition at 14:32 on that day, when the centroid wavelength dramatically moved into 572.82nm as indicated in Figure 7.20.

Comparing to that in the sunny weather at 9:53 and 12:30, the centroid wavelength under the overcast condition as 572.82nm is much closer to that of the average white light, which is 555nm. This is probably because that the direct sun light is more like a yellow-white color light as indicated in Figure 7.11, and after filtering and diffusing by heavy clouds, daylight becomes softer and whiter as shown in Figure 7.15 and Figure 7.21. Figure 7.21 presents the wavelength recorded for the natural daylight on an overcast day, 2nd Nov 2008, as a reference of the daylight data under the overcast condition for this test, where the centroid wavelength is 545.07nm, which is close to that of the average white light at 555nm.

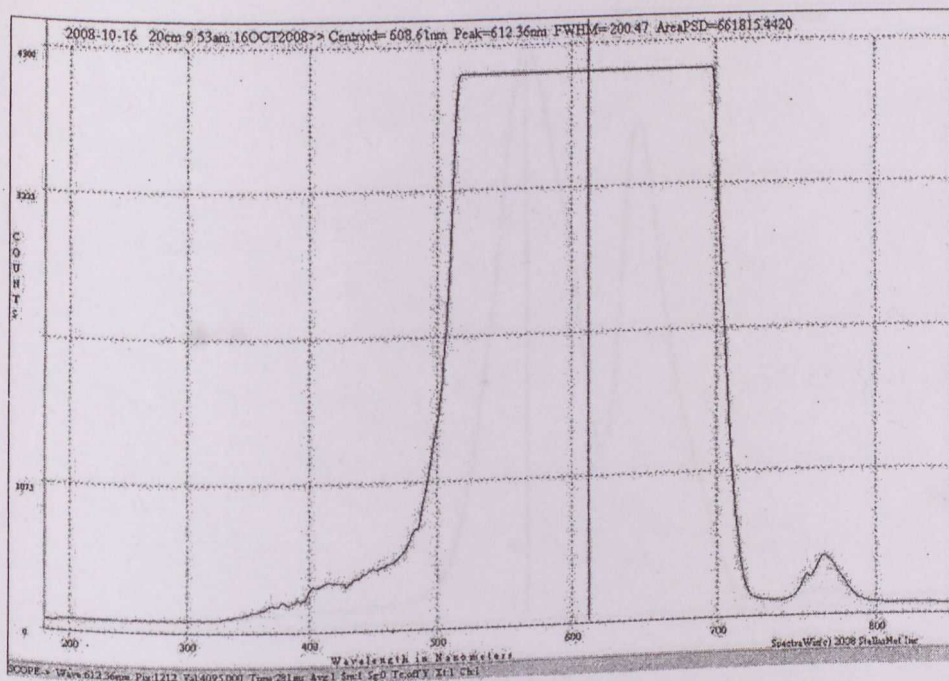


Figure 7.18: wavelength Scope mode 20cm 9:53, 16OCT2008

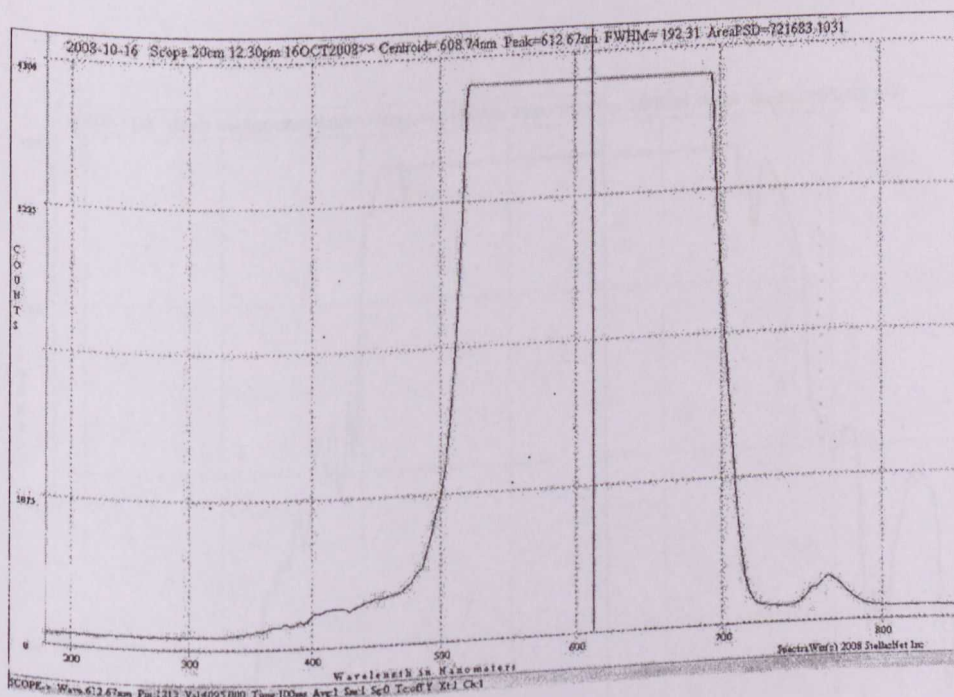


Figure 7.19: wavelength Scope mode 20cm 12:30, 16OCT2008



Figure 7.20: wavelength Scope mode 20cm 14:32, 16OCT2008

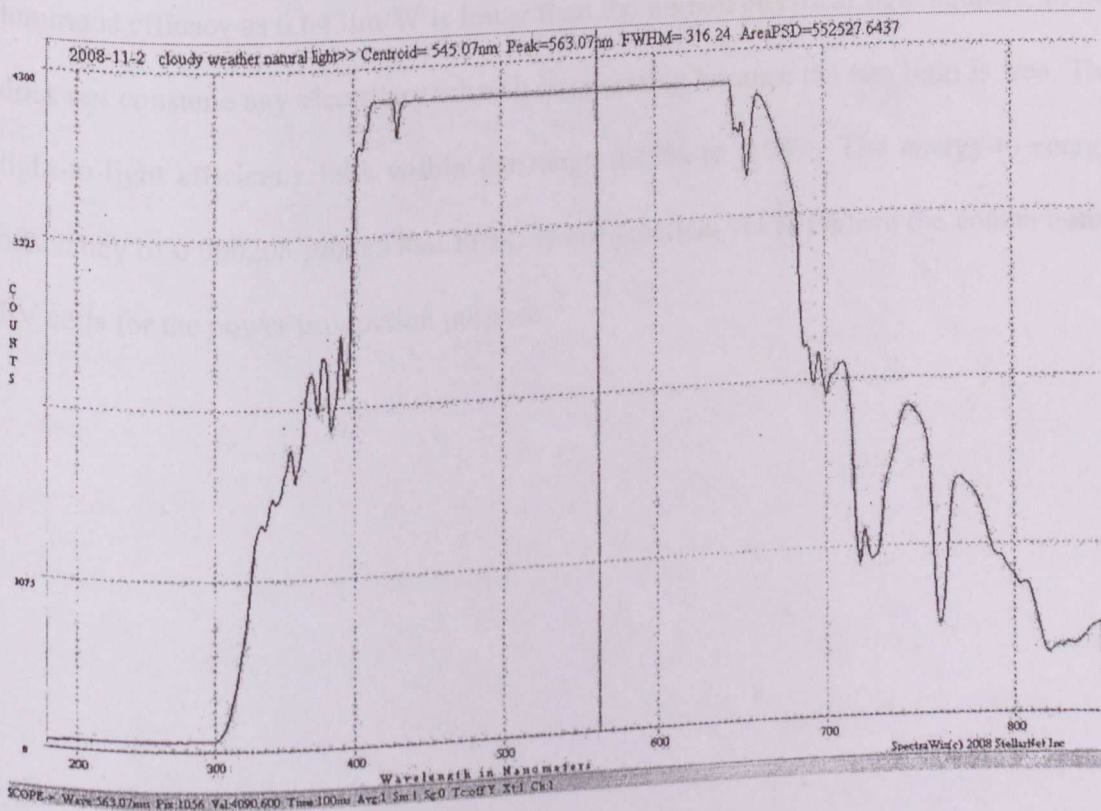


Figure 7.21: Scope mode natural daylight overcast 2nd Nov 2008

7.9 Summary

From 24th May 2008 to 23rd November 2008, a 6-month outdoor trial run and monitoring has been conducted for the fabricated fluorescent fibers solar concentrator (FFSC) system. A potential in remote indoor daylighting purpose for the application in building integration has been revealed by the reasonable radiation-to-radiation efficiency with a mean value of 0.057, the acceptable lighting effect up to 114.1 lumens, and the satisfactory match to the natural light in color. The negative trend between the radiation-to-radiation efficiency (η_r) and the solar radiation is detected. The wavelength tests and the CIE color analysis reveal that the FFSC light output has a satisfactory match to the natural light, and it is comforting to human eyes. Even though the luminous efficacy as 0.643lm/W is lower than the normal electrical light sources, FFSC does not consume any electricity when it is operating because the sun light is free. The light-to-light efficiency falls within the range 0.49% to 0.64%. The energy-to-energy efficiency of 0.000268 proves that FFSC is not practical yet to replace the conventional PV cells for the power production purpose.

Chapter 8

Conclusions and Recommendations

8.1 Conclusions

In conclusion, the three main objectives have been fully achieved in this research. The three main objectives of this research are:

- a) to identify the working principles and to extract the limitations of the present daylighting related devices, and
- b) to develop a new concept to avoid or to mitigate the limitations of the present daylighting related devices and to fabricate a device based on the new concept, and
- c) to assess the performance of the fabricated new device for remote indoor daylighting purposes through its trial run.

The 1st objective is achieved through literature reviews on the natural lighting related devices as presented in Chapter 2 as well as through the discussions on the necessity of FFSC as presented in the first section of Chapter 4. Daylight has a disadvantage of not

being able to reach deeper areas in a building such as storerooms, basements, and corridors, and it brings the heat gain with the light. Light pipes and optical fibers were expected to transfer daylight to unreached areas, but light pipes have their difficulties in wiring and the optical fiber needs a pointolite for the light transportation. Solar concentrators are only sensitive for the beam radiation and they function poorly in overcast sky conditions. Even under a clear sky condition, trackers are always needed for conventional solar concentrators. Static concentrators always come with a poor concentration rate without a tracker, and the light concentrated by normal luminescent solar concentrators could not be transported by optical fibers to a remote place since the light produced by LSCs is not a pointolite.

The 2nd objective is achieved through the concept design and the fabrication process as described in Chapter 4. A new concept, which is to use fluorescent fibers for solar concentration and to use clear optical fiber bundles to transport the absorbed daylight into a target area for remote indoor daylighting purposes, has been developed by the author. Accordingly, a new device named “fluorescent fiber solar concentrator” (FFSC) is designed and fabricated in this study based on the concept.

The last objective is to monitor the performance of the fabricated new device in remote indoor daylighting purposes through its trial run, and this is fulfilled through a 6-month experimentation as discussed in Chapters 5, 6, and 7. Through the 6-month experimentation, the fabricated $1200\text{mm} \times 1200\text{mm}$ solar concentrator (FFSC) consisting of 150 pieces of three-color 1m long fluorescent fibers with the diameter of 2mm has been mounted on the roof of a University building, and the concentrated light is transported to a remote dark room through the 10m long, 2mm diameter clear optical

fiber bundles. Outdoor testing for remote indoor daylighting and power production evaluation has been conducted from 24th May 2008 to 23rd November 2008.

The negative trend between the radiation-to-radiation efficiency and the solar radiation is detected and analyzed. The low energy-to-energy efficiency value of 0.000268 indicates that FFSC is not practical yet to replace the conventional PV cells for power production. However, the reasonable radiation-to-radiation efficiency with a mean value of 0.057 and the acceptable lighting effect up to 114.1 lumens reveal FFSC a potential in remote indoor daylighting for the application in building integration. The wavelength test and the CIE color analysis reveal that the FFSC light output has a satisfactory match to the natural light in color. Since the sun light is free, even though the luminous efficacy as 0.643lm/W is lower than the normal electrical light sources, FFSC does not consume any electricity when it is operating. The light-to-light efficiency falls within the range 0.49% to 0.64% and it is expected to be raised by increasing the diameter of the fluorescent fibers embedded in FFSC. Even though the light-to-light efficiency of FFSC appears lower than that of the LSC produced by Earp et al. (2004), there is no comparability between FFSC and Earp et al.'s LSC because the cross section of the fluorescent fiber in FFSC is a 12.56m² circular section while that of the Earp et al.'s LSC is a 270m² rectangular section, and the size and form of the cross section could impact on the proportion of photons trapped. FFSC has a greater advantage in wiring as it is designed for, because its media for light transportation are optical fibers, which is difficult for the LSC produced by Earp et al. (2004) to achieve. Moreover, comparing to the conventional artificial lighting devices powered by PV cells, which convert light to electricity and then convert it back to light again losing a lot of efficiency in multi-converting, the idea of FFSC as a shortcut light-to-light conversion is considered to have a more efficient future.

8.2 Potential applications of FFSC

In light of the revealed potentials in remote indoor daylighting for the application in building integration, and dependent on the potential dramatic commercial success of fluorescent fibers in the future, FFSC systems could probably be applied for the illumination in underground areas of buildings or constructions during the daytime. Since the FFSC plate does not rely on only beam irradiation, it could be placed anywhere there is sufficient light, no matter the light source is the beam irradiation or the diffuse irradiation or even the electrical light. For example, the FFSC plate can be placed vertically in the south facade of a building in the northern hemisphere. The proposed underground areas to be illuminated by FFSC systems could be the car park levels in shopping complexes, convention centers, and some office buildings.

FFSC system could also be applied to illuminate the inner areas in a building. Where there is insufficient daylight, an artificial light source is always needed during the daytime. Illumination produced by FFSC could complement the side lighting (e.g. light from windows), especially for the space in the deep interior of a building. These inner areas include such as meeting rooms, corridors, and so on.

Since electro circuits are not needed in the FFSC system, there is no any risk for short circuits while this system is operating. Hence, potentially FFSC systems are quite suitable for subaqueous illumination during the daytime, especially for the underwater areas where the sunlight is not able to penetrate through effectively. Because of this

kind of attribute, some extremely moist operation environments are also suitable for FFSC systems to be applied in when a durative illumination is needed during the daytime. Also because there is no electro circuit needed, FFSC systems do not have any risk of fire caused by the electrical current in inflammable gas conditions.

8.3 Recommendations for Future Research

The following areas are recommended for future study:

Firstly, in future study, the fluorescent fibers with a large diameter, say 10mm diameter, are recommended in the FFSC system. This will increase the light-to-light efficiency of FFSC and it does not bring extra difficulties in wiring. A study on the relationship between the diameters and the light-to-light efficiency of fluorescent fibers is recommended.

Secondly, cost evaluations for the fluorescent fiber solar concentrator (FFSC) or for other types of new designed fluorescent solar concentrators could probably be conducted in the future for the commercialization purpose. The cost evaluations for FFSC have not been conducted in this research because it is still on the experimental stage and the market for the fluorescent fibers is not yet mature.

Thirdly, as experimentations for FFSC were only conducted in the tropic zone especially in the country of Malaysia, future monitoring activities are recommended in the frigid zone and the temperate zone.

Next, based on the monitored 10167 sets of effective data during the 6 months, the system radiation-to-radiation efficiency (η_r) presents a negative trend with the solar radiation PY1. The knowledge for the reason why this kind of negative trend occurs may be beyond the author's specializing field. However, being aided by specialists with proper fields of knowledge, say, knowledge in optical physics or hylology, the answer is expected to be revealed in future study.

Finally, studies on new ideas in the FFSC structural design itself are also encouraged since improvements could probably be made in the structural design to enhance the device efficiency, to save materials, or to accommodate with the large-scale installation.

References

- Aizenberg, J.B., Bukhman, G.B., & Pyatigorsky, V.M. (1975). A new principle of lighting premises by means of the illuminating devices with slit lightguides, in *Proceedings of the 18th Session of the Commission Internationale de l'Eclairage, London*, 412-415.
- Allsop, T., Webb, D.J., & Bennion, I. (2002). A high sensitivity long period grating Mach-Zehnder refractometer, in: *The 15th Optical Fiber Sensors Conference Technical Digest*, Portland, OR, 123-126.
- Al-Marwaei, M., & Carter, D.J. (2006). A field study of tubular daylight guidance installations. *Lighting Research and Technology*. 38(3), 1-18.
- Andre, E. (2002). Daylighting by optical fibre. *Master's Thesis*, Lulea University of Technology, Sweden.
- Aries, M.B.C. & Newsham, G.R. (2008). Effect of daylight saving time on lighting energy use: a literature review. *Energy Policy*. 36(6), 1858-1866.
- Arregui, F.J., Galbarra, D., Matias, I.R., Cooper, K.L., & Claus, R.O. (2002). ZrO₂ thin films deposited by the electrostatic self-assembly method on optical fibers for ammonia detection, in: *The 15th Optical Fiber Sensors Conference Technical Digest*, Portland, OR, 265-268.
- Barnham, K.W.J., Marques, J.L., Hassard, J., & Brien, P.O. (2000). Quantum dot concentrator and thermodynamic model for the global red-shift, *Al. Phys. Lett.* 76(9), 1197-1199.
- Barnoski, M.K., & Jensen, S.M. (1976). Fiber waveguides: a novel technique for investigating attenuation characteristics, *Al. Opt.* 15, 2112-2115.
- Batchelder, J.S., Zewail, A.H., & Cole, T. (1979). Luminescent Solar Concentrators. Theory of operation and techniques for performance evaluation. *Alid Optics*. 18 (18), 3090-3110.
- Beckman, W.A., Schlegel, G.O., Klein, S.A., Wood, B.D., & Muhs, J.D.M. (2003). A TRNSYS model of a full spectrum hybrid lighting system. *Proceedings of ISES Solar World Congress*, Gothenburg, Sweden.
- Beller, J. (1998). OTDRs and backscatter measurements, in: D. Derickson (Ed.), *Fiber Optic Test and Measurement*, Prentice Hall, Uer Saddle River, NJ, Chap. 11, 434-474.
- Beltran, L.O., Lee, E.S., & Selkowitz, S.E. (1997). Advanced ommended Practice for the Lumen Method of Daylight optical daylighting systems: light shelves and light pipes. J. Calculations, IESNA, New York, RP-23-1989. *Illum. Eng. Soc.* 26, p91.

- Blyler, L. (1999). Material Science and Technology for POF. in *Proc. Eighth Conference on Plastic Optical Fibers and Applications POF'99*, Chiba, Japan, 196-200.
- Bouchet, B., & Fontoynt, M. (1996). Daylighting of underground spaces: design rules. *Energy and Buildings* 23(3), 293-298.
- Bouma, G.D., Atkinson, G.B.J., & Dixon, B.R. (1995). *A handbook of social science research*. Oxford University Press, Oxford and New York.
- Bouquet, F.L., Helms, R.G., & Maag, C.R. (1987). Recent advances in long-lived mirrors for terrestrial and space applications, *Sol. Energy Mater.* 16, 423-433.
- Boyce, P. (2009). *Reviews of Technical Reports on Daylight and Productivity*. from: http://www.lrc.rpi.edu/programs/daylighting/rp_technicalreviews.asp
- BRE. Energy consumption guide. (1997). *Energy use in offices, energy efficiency best practice programme*. Garston, Watford.
- Building Regulations (2006). *The Building Regulations*. Office of the Deputy Prime Minister, UK, from: <http://www.odpm.gov.uk/index.asp?id/41130474>
- Carbon Trust. (2009). Online on the World Wide Web: <http://www.thecarbontrust.co.uk/carbontrust/>
- Cariou, J.M., Dugas, J., & Martin, L. (1982). Transport of solar energy with optical fibers. *Solar Energy*. 29 (5), 397-406.
- Cariou, J.M., Martin, L., & Dugas, J. (1980). Advances in Ceramics. *Physics of Fiber Optics*. 2, 557-563.
- Carter, D.J. (2004). Developments in tubular daylight guidance systems. *Building Research & Information*. 32(3), 220-234.
- Carter, D.J. (2008). Tubular guidance systems for daylight: UK case studies. *Building Research & Information*. 36(5), 520-535.
- Chattena, A.J., Barnhama, K.W.J., Buxtonb, B.F., Ekins-Daukesa, N.J., & Malik, M.A. (2003). A new approach to modeling quantum dot concentrators. *Solar Energy Materials & Solar Cells*. 75, 363-371.
- Chel, A., Tiwari, G.N., & Chandra, A. (2009). A model for estimation of daylight factor for skylight: An experimental validation using pyramid shape skylight over vault roof mud-house in New Delhi (India). *Al Energy*. doi:10.1016/j.apenergy.2009.03.004.
- Chia, S.L., Hamdan, M.A., & Dilshan, R.O. (2006). Impact of solar radiation on high-rise built form in tropical climate. *Energy in Buildings: Sustainable Symbiosis*. Book edited by Azni Zain-Ahmed, Samirah Abdul Rahman, Sulaiman Shaari. UPENA, Universiti Teknologi MARA, Shah Alam, Malaysia. 145-162.
- CIE Publication. (1986). No.15.2, *Colorimetry*, Second Edition.

Commission Internationale de l'Eclairage. (2002). Hollow Light Guides. *Technical Report*. TC 3-30, Vienna.

Compagnon, R., Scartezzini, J.L., & Paule, B. (1993). Application of nonimaging optics to the development of new daylighting systems. *Proceedings of ISES Solar World Congress*. Budapest, Hungary.

Creswell, J.W. (1994). *Research design: Qualitative & quantitative approaches*. Sage Publications, Thousand Oaks, Calif.

Crisp, V.H.C., Littlefair, P.J., Cooper, I., & McKennan, G. (1988). *Daylighting as a passive solar energy option: and assessment of its potential in non-domestic buildings*. Report BR129, BRE, Garston, UK.

Czanderna, A.W. (1981). Stability of interfaces in solar energy materials, *Sol. Energy Mater.* 5, 349 - 377.

Danny, H.W.L., Chris, C.S.L., & Joseph, C.L. (2005). Predicting daylight illuminance on inclined surfaces using sky luminance data. *Energy*. 30, 1649-1665.

Daum, W., Hoffman, A., & Strecker, U. (1994). Influence of chemicals on the durability of polymer optical fibers. in *Proc. Third International Conference on Plastic Optical Fibres and Applications POF'94*, Yokohama, Japan, 111-114.

Denscombe, M. (1998). *The Good Research Guide*. Buckingham. Open University Press.

Department of Environment, Farming and Rural Affairs, UK. (2009). Online on the World Wide Web:

<http://www.defra.gov.uk/environment/ccl/>

Dilshan, R.O., Hamidan, A.M., & Nor, H.M. (2006). Impact of solar shading geometry on building energy use in hot humid climates with special reference to Malaysia. *Energy in Buildings: Sustainable Symbiosis*. Book edited by Azni Zain-Ahmed, Samirah Abdul Rahman, Sulaiman Shaari. UPENA, Universiti Teknologi MARA, Shah Alam, Malaysia. 183-204.

Djamila, R.S. (1996). Adoption of Optical Fibres or of Optical Light Films in Architecture. *World Renewable Energy Congress*. Denver, USA.

Duffie, J.A. (1962). New materials in solar energy utilization, *Sol. Energy*. 6 (3), 114-118.

Dugay, M.A., & Edgar, R.M. (1977). Lighting with sunlight using sun tracking concentrators. *Applied Optics*, 16(5), 1444-1446.

Earp, A.A., Geoff, B.S., Jim, F., & Paul, S. (2004). Optimisation of a three-colour luminescent solar concentrator daylighting system. *Solar Energy Materials & Solar Cells*. 84, 411 - 426.

Eben, K. (1993). Let the sun shine in. *Lighting Design and Application*. 23(5), 41-46.

- Egan, D.M. (1983). *Concepts in Architectural Lighting*. Mc.Graw Hill.
- Ejhed, J. (2001). Daylight quantities acceptance studies in the Arthelio project, in *Proceedings of the 9th LUX Europa Congress*, Reykjavik, Iceland, 1, 22-25.
- Elmaualim, A.A., Smith, S, Riffat, S.B., & Shaou, L. (1999). Evaluation of dichroic material for enhancing light pipe/natural ventilation and daylighting in an integrated system. *AI Energy*. 62(2), 53-66.
- Enedir, G., & John, A.T. (2006). Evaluating the potential for energy savings on lighting by integrating fibre optics in buildings. *Building and Environment*. 41, 1611-1621.
- Eng, K.S. (2007). *The Knowledge Acquisition for Construction Site Layout Planning*. Thesis for Doctor of Philosophy. University of Malaya. Kuala Lumpur.
- EPA, Environmental Protection Agency. (1999). *EPA Energy Star Buildings and Green Lights Snapshot*. Washington, DC.
- Estrada, C.A., Jaramillo, O.A., & Acosta, R. (2007). Arancibia-Bulnes, Heat transfer analysis in a calorimeter for concentrated solar radiation measurements, *Sol. Energy*. 81, 1306-1313.
- Evenson, S.A., & Rawicz, A.H. (1995). Thin-film luminescent concentrators for position-sensitive devices: a cookbook. *AI. Opt.* 34, 7302- 7306.
- Fellows, R., & Liu, A. (2003). *Research Methods for Construction*. 2nd edition. Blackwell Science Ltd.
- Fontoynt, M. (2005). Long term assessment of costs associated with lighting and daylighting, in *Proceedings of the LUX Europa*, Berlin, Germany, 227-230.
- Fraas, L.J.A., Sundaram, V., Dinh, V., Davenport, T., & Yerkes, J. (1990). Over 35% efficient GaAs/GaSb stacked concentrator cell assemblies for terrestrial applications, in: *21st IEEE Photovoltaics Specialists Conference*, Orlando, FL.
- Franzetti, C., Fraisse, G., & Achard, G. (2004). Influence of the coupling between daylight and artificial lighting on thermal loads in office buildings. *Energy Buildings*. 36, 117-126.
- Garcia-Hansen, V., & Edmonds, I. (2003). Natural illumination of deep-plan office buildings: light pipe strategies. *Proceedings of ISES Solar World Congress*. Gothenburg, Sweden.
- Geoffrey, B.S. (2004). Materials and systems for efficient lighting and delivery of daylight. *Solar Energy Materials & Solar Cells*. 84, 395 - 409.
- Goetzberger, A., & Greubel, W. (1977). Solar energy conversion with fluorescent collectors, *AI. Phys*. 14, 123 - 139.

- Goetzberger, A., Stahl, W., & Wittwer, V. (1985). Physical limitations of the concentration of direct and diffuse radiation, in: *Proceedings of the Sixth European Photovoltaic Solar Energy Conference*, Reidel, Dordrecht, 209 – 215.
- Goldschmidt, J.C., Marius, P., Armin, B.S., Henning, H., Frank, D., Stefan, W.G., & Gerhard, W. (2009). Increasing the efficiency of fluorescent concentrator systems. *Solar Energy Materials & Solar Cells*. 93, 176–182.
- Granqvist, C.G. (2003). Solar Energy Materials, *Adv. Mater.* 15 (21), 1789 – 1803.
- Grattan, K.T.V., & Meggitt, B.T. (Eds.). (1998). Optical Fiber Sensor Technology, Vol. 2, *Devices and Technology*, Chapman & Hall, London.
- Grattan, K.T.V., & Meggitt, B.T. (Eds.). (1999). Optical Fiber Sensor Technology, Vol. 3, *Applications and Systems*, Kluwer Academic Publishers, Boston.
- Guerrero, H., Guinea, G.V., & Zoido, J. (1998). Mechanical properties of polycarbonate optical fibers. *Fiber and Integrated Optics*, 17, p231.
- Guerrero, H., Zoido, J., Escudero, J. L., & Bernabeu, E. (1993). Characterization and sensor applications of polycarbonate optical fibers. in *Proc. Second International Conference on Plastic Optical Fibres and Applications _POF'93*, The Hague, Holland, 166-170.
- Hammam, M., El-Mansy, M.K., El-Bashir, S.M., & El-Shaarawy, M.G. (2007). Performance evaluation of thin-film solar concentrators for greenhouse applications. *Desalination*, 209 (2007), 244–250.
- Hasdemir, B. (1995). A new method for the estimation of lacking daylight illumination data by using available meteorological data. *Ph.D. Thesis, Middle East Technical University*, Ankara, Turkey.
- Hellstrom, B., Adsten, M., Nostell, P., Karlsson, B., & Wackelgard, E. (2003). The impact of optical and thermal properties on the performance of flat plate solar collectors, *Renew. Energy*. 28, 331-344.
- Hicks, A., & Wright, J. (2000). Novel polymeric multilayer optical films offer performance improvements for lighting systems, in *Proceedings of the CIBSE National Lighting Conference*, 26–32.
- Hill, K.O., Fujii, Y., Johnson, D.C., & Kawasaki, B.S. (1978). Photosensitivity in optical fiber waveguides: application to reflection filter fabrication, *Appl. Phys. Lett.* 32, 647–649.
- Inaudi, D., & Casanova, N. (2002). SMART-TEC: bringing fiber optic sensors into concrete applications, in: *The 15th Optical Fiber Sensors Conference Technical Digest*, Portland, OR, 27–30.
- ISO/CIE10526-1991. (1991). *CIE standard colorimetric illuminants*.

- James, S.W., Rees, N.D., Tatam, R.P., & Ashwell, G.J. (2002). Optical fiber long period gratings with thin film overlays, in: *The 15th Optical Fiber Sensors Conference Technical Digest*, Portland, OR, 119–122.
- Joseba, Z., & Jon, A. (2001). Plastic Optical Fibers: An Introduction to Their Technological Processes and Applications. *Optical Fiber Technology*. 7, 101–140.
- Kaino, T. (1992). Polymer optical fibers. *Proceeding of Polymers for Lightwave and Integrated Optics*. Dekker, New York.
- Kamaruzzaman, S., Mohd, Y.O., & Baharudin, Y. (2006). Large scale solar assisted water heating systems for public and commercial buildings. *Energy in Buildings: Sustainable Symbiosis*. Book edited by Azni Zain-Ahmed, Samirah Abdul Rahman, Sulaiman Shaari. UPENA, Universiti Teknologi MARA, Shah Alam, Malaysia. 247–258.
- Kandilli, C., Ulgen, K., & Hepbasli, A. (2007). Exergetic assessment of transmission concentrated solar energy systems via optical fibres for building applications, *Energy and Buildings*, doi:10.1016/j.enbuild.2008.02.021.
- Kim, S., Jeong, Y., Kim, S., Kwon, J., Park, N., & Lee, B. (2000). Control of the characteristics of a long-period grating by cladding etching, *Al. Opt.* 39 (13), 2038–2042.
- Kischkoweit, L.M. (1998). Application of new developed daylighting systems in real case studies. *Daylighting '98 Conference Proceedings*, Ontario, Canada, 255–259.
- Klotz, F.H. (1995). PV systems with V-trough concentration and passive tracking concept and economic potential in Europe, *Proceedings of the 13th European PV Solar Energy Conference*, Nice, 23–27 October, 1995, 1060–1063.
- Kocifaj, M. (2009). Efficient tubular light guide with two-component glazing with Lambertian diffuser and clear glass. *Applied Energy*. 86, 1031–1036.
- Koike, Y., Ishigure, T., & Nihei, E. (1995). High-bandwidth graded index polymer optical fiber, *J. Light Technol.* 13, p1475.
- Koster, H. (2000). Tageslichtlenksysteme. *Neuester Stand der Technik*. Licht 7–8 Germany.
- Laar, M., & Friedrich, W.G. (2002). German developments in daylight guidance systems: an overview. *Building Research & Information*. 30(4), 282–301.
- Lam, J.C., & Chan, A.L.S. (1995). Energy audits and surveys of air-conditioning. *Proceedings of the Australian and New Zealand Architectural Science Association Conference*. Australian National University, Australia, p49.
- Lam, J.C., & Li, D.H.W. (1996). *Energy Convers. Manage.* 37 (12) 1703 – 1711.
- Lee, Y.W., & Lee, B. (2002). High resolution cryogenic optical fiber sensor system using erbium-doped fiber, *Sensors Actuators. Applied Phys.* 96 (1), 25–27.

Leslie, R.P. (2003). Capturing the daylight dividend in buildings: Why and how. *Building Environ.* 38, 381–385.

Li, D.H.W., & Lam, J.C. (2001). Evaluation of lighting performance in office buildings with daylighting controls. *Energy Buildings.* 33, 793–803.

Littlefair, P.J. (1996). *Designing buildings with innovative daylighting*, Construction Research Communications Ltd.

Luque, A., Martí, A., Bett, A., Andreev, V.M., Jaussaud, C., Roosmalen, J.A.M. van, Alonso, J., Rauber, A., Strobl, G., Stolz, W., Algora, C., Bitnar, B., Gombert, A., Stanley, C., Wahnou, P., Conesa, J.C., Van-Sark, W.G.J.H.M., Meijerink, A., Van-Klink, G.P.M., Barnham, K., Danz, R., Meyer, T., Luque-Heredia, I., Kenny, R., Christofides, C., Sala, G., & Benítez, P. (2005). FULLSPECTRUM: a new PV wave making more efficient use of the solar spectrum. *Sol. Energy Mater. Sol. Cells.* 87, 467–479.

Marazuela, M.D., & Moreno-Bondi, M.C. (2002). Fiber-optic biosensors: an overview, *Anal. Bioanal. Chem.* 372, 664–682.

Maria, B., Anna, H., Bjorn, K., Johan, N., & Arne, R. (2004). Optical properties, durability, and system aspects of a new aluminium-polymer-laminated steel reflector for solar concentrators. *Solar Energy Materials & Solar Cells.* 82 (2004), 387–412.

Martin, K.L. (2002). An overview of daylighting systems. *Solar Energy.* 73(2), 77–82.

Masato, M., & Toshiro, M. (2005). Static solar concentrator with vertical flat plate photovoltaic cells and switchable white/transparent bottom plate. *Solar Energy Materials & Solar Cells.* 87, 299 – 309.

McDaniels, D.K., Lowndes, D.H., Mathew, H., Reynolds, J., & Gray, R. (1975). Enhanced solar energy collection using reflector-solar thermal collector combinations. *Sol. Energy.* 17(1975), p277.

Melnik, I.S., & Rawicz, A.H. (1997). Thin-film luminescent concentrators for position-sensitive devices. *Al. Opt.* 36, 9025–9033.

Meltz, G., Morey, W.W., & Glenn, W.H. (1989). Formation of Bragg gratings in optical fibers by a transverse holographic method, *Opt. Lett.* 14, 823–825.

Melville, S. (1996). *Research methodology: an introduction for science & engineering students.* Juta & Co. Ltd.

Micic, O.I., Curtis, C.J., Jones, K.M., Nozik, A.J., & Sprague, J.R. (1994). Synthesis and characterisation of InP quantumdots, *J. Phys. Chem.* 98, 4966–4969.

Micic, O.I., Cheong, H.M., Fu, H., Zunger, A., Sprague, J.R., Mascarenhas, A., & Nozik, A.J. (1997). Size dependent spectroscopy of InP quantumdots, *J. Phys. Chem. B* 101, 4904–4912.

Mills, E., & Orlando, E. (2002). Why we are here: the \$230-billion global lighting energy bill. In: *Proceedings of the right fifth conference, Nice, France*. 369-385.

Mingozi, A., Bottiglioni, S., & Casalone, R. (2001). An innovative system for daylight collecting and transport for long distances and mixing with artificial light coming from hollow light guides, in *Proceedings of the 9th LUX Europa Congress*, Reykjavik, 1, 12-21.

Monodraught. (1997). *Sunpipe information leaflet*. Monodraught Ltd.

Mora, M.B. de la, Jaramillo, O.A., Navaa, R., Taguena-Martinez, J., Rio, J.A.del. (2009). *Solar Energy Materials & Solar Cells*. doi:10.1016/j.solmat.2009.01.007.

Morris, V.L. (1980). Cleaning agents and techniques for concentrating solar collectors, *Sol. Energy Mater.* 3, 35-55.

Muhs, J.D. (2000). Design and analysis of hybrid solar lighting and full-spectrum solar energy systems. *Solar 2000, 16 - 21 July 2000*, American Solar Energy Society.

Muneer, T., & Jenkins, D. (2004). The value and estimated savings of light pipe use in windowless environments. *Light and Engineering*. 12(3), 5-14.

Murofushi, H. (1996). Low loss perfluorinated POF. *Proceeding of Fifth International Conference on Plastic Optical Fibres and Applications _POF'96*, Paris, France. 17-23.

Mwamburi, M.E.W., & Roos, A. (2000). Preparation of solar selective SnOx: F coated aluminium reflector surfaces, *Thin Solid Films*. 374, 1-9.

Nann, S. (1991). Potentials for tracking photovoltaic systems and V-troughs in moderate climates, *Sol. Energy*. 45, p385.

Naritomi, M. (1996). CYTOP-Amorphous Fluoropolymers for low loss POF. in *POF Asia Pacific Forum 1996*, Tokyo, Japan.

Neuman, W.L. (2003). *Social Research Methods: Qualitative and Quantitative Approaches*. 5th edition. Pearson Education Inc.

Ngai, P.Y. (1983). Solar illumination for interior spaces, *Lighting Design and Application*, 13(4), 26-33.

Nihei, E., Ishigure, T., Tanio, N., & Koike, Y. (1997). Present prospect of graded index plastic optical fiber in telecommunications. *IEICE Trans. Electron.* vol. E-80-c, 117-122.

Oakley, G., Riffat, S.B., & Shao, L. (2000). Daylight performance of lightpipes. *Solar Energy*. 69(2), 89-98.

Orellana, G., & Moreno-Bondi, M.C. (2002). From molecular engineering of luminescent indicators to environmental analytical chemistry in the field with fiber-optic (bio) sensors, in: *The 15th Optical Fiber Sensors Conference Technical Digest*, Portland, OR, 115-118.

- Othonos, A., & Kalli, K. (1999). *Fiber Bragg Gratings: Fundamentals and Applications in Telecommunications and Sensing*, Artech House, Boston.
- Page, J., Kaempf, J., & Scatrezzini, J.L. (2003). Assessing daylighting performances of electrochromic glazings coupled to an anidolic device. *Proceedings of ISES Solar World Congress*. Gothenburg, Sweden.
- Paroncini, M., Calcagni, B., & Corvaro, F. (2007). Monitoring of a light-pipe system. *Solar Energy*. 81, 1180-1186.
- Peacock, A.D., Newborough, M., & Banfill, P.F.G. (2005). Technology assessment for the existing built-asset base (TARBASE), WREC, Aberdeen, May 22-27.
- Peng G.D. and Chu P.L. (2002). Optical fiber hydrophone systems, in: F.T.S. Yu, S. Yin (Eds.), *Fiber Optic Sensors*, Dekker, New York, Chap. 9, 417-447.
- Peng, X., Schlamp, M.C., Kadavanich, A.V., & Alivisatos, A.P. (1997). Epitaxial Growth of Highly Luminescent CdSe/CdS Core/Shell Nanocrystals with Photostability and Electronic Accessibility. *J. Am. Chem. Soc.* 119, 7019-7029
- Pohl, W., & Anselm, C. (2001). Report of EC-funded Joule-Craft Research Project: Development of an Economic and Energy saving Heliostat Technology for Room Illumination, *Publishable Final Report*, Contract No. JOR3-CT98-7042, Bartenbach LichtLabor GmbH, Aldrans.
- Pohl, W., & Anselm, C. (2002). Natural room illumination using sunlight. *Proceedings of World Renewable Energy Congress VII (WREC 2002)*, Cologne, Germany.
- Poulek, V., & Libra, M. (2000). A new low-cost tracking ridge concentrator. *Solar Energy Materials & Solar Cells*. 61, 199-202.
- Rabl, A. (1980). Concentrating collectors, in A. Dickinson and M. Cheremisinoff (eds): *Solar Energy Technology Handbook*, Marcel Dekker, New York.
- Rapp, C.F., & Boling, N.L. (1978). Luminescent solar concentrators, in: *Proceedings of the 13th Photovoltaic Specialists Conference, IEEE*, New York, 690 - 693.
- Reisfeld, R. (2001). Prospects of sol-gel technology towards luminescent materials, *Opt. Mater.* 16, 1-7.
- Reisfeld, R., & Jorgensen, C.K. (1982). Luminescent Solar Concentrators for energy conversion. *Structure and Bonding*. 49, 1-36.
- Richards, B.S. (2006). Enhancing the performance of silicon solar cells via the application of passive luminescence conversion layers. *Solar Energy Materials & Solar Cells*. 90 (2006), 2329-2337.
- Ries, H., Zaibel, R., Dagan, E., & Karni, J. (1995). An astigmatic corrected target-aligned heliostat for high concentration. *Solar Energy Materials and Solar Cells*. 37 (2), 191-202.

- Robert, C.A., & Ernest, J.M. (2006). *Report of the Energy Research Council*. Massachusetts Institute of Technology. Cambridge, Massachusetts, USA.
- Roos, A., Ribbing, C.G., & Karlsson, B. (1989). Stainless steel solar mirrors: A material feasibility study, *Sol. Energy Mater.* 18, 233 - 240.
- Sabarinah, S.A. (2006). Thermal comfort and building performance of naturally ventilated apartment building in the Klang Valley: A simulation study. *Energy in Buildings: Sustainable Symbiosis*. Book edited by Azni Zain-Ahmed, Samirah Abdul Rahman, Sulaiman Shaari. UPENA, Universiti Teknologi MARA, Shah Alam, Malaysia. 115-132.
- Sala, M., Milanesi, F., Ceccherini, & NeW, L. (1993). Fresnel Lenses and Plastic Optic Fibers for Natural lighting. *Solar Energy in Architecture and urban Planning 3rd European Conference on Architecture* (Book of Abstracts), p14.
- Sanders, G.A., Blake, J.N., Rose, A.H., Rahmatian, F., & Herdman, C. (2002). Commercialization of fiber-optic current and voltage sensors at NxtPhase, in: *The 15th Optical Fiber Sensors Conference Technical Digest*, Portland, 31-34.
- Sato, M., Ishigure, T., & Koike, Y. (2000). Thermally stable high-bandwidth graded index polymer optical fiber. *J. Light. Technol.* 18(7), p952.
- Schiler, M. (1992). *Simplified design of Building Lighting*. John Wiley.
- Schissel, P., Jorgensen, G., Kennedy, C., & Goggin, R. (1994). Silvered-PMMA reflectors, *Sol. Energy Mater. Sol. Cells*, 33, 183-197.
- Schmela, M. (2003). *A bullish PV Year: Market Survey on Worlds Cell Production in 2002*. Photon Int.42-48.
- Shao, L., Riffat, S.B., Yohannes, I., & Elmualim, A.A. (1998). Measurement and modelling of light pipe for energy efficient lighting. *CIBSE National Lighting Conference Paper*.
- Sorin, W.V. (1998). Optical reflectometry for component characterization, in: D. Derickson (Ed.), *Fiber Optic Test and Measurement*, Prentice Hall, Uer Saddle River, NJ, Chap. 10, 383-433.
- Surapong, C., Siriwat, C., & Liu, R. (2000). Daylighting through light pipes in the tropics. *Solar Energy*. 69(4); 331-341.
- Swanson, R.M. (2000). The Promise of Concentrators, *Prog. Photovoltaics: Res. Al.* 8 (Millennium Special Issue), 93-111.
- Sweitzer, G. (1993). Three advanced daylighting technologies for offices. *Energy*. 8(2), 107-114.
- Thevenaz, L., Facchini, M., Fellay, A., Robert, P., Inaudi, D., & Dardel, B. (1999). Monitoring of large structures using distributed Brillouin fiber sensing, in: *Proceedings of the 13th International Conference on Optical Fiber Sensors (OFS-13)*, cited from Kyongju, Korea, in: *Proc. SPIE 1999*, 3746, 345-348.

- Udd, E. (2002). Overview of fiber optic sensors, in: F.T.S. Yu, S. Yin (Eds.), *Fiber Optic Sensors*, Dekker, New York, Chap. 1, 1-39.
- Uematsu, T, Yazawa, Y., Miyamura, Y., Muramatsu, S., Ohtsuka, H., Tsutsui, K., & Warabisako, T. (2001). Static concentrator photovoltaic module with prism array. *Solar Energy Materials & Solar Cells*. 67, 415-423.
- Unver, R., Ozturk, L., Adiguzel, S., & Celik, O. (2003). Effect of the facade alternatives on the daylight illuminance in offices. *Energy Buildings*. 35, 737-746.
- Vali, V., & Shorthill, R.W. (1976). Fiber ring interferometer, *Al. Opt.*, 15, 1099-1100.
- Wapedia. (2009). Online on the World Wide Web:
http://wapedia.mobi/en/Luminous_efficacy
- Webb, A.R. (2006). Considerations for lighting in the built environment: non-visual effects of light. *Energy Build.* 38(7), 721-727.
- Webb, D.J., Hathaway, M.W., Jackson, D.A., Jones, S., Zhang, L., & Bennion, I. (2000). First in-vivo trials of a fiber Bragg grating based temperature profiling system, *J. Biomed. Opt.* 5 (1), 45-50.
- Weber, W.H., & Lambe, J. (1976). Luminescent greenhouse collector for solar radiation. *Alie Optics*. 15 (10), 2299 - 2300.
- Whitehead, L., Nodwell, R.A., & Curzon, F.L. (1982). New efficient guide for interior illumination. *Alie Optics*, 21(15), 2755-2757.
- Whitfield, G.R., Bentley, R.W., & Burton, J.D. (1995). Increasing the cost-effectiveness of small solar photovoltaic pumping systems. *Renew. Energy*. 6 (5-6), 469-475.
- Wikipedia. (2009a). Online on the World Wide Web:
http://en.wikipedia.org/wiki/Main_Page
- Wikipedia. (2009b). Online on the World Wide Web:
http://en.wikipedia.org/wiki/Incandescent_light_bulb
- Wittwer, V., Goetzberger, A., Heidler, K., & Zastrow, A. (1981). Theory of fluorescent planar concentrators and experimental results, *J. Lumin.* 24/25, 873-876.
- Wittwer, V., Stahl, W., & Goetzberger, A. (1984). Fluorescent planar concentrators. *Sol. Energy Mater.* 11, 187-197.
- Wyszecki, G., & Stiles, W.S. (1982). *Color Science: Concepts and Methods*, John Wiley and Sons, Inc., New York.
- Yamaguchi, M., & Luque, A. (1999). High efficiency and high concentration in photovoltaics, *IEEE Trans. Electron Dev.* 46 (10), 2139-2144.
- Yoshi, O. (2000). CIE Fundamentals for Color Measurements. *Paper for IS&T NIP16 Conference*, Vancouver, Canada, Oct. 16-20.

Yoshi, O. (2004), Color Rendering and Luminous Efficacy of White LED Spectra, *Proc. of SPIE (Fourth International Conference on Solid State Lighting)*, 5530, SPIE, Bellingham, WA. doi:10.1117/12.565757.

Yu, F.T.S., & Yin, S. (2002). *Fiber Optic Sensors*, Dekker, New York.

Zubia, J., Arrue, J., & Mendioroz, A. (1997). Theoretical analysis of the torsion induced optical effect in plastic optical fibers. *Opt. Fiber Technol.*, 3, p162.

Bibliography

- American Council for an Energy-Efficient Economy. (2000). *American Council for an Energy-Efficient Economy. One of a Series of ACEEE White Papers on the Role of Energy Efficiency in Electric Utility Restructuring*. WASHINGTON, DC.
- Atif, M.R., Love, J.A., & Littlefair, P. (1997). Daylighting Monitoring Protocols & Procedures for Buildings, *Report NRCC-41369*.
- Azni, Z.A. (2008). Integrating Sustainable Energy in Buildings: A Case Study in Malaysia. *FAU Conference*, Copenhagen, Denmark, 14-15.
- Azni, Z.A., Samirah, A.R., & Sulaiman, S. (2006). *Energy in Buildings: Sustainable Symbiosis*. UPENA. Malaysia.
- Barth, S.A., & Hubbard, C.L. (2002). *Port, International Patent Application WO 02/41041 A2*.
- Batchelder, J.S., Zewail, A.H., & Cole, T. (1981). Luminescent Solar Concentrators. Experimental and theoretical analysis of their possible efficiencies. *Applied Optics*. 20 (21), 3733 - 3754.
- Boettcher, J.A. (2003). Laminate performance results of metal free and color neutral solar reflecting film, *Proceedings of Glass Processing Days Conference*, June 2003, 538 - 539.
- Bohren, C.F., & Huffman, D.R. (1998). *Absorption and Scattering of Light by Small Particles*, Wiley Science Paperback Series, Wiley-Interscience, New York, 1998.
- ARTICLE IN PRESS.
- BRE Building Research Establishment. (1986a). *BRE Digest 309: Estimating daylight in buildings: Part 1*. Building Research Establishment Digest, Watford, England.
- BRE Building Research Establishment. (1986b). *BRE Digest 310: Estimating daylight in buildings: Part 2*. Building Research Establishment Digest, Watford, England.
- Byoungcho, L. (2003). Review of the present status of optical fiber sensors. *Optical Fiber Technology*. 9, 57-79.
- Caddet. (1997). *Saving energy with energy efficiency in hospitals*. Maxi Brochure 05, (IEA and OECD, Netherlands).
- Canziani, R., Peron, F., & Rossi, G. (2004). Daylight and energy performances of a new type of light pipe. *Energy and Buildings*. 36(11), 1163-76.
- Carmody, J., Selkowitz, S., & Heschong, L. (1996). *Residential windows: a guide to new technologies and energy performance*. New York, USA: WW Norton & Company.

- Carrascosa, M., Unamuno, S., & Agullo-Lopez, F. (1983). Monte Carlo simulation of the performance of PMMA luminescent solar collectors. *Applied Optics*. 22 (20), 3236 - 3241.
- Carter, D.J. (2002). The measured and predicted performance of passive solar light pipe systems. *Lighting Research and Technology*, 34(1), 39-52.
- Carter, D.J. (2003). Human response to interiors lit using light pipe systems, in *Proceedings of Illuminat 2003*, Cluj-Napoca, Romania, vol. 1, 11-1-11-10.
- Cawthorne, D. (1991). *Buildings, Lighting and the Biological Clock*. Martin Centre for Architectural and Urban Studies, University of Cambridge, Cambridge.
- Chirarattananon, S., Chedsiri, S., & Renshen, L. (2000). Daylighting through light pipes in the tropics. *Solar Energy*. 69(4), 331 - 41.
- Choi, A.S., & Mistrick, R.G. (1999). Analysis of daylight responsive dimming system performance. *Building and Environment*. 34(3), 231 - 43.
- Choi, A.S., & Sung, M.K. (2000). Development of a daylight responsive dimming system and preliminary evaluation of system performance. *Building and Environment*. 35(7), 663 - 76.
- Commission of the European Communities. (1993). In: Baker NV, Fanchiotti A, Steemers KA, editors. *Daylighting in architecture: a European reference book*. Directorate-General XII for Science, Research and Development. London: James & James (Science Publishers) Ltd.
- Liang, D., Monteiro, L.F., Teixeira, M.R., Monteiro, M.L.F., & Collares-Pereira, M. (1998). Fibre-optic solar energy transmission and concentration, *Solar Energy Materials and Solar Cells*. 54, 323 - 331.
- Department of Trade and Industry. (1999). *UK Energy Sector Indicators*, London.
- Duffie, J.A., & Beckman, W.A. (1991). *Solar Engineering of Thermal Processes*, second ed. John Wiley and Sons.
- Dwivedi, S.K. (2007). *A textbook of engineering physics*. New Delhi, I.K.
- Dye, D., Wood, B.D., Fraas, L.M., & Muhs, J.D. (2003). Optical design of an infrared non-imaging device for a full spectrum solar energy system. In: *International Solar Energy Conference*, Kohala Coast, Hawaii Island, March 15 - 18.
- Earl, D., & Muhs, J.D. (2001). Preliminary results on luminaire design for hybrid solar lighting systems. *Proceeding of Forum 2001: Solar Energy: The Power to Choose*, April 21 - 25.
- Earl, D.D., Maxey, C.L., & Muhs, J.D. (2003). Performance of new hybrid solar lighting luminaire design. In: *International Solar Energy Conference*, Kohala Coast, Hawaii Island, March 15 - 18.

- Earl, D.D., & Muhs, J.D. (2003). Modeling and evaluation of chromatic variations in a hybrid solar/electric lighting system. In: *International Solar Energy Conference*, Kohala Coast, Hawaii Island, March 15 - 18.
- Edmonds, I.R., & Greenup, P.J. (2002). Daylighting in the tropics. *Solar Energy*. 73(2), 111 - 121.
- Edmonds, I.E., Repel, J., & Jardine, P. (1997). *Light Research Technology*. 29, 23 - 32.
- Edmonds, I.R., Moore, G.I., Smith, G.B., & Swift, P.D. (1995). *Light Research Technology*. 27, 27 - 35.
- Fay, C. (2003). Daylighting and productivity, a literature review. *International Solar Energy Conference*, Kohala Coast, Hawaii Island, March 15 - 18.
- Feng, Z., Narendran, N., & Van, J. D. (2002). *Proceeding of SPIE, Solid State Light. II* 4776, 206 - 214.
- Franta, G., & Anstead, K. (1993). *Daylighting Offers Great Oortunities*, American Institute of Architects, Washington, DC.
- FSEC. (2006). *About window films*. Florida: Florida Solar Energy Center, from <http://www.fsec.ucf.edu/en/consumer/buildings/homes/windows/films.htm>.
- Ghisi, E., & Tinker, J.A. (2005). An Ideal Window Area concept for energy efficient integration of daylight and artificial light in buildings. *Building and Environment*. 40(1), 51 - 61.
- Ghisi, E. (2002). *The use of fibre optics on energy efficient lighting in buildings*. PhD thesis, School of Civil Engineering, University of Leeds.
- Glenigan. (1998). *Griffiths Electrical Installations Price Book*, Glenigan Cost Information Service, Bournemouth.
- Granqvist, C.G. (1991). Energy efficient windows: present and forthcoming technology, in: C.G. Granqvist (Ed.), *Material Science for Solar Energy Conversion Systems*, Pergamon, Oxford, UK.
- Gruzen Samton LLP, & Hayden McKay Lighting Design Inc. (2005). *Manual for quality, energy efficient lighting*. New York: Department of Design and Construction.
- Gueymard, C. (2000). Prediction and performance assessment of mean hourly global radiation. *Solar Energy*. 68 (3).
- Guide, F. (1999). *Energy efficiency in buildings*. Chartered Institute of Building Services Engineers.
- Halliday, & David. (2001). *Fundamentals of physics*. John Wiley & Sons.

- Hamiza, I. (2005). Energy Efficient Buildings. *Energy Smart*. Quarter 1, Issue 0017. Malaysia.
- Hassan, B. (2006). Energy Management Practice in Buildings. *Seminar on Energy Efficiency in Buildings – How to Achieve Immediate Savings*, 24th January, 2006 at Crowne Plaza Mutiara Hotel, Kuala Lumpur.
- Hermann, A.M. (1982). Luminescent Solar Concentrators: a review. *Solar Energy*. 29 (4), 323 – 329.
- Hopkinson, R.G., Petherbridge, P., & Longmore, J. (1966). *Daylighting*. London: Heinemann.
- Hui, S.C.M., & Muller, H.F.O. (2001). *Architecture Science Review*. 44, 221 – 226.
- Illuminating Engineering Society of North America (IESNA). (2003). *The IESNA Lighting Handbook: Reference and Application*. Illuminating Engineering Society of North America, New York, NY.
- Jaramillo, O.A., Rio, J.A. del., & Huelsz, G. (1999). A thermal study of optical fibres transmitting concentrated solar energy, *J. Phys. D: Allied Physics*. 32, 1000 – 1005.
- Jaramillo, O.A., & Rio, J.A. del. (2002). Optical fibres for a mini-dish/Stirling system: thermodynamic optimization, *J. Phys. D: Allied Physics*. 35, 1241 – 1250.
- Jaramillo, O.A., Huelsz, G., & Rio, J.A. del. (2002). A theoretical and experimental thermal study of SiO₂ optical fibres transmitting concentrated radiative energy, *J. Phys. D: Allied Physics*. 35, 95 – 102.
- Jenkins, D., & Muneer, T. (2003). Modelling light-pipe performances: a natural daylighting solution. *Building and Environment*. 38(7), 965 – 72.
- Jim, J. (2006). *Energy Efficiency Opportunities in Ontario Hospitals*, Ontario USA.
- Johnson, K., & Selkowitz, S. (1986). Lightguide design principles, in *Proceedings of the 2nd International Daylighting Conference*, Long Beach, CA, 182–198.
- Kalogirou, S.A. (2004). Solar thermal collectors and applications, *Progress in Energy and Combustion Science*, 30, 231 – 295.
- Kevin, B. (2001). *Energy Efficiency in Africa for Sustainable Development: A South African Perspective*. Energy Research Institute, University of Cape Town.
- Kinney, L., & Burnett, T. (2002). Innovations in direct beam daylighting systems, *Right Light 5 Conference Proceedings*, 29-31/5, Nice, France, 425 – 427.
- Koroneos, C., Spachos, T., & Moussiopoulos, N. (2003). Exergy analysis of renewable energy sources. *Renewable Energy*. 28, 295 – 310.
- Kribus, O., Zik, J., & Karni, J. (2000). Optical fibres and solar power generation. *Solar Energy*. 68, 405 – 416.

- Lancashire, D.S., & Fox, A.E. (1996). Lighting: the way to building efficiency. *Consulting-Specifying Engineer*. 34(6).
- Leslie, R.P. (1986). Core daylighting: building code issues, in *Proceedings of the 2nd International Daylighting Conference*, Long Beach, CA, 407-410.
- Leslie, R.P. (2002). Capturing the daylight dividend in buildings: why and how? *Building and Environment*. 38 (2003), p381.
- Li, B.J., & Cao, W.J. (1992). Analysis of light transmitting way on solar energy lighting. *17th National Passive Solar Conference*. (S. Burley and M.E Arden Ed.), 93-98.
- Loe, D., & Rowlands, E. (1996). The art and science of lighting. *Lighting Research and Technology*. 28(4), 153-164.
- Max Home. (2009). *High performance building services and products*, from: <http://www.fle-enterprises.com/info/builders>.
- Maxey, L.D., Cates, M.R., & Jaiswal, S.L. (2003). Efficient optical couplings for fiber-distributed solar lighting. In: *International Solar Energy Conference*, Kohala Coast, Hawaii Island, March 15 - 18.
- Mirkovich, D.N. (1993). Assessment of beam lighting systems for interior core illumination in multi-storey commercial buildings, *ASHRAE Transactions*, 99(1), 1106-1116.
- MS1525. (2001). *Code of Practice on Energy Efficiency and use of Renewable Energy for non-residential buildings*.
- Kaushika, N.D., & Reddy, K.S. (2000). Performance of a low cost solar paraboloidal dish steam generating system. *Energy Conversion&Management*. 41, 713-726.
- National Lighting Product Information Program (NLPIP). (1999). *Dimming Electronic Ballasts, Specifier Reports*, vol. 7, no. 3, October. Available from <<http://www.lrc.rpi.edu>>.
- Office of the Deputy Prime Minister, UK. (2002). *The Building Regulations*, HMSO, London.
- Ozturk, H.H. (2004). Experimental determination of energy and exergy efficiency of the solar parabolic-cooker. *Solar Energy*. 77, 67-71.
- Papadopoulos, A., Katsafados, P., Kallos, G., & Nickovic, S. (2002). The weather forecasting system for Poseidon-An overview. *The Global Atmosphere and Ocean System Journal*. 8 (2-3), 219 - 237.
- Petela, R. (2005). Exergy analysis of the solar cylindrical-parabolic cooker, *Solar Energy*. 79, 221 - 233.
- Pouleik, V., & Libra, M. (1998). New Solar Tracker, *Sol. Energy Mater. Sol. Cells*. 51, 113.

- Public work and Government Services Canada. (2002). *Daylighting guide for Canadian commercial buildings*. Canada: Public work and Government Services Canada.
- Rubin, E.S., & Davidson, C.I. (2001). *Introduction to Engineering & the Environment*, McGraw-Hill, Boston.
- Schlegel, G. (2003). *A TRNSYS model of a hybrid lighting system*. M.S. Thesis, Solar Energy Laboratory, University of Wisconsin-Madison, USA.
- Selkowitz, S., Rubin, M., & Stearns, B. (1982). *Fluorescent concentrators for daylighting applications*. University of California, California, p29.
- Sharples, S., Stewart, L., & Tregenza, P.R. (2001). Glazing daylight transmittances: a field survey of windows in urban areas. *Building and Environment*. 36(4), 503-509.
- Singh, N., Kaushik, S.C., & Misra, R.D. (2000). Exergetic analysis of a solar thermal power system, *Renewable Energy*. 19 (2000), 135-143.
- Smith, G.B. (2003). Nanostructured thin films, in: W.S. Weiglhofer, A. Lakhtakia (Eds.), *Introduction to Complex Mediums for Optics and Electromagnetics*, SPIE, Bellingham, WA, USA.
- Society of Light and Lighting. (2001). *Code for Interior Lighting*, SLL, London.
- Stewart, & Oscar M. (1957). *Physics : a textbook for colleges*. Newell S. Gingrich. Ginn.
- Swift, P.D., Smith, G.B., & Franklin, J. (1999). Light to light efficiencies in Luminescent Solar Concentrators. In: *Proceedings of SPIE Conference on Solar Optical Materials*, Denver, CO, 21 - 28.
- Tekelioglu, M., & Wood, B.D. (2003). Thermal management of the polymethylmethacrylate (PMMA) core optical fiber for use in hybrid solar lighting. In: *International Solar Energy Conference*, Kohala Coast, Hawaii Island, March 15 - 18.
- Thomas, W.R.L., Drake, J.M., & Lesiecki, M.L. (1983). Light transport in planar Luminescent Solar Concentrators: the role of matrix losses. *Applied Optics*. 22 (21), 3440-3450.
- Thong, & Saw-pak. (1969). *Textbook of physics*. Pan-Asian Publications.
- Tyagi, S.K., Shengwei, W., Singhal, M.K., Kaushik, S.C., & Park, S.R. (2007). Exergy analysis and parametric study of concentrating type solar collectors, *International Journal of Thermal Sciences*. 46 (12), 1304 - 1310.
- Ulgen, K., & Hepbasli, A. (2004). Solar radiation models. part 1: a review. *Energy Sources*. 26, 507 - 520.
- Van de Hulst, H.C. (1981). *Light Scattering by Small Particles*, Dover Publications Inc., New York.

Wang, C., Abdul-Rahman, H., & S.P. Rao. (2008). A Design of Fluorescent Fiber Solar Concentrator (FFSC) and Outdoor Testing for Remote Indoor Daylighting and Power production Evaluation for Building Integration. *Journal of Design and the Built Environment*. 4(1), 97-114.

West, S. (2001). Improving the sustainable development of building stock by the implementation of energy efficient, climate control technologies. *Building and Environment*. 36(3), 281 - 9.

Wilfried, G.J.H.M. van S., Keith, W.J. B., Lenneke, H.S., Amanda, J. C., Andreas, B., Andreas, M., Sarah, J. McCormack, R.K., Daniel, J.F., Rahul, B., Evert, E.B., Antonius, R.B., Tristram, B., Jana, Q., Manus, K., Toby, M., De-Mello, D.C., Andries, M., & Daniel, V. (2008). Luminēcent Solar Concentrators: A review of recent results. *Optical Society of America*. Vol. 16, No. 26. OPTICS EXPRESS 21773.

Wilson, M., Jacobs, A., Solomon, J., Fontoynt, M., Pohl, W., Tsangrassoulis, A., & Jorve, M. (2002). Creating sunlight rooms in non-daylit spaces, In: *Right Light 5, 5th International Conference on Energy Efficient Lighting*, Nice, France, 29 - 31 May.

Wittwer, V., Goetzberger, A., & Heidler, K. (1982). Fluorescent planar concentrator (FPC) Monte Carlo computer model limit efficiency and latest experimental results. In: *Proceedings of 4th E.C. Photovoltaic Solar Energy Conference*, Stresa, Italy, 682-686.

Wright, M. (1994). Les fontaines de saint James Park, Londres. *Revue internationale de r~clairage*. 1994/3, 98-99.

Zastrow, A., & Wittwer, V. (1986). Daylighting with fluorescent concentrators and highly reflective silver-coated plastic films: a new alication for new materials. SPIE, *Optical Materials Technology for Energy Efficiency and Solar Energy Conversion* 653, 93-100.

Zeguers, J.D.M., & Jacobs, M.J.M. (1997). Energy saving and-perception of visual comfort, in *Proceedings of LUX Europa*, vol. 1, 761-782.

Zhang, Z.Y., & Grattan, K.T.V. (1999). Commercial activity in optical fiber sensors, in: K.T.V. Grattan, B.T. Meggitt (Eds.), *Optical Fiber Sensor Technology*, Vol. 3: Alications and Systems, Kluwer Academic Publishers, Boston, 1999, Chap. 10, 257-306.

Zik, O., Karni, J., & Kribus, A. (1999). The Trof (Tower Reflector with Optical Fibres): A new degree of freedom for solar energy systems. *Solar Energy*. 67, 13 - 22.

APPENDIX A: Wavelength Testing Diagram

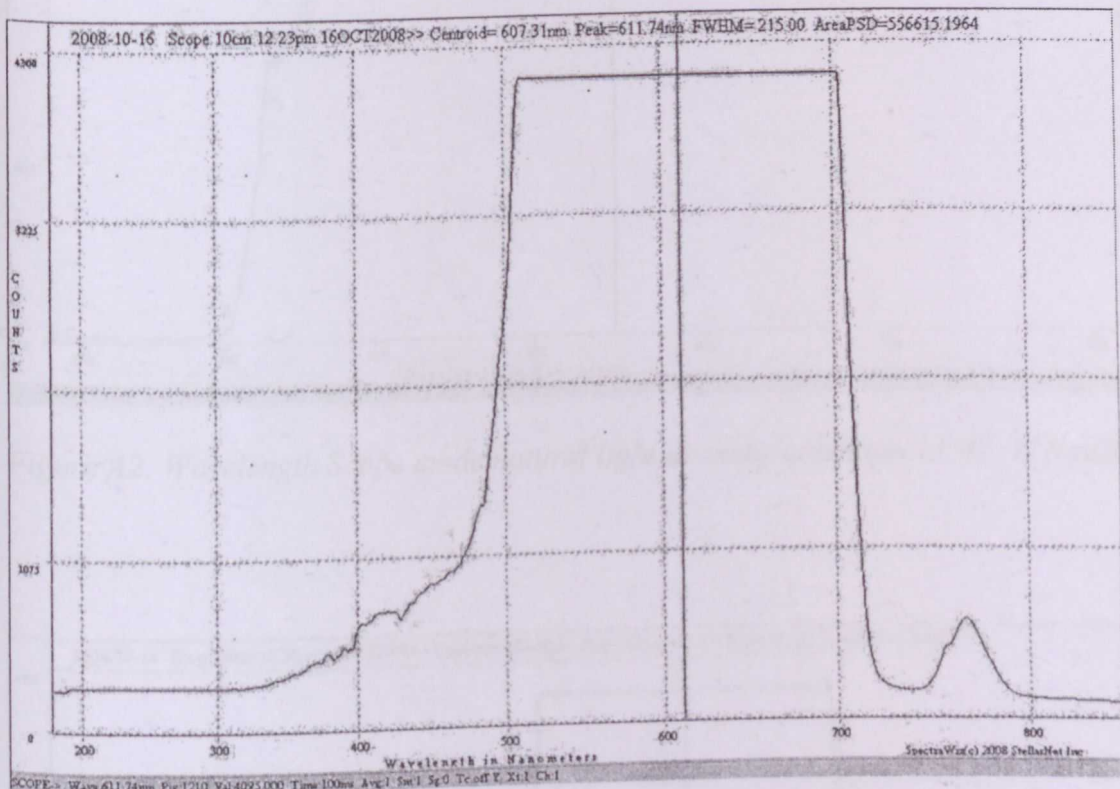


Figure A1: Wavelength Scope mode 10cm 12:23 16OCT2008

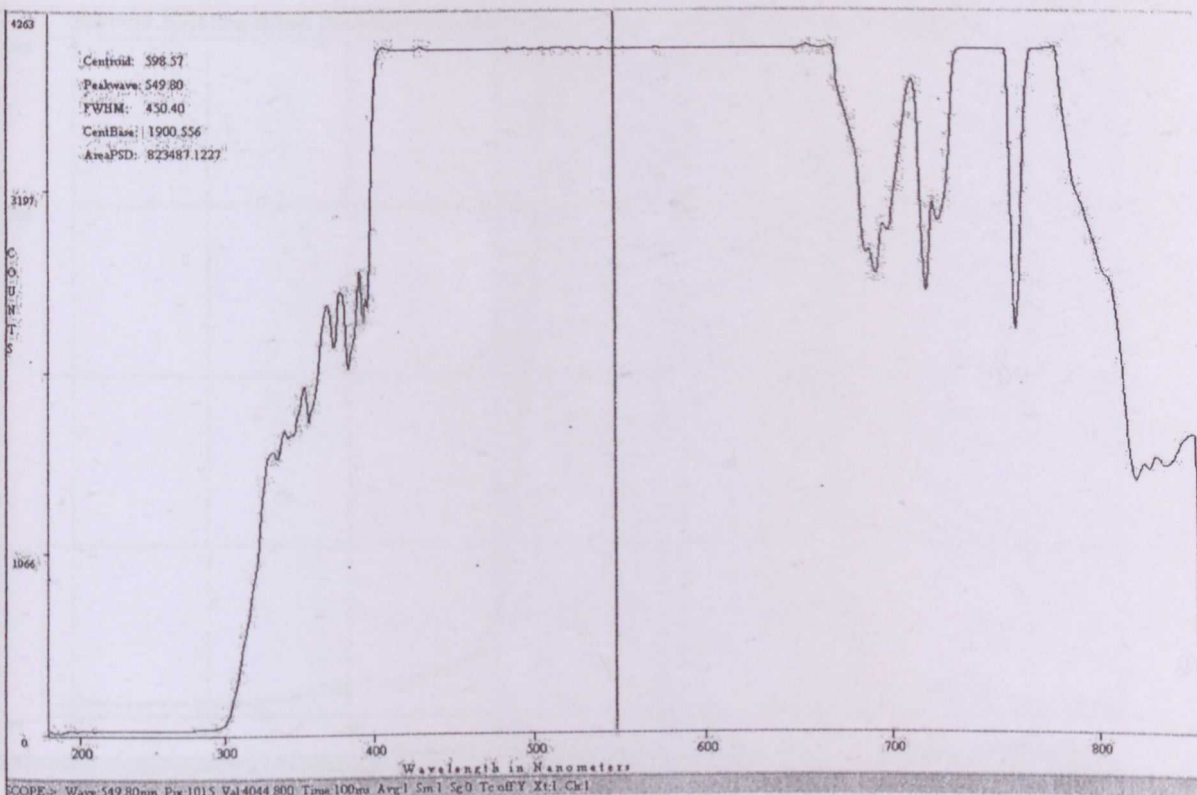


Figure A2: Wavelength Scope mode natural light at sunny condition 11:47, 12Nov2008

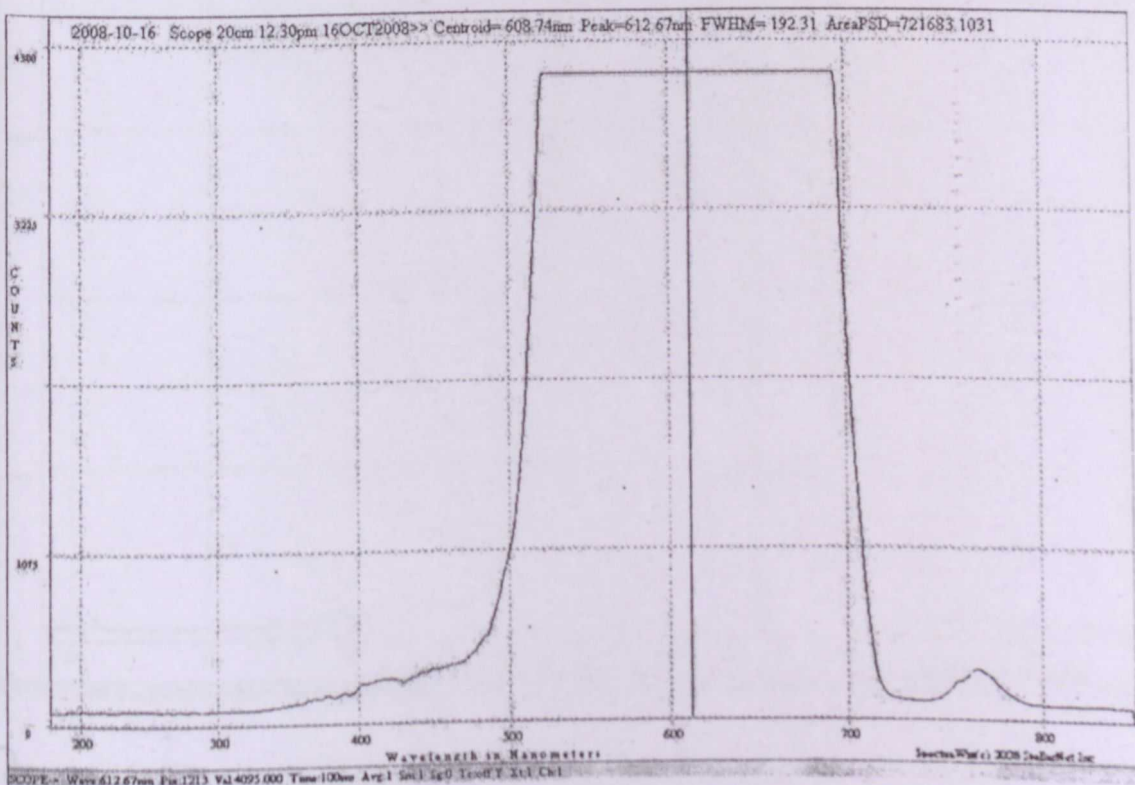


Figure A3: Wavelength Scope mode 20cm 12:30, 16OCT2008

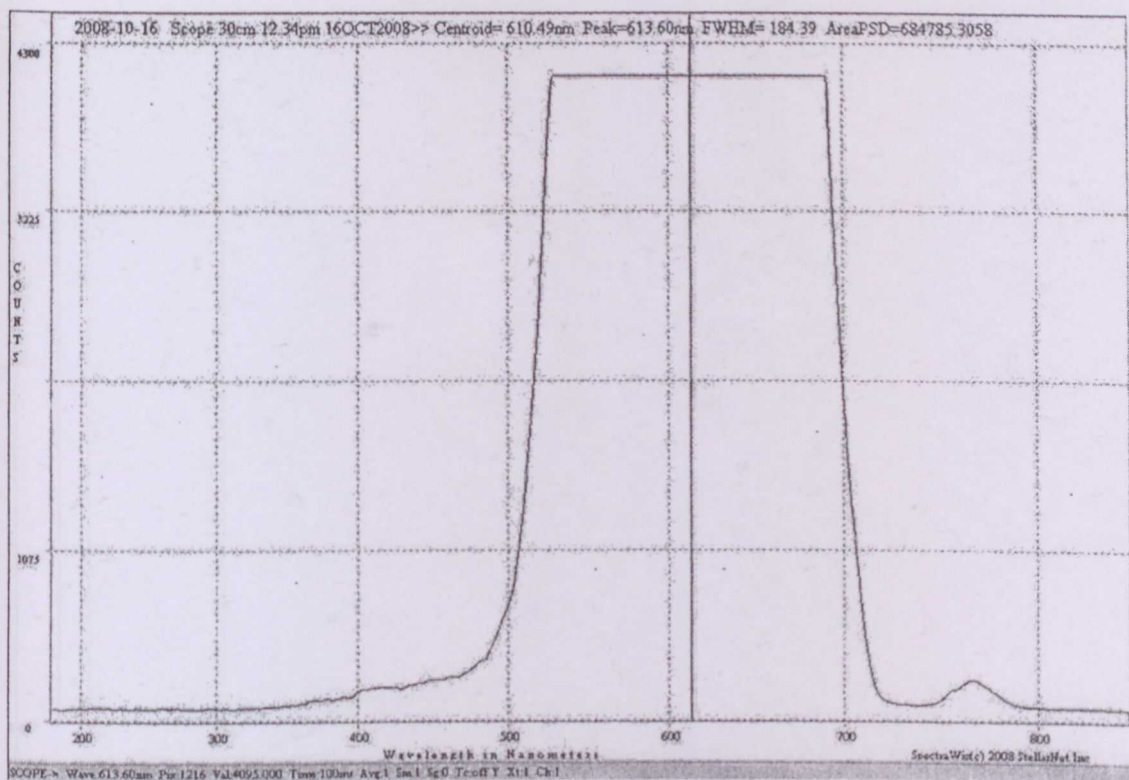


Figure A4: Wavelength Scope mode 30cm 12:34, 16OCT2008

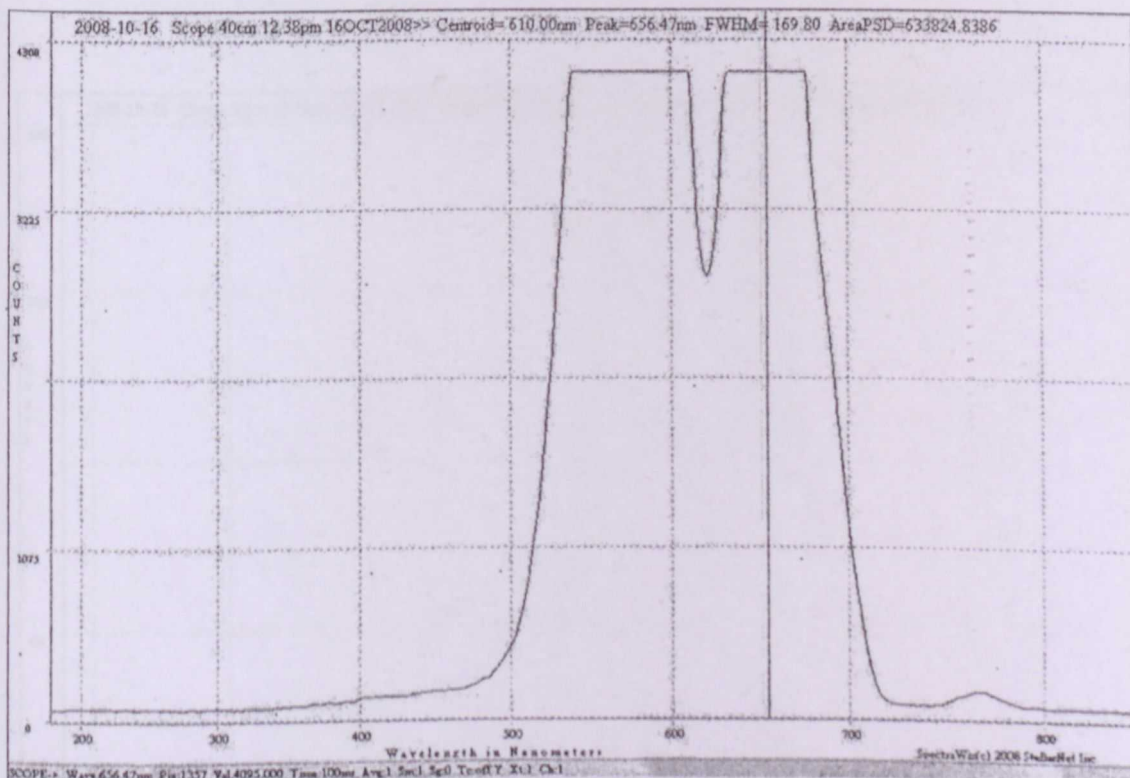


Figure A5: Wavelength Scope mode 40cm 12:37, 16OCT2008

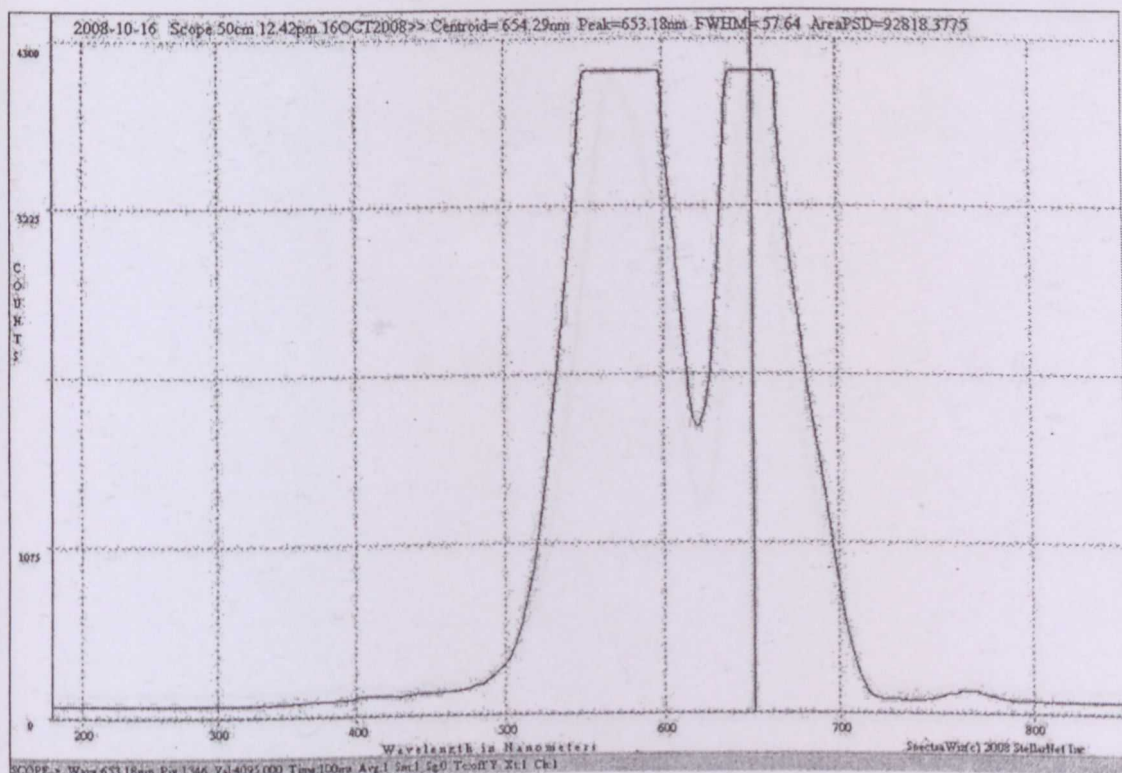


Figure A6: Wavelength Scope mode 50cm 12:42, 16OCT2008

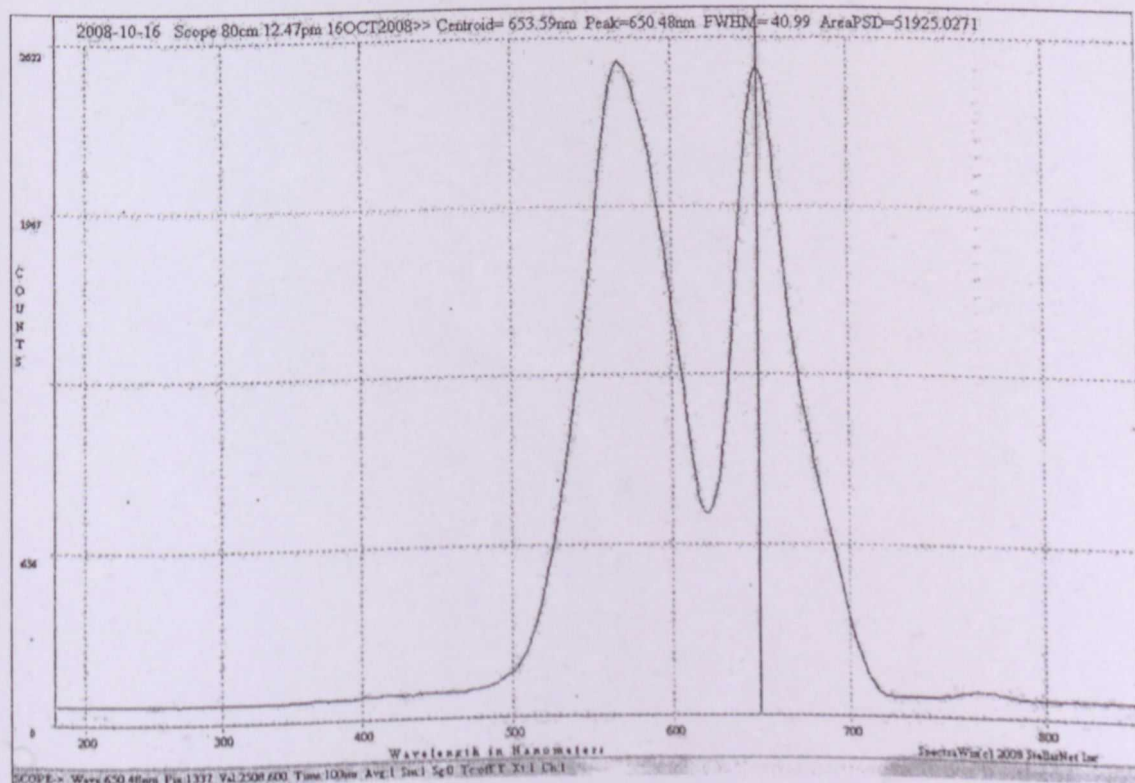


Figure A7: Wavelength Scope mode 80cm 12:47, 16OCT2008

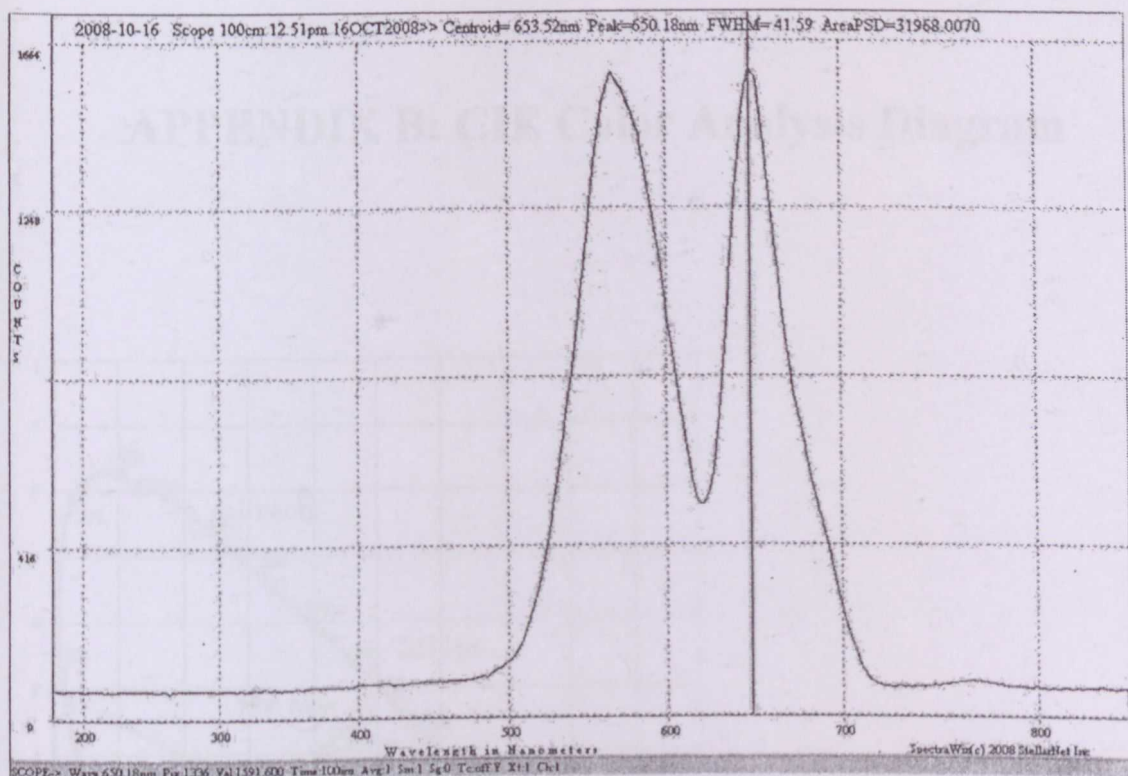
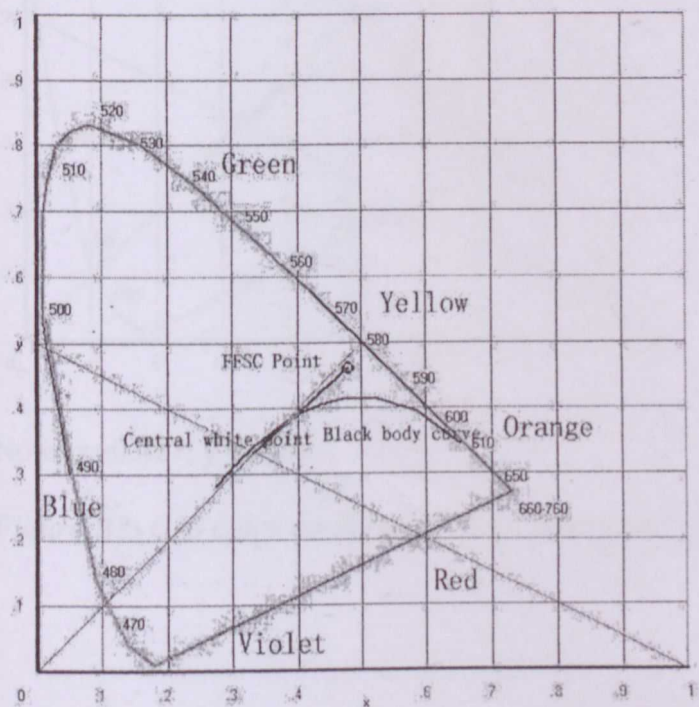


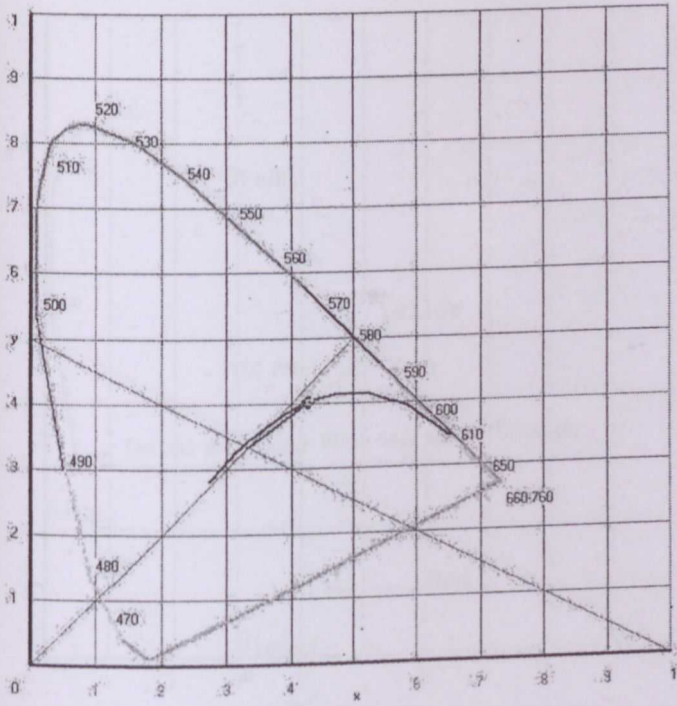
Figure A8: Wavelength Scope mode 100cm 12:51, 16OCT2008

APPENDIX B: CIE Color Analysis Diagram



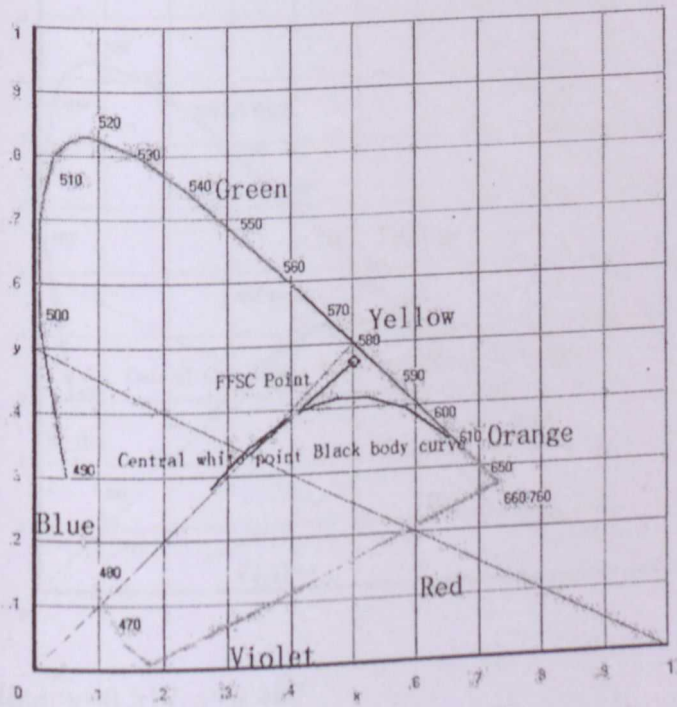
Note: $x=0.479$, $y=0.460$

Figure B1: CIE color analysis 10cm 12:27, 16OCT2008



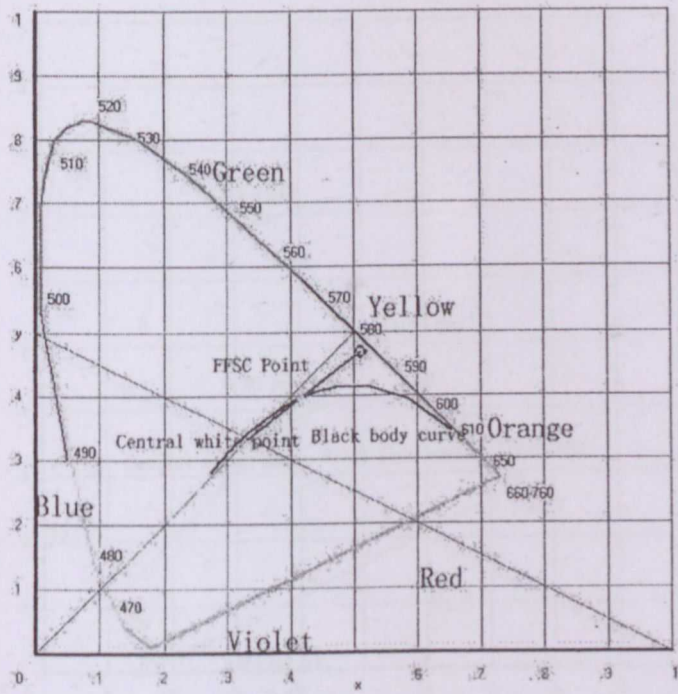
Note: $x=0.427$, $y=0.401$

Figure B2: CIE color analysis for direct sun light 11:33, 12Nov2008



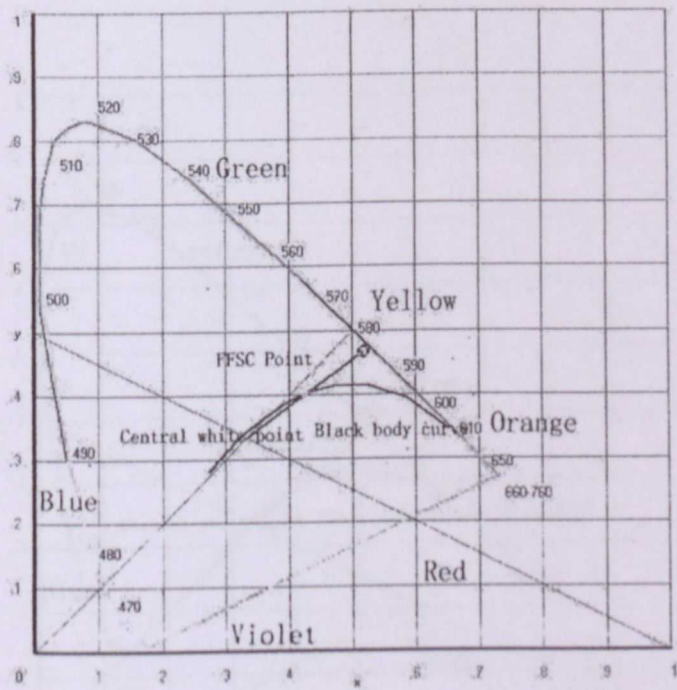
Note: $x=0.502$, $y=0.470$

Figure B3: CIE color analysis 20cm 12:33, 16OCT2008



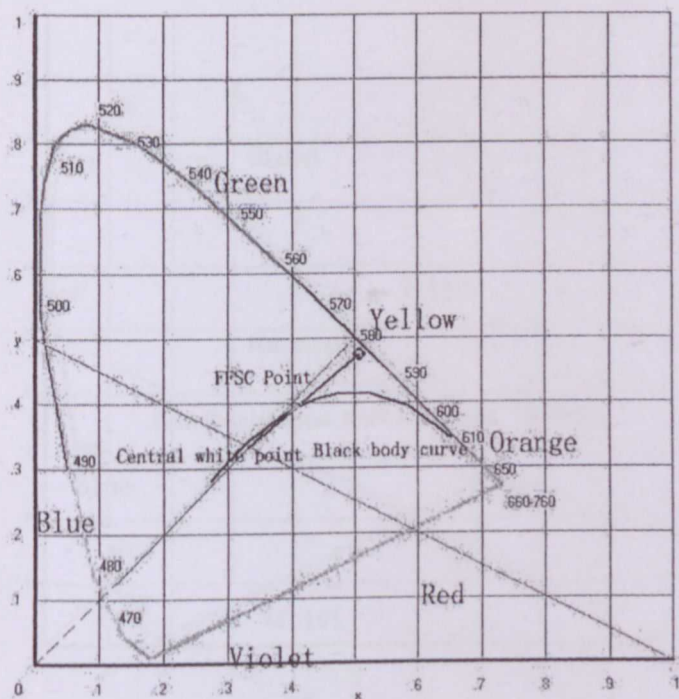
Note: $x=0.510$, $y=0.468$

Figure B4: CIE color analysis 30cm 12:36, 16OCT2008



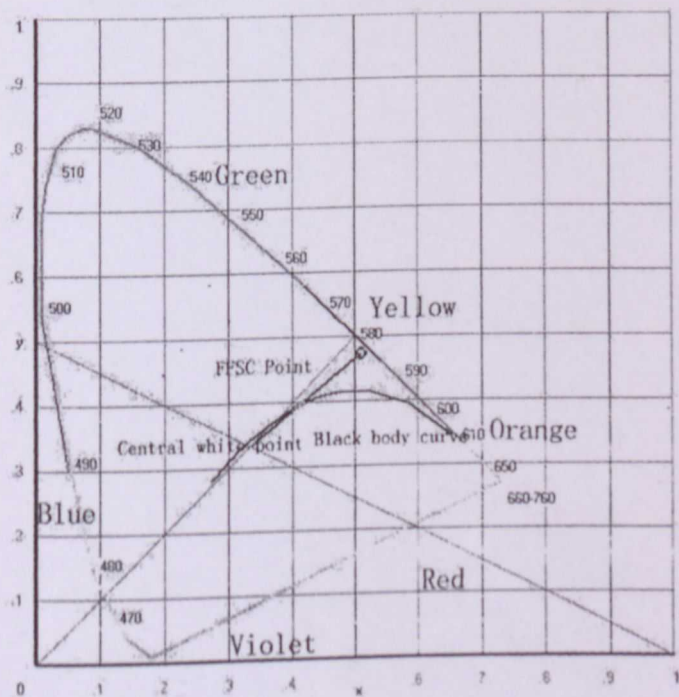
Note: $x=0.517$, $y=0.467$

Figure B5: CIE color analysis 40cm 12:47, 16OCT2008



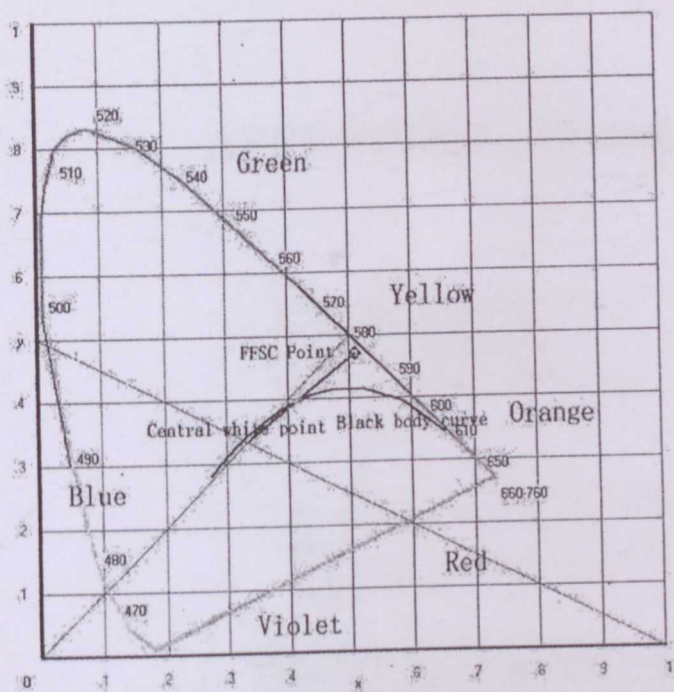
Note: $x=0.508$, $y=0.475$

Figure B6: CIE color analysis 50cm 12:47, 16OCT2008



Note: $x=0.510$, $y=0.472$

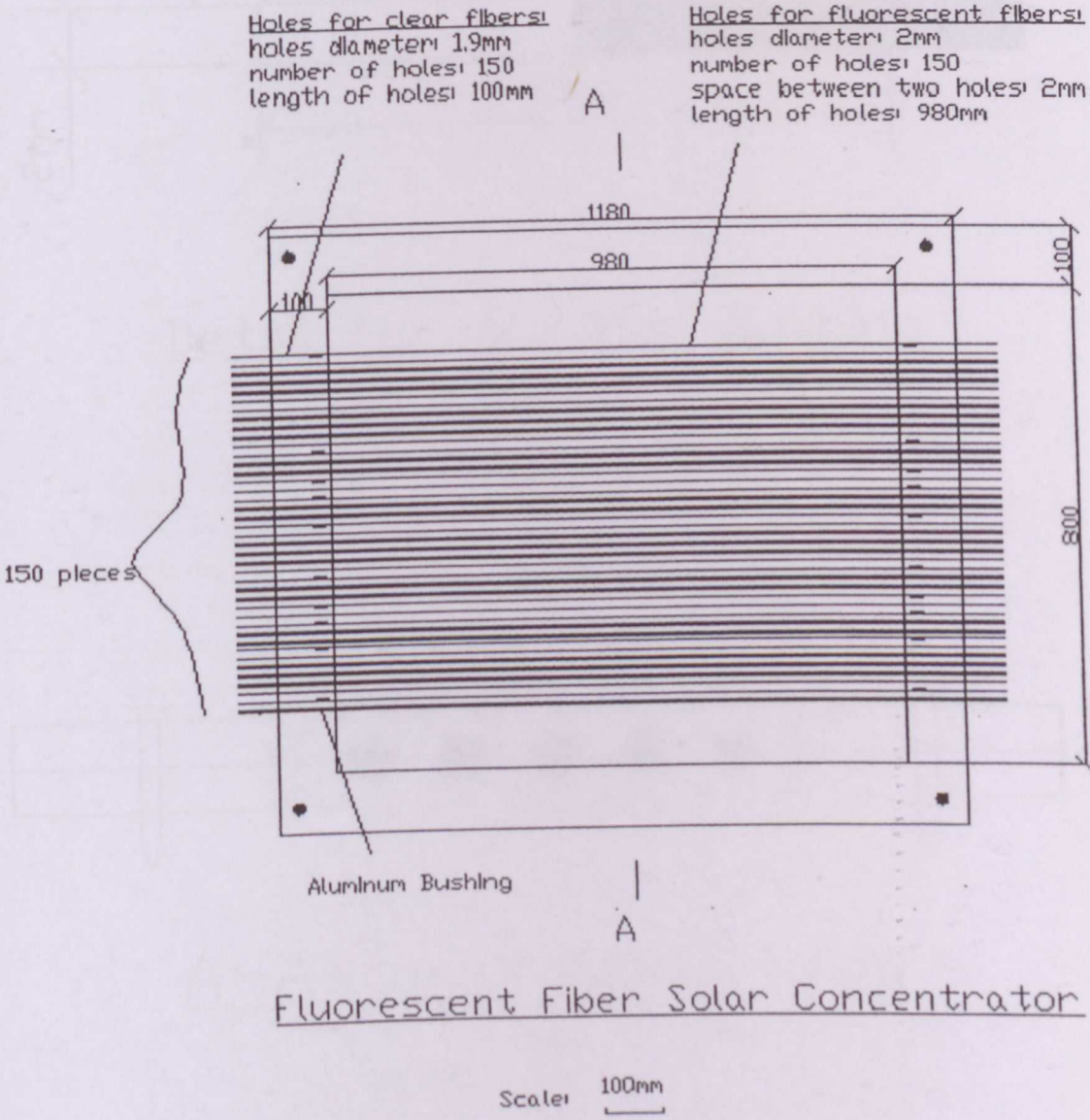
Figure B7: CIE color analysis 80cm 12:50, 16OCT2008



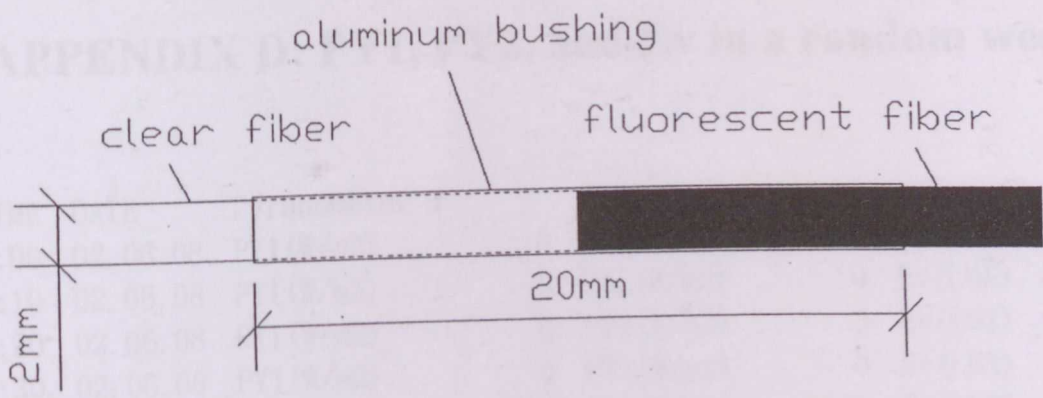
Note: $x=0.509$, $y=0.469$

Figure B8: CIE color analysis 100cm 12:52, 16OCT2008

APPENDIX C: Drawings of FFSC

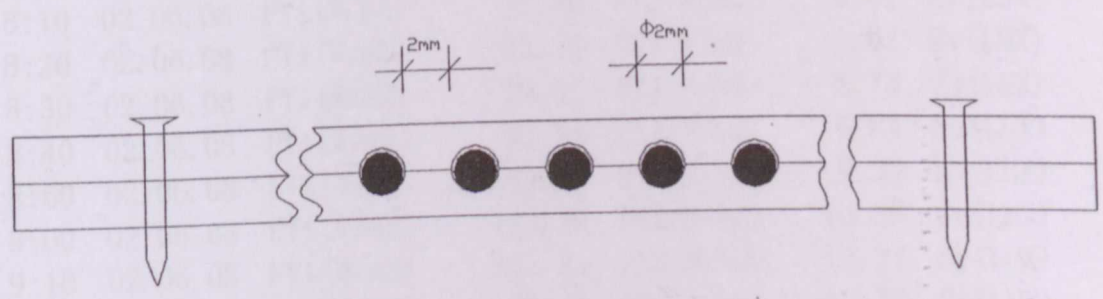


Fluorescent Fiber Solar Concentrator



Detail for Aluminum Bushing

scale: 1mm



A-A sectional view

scale: 1mm

APPENDIX D: PY1, PY2, and Ev in a random week

TIME	DATE	Pyranometer 1	Pyranometer 2	LUX sensor	
6:00	02. 06. 08	PY1 (W/m2)	0 PY2 (W/m2)	0 Ev (LUX)	0
6:10	02. 06. 08	PY1 (W/m2)	0 PY2 (W/m2)	0 Ev (LUX)	0
6:20	02. 06. 08	PY1 (W/m2)	0 PY2 (W/m2)	0 Ev (LUX)	0
6:30	02. 06. 08	PY1 (W/m2)	0 PY2 (W/m2)	0 Ev (LUX)	0
6:40	02. 06. 08	PY1 (W/m2)	0.2 PY2 (W/m2)	0.18 Ev (LUX)	12
6:50	02. 06. 08	PY1 (W/m2)	0 PY2 (W/m2)	0 Ev (LUX)	0
7:00	02. 06. 08	PY1 (W/m2)	0 PY2 (W/m2)	0 Ev (LUX)	0
7:10	02. 06. 08	PY1 (W/m2)	8.93 PY2 (W/m2)	0 Ev (LUX)	0
7:20	02. 06. 08	PY1 (W/m2)	16.83 PY2 (W/m2)	0 Ev (LUX)	0
7:30	02. 06. 08	PY1 (W/m2)	28.27 PY2 (W/m2)	2.03 Ev (LUX)	0
7:40	02. 06. 08	PY1 (W/m2)	44.69 PY2 (W/m2)	3.14 Ev (LUX)	0
7:50	02. 06. 08	PY1 (W/m2)	52.18 PY2 (W/m2)	3.7 Ev (LUX)	0
8:00	02. 06. 08	PY1 (W/m2)	60.7 PY2 (W/m2)	4.25 Ev (LUX)	0
8:10	02. 06. 08	PY1 (W/m2)	52.39 PY2 (W/m2)	4.07 Ev (LUX)	12
8:20	02. 06. 08	PY1 (W/m2)	51.55 PY2 (W/m2)	4.07 Ev (LUX)	0
8:30	02. 06. 08	PY1 (W/m2)	79.41 PY2 (W/m2)	5.73 Ev (LUX)	167
8:40	02. 06. 08	PY1 (W/m2)	95.84 PY2 (W/m2)	6.84 Ev (LUX)	192
8:50	02. 06. 08	PY1 (W/m2)	122.24 PY2 (W/m2)	8.32 Ev (LUX)	231
9:00	02. 06. 08	PY1 (W/m2)	152.39 PY2 (W/m2)	10.36 Ev (LUX)	282
9:10	02. 06. 08	PY1 (W/m2)	185.23 PY2 (W/m2)	12.21 Ev (LUX)	346
9:20	02. 06. 08	PY1 (W/m2)	189.18 PY2 (W/m2)	12.77 Ev (LUX)	359
9:30	02. 06. 08	PY1 (W/m2)	261.33 PY2 (W/m2)	16.84 Ev (LUX)	475
9:40	02. 06. 08	PY1 (W/m2)	293.13 PY2 (W/m2)	18.87 Ev (LUX)	526
9:50	02. 06. 08	PY1 (W/m2)	283.78 PY2 (W/m2)	18.32 Ev (LUX)	513
10:00	02. 06. 08	PY1 (W/m2)	281.7 PY2 (W/m2)	19.43 Ev (LUX)	552
10:10	02. 06. 08	PY1 (W/m2)	329.72 PY2 (W/m2)	20.54 Ev (LUX)	552
10:20	02. 06. 08	PY1 (W/m2)	246.56 PY2 (W/m2)	15.17 Ev (LUX)	411
10:30	02. 06. 08	PY1 (W/m2)	212.88 PY2 (W/m2)	13.51 Ev (LUX)	359
10:40	02. 06. 08	PY1 (W/m2)	279.62 PY2 (W/m2)	16.84 Ev (LUX)	462
10:50	02. 06. 08	PY1 (W/m2)	368.6 PY2 (W/m2)	21.09 Ev (LUX)	578
11:00	02. 06. 08	PY1 (W/m2)	716.63 PY2 (W/m2)	39.97 Ev (LUX)	1130
11:10	02. 06. 08	PY1 (W/m2)	455.09 PY2 (W/m2)	26.83 Ev (LUX)	770
11:20	02. 06. 08	PY1 (W/m2)	428.06 PY2 (W/m2)	22.76 Ev (LUX)	655
11:30	02. 06. 08	PY1 (W/m2)	180.87 PY2 (W/m2)	10.36 Ev (LUX)	308
11:40	02. 06. 08	PY1 (W/m2)	160.7 PY2 (W/m2)	9.43 Ev (LUX)	269
11:50	02. 06. 08	PY1 (W/m2)	221.2 PY2 (W/m2)	14.43 Ev (LUX)	411
12:00	02. 06. 08	PY1 (W/m2)	288.35 PY2 (W/m2)	19.24 Ev (LUX)	513
12:10	02. 06. 08	PY1 (W/m2)	307.48 PY2 (W/m2)	20.72 Ev (LUX)	552
12:20	02. 06. 08	PY1 (W/m2)	239.29 PY2 (W/m2)	17.02 Ev (LUX)	462

12:30	02.06.08	PY1 (W/m2)	237.62	PY2 (W/m2)	16.65	Ev (LUX)	449
12:40	02.06.08	PY1 (W/m2)	234.3	PY2 (W/m2)	16.47	Ev (LUX)	436
12:50	02.06.08	PY1 (W/m2)	166.52	PY2 (W/m2)	11.84	Ev (LUX)	321
13:00	02.06.08	PY1 (W/m2)	154.46	PY2 (W/m2)	10.91	Ev (LUX)	295
13:10	02.06.08	PY1 (W/m2)	105.19	PY2 (W/m2)	7.95	Ev (LUX)	218
13:20	02.06.08	PY1 (W/m2)	104.57	PY2 (W/m2)	7.77	Ev (LUX)	218
13:30	02.06.08	PY1 (W/m2)	135.34	PY2 (W/m2)	10.36	Ev (LUX)	295
13:40	02.06.08	PY1 (W/m2)	149.27	PY2 (W/m2)	11.47	Ev (LUX)	308
13:50	02.06.08	PY1 (W/m2)	211.85	PY2 (W/m2)	15.73	Ev (LUX)	436
14:00	02.06.08	PY1 (W/m2)	838.46	PY2 (W/m2)	56.07	Ev (LUX)	1451
14:10	02.06.08	PY1 (W/m2)	893.34	PY2 (W/m2)	61.07	Ev (LUX)	1605
14:20	02.06.08	PY1 (W/m2)	164.86	PY2 (W/m2)	11.84	Ev (LUX)	346
14:30	02.06.08	PY1 (W/m2)	144.69	PY2 (W/m2)	9.62	Ev (LUX)	295
14:40	02.06.08	PY1 (W/m2)	277.75	PY2 (W/m2)	17.95	Ev (LUX)	488
14:50	02.06.08	PY1 (W/m2)	554.46	PY2 (W/m2)	34.98	Ev (LUX)	937
15:00	02.06.08	PY1 (W/m2)	835.34	PY2 (W/m2)	50.89	Ev (LUX)	1323
15:10	02.06.08	PY1 (W/m2)	955.09	PY2 (W/m2)	54.04	Ev (LUX)	1387
15:20	02.06.08	PY1 (W/m2)	269.85	PY2 (W/m2)	17.58	Ev (LUX)	488
15:30	02.06.08	PY1 (W/m2)	882.32	PY2 (W/m2)	51.45	Ev (LUX)	1310
15:40	02.06.08	PY1 (W/m2)	780.24	PY2 (W/m2)	46.45	Ev (LUX)	1181
15:50	02.06.08	PY1 (W/m2)	756.13	PY2 (W/m2)	46.45	Ev (LUX)	1181
16:00	02.06.08	PY1 (W/m2)	690.85	PY2 (W/m2)	43.12	Ev (LUX)	1117
16:10	02.06.08	PY1 (W/m2)	656.34	PY2 (W/m2)	40.34	Ev (LUX)	1027
16:20	02.06.08	PY1 (W/m2)	580.24	PY2 (W/m2)	37.2	Ev (LUX)	976
16:30	02.06.08	PY1 (W/m2)	388.98	PY2 (W/m2)	26.65	Ev (LUX)	732
16:40	02.06.08	PY1 (W/m2)	813.92	PY2 (W/m2)	46.82	Ev (LUX)	1181
16:50	02.06.08	PY1 (W/m2)	613.3	PY2 (W/m2)	35.16	Ev (LUX)	924
17:00	02.06.08	PY1 (W/m2)	766.94	PY2 (W/m2)	39.42	Ev (LUX)	1014
17:10	02.06.08	PY1 (W/m2)	504.78	PY2 (W/m2)	27.2	Ev (LUX)	706
17:20	02.06.08	PY1 (W/m2)	457.17	PY2 (W/m2)	23.87	Ev (LUX)	603
17:30	02.06.08	PY1 (W/m2)	330.76	PY2 (W/m2)	17.76	Ev (LUX)	462
17:40	02.06.08	PY1 (W/m2)	167.56	PY2 (W/m2)	9.43	Ev (LUX)	282
17:50	02.06.08	PY1 (W/m2)	177.96	PY2 (W/m2)	11.1	Ev (LUX)	295
18:00	02.06.08	PY1 (W/m2)	76.71	PY2 (W/m2)	4.62	Ev (LUX)	0

6:00	03.06.08	PY1 (W/m2)	0	PY2 (W/m2)	0	Ev (LUX)	0
6:10	03.06.08	PY1 (W/m2)	0	PY2 (W/m2)	0	Ev (LUX)	0
6:20	03.06.08	PY1 (W/m2)	0	PY2 (W/m2)	0	Ev (LUX)	0
6:30	03.06.08	PY1 (W/m2)	0	PY2 (W/m2)	0	Ev (LUX)	0
6:40	03.06.08	PY1 (W/m2)	0	PY2 (W/m2)	0	Ev (LUX)	12
6:50	03.06.08	PY1 (W/m2)	0	PY2 (W/m2)	0.18	Ev (LUX)	12
7:00	03.06.08	PY1 (W/m2)	2.28	PY2 (W/m2)	0	Ev (LUX)	0
7:10	03.06.08	PY1 (W/m2)	12.68	PY2 (W/m2)	0	Ev (LUX)	0
7:20	03.06.08	PY1 (W/m2)	18.71	PY2 (W/m2)	0	Ev (LUX)	0
7:30	03.06.08	PY1 (W/m2)	21.82	PY2 (W/m2)	0	Ev (LUX)	0

7:40	03.06.08	PY1 (W/m2)	34.92	PY2 (W/m2)	2.96	Ev (LUX)	0
7:50	03.06.08	PY1 (W/m2)	44.07	PY2 (W/m2)	3.51	Ev (LUX)	0
8:00	03.06.08	PY1 (W/m2)	61.12	PY2 (W/m2)	4.62	Ev (LUX)	154
8:10	03.06.08	PY1 (W/m2)	94.38	PY2 (W/m2)	6.47	Ev (LUX)	218
8:20	03.06.08	PY1 (W/m2)	109.77	PY2 (W/m2)	7.58	Ev (LUX)	231
8:30	03.06.08	PY1 (W/m2)	207.06	PY2 (W/m2)	11.47	Ev (LUX)	334
8:40	03.06.08	PY1 (W/m2)	154.88	PY2 (W/m2)	10.17	Ev (LUX)	308
8:50	03.06.08	PY1 (W/m2)	261.53	PY2 (W/m2)	14.43	Ev (LUX)	436
9:00	03.06.08	PY1 (W/m2)	238.87	PY2 (W/m2)	14.06	Ev (LUX)	411
9:10	03.06.08	PY1 (W/m2)	297.08	PY2 (W/m2)	16.65	Ev (LUX)	513
9:20	03.06.08	PY1 (W/m2)	331.8	PY2 (W/m2)	18.69	Ev (LUX)	565
9:30	03.06.08	PY1 (W/m2)	262.37	PY2 (W/m2)	16.28	Ev (LUX)	462
9:40	03.06.08	PY1 (W/m2)	421.2	PY2 (W/m2)	24.24	Ev (LUX)	680
9:50	03.06.08	PY1 (W/m2)	306.86	PY2 (W/m2)	18.87	Ev (LUX)	552
10:00	03.06.08	PY1 (W/m2)	432.22	PY2 (W/m2)	23.87	Ev (LUX)	693
10:10	03.06.08	PY1 (W/m2)	334.92	PY2 (W/m2)	20.91	Ev (LUX)	629
10:20	03.06.08	PY1 (W/m2)	593.55	PY2 (W/m2)	33.31	Ev (LUX)	1014
10:30	03.06.08	PY1 (W/m2)	620.99	PY2 (W/m2)	35.16	Ev (LUX)	1053
10:40	03.06.08	PY1 (W/m2)	602.28	PY2 (W/m2)	34.05	Ev (LUX)	1040
10:50	03.06.08	PY1 (W/m2)	335.96	PY2 (W/m2)	23.13	Ev (LUX)	745
11:00	03.06.08	PY1 (W/m2)	723.28	PY2 (W/m2)	38.31	Ev (LUX)	1233
11:10	03.06.08	PY1 (W/m2)	695.42	PY2 (W/m2)	37.57	Ev (LUX)	1207
11:20	03.06.08	PY1 (W/m2)	861.12	PY2 (W/m2)	45.9	Ev (LUX)	1477
11:30	03.06.08	PY1 (W/m2)	343.45	PY2 (W/m2)	21.46	Ev (LUX)	668
11:40	03.06.08	PY1 (W/m2)	541.78	PY2 (W/m2)	31.09	Ev (LUX)	937
11:50	03.06.08	PY1 (W/m2)	449.06	PY2 (W/m2)	27.2	Ev (LUX)	809
12:00	03.06.08	PY1 (W/m2)	320.37	PY2 (W/m2)	19.61	Ev (LUX)	603
12:10	03.06.08	PY1 (W/m2)	833.05	PY2 (W/m2)	39.79	Ev (LUX)	1181
12:20	03.06.08	PY1 (W/m2)	1018.5	PY2 (W/m2)	46.64	Ev (LUX)	1336
12:30	03.06.08	PY1 (W/m2)	1025.36	PY2 (W/m2)	47.93	Ev (LUX)	1348
12:40	03.06.08	PY1 (W/m2)	375.05	PY2 (W/m2)	22.39	Ev (LUX)	655
12:50	03.06.08	PY1 (W/m2)	1064.65	PY2 (W/m2)	53.11	Ev (LUX)	1503
13:00	03.06.08	PY1 (W/m2)	598.33	PY2 (W/m2)	33.68	Ev (LUX)	1002
13:10	03.06.08	PY1 (W/m2)	484.61	PY2 (W/m2)	28.31	Ev (LUX)	835
13:20	03.06.08	PY1 (W/m2)	341.99	PY2 (W/m2)	19.43	Ev (LUX)	552
13:30	03.06.08	PY1 (W/m2)	311.22	PY2 (W/m2)	17.58	Ev (LUX)	488
13:40	03.06.08	PY1 (W/m2)	1086.9	PY2 (W/m2)	51.08	Ev (LUX)	1426
13:50	03.06.08	PY1 (W/m2)	643.86	PY2 (W/m2)	36.46	Ev (LUX)	1053
14:00	03.06.08	PY1 (W/m2)	353.63	PY2 (W/m2)	20.91	Ev (LUX)	603
14:10	03.06.08	PY1 (W/m2)	397.5	PY2 (W/m2)	23.5	Ev (LUX)	668
14:20	03.06.08	PY1 (W/m2)	272.34	PY2 (W/m2)	16.1	Ev (LUX)	475
14:30	03.06.08	PY1 (W/m2)	346.36	PY2 (W/m2)	19.98	Ev (LUX)	578
14:40	03.06.08	PY1 (W/m2)	824.32	PY2 (W/m2)	39.42	Ev (LUX)	1091
14:50	03.06.08	PY1 (W/m2)	286.27	PY2 (W/m2)	15.54	Ev (LUX)	449
15:00	03.06.08	PY1 (W/m2)	286.9	PY2 (W/m2)	15.91	Ev (LUX)	449
15:10	03.06.08	PY1 (W/m2)	260.49	PY2 (W/m2)	14.8	Ev (LUX)	436

15:20	03.06.08	PY1 (W/m2)	277.75	PY2 (W/m2)	16.1	Ev (LUX)	449
15:30	03.06.08	PY1 (W/m2)	66.11	PY2 (W/m2)	4.44	Ev (LUX)	0
15:40	03.06.08	PY1 (W/m2)	23.9	PY2 (W/m2)	2.03	Ev (LUX)	0
15:50	03.06.08	PY1 (W/m2)	18.5	PY2 (W/m2)	0	Ev (LUX)	0
16:00	03.06.08	PY1 (W/m2)	12.26	PY2 (W/m2)	0	Ev (LUX)	0
16:10	03.06.08	PY1 (W/m2)	8.73	PY2 (W/m2)	0	Ev (LUX)	0
16:20	03.06.08	PY1 (W/m2)	63.2	PY2 (W/m2)	4.99	Ev (LUX)	154
16:30	03.06.08	PY1 (W/m2)	95.01	PY2 (W/m2)	7.03	Ev (LUX)	218
16:40	03.06.08	PY1 (W/m2)	96.88	PY2 (W/m2)	7.03	Ev (LUX)	205
16:50	03.06.08	PY1 (W/m2)	84.61	PY2 (W/m2)	6.29	Ev (LUX)	179
17:00	03.06.08	PY1 (W/m2)	118.29	PY2 (W/m2)	8.14	Ev (LUX)	231
17:10	03.06.08	PY1 (W/m2)	110.39	PY2 (W/m2)	7.77	Ev (LUX)	231
17:20	03.06.08	PY1 (W/m2)	174.42	PY2 (W/m2)	11.47	Ev (LUX)	308
17:30	03.06.08	PY1 (W/m2)	122.24	PY2 (W/m2)	8.88	Ev (LUX)	244
17:40	03.06.08	PY1 (W/m2)	115.17	PY2 (W/m2)	8.14	Ev (LUX)	231
17:50	03.06.08	PY1 (W/m2)	124.32	PY2 (W/m2)	8.69	Ev (LUX)	244
18:00	03.06.08	PY1 (W/m2)	149.48	PY2 (W/m2)	9.99	Ev (LUX)	269

6:00	04.06.08	PY1 (W/m2)	0	PY2 (W/m2)	0	Ev (LUX)	0
6:10	04.06.08	PY1 (W/m2)	0	PY2 (W/m2)	0	Ev (LUX)	0
6:20	04.06.08	PY1 (W/m2)	0	PY2 (W/m2)	0	Ev (LUX)	0
6:30	04.06.08	PY1 (W/m2)	0	PY2 (W/m2)	0	Ev (LUX)	0
6:40	04.06.08	PY1 (W/m2)	0	PY2 (W/m2)	0	Ev (LUX)	0
6:50	04.06.08	PY1 (W/m2)	0	PY2 (W/m2)	0	Ev (LUX)	0
7:00	04.06.08	PY1 (W/m2)	5.19	PY2 (W/m2)	0	Ev (LUX)	0
7:10	04.06.08	PY1 (W/m2)	9.77	PY2 (W/m2)	0	Ev (LUX)	0
7:20	04.06.08	PY1 (W/m2)	16.83	PY2 (W/m2)	0	Ev (LUX)	0
7:30	04.06.08	PY1 (W/m2)	41.37	PY2 (W/m2)	2.59	Ev (LUX)	0
7:40	04.06.08	PY1 (W/m2)	40.33	PY2 (W/m2)	3.51	Ev (LUX)	0
7:50	04.06.08	PY1 (W/m2)	31.8	PY2 (W/m2)	3.51	Ev (LUX)	0
8:00	04.06.08	PY1 (W/m2)	51.76	PY2 (W/m2)	4.81	Ev (LUX)	154
8:10	04.06.08	PY1 (W/m2)	148.23	PY2 (W/m2)	8.32	Ev (LUX)	231
8:20	04.06.08	PY1 (W/m2)	185.03	PY2 (W/m2)	9.99	Ev (LUX)	282
8:30	04.06.08	PY1 (W/m2)	223.9	PY2 (W/m2)	11.66	Ev (LUX)	334
8:40	04.06.08	PY1 (W/m2)	238.04	PY2 (W/m2)	12.77	Ev (LUX)	385
8:50	04.06.08	PY1 (W/m2)	274.84	PY2 (W/m2)	14.99	Ev (LUX)	449
9:00	04.06.08	PY1 (W/m2)	320.58	PY2 (W/m2)	17.39	Ev (LUX)	526
9:10	04.06.08	PY1 (W/m2)	361.95	PY2 (W/m2)	19.8	Ev (LUX)	629
9:20	04.06.08	PY1 (W/m2)	384.61	PY2 (W/m2)	21.28	Ev (LUX)	680
9:30	04.06.08	PY1 (W/m2)	406.65	PY2 (W/m2)	22.2	Ev (LUX)	706
9:40	04.06.08	PY1 (W/m2)	479.83	PY2 (W/m2)	26.09	Ev (LUX)	835
9:50	04.06.08	PY1 (W/m2)	507.9	PY2 (W/m2)	27.2	Ev (LUX)	873
10:00	04.06.08	PY1 (W/m2)	522.66	PY2 (W/m2)	28.5	Ev (LUX)	899
10:10	04.06.08	PY1 (W/m2)	578.37	PY2 (W/m2)	31.27	Ev (LUX)	976
10:20	04.06.08	PY1 (W/m2)	586.07	PY2 (W/m2)	31.83	Ev (LUX)	976

10:30	04.06.08	PY1 (W/m2)	596.88	PY2 (W/m2)	32.57	Ev (LUX)	989
10:40	04.06.08	PY1 (W/m2)	631.8	PY2 (W/m2)	34.24	Ev (LUX)	1027
10:50	04.06.08	PY1 (W/m2)	646.15	PY2 (W/m2)	33.68	Ev (LUX)	1040
11:00	04.06.08	PY1 (W/m2)	725.36	PY2 (W/m2)	36.09	Ev (LUX)	1181
11:10	04.06.08	PY1 (W/m2)	768.6	PY2 (W/m2)	39.42	Ev (LUX)	1310
11:20	04.06.08	PY1 (W/m2)	765.28	PY2 (W/m2)	37.75	Ev (LUX)	1233
11:30	04.06.08	PY1 (W/m2)	849.89	PY2 (W/m2)	42.56	Ev (LUX)	1374
11:40	04.06.08	PY1 (W/m2)	897.5	PY2 (W/m2)	45.9	Ev (LUX)	1438
11:50	04.06.08	PY1 (W/m2)	876.5	PY2 (W/m2)	44.23	Ev (LUX)	1348
12:00	04.06.08	PY1 (W/m2)	931.18	PY2 (W/m2)	45.34	Ev (LUX)	1387
12:10	04.06.08	PY1 (W/m2)	979.83	PY2 (W/m2)	45.53	Ev (LUX)	1374
12:20	04.06.08	PY1 (W/m2)	956.75	PY2 (W/m2)	44.41	Ev (LUX)	1336
12:30	04.06.08	PY1 (W/m2)	997.5	PY2 (W/m2)	48.49	Ev (LUX)	1490
12:40	04.06.08	PY1 (W/m2)	1039.29	PY2 (W/m2)	53.48	Ev (LUX)	1618
12:50	04.06.08	PY1 (W/m2)	1064.65	PY2 (W/m2)	55.52	Ev (LUX)	1695
13:00	04.06.08	PY1 (W/m2)	1107.06	PY2 (W/m2)	56.26	Ev (LUX)	1708
13:10	04.06.08	PY1 (W/m2)	609.97	PY2 (W/m2)	34.24	Ev (LUX)	1027
13:20	04.06.08	PY1 (W/m2)	1027.85	PY2 (W/m2)	48.67	Ev (LUX)	1490
13:30	04.06.08	PY1 (W/m2)	1093.97	PY2 (W/m2)	52.37	Ev (LUX)	1528
13:40	04.06.08	PY1 (W/m2)	636.38	PY2 (W/m2)	32.2	Ev (LUX)	950
13:50	04.06.08	PY1 (W/m2)	1097.29	PY2 (W/m2)	54.04	Ev (LUX)	1477
14:00	04.06.08	PY1 (W/m2)	1040.74	PY2 (W/m2)	52	Ev (LUX)	1451
14:10	04.06.08	PY1 (W/m2)	1059.45	PY2 (W/m2)	50.89	Ev (LUX)	1387
14:20	04.06.08	PY1 (W/m2)	1135.75	PY2 (W/m2)	54.41	Ev (LUX)	1464
14:30	04.06.08	PY1 (W/m2)	356.13	PY2 (W/m2)	23.32	Ev (LUX)	680
14:40	04.06.08	PY1 (W/m2)	218.71	PY2 (W/m2)	14.62	Ev (LUX)	423
14:50	04.06.08	PY1 (W/m2)	393.34	PY2 (W/m2)	24.61	Ev (LUX)	693
15:00	04.06.08	PY1 (W/m2)	849.27	PY2 (W/m2)	43.12	Ev (LUX)	1104
15:10	04.06.08	PY1 (W/m2)	954.67	PY2 (W/m2)	49.6	Ev (LUX)	1271
15:20	04.06.08	PY1 (W/m2)	289.39	PY2 (W/m2)	18.5	Ev (LUX)	526
15:30	04.06.08	PY1 (W/m2)	195.84	PY2 (W/m2)	12.4	Ev (LUX)	359
15:40	04.06.08	PY1 (W/m2)	167.98	PY2 (W/m2)	10.17	Ev (LUX)	308
15:50	04.06.08	PY1 (W/m2)	182.95	PY2 (W/m2)	10.73	Ev (LUX)	308
16:00	04.06.08	PY1 (W/m2)	437.62	PY2 (W/m2)	20.35	Ev (LUX)	501
16:10	04.06.08	PY1 (W/m2)	355.3	PY2 (W/m2)	17.76	Ev (LUX)	436
16:20	04.06.08	PY1 (W/m2)	209.77	PY2 (W/m2)	11.84	Ev (LUX)	295
16:30	04.06.08	PY1 (W/m2)	54.67	PY2 (W/m2)	3.7	Ev (LUX)	0
16:40	04.06.08	PY1 (W/m2)	33.88	PY2 (W/m2)	2.59	Ev (LUX)	0
16:50	04.06.08	PY1 (W/m2)	6.44	PY2 (W/m2)	0	Ev (LUX)	0
17:00	04.06.08	PY1 (W/m2)	0	PY2 (W/m2)	0	Ev (LUX)	0
17:10	04.06.08	PY1 (W/m2)	0	PY2 (W/m2)	0	Ev (LUX)	0
17:20	04.06.08	PY1 (W/m2)	0	PY2 (W/m2)	0	Ev (LUX)	0
17:30	04.06.08	PY1 (W/m2)	4.15	PY2 (W/m2)	0	Ev (LUX)	0
17:40	04.06.08	PY1 (W/m2)	6.02	PY2 (W/m2)	0	Ev (LUX)	0
17:50	04.06.08	PY1 (W/m2)	6.23	PY2 (W/m2)	0	Ev (LUX)	0
18:00	04.06.08	PY1 (W/m2)	9.14	PY2 (W/m2)	0	Ev (LUX)	0

6:00	05.06.08	PY1 (W/m2)	0	PY2 (W/m2)	0	Ev (LUX)	0
6:10	05.06.08	PY1 (W/m2)	0	PY2 (W/m2)	0	Ev (LUX)	0
6:20	05.06.08	PY1 (W/m2)	0	PY2 (W/m2)	0	Ev (LUX)	0
6:30	05.06.08	PY1 (W/m2)	0	PY2 (W/m2)	0	Ev (LUX)	0
6:40	05.06.08	PY1 (W/m2)	0	PY2 (W/m2)	0	Ev (LUX)	0
6:50	05.06.08	PY1 (W/m2)	0	PY2 (W/m2)	0	Ev (LUX)	0
7:00	05.06.08	PY1 (W/m2)	4.98	PY2 (W/m2)	0	Ev (LUX)	0
7:10	05.06.08	PY1 (W/m2)	11.43	PY2 (W/m2)	0	Ev (LUX)	0
7:20	05.06.08	PY1 (W/m2)	24.32	PY2 (W/m2)	0	Ev (LUX)	0
7:30	05.06.08	PY1 (W/m2)	38.25	PY2 (W/m2)	3.33	Ev (LUX)	25
7:40	05.06.08	PY1 (W/m2)	58.21	PY2 (W/m2)	4.07	Ev (LUX)	0
7:50	05.06.08	PY1 (W/m2)	84.82	PY2 (W/m2)	5.36	Ev (LUX)	167
8:00	05.06.08	PY1 (W/m2)	92.93	PY2 (W/m2)	6.84	Ev (LUX)	205
8:10	05.06.08	PY1 (W/m2)	206.02	PY2 (W/m2)	11.66	Ev (LUX)	334
8:20	05.06.08	PY1 (W/m2)	262.16	PY2 (W/m2)	14.62	Ev (LUX)	411
8:30	05.06.08	PY1 (W/m2)	298.12	PY2 (W/m2)	17.02	Ev (LUX)	488
8:40	05.06.08	PY1 (W/m2)	321.2	PY2 (W/m2)	17.95	Ev (LUX)	513
8:50	05.06.08	PY1 (W/m2)	347.4	PY2 (W/m2)	19.24	Ev (LUX)	578
9:00	05.06.08	PY1 (W/m2)	327.02	PY2 (W/m2)	18.13	Ev (LUX)	578
9:10	05.06.08	PY1 (W/m2)	355.3	PY2 (W/m2)	19.61	Ev (LUX)	629
9:20	05.06.08	PY1 (W/m2)	397.71	PY2 (W/m2)	21.83	Ev (LUX)	693
9:30	05.06.08	PY1 (W/m2)	436.59	PY2 (W/m2)	23.13	Ev (LUX)	745
9:40	05.06.08	PY1 (W/m2)	476.29	PY2 (W/m2)	24.8	Ev (LUX)	783
9:50	05.06.08	PY1 (W/m2)	417.04	PY2 (W/m2)	22.39	Ev (LUX)	706
10:00	05.06.08	PY1 (W/m2)	500.41	PY2 (W/m2)	26.28	Ev (LUX)	822
10:10	05.06.08	PY1 (W/m2)	624.32	PY2 (W/m2)	33.12	Ev (LUX)	1014
10:20	05.06.08	PY1 (W/m2)	357.38	PY2 (W/m2)	21.83	Ev (LUX)	642
10:30	05.06.08	PY1 (W/m2)	575.88	PY2 (W/m2)	32.38	Ev (LUX)	976
10:40	05.06.08	PY1 (W/m2)	757.79	PY2 (W/m2)	40.16	Ev (LUX)	1207
10:50	05.06.08	PY1 (W/m2)	780.24	PY2 (W/m2)	39.05	Ev (LUX)	1207
11:00	05.06.08	PY1 (W/m2)	920.37	PY2 (W/m2)	43.49	Ev (LUX)	1336
11:10	05.06.08	PY1 (W/m2)	933.05	PY2 (W/m2)	40.9	Ev (LUX)	1297
11:20	05.06.08	PY1 (W/m2)	276.09	PY2 (W/m2)	14.8	Ev (LUX)	449
11:30	05.06.08	PY1 (W/m2)	965.07	PY2 (W/m2)	44.41	Ev (LUX)	1400
11:40	05.06.08	PY1 (W/m2)	887.11	PY2 (W/m2)	42.38	Ev (LUX)	1271
11:50	05.06.08	PY1 (W/m2)	999.37	PY2 (W/m2)	46.08	Ev (LUX)	1387
12:00	05.06.08	PY1 (W/m2)	686.48	PY2 (W/m2)	33.68	Ev (LUX)	1040
12:10	05.06.08	PY1 (W/m2)	973.38	PY2 (W/m2)	38.12	Ev (LUX)	1130
12:20	05.06.08	PY1 (W/m2)	317.04	PY2 (W/m2)	16.65	Ev (LUX)	501
12:30	05.06.08	PY1 (W/m2)	235.34	PY2 (W/m2)	13.14	Ev (LUX)	398
12:40	05.06.08	PY1 (W/m2)	327.23	PY2 (W/m2)	18.69	Ev (LUX)	539
12:50	05.06.08	PY1 (W/m2)	1025.15	PY2 (W/m2)	48.86	Ev (LUX)	1387
13:00	05.06.08	PY1 (W/m2)	350.72	PY2 (W/m2)	21.65	Ev (LUX)	629
13:10	05.06.08	PY1 (W/m2)	802.91	PY2 (W/m2)	39.23	Ev (LUX)	1143

13:20	05.06.08	PY1 (W/m2)	337.83	PY2 (W/m2)	19.43	Ev (LUX)	552
13:30	05.06.08	PY1 (W/m2)	388.14	PY2 (W/m2)	22.39	Ev (LUX)	655
13:40	05.06.08	PY1 (W/m2)	987.73	PY2 (W/m2)	48.3	Ev (LUX)	1348
13:50	05.06.08	PY1 (W/m2)	1022.03	PY2 (W/m2)	50.15	Ev (LUX)	1374
14:00	05.06.08	PY1 (W/m2)	332.43	PY2 (W/m2)	19.06	Ev (LUX)	565
14:10	05.06.08	PY1 (W/m2)	392.93	PY2 (W/m2)	22.58	Ev (LUX)	642
14:20	05.06.08	PY1 (W/m2)	464.65	PY2 (W/m2)	22.76	Ev (LUX)	616
14:30	05.06.08	PY1 (W/m2)	146.15	PY2 (W/m2)	8.69	Ev (LUX)	256
14:40	05.06.08	PY1 (W/m2)	69.43	PY2 (W/m2)	4.25	Ev (LUX)	0
14:50	05.06.08	PY1 (W/m2)	26.19	PY2 (W/m2)	0	Ev (LUX)	0
15:00	05.06.08	PY1 (W/m2)	16.42	PY2 (W/m2)	0	Ev (LUX)	0
15:10	05.06.08	PY1 (W/m2)	5.61	PY2 (W/m2)	0	Ev (LUX)	0
15:20	05.06.08	PY1 (W/m2)	4.36	PY2 (W/m2)	0	Ev (LUX)	0
15:30	05.06.08	PY1 (W/m2)	9.35	PY2 (W/m2)	0	Ev (LUX)	0
15:40	05.06.08	PY1 (W/m2)	14.96	PY2 (W/m2)	0	Ev (LUX)	0
15:50	05.06.08	PY1 (W/m2)	35.34	PY2 (W/m2)	2.96	Ev (LUX)	0
16:00	05.06.08	PY1 (W/m2)	64.44	PY2 (W/m2)	4.99	Ev (LUX)	167
16:10	05.06.08	PY1 (W/m2)	87.11	PY2 (W/m2)	6.29	Ev (LUX)	192
16:20	05.06.08	PY1 (W/m2)	104.98	PY2 (W/m2)	7.4	Ev (LUX)	205
16:30	05.06.08	PY1 (W/m2)	114.34	PY2 (W/m2)	7.95	Ev (LUX)	231
16:40	05.06.08	PY1 (W/m2)	115.38	PY2 (W/m2)	7.95	Ev (LUX)	231
16:50	05.06.08	PY1 (W/m2)	80.45	PY2 (W/m2)	5.55	Ev (LUX)	167
17:00	05.06.08	PY1 (W/m2)	40.33	PY2 (W/m2)	3.14	Ev (LUX)	0
17:10	05.06.08	PY1 (W/m2)	64.86	PY2 (W/m2)	4.62	Ev (LUX)	0
17:20	05.06.08	PY1 (W/m2)	102.07	PY2 (W/m2)	6.84	Ev (LUX)	192
17:30	05.06.08	PY1 (W/m2)	100.62	PY2 (W/m2)	7.03	Ev (LUX)	192
17:40	05.06.08	PY1 (W/m2)	83.16	PY2 (W/m2)	5.92	Ev (LUX)	179
17:50	05.06.08	PY1 (W/m2)	80.04	PY2 (W/m2)	5.55	Ev (LUX)	154
18:00	05.06.08	PY1 (W/m2)	42.82	PY2 (W/m2)	3.14	Ev (LUX)	0

6:00	06.06.08	PY1 (W/m2)	0	PY2 (W/m2)	0	Ev (LUX)	0
6:10	06.06.08	PY1 (W/m2)	0	PY2 (W/m2)	0	Ev (LUX)	0
6:20	06.06.08	PY1 (W/m2)	0	PY2 (W/m2)	0	Ev (LUX)	0
6:30	06.06.08	PY1 (W/m2)	0	PY2 (W/m2)	0	Ev (LUX)	0
6:40	06.06.08	PY1 (W/m2)	0	PY2 (W/m2)	0	Ev (LUX)	0
6:50	06.06.08	PY1 (W/m2)	0	PY2 (W/m2)	0	Ev (LUX)	0
7:00	06.06.08	PY1 (W/m2)	3.32	PY2 (W/m2)	0	Ev (LUX)	0
7:10	06.06.08	PY1 (W/m2)	8.73	PY2 (W/m2)	0	Ev (LUX)	0
7:20	06.06.08	PY1 (W/m2)	18.5	PY2 (W/m2)	0	Ev (LUX)	0
7:30	06.06.08	PY1 (W/m2)	34.09	PY2 (W/m2)	2.59	Ev (LUX)	0
7:40	06.06.08	PY1 (W/m2)	48.44	PY2 (W/m2)	3.51	Ev (LUX)	0
7:50	06.06.08	PY1 (W/m2)	66.32	PY2 (W/m2)	3.88	Ev (LUX)	0
8:00	06.06.08	PY1 (W/m2)	53.43	PY2 (W/m2)	3.88	Ev (LUX)	0
8:10	06.06.08	PY1 (W/m2)	67.98	PY2 (W/m2)	4.81	Ev (LUX)	167
8:20	06.06.08	PY1 (W/m2)	87.31	PY2 (W/m2)	6.1	Ev (LUX)	192

8:30	06.06.08	PY1 (W/m2)	96.46	PY2 (W/m2)	6.66	Ev (LUX)	205
8:40	06.06.08	PY1 (W/m2)	110.39	PY2 (W/m2)	7.58	Ev (LUX)	244
8:50	06.06.08	PY1 (W/m2)	131.8	PY2 (W/m2)	8.51	Ev (LUX)	269
9:00	06.06.08	PY1 (W/m2)	152.59	PY2 (W/m2)	9.99	Ev (LUX)	321
9:10	06.06.08	PY1 (W/m2)	174.42	PY2 (W/m2)	10.91	Ev (LUX)	346
9:20	06.06.08	PY1 (W/m2)	199.79	PY2 (W/m2)	12.4	Ev (LUX)	385
9:30	06.06.08	PY1 (W/m2)	239.29	PY2 (W/m2)	14.62	Ev (LUX)	462
9:40	06.06.08	PY1 (W/m2)	281.49	PY2 (W/m2)	16.65	Ev (LUX)	513
9:50	06.06.08	PY1 (W/m2)	337.21	PY2 (W/m2)	19.61	Ev (LUX)	616
10:00	06.06.08	PY1 (W/m2)	401.24	PY2 (W/m2)	22.95	Ev (LUX)	719
10:10	06.06.08	PY1 (W/m2)	459.66	PY2 (W/m2)	26.09	Ev (LUX)	809
10:20	06.06.08	PY1 (W/m2)	459.87	PY2 (W/m2)	27.76	Ev (LUX)	847
10:30	06.06.08	PY1 (W/m2)	523.7	PY2 (W/m2)	30.9	Ev (LUX)	924
10:40	06.06.08	PY1 (W/m2)	529.1	PY2 (W/m2)	31.46	Ev (LUX)	924
10:50	06.06.08	PY1 (W/m2)	522.86	PY2 (W/m2)	30.72	Ev (LUX)	873
11:00	06.06.08	PY1 (W/m2)	393.34	PY2 (W/m2)	24.06	Ev (LUX)	693
11:10	06.06.08	PY1 (W/m2)	460.08	PY2 (W/m2)	27.94	Ev (LUX)	809
11:20	06.06.08	PY1 (W/m2)	516	PY2 (W/m2)	30.35	Ev (LUX)	873
11:30	06.06.08	PY1 (W/m2)	333.47	PY2 (W/m2)	20.54	Ev (LUX)	578
11:40	06.06.08	PY1 (W/m2)	343.24	PY2 (W/m2)	20.35	Ev (LUX)	578
11:50	06.06.08	PY1 (W/m2)	381.28	PY2 (W/m2)	22.76	Ev (LUX)	629
12:00	06.06.08	PY1 (W/m2)	536.79	PY2 (W/m2)	30.9	Ev (LUX)	873
12:10	06.06.08	PY1 (W/m2)	506.44	PY2 (W/m2)	29.24	Ev (LUX)	822
12:20	06.06.08	PY1 (W/m2)	522.03	PY2 (W/m2)	30.16	Ev (LUX)	835
12:30	06.06.08	PY1 (W/m2)	575.88	PY2 (W/m2)	32.75	Ev (LUX)	924
12:40	06.06.08	PY1 (W/m2)	738.87	PY2 (W/m2)	37.94	Ev (LUX)	1053
12:50	06.06.08	PY1 (W/m2)	482.95	PY2 (W/m2)	26.65	Ev (LUX)	745
13:00	06.06.08	PY1 (W/m2)	337	PY2 (W/m2)	19.61	Ev (LUX)	552
13:10	06.06.08	PY1 (W/m2)	498.96	PY2 (W/m2)	27.02	Ev (LUX)	770
13:20	06.06.08	PY1 (W/m2)	670.68	PY2 (W/m2)	34.61	Ev (LUX)	1002
13:30	06.06.08	PY1 (W/m2)	717.67	PY2 (W/m2)	36.83	Ev (LUX)	1040
13:40	06.06.08	PY1 (W/m2)	650.31	PY2 (W/m2)	33.87	Ev (LUX)	937
13:50	06.06.08	PY1 (W/m2)	589.6	PY2 (W/m2)	31.27	Ev (LUX)	860
14:00	06.06.08	PY1 (W/m2)	796.25	PY2 (W/m2)	41.27	Ev (LUX)	1117
14:10	06.06.08	PY1 (W/m2)	793.97	PY2 (W/m2)	41.45	Ev (LUX)	1143
14:20	06.06.08	PY1 (W/m2)	593.76	PY2 (W/m2)	32.01	Ev (LUX)	899
14:30	06.06.08	PY1 (W/m2)	682.95	PY2 (W/m2)	36.09	Ev (LUX)	1027
14:40	06.06.08	PY1 (W/m2)	370.68	PY2 (W/m2)	22.2	Ev (LUX)	629
14:50	06.06.08	PY1 (W/m2)	777.75	PY2 (W/m2)	40.9	Ev (LUX)	1117
15:00	06.06.08	PY1 (W/m2)	829.93	PY2 (W/m2)	44.41	Ev (LUX)	1194
15:10	06.06.08	PY1 (W/m2)	928.89	PY2 (W/m2)	49.6	Ev (LUX)	1297
15:20	06.06.08	PY1 (W/m2)	951.55	PY2 (W/m2)	51.26	Ev (LUX)	1336
15:30	06.06.08	PY1 (W/m2)	885.23	PY2 (W/m2)	47.93	Ev (LUX)	1246
15:40	06.06.08	PY1 (W/m2)	834.3	PY2 (W/m2)	46.64	Ev (LUX)	1194
15:50	06.06.08	PY1 (W/m2)	782.74	PY2 (W/m2)	43.67	Ev (LUX)	1117
16:00	06.06.08	PY1 (W/m2)	696.88	PY2 (W/m2)	39.05	Ev (LUX)	976

16:10	06.06.08	PY1 (W/m2)	673.38	PY2 (W/m2)	37.38	Ev (LUX)	924
16:20	06.06.08	PY1 (W/m2)	625.36	PY2 (W/m2)	35.35	Ev (LUX)	899
16:30	06.06.08	PY1 (W/m2)	644.49	PY2 (W/m2)	35.53	Ev (LUX)	886
16:40	06.06.08	PY1 (W/m2)	216.63	PY2 (W/m2)	14.99	Ev (LUX)	423
16:50	06.06.08	PY1 (W/m2)	610.6	PY2 (W/m2)	33.31	Ev (LUX)	822
17:00	06.06.08	PY1 (W/m2)	517.67	PY2 (W/m2)	28.87	Ev (LUX)	719
17:10	06.06.08	PY1 (W/m2)	472.76	PY2 (W/m2)	26.46	Ev (LUX)	655
17:20	06.06.08	PY1 (W/m2)	432.64	PY2 (W/m2)	23.69	Ev (LUX)	603
17:30	06.06.08	PY1 (W/m2)	407.27	PY2 (W/m2)	22.58	Ev (LUX)	578
17:40	06.06.08	PY1 (W/m2)	356.75	PY2 (W/m2)	18.69	Ev (LUX)	488
17:50	06.06.08	PY1 (W/m2)	71.72	PY2 (W/m2)	13.32	Ev (LUX)	359
18:00	06.06.08	PY1 (W/m2)	67.35	PY2 (W/m2)	7.95	Ev (LUX)	231

6:00	07.06.08	PY1 (W/m2)	0	PY2 (W/m2)	0	Ev (LUX)	0
6:10	07.06.08	PY1 (W/m2)	0	PY2 (W/m2)	0	Ev (LUX)	0
6:20	07.06.08	PY1 (W/m2)	0	PY2 (W/m2)	0	Ev (LUX)	0
6:30	07.06.08	PY1 (W/m2)	0	PY2 (W/m2)	0	Ev (LUX)	0
6:40	07.06.08	PY1 (W/m2)	0	PY2 (W/m2)	0	Ev (LUX)	0
6:50	07.06.08	PY1 (W/m2)	0	PY2 (W/m2)	0.18	Ev (LUX)	0
7:00	07.06.08	PY1 (W/m2)	0	PY2 (W/m2)	0	Ev (LUX)	0
7:10	07.06.08	PY1 (W/m2)	6.44	PY2 (W/m2)	0	Ev (LUX)	0
7:20	07.06.08	PY1 (W/m2)	12.05	PY2 (W/m2)	0	Ev (LUX)	0
7:30	07.06.08	PY1 (W/m2)	9.97	PY2 (W/m2)	0	Ev (LUX)	0
7:40	07.06.08	PY1 (W/m2)	23.49	PY2 (W/m2)	0	Ev (LUX)	0
7:50	07.06.08	PY1 (W/m2)	59.45	PY2 (W/m2)	3.88	Ev (LUX)	0
8:00	07.06.08	PY1 (W/m2)	64.65	PY2 (W/m2)	4.07	Ev (LUX)	0
8:10	07.06.08	PY1 (W/m2)	84.19	PY2 (W/m2)	5.18	Ev (LUX)	154
8:20	07.06.08	PY1 (W/m2)	141.58	PY2 (W/m2)	7.95	Ev (LUX)	231
8:30	07.06.08	PY1 (W/m2)	196.46	PY2 (W/m2)	9.99	Ev (LUX)	256
8:40	07.06.08	PY1 (W/m2)	186.27	PY2 (W/m2)	11.66	Ev (LUX)	321
8:50	07.06.08	PY1 (W/m2)	312.47	PY2 (W/m2)	15.73	Ev (LUX)	449
9:00	07.06.08	PY1 (W/m2)	439.29	PY2 (W/m2)	21.46	Ev (LUX)	616
9:10	07.06.08	PY1 (W/m2)	470.47	PY2 (W/m2)	23.32	Ev (LUX)	680
9:20	07.06.08	PY1 (W/m2)	476.29	PY2 (W/m2)	24.06	Ev (LUX)	719
9:30	07.06.08	PY1 (W/m2)	512.47	PY2 (W/m2)	26.09	Ev (LUX)	796
9:40	07.06.08	PY1 (W/m2)	528.69	PY2 (W/m2)	27.2	Ev (LUX)	822
9:50	07.06.08	PY1 (W/m2)	602.28	PY2 (W/m2)	30.16	Ev (LUX)	912
10:00	07.06.08	PY1 (W/m2)	651.35	PY2 (W/m2)	33.12	Ev (LUX)	1014
10:10	07.06.08	PY1 (W/m2)	673.59	PY2 (W/m2)	34.24	Ev (LUX)	1040
10:20	07.06.08	PY1 (W/m2)	779	PY2 (W/m2)	38.49	Ev (LUX)	1143
10:30	07.06.08	PY1 (W/m2)	322.03	PY2 (W/m2)	18.87	Ev (LUX)	552
10:40	07.06.08	PY1 (W/m2)	465.48	PY2 (W/m2)	25.91	Ev (LUX)	770
10:50	07.06.08	PY1 (W/m2)	401.45	PY2 (W/m2)	22.58	Ev (LUX)	655
11:00	07.06.08	PY1 (W/m2)	401.03	PY2 (W/m2)	22.95	Ev (LUX)	642
11:10	07.06.08	PY1 (W/m2)	583.99	PY2 (W/m2)	31.64	Ev (LUX)	899

11:20	07.06.08	PY1 (W/m2)	696.04	PY2 (W/m2)	38.49	Ev (LUX)	1117
11:30	07.06.08	PY1 (W/m2)	1099.37	PY2 (W/m2)	56.26	Ev (LUX)	1644
11:40	07.06.08	PY1 (W/m2)	495.01	PY2 (W/m2)	27.02	Ev (LUX)	770
11:50	07.06.08	PY1 (W/m2)	481.91	PY2 (W/m2)	27.57	Ev (LUX)	770
12:00	07.06.08	PY1 (W/m2)	412.47	PY2 (W/m2)	23.32	Ev (LUX)	655
12:10	07.06.08	PY1 (W/m2)	574.84	PY2 (W/m2)	32.38	Ev (LUX)	899
12:20	07.06.08	PY1 (W/m2)	287.94	PY2 (W/m2)	16.47	Ev (LUX)	449
12:30	07.06.08	PY1 (W/m2)	259.25	PY2 (W/m2)	14.43	Ev (LUX)	411
12:40	07.06.08	PY1 (W/m2)	334.51	PY2 (W/m2)	19.61	Ev (LUX)	526
12:50	07.06.08	PY1 (W/m2)	563.82	PY2 (W/m2)	32.75	Ev (LUX)	899
13:00	07.06.08	PY1 (W/m2)	329.52	PY2 (W/m2)	19.8	Ev (LUX)	526
13:10	07.06.08	PY1 (W/m2)	353.01	PY2 (W/m2)	20.91	Ev (LUX)	565
13:20	07.06.08	PY1 (W/m2)	367.98	PY2 (W/m2)	21.83	Ev (LUX)	578
13:30	07.06.08	PY1 (W/m2)	290.85	PY2 (W/m2)	17.76	Ev (LUX)	462
13:40	07.06.08	PY1 (W/m2)	297.92	PY2 (W/m2)	17.76	Ev (LUX)	488
13:50	07.06.08	PY1 (W/m2)	353.84	PY2 (W/m2)	20.91	Ev (LUX)	552
14:00	07.06.08	PY1 (W/m2)	472.76	PY2 (W/m2)	27.57	Ev (LUX)	719
14:10	07.06.08	PY1 (W/m2)	463.4	PY2 (W/m2)	26.83	Ev (LUX)	719
14:20	07.06.08	PY1 (W/m2)	393.97	PY2 (W/m2)	22.58	Ev (LUX)	616
14:30	07.06.08	PY1 (W/m2)	491.26	PY2 (W/m2)	27.57	Ev (LUX)	745
14:40	07.06.08	PY1 (W/m2)	376.09	PY2 (W/m2)	21.46	Ev (LUX)	590
14:50	07.06.08	PY1 (W/m2)	383.78	PY2 (W/m2)	22.02	Ev (LUX)	578
15:00	07.06.08	PY1 (W/m2)	324.74	PY2 (W/m2)	18.87	Ev (LUX)	501
15:10	07.06.08	PY1 (W/m2)	260.49	PY2 (W/m2)	15.17	Ev (LUX)	411
15:20	07.06.08	PY1 (W/m2)	305.61	PY2 (W/m2)	17.76	Ev (LUX)	462
15:30	07.06.08	PY1 (W/m2)	242.82	PY2 (W/m2)	14.25	Ev (LUX)	372
15:40	07.06.08	PY1 (W/m2)	231.18	PY2 (W/m2)	13.69	Ev (LUX)	359
15:50	07.06.08	PY1 (W/m2)	164.65	PY2 (W/m2)	9.8	Ev (LUX)	269
16:00	07.06.08	PY1 (W/m2)	134.51	PY2 (W/m2)	8.32	Ev (LUX)	231
16:10	07.06.08	PY1 (W/m2)	132.84	PY2 (W/m2)	8.14	Ev (LUX)	218
16:20	07.06.08	PY1 (W/m2)	103.32	PY2 (W/m2)	6.84	Ev (LUX)	192
16:30	07.06.08	PY1 (W/m2)	99.37	PY2 (W/m2)	6.66	Ev (LUX)	179
16:40	07.06.08	PY1 (W/m2)	108.52	PY2 (W/m2)	7.21	Ev (LUX)	192
16:50	07.06.08	PY1 (W/m2)	83.99	PY2 (W/m2)	5.73	Ev (LUX)	154
17:00	07.06.08	PY1 (W/m2)	58.83	PY2 (W/m2)	4.25	Ev (LUX)	0
17:10	07.06.08	PY1 (W/m2)	45.32	PY2 (W/m2)	3.33	Ev (LUX)	0
17:20	07.06.08	PY1 (W/m2)	49.48	PY2 (W/m2)	3.51	Ev (LUX)	0
17:30	07.06.08	PY1 (W/m2)	61.95	PY2 (W/m2)	4.44	Ev (LUX)	0
17:40	07.06.08	PY1 (W/m2)	51.55	PY2 (W/m2)	3.51	Ev (LUX)	0
17:50	07.06.08	PY1 (W/m2)	45.11	PY2 (W/m2)	3.14	Ev (LUX)	0
18:00	07.06.08	PY1 (W/m2)	7.48	PY2 (W/m2)	0	Ev (LUX)	0

6:00	08.06.08	PY1 (W/m2)	0	PY2 (W/m2)	0	Ev (LUX)	0
6:10	08.06.08	PY1 (W/m2)	0	PY2 (W/m2)	0	Ev (LUX)	0
6:20	08.06.08	PY1 (W/m2)	0	PY2 (W/m2)	0.18	Ev (LUX)	0

6:30	08.06.08	PY1 (W/m ²)	0	PY2 (W/m ²)	0.18	Ev (LUX)	0
6:40	08.06.08	PY1 (W/m ²)	0	PY2 (W/m ²)	0	Ev (LUX)	0
6:50	08.06.08	PY1 (W/m ²)	0	PY2 (W/m ²)	0.18	Ev (LUX)	0
7:00	08.06.08	PY1 (W/m ²)	0	PY2 (W/m ²)	0	Ev (LUX)	0
7:10	08.06.08	PY1 (W/m ²)	0	PY2 (W/m ²)	0.18	Ev (LUX)	12
7:20	08.06.08	PY1 (W/m ²)	2.49	PY2 (W/m ²)	0	Ev (LUX)	0
7:30	08.06.08	PY1 (W/m ²)	5.4	PY2 (W/m ²)	0	Ev (LUX)	0
7:40	08.06.08	PY1 (W/m ²)	9.14	PY2 (W/m ²)	0	Ev (LUX)	0
7:50	08.06.08	PY1 (W/m ²)	13.51	PY2 (W/m ²)	0	Ev (LUX)	0
8:00	08.06.08	PY1 (W/m ²)	18.91	PY2 (W/m ²)	0	Ev (LUX)	0
8:10	08.06.08	PY1 (W/m ²)	25.36	PY2 (W/m ²)	2.22	Ev (LUX)	0
8:20	08.06.08	PY1 (W/m ²)	38.66	PY2 (W/m ²)	3.14	Ev (LUX)	0
8:30	08.06.08	PY1 (W/m ²)	61.33	PY2 (W/m ²)	4.44	Ev (LUX)	0
8:40	08.06.08	PY1 (W/m ²)	105.61	PY2 (W/m ²)	7.58	Ev (LUX)	218
8:50	08.06.08	PY1 (W/m ²)	155.3	PY2 (W/m ²)	11.1	Ev (LUX)	295
9:00	08.06.08	PY1 (W/m ²)	131.8	PY2 (W/m ²)	9.43	Ev (LUX)	256
9:10	08.06.08	PY1 (W/m ²)	144.9	PY2 (W/m ²)	10.73	Ev (LUX)	282
9:20	08.06.08	PY1 (W/m ²)	166.52	PY2 (W/m ²)	11.84	Ev (LUX)	308
9:30	08.06.08	PY1 (W/m ²)	212.26	PY2 (W/m ²)	14.8	Ev (LUX)	385
9:40	08.06.08	PY1 (W/m ²)	271.72	PY2 (W/m ²)	18.69	Ev (LUX)	488
9:50	08.06.08	PY1 (W/m ²)	297.08	PY2 (W/m ²)	20.17	Ev (LUX)	539
10:00	08.06.08	PY1 (W/m ²)	314.76	PY2 (W/m ²)	21.65	Ev (LUX)	578
10:10	08.06.08	PY1 (W/m ²)	336.59	PY2 (W/m ²)	22.76	Ev (LUX)	590
10:20	08.06.08	PY1 (W/m ²)	376.92	PY2 (W/m ²)	25.17	Ev (LUX)	668
10:30	08.06.08	PY1 (W/m ²)	373.8	PY2 (W/m ²)	24.61	Ev (LUX)	655
10:40	08.06.08	PY1 (W/m ²)	357.17	PY2 (W/m ²)	23.69	Ev (LUX)	616
10:50	08.06.08	PY1 (W/m ²)	381.7	PY2 (W/m ²)	24.8	Ev (LUX)	642
11:00	08.06.08	PY1 (W/m ²)	393.34	PY2 (W/m ²)	25.17	Ev (LUX)	655
11:10	08.06.08	PY1 (W/m ²)	397.71	PY2 (W/m ²)	26.09	Ev (LUX)	668
11:20	08.06.08	PY1 (W/m ²)	477.54	PY2 (W/m ²)	30.9	Ev (LUX)	822
11:30	08.06.08	PY1 (W/m ²)	492.93	PY2 (W/m ²)	32.01	Ev (LUX)	860
11:40	08.06.08	PY1 (W/m ²)	499.16	PY2 (W/m ²)	32.2	Ev (LUX)	860
11:50	08.06.08	PY1 (W/m ²)	591.26	PY2 (W/m ²)	37.57	Ev (LUX)	1014
12:00	08.06.08	PY1 (W/m ²)	582.32	PY2 (W/m ²)	36.09	Ev (LUX)	976
12:10	08.06.08	PY1 (W/m ²)	596.88	PY2 (W/m ²)	36.27	Ev (LUX)	976
12:20	08.06.08	PY1 (W/m ²)	693.13	PY2 (W/m ²)	41.08	Ev (LUX)	1117
12:30	08.06.08	PY1 (W/m ²)	652.59	PY2 (W/m ²)	38.31	Ev (LUX)	1040
12:40	08.06.08	PY1 (W/m ²)	508.52	PY2 (W/m ²)	28.87	Ev (LUX)	770
12:50	08.06.08	PY1 (W/m ²)	456.96	PY2 (W/m ²)	26.09	Ev (LUX)	693
13:00	08.06.08	PY1 (W/m ²)	368.6	PY2 (W/m ²)	21.28	Ev (LUX)	565
13:10	08.06.08	PY1 (W/m ²)	335.55	PY2 (W/m ²)	19.24	Ev (LUX)	526
13:20	08.06.08	PY1 (W/m ²)	354.46	PY2 (W/m ²)	20.54	Ev (LUX)	552
13:30	08.06.08	PY1 (W/m ²)	426.61	PY2 (W/m ²)	24.24	Ev (LUX)	642
13:40	08.06.08	PY1 (W/m ²)	350.51	PY2 (W/m ²)	20.35	Ev (LUX)	539
13:50	08.06.08	PY1 (W/m ²)	252.59	PY2 (W/m ²)	14.8	Ev (LUX)	411
14:00	08.06.08	PY1 (W/m ²)	252.39	PY2 (W/m ²)	14.62	Ev (LUX)	411

14:10	08.06.08	PY1 (W/m2)	271.1	PY2 (W/m2)	15.73	Ev (LUX)	423
14:20	08.06.08	PY1 (W/m2)	308.73	PY2 (W/m2)	17.76	Ev (LUX)	488
14:30	08.06.08	PY1 (W/m2)	332.01	PY2 (W/m2)	19.24	Ev (LUX)	513
14:40	08.06.08	PY1 (W/m2)	400.2	PY2 (W/m2)	23.13	Ev (LUX)	603
14:50	08.06.08	PY1 (W/m2)	389.6	PY2 (W/m2)	22.39	Ev (LUX)	603
15:00	08.06.08	PY1 (W/m2)	340.12	PY2 (W/m2)	19.61	Ev (LUX)	526
15:10	08.06.08	PY1 (W/m2)	322.24	PY2 (W/m2)	18.69	Ev (LUX)	513
15:20	08.06.08	PY1 (W/m2)	299.58	PY2 (W/m2)	17.76	Ev (LUX)	475
15:30	08.06.08	PY1 (W/m2)	258.62	PY2 (W/m2)	15.17	Ev (LUX)	398
15:40	08.06.08	PY1 (W/m2)	214.55	PY2 (W/m2)	12.58	Ev (LUX)	346
15:50	08.06.08	PY1 (W/m2)	195.84	PY2 (W/m2)	11.47	Ev (LUX)	308
16:00	08.06.08	PY1 (W/m2)	199.37	PY2 (W/m2)	11.84	Ev (LUX)	321
16:10	08.06.08	PY1 (W/m2)	172.34	PY2 (W/m2)	10.17	Ev (LUX)	282
16:20	08.06.08	PY1 (W/m2)	190.85	PY2 (W/m2)	11.47	Ev (LUX)	308
16:30	08.06.08	PY1 (W/m2)	228.48	PY2 (W/m2)	13.32	Ev (LUX)	359
16:40	08.06.08	PY1 (W/m2)	194.8	PY2 (W/m2)	11.47	Ev (LUX)	321
16:50	08.06.08	PY1 (W/m2)	151.35	PY2 (W/m2)	9.06	Ev (LUX)	244
17:00	08.06.08	PY1 (W/m2)	145.32	PY2 (W/m2)	8.51	Ev (LUX)	244
17:10	08.06.08	PY1 (W/m2)	153.43	PY2 (W/m2)	9.06	Ev (LUX)	244
17:20	08.06.08	PY1 (W/m2)	144.49	PY2 (W/m2)	8.51	Ev (LUX)	231
17:30	08.06.08	PY1 (W/m2)	128.06	PY2 (W/m2)	7.77	Ev (LUX)	218
17:40	08.06.08	PY1 (W/m2)	124.53	PY2 (W/m2)	7.4	Ev (LUX)	205
17:50	08.06.08	PY1 (W/m2)	96.88	PY2 (W/m2)	5.92	Ev (LUX)	179
18:00	08.06.08	PY1 (W/m2)	75.46	PY2 (W/m2)	4.62	Ev (LUX)	0



Calibration & Test Certificates

Skye Instruments Ltd
21, Ddole Enterprise Park
Llandrindod Wells
Powys LD1 6DF

Tel: 01597 824811 Fax: 01597 824812
Email: skyemail@skyeinstruments.com
Web: www.skyeinstruments.com



**SKYE INSTRUMENTS LTD.
21, DDOLE ENTERPRISE PARK,
LLANDRINDOD WELLS,
POWYS LD1 6DF U.K.**

TEL: +44 (0) 1597 824811 FAX: +44 (0) 1597 824812
E-Mail: skyemail@skyeinstruments.com

CALIBRATION CERTIFICATES ENCLOSED:

DataHog / MiniMet datalogger

Relative Humidity / Air Temperature

Relative Humidity

Air Temperature

Light Sensor 1.....

Light Sensor 2.....

Light Meter.....

Wind Speed

Raingauge

Air Pressure – Manufacturers calibration

Air Pressure – Datalogger factors

Water Level

Soil Moisture Tensiometers

Other.....

Other.....

Other.....

MiniMet Service Contract Order Form



**SKYE INSTRUMENTS LTD.
21, DDOLE ENTERPRISE PARK,
LLANDRINDOD WELLS,
POWYS LD1 6DF U.K.**

TEL: +44 (0) 1597 824811 FAX: +44 (0) 1597 824812
E-Mail: skyemail@skyeinstruments.com

DATAHOG2 / MINIMET2

Datalogger Factory Default settings

If you have just received a new datalogger, it will have been set up with the following default factory settings.

If your datalogger has just been serviced or recalibrated by Skye your own settings will have not been altered.

Datalogger settings will become operational as soon as power applied. Please follow the instructions attached to the logger base to press PSU reset button inside the battery compartment.

LOGGER TIME	Greenwich Mean Time
LOGGER DATE	Current DD.MM.YY
LOGGER MODE	Continuous logging (Stop / Start mode is disabled)
SAMPLE INTERVAL	30 seconds (except for raingauge channels which are set to 30 minutes to store total not averaged rainfall per interval)
AVERAGE INTERVAL	30 minutes
MEMORY FULL MODE	Overwrite oldest record when full
DATAFILE IDENTIFIER	12 characters made up from the loggers 5 figure serial number plus xxxtxt e.g. for logger with serial number 12345 the DataFile Identifier will be 12345 xxxtxt
CALIBRATION FACTORS	If the logger is supplied with sensors as a system, all necessary sensor calibration factors have been entered. Please see the Datalogger Hardware Configuration Certificate.

THESE LOGGER SETTINGS MAY BE CHANGED OR CUSTOMIZED TO YOUR OWN PREFERENCES

Please see the Datalogger Manual for details.



SKYE INSTRUMENTS LTD.
21, DDOLE ENTERPRISE PARK,
LLANDRINDOD WELLS,
POWYS. LD1 6DF. U.K.

TEL: +44 (0) 1597 824811 FAX: +44 (0) 1597 824812
email: skyemail@skyeinstruments.com
website: www.skyeinstruments.com

CALIBRATION CERTIFICATE

NO: PYR/ 5657 1207

UNIT TYPE

PYRANOMETER SENSOR

SERIAL NO:-

SKS 1110/I 1107 33461

OUTPUTS:-

0.05024 $\mu\text{A} / \text{watt m}^{-2}$

10.000 $\mu\text{V} / \text{watt m}^{-2}$

DATE OF CALIBRATION

04/09/2007

A/D UNIT

E2168

Calibrated outdoors under natural daylight conditions by the ratiometric method, against a WMO Secondary Standard Pyranometer, which is traceable to the World Ratiometric Reference via the Met Office standard cavity radiometer.

Uncertainty + 5% (typically + 3%) based on an estimated confidence of not less than 95%.

Calibrated By:-

D. TROTTER

Checked By:-

A. Melling

Issue Date:-

05.12.07

THIS UNIT IS DUE FOR RECALIBRATION WITHIN 2 YEARS OF THE ABOVE
CALIBRATION DATE.



SKYE INSTRUMENTS LTD.
21, DDOLLE ENTERPRISE PARK,
LLANDRINDOD WELLS,
POWYS. LD1 6DF. U.K.
TEL: +44 (0) 1597 824811 FAX: +44 (0) 1597 824812
email: skyemail@skyeinstruments.com
website: www.skyeinstruments.com

CALIBRATION CERTIFICATE

NO: PYR/ 5658 1207

UNIT TYPE PYRANOMETER SENSOR

SERIAL NO:- SKS 1110/I 1107 33462

OUTPUTS: 0.05644 $\mu\text{A} / \text{watt m}^{-2}$

10.22 $\mu\text{V} / \text{watt m}^{-2}$ with 30m cable

DATE OF CALIBRATION 04/09/2007

A/D UNIT E2168

Calibrated outdoors under natural daylight conditions by the ratiometric method, against a WMO Secondary Standard Pyranometer, which is traceable to the World Ratiometric Reference via the Met Office standard cavity radiometer. Uncertainty + 5% (typically + 3%) based on an estimated confidence of not less than 95%.

Calibrated By:-

D. TROTTER

Checked By:-

A. Myling

Issue Date:-

06.12.07

THIS UNIT IS DUE FOR RECALIBRATION WITHIN 2 YEARS OF THE ABOVE CALIBRATION DATE.



SKYE INSTRUMENTS LTD.
21, DDOLE ENTERPRISE PARK,
LLANDRINDOD WELLS,
POWYS. LD1 6DF. U.K.

TEL: +44 (0) 1597 824811 FAX: +44 (0) 1597 824812
E-Mail: skyemail@skyeinstruments.com

CALIBRATION CERTIFICATE No: LUX/565/1207

UNIT TYPE :- PHOTOMETRIC SENSOR (LUX CALIBRATION)
.....
SERIAL NO. :- SKL 310/I 1107 33463
.....
OUTPUTS :- 0.1597 μ A per kLux
.....
100.0 μ V per kLux
.....
DATE OF CALIBRATION :- NOVEMBER 2007
.....
LAMP REFERENCE :- SK3
.....
A/D UNIT:- 039 353
.....

Calibrated against a National Physical Laboratory UK reference standard lamp.
Uncertainty $\pm 5\%$ (typically $\pm 3\%$) based on an estimated confidence of not less than 95%.

CALIBRATED BY:- D. PROFFER DATE:- 13.11.07
CHECKED :- A. McVey DATE:- 05.12.07

THIS UNIT IS DUE FOR RECALIBRATION WITHIN 2 YEARS OF THE ABOVE
CALIBRATION DATE.

DATE OF LAST CALIBRATION :- N/A
.....
% CHANGE SINCE LAST CALIBRATION :- N/A
.....

Single Channel Light Sensors



WEEE Mark

If you want to dispose of this product, do not mix with general household waste. There are separate collection systems for used electronic products in accordance with legislation under the WEEE Directive and is effective only within the European Union.

Updated August 2004

SINGLE CHANNEL LIGHT SENSORS

CONTENTS

1	INTRODUCTION	3
2	LIGHT SENSORS FOR MEASURING FROM ANY LIGHT SOURCE.....	3
3	LIGHT SENSORS FOR TOTAL SOLAR RADIATION.....	3
4	POSITIONING OF ALL TYPES OF SENSOR.	4
5	COSINE CORRECTION.	4
6	SENSOR MAINTENANCE.....	4
7	CONNECTIONS.	5
8	NON-STANDARD SENSORS.....	5
APPENDIX 1 – RESPONSE CURVES		7
APPENDIX 2 – COSINE CORRECTION.....		8
APPENDIX 3 - WIRE CONNECTIONS.....		9
APPENDIX 4 - SPECIFICATIONS		10

SINGLE CHANNEL LIGHT SENSORS

1 INTRODUCTION

Skye Instruments Limited family of specialist light sensors include sensors to measure different parts of the ultra violet, visible and infra-red spectrum for a wide range of applications.

All sensors use high quality photodiodes and spectral filters, and are individually calibrated to National Standards. Each is supplied with a traceable Calibration Certificate.

The single channel Light Sensors are fully waterproof and guaranteed submersible to 4m depth. They are ideal for monitoring light levels in all environments around the world.

There are five types of sensor in this range, three PAR or Photosynthetically Active Radiation sensors (PAR Quantum, PAR Special and PAR Energy), a total solar radiation Pyranometers plus Lux sensors for human or animal studies.

This manual covers the non-amplified output sensor versions, where the output signal comes direct from the sensor photodiode. Amplified versions and add on amplifiers are also available from Skye, please enquire for details.

These sensors are cosine corrected, which means that they accept incoming light according to Lambert's Cosine Law. Essentially this means that light is measured from the hemisphere directly above the sensor.

2 LIGHT SENSORS FOR MEASURING FROM ANY LIGHT SOURCE

SKP 210 - PAR Special
SKP 215 - PAR Quantum
SKL 310 - LUX Sensor
SKE 510 - PAR Energy Sensor

PAR (Photosynthetically
Active
Radiation)

These four sensors have cosine - corrected heads, each containing a semi conductor diode and filter system responding to light according to the response curves in Appendix 1.

They are all fully waterproof and may be left exposed to rain and used in humid climates. They are guaranteed for underwater use up to 4m depth.

Each sensor has been calibrated against a reference lamp, whose own calibration has been carried out at the National Physical Laboratory (N.P.L.). They are calibrated for use with any natural or artificial light source.

3 LIGHT SENSORS FOR TOTAL SOLAR RADIATION

SKS 1110 - Silicon Cell Pyranometer

The pyranometer cosine corrected head contains a special high grade silicon photocell, sensitive to light between 350 and 1100nm. The head is completely sealed and can be left indefinitely in exposed conditions.

This sensor has been calibrated under open-sky conditions, against reference pyranometers and hence referred to the World Radiometric Reference. The calibration thus refers to Solar energy in the waveband 00nm to 3000nm, i.e. the acceptance band of thermopile pyranometers.

SINGLE CHANNEL LIGHT SENSORS

Because of the different spectral responses of the silicon photocell and the thermopiles, to obtain accurate readings the unit must be used in the same conditions as its calibration, i.e. under open sky only. The calibration of the SKS 1110 silicon cell pyranometer is not valid for measuring solar radiation inside glasshouses or polytunnels etc.

Different conditions of sun, cloud, etc., will slightly affect calibration, but absolute errors will always be within 5% and typically much better than 3%.

Linearity is excellent, with a maximum of 1% deviation up to levels of 3000 watts/sq.m (greater than normal solar irradiance).

4 POSITIONING OF ALL TYPES OF SENSOR.

For accurate positioning of the sensor Skye recommend the use of a levelling unit (SKM 221). Great care should be given to the placing of the sensor, in order to achieve accurate and repeatable results. Avoid objects, trees, etc., that will shade the sensor selectively, compared with the areas under study.

5 COSINE CORRECTION.

Since the sensor is intended to measure light falling on a horizontal plane (i.e. the ground), it is designed to collect light from the whole hemisphere of sky above it. This is why light sensors are cosine corrected.

Light rays perpendicular to the sensor are fully measured, while those at 90° are not accepted (they pass parallel to the surface of the plane or the ground and never intercept it). Rays at intermediate angles are treated according to the cosine of their angle to the perpendicular. Imagine the sun overhead, you feel its rays strongest when directly overhead, and much weaker when the sun is near the horizon. The sensor measures light from the different angles in a similar way, stronger when overhead than at low angles.

The cosine response of the sensor is shown in Appendix 2. The cosine errors to angle of 70° are minimal and are less than 5% to an angle of 80°. The graph shows the actual response of the sensor as a Percentage of the ideal response. At 90°, even the most insignificant acceptance of light represents an infinite error, and because of this, accurate plotting beyond 85° is not practical. Errors from such low angle light in nature are generally not material in most studies.

6 SENSOR MAINTENANCE

Light Sensors require very little maintenance apart from keeping the top light collecting surface (small white diffusing disc) clean and dust free. This can be done using a soft cloth dampened with de-ionised water. Take care not to scratch this surface as this may affect the sensor calibration.

Skye Instruments light sensors and meters are recommended to be calibrated every 2 years. Please return to Skye where the sensor will be calibrated against the reference lamp and a new calibration certificate issued.

SINGLE CHANNEL LIGHT SENSORS

7 CONNECTIONS.

Connection to obtain either mV or microamp output is shown in Appendix 3. Please note that external voltages must not be applied to the sensor, the silicon photocell and precision resistive elements may be damaged by reverse voltage or excess current.

8 NON-STANDARD SENSORS.

The sensor part number may include a suffix as follows:

/LT

These sensors have been fitted with cable suitable for low temperatures. Whilst the special cable is rated for use at low temperatures, it is still advisable to avoid undue stress, movement, etc., of the cable when at low temperatures. A special modified levelling unit (SKM 221S) is available to give extra support to the cable and minimise unnecessary movement.

A voltage only output is available. The red wire is the positive output and the blue wire is the ground/screen. All other sensor specifications remain the same.

/S

These sensors have a 3 core cable, and a grey wire connected to the screen on the tail end only - there is no connection inside the sensor.

All other specifications remain the same.

/V

These sensors have a voltage output only.

The red wire is the positive output and the blue wire is the ground / screen. All other specifications remain the same.

/I

These sensors have been fitted with a 5 pin plug for a Skye DataHog logger connection and wired for a current input socket of the logger, as shown below:

Pin 1	not connected
Pin 2	not connected
Pin 3	Red
Pin 4	Blue
Pin 5	Green

SINGLE CHANNEL LIGHT SENSORS

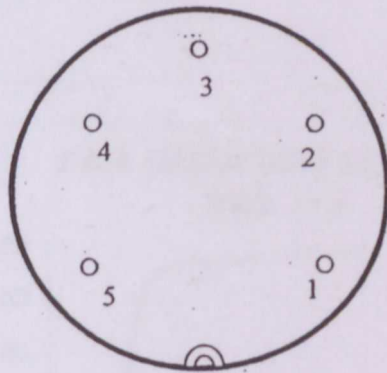
/D/I

These sensors have been fitted with a 5 pin plug for a Skye DataHog logger connection and wired for a differential voltage input socket of the logger, as shown below:

Pin 1		not connected
Pin 2	Blue	Linked to Pin 3
Pin 3	Red	Linked to Pin 2
Pin 4	Grey	Linked to Pin 5
Pin 5		Linked to Pin 4

DATAHOG WATERPROOF BINDER 5 PIN PLUG

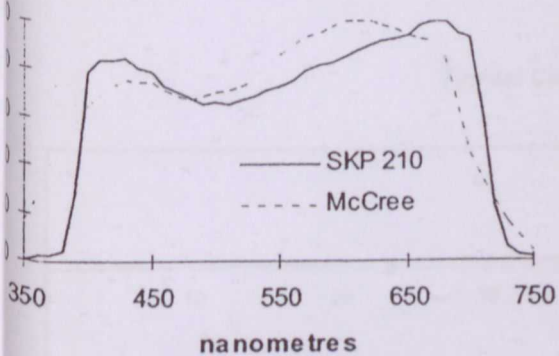
OUTSIDE PIN VIEW



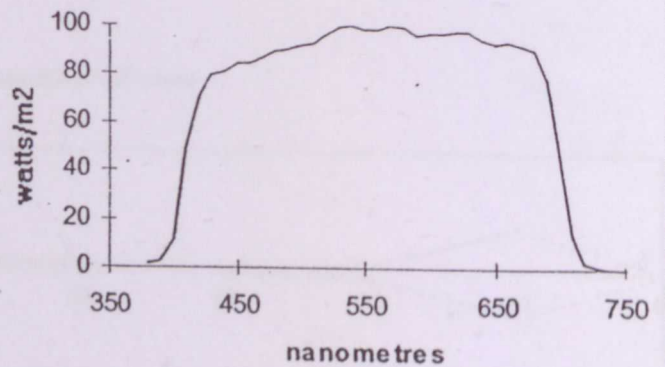
SINGLE CHANNEL LIGHT SENSORS

APPENDIX I - RESPONSE CURVES

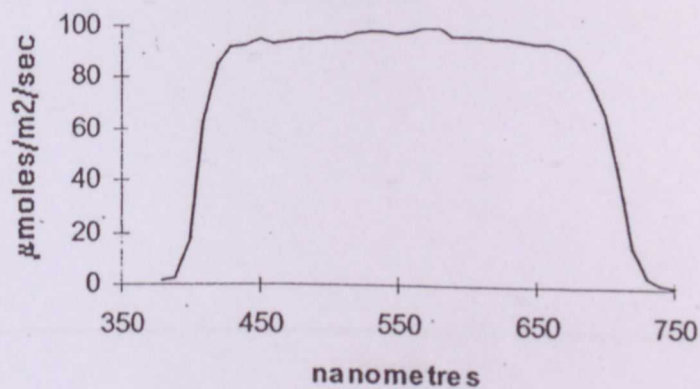
PAR SPECIAL SKP 210



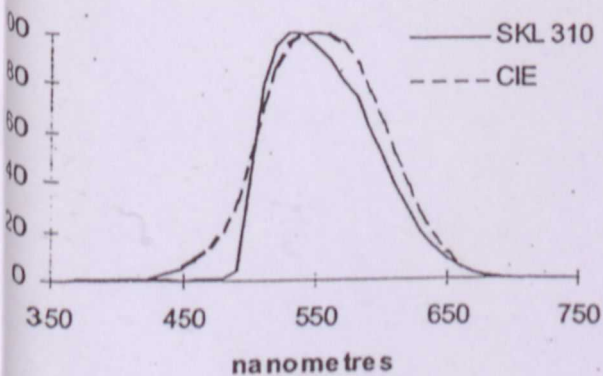
ENERGY SENSOR SKE 510



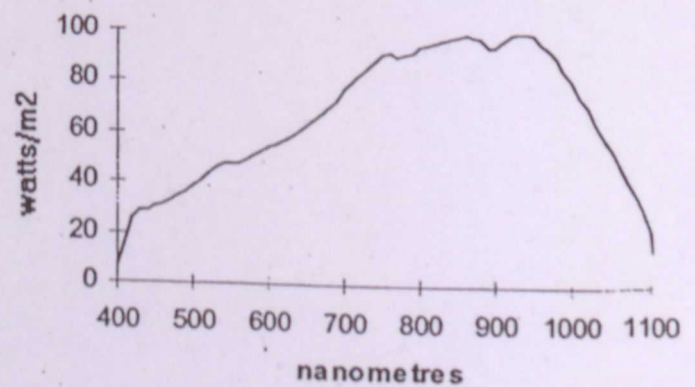
PAR QUANTUM SENSOR
SKP 215



LUX SENSOR SKL 310



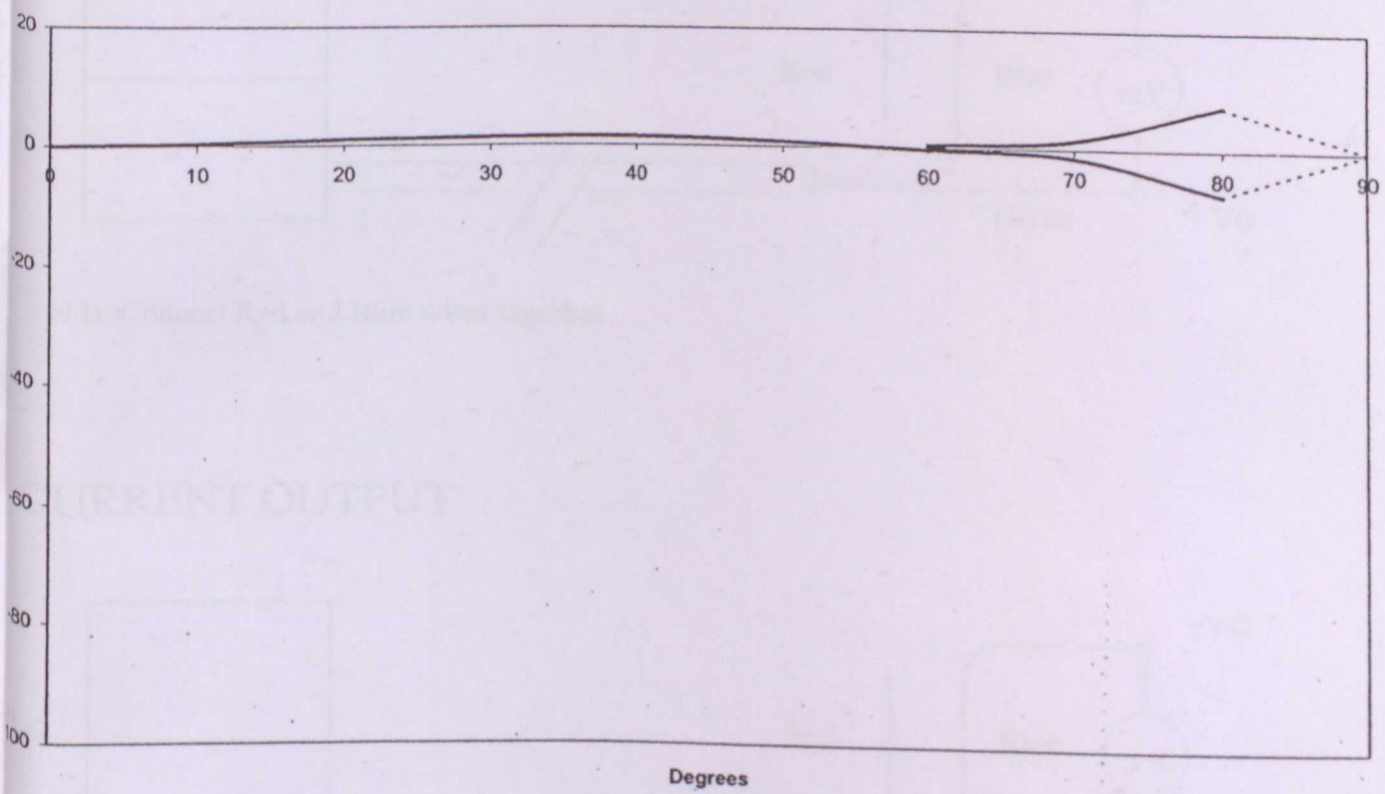
PYRANOMETER SKS 1110



SINGLE CHANNEL LIGHT SENSORS

APPENDIX 2 – COSINE CORRECTION

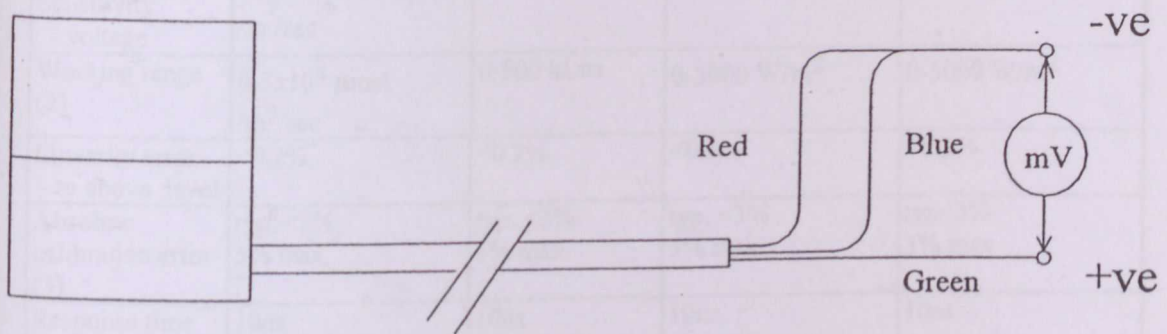
Typical Cosine Response Error Window



SINGLE CHANNEL LIGHT SENSORS

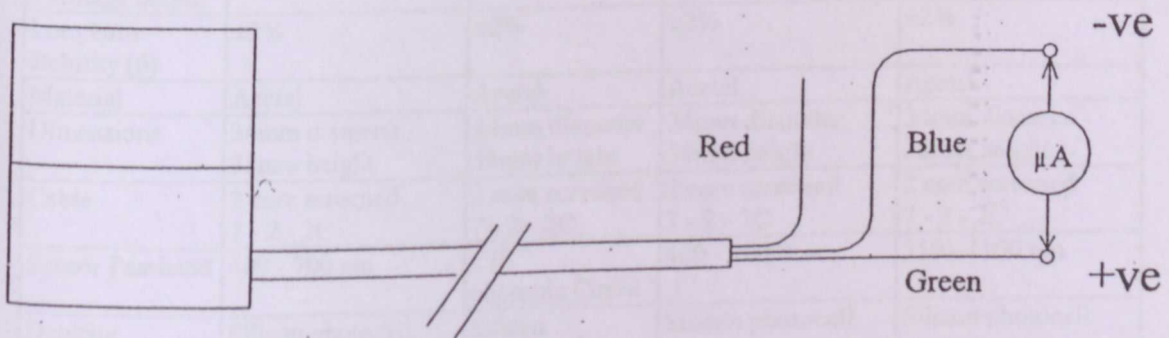
APPENDIX 3 - WIRE CONNECTIONS

VOLTAGE OUTPUT



N.B. Connect Red and Blue wires together.

CURRENT OUTPUT



N.B. Red wire left disconnected.

SINGLE CHANNEL LIGHT SENSORS

APPENDIX 4 - SPECIFICATIONS

	SKP 210/212/215	SKL 310/315	SKE 510/515	SKS 1110
Sensitivity - current (1)	1.6 μ A/ 100 μ mol /m ² /sec	1.5 μ A/ 10 kLux	3.5 μ A/ 100 W/m ²	5 μ A/ 100Wm ²
Sensitivity - voltage	1 mV/ 100 μ mol /m ² /sec	1mV/ 10 kLux	1mV/ 100W/m ²	1mV/100W/m ²
Working range (2)	0-5x10 ⁴ μ mol /m ² /sec	0-500 kLux	0-5000 W/m ²	0-5000 W/m ²
Linearity error - to above level	<0.2%	<0.2%	<0.2%	<0.2%
Absolute calibration error (3)	typ. <3% 5% max.	typ. <3% 5% max.	typ. <3% 5% max.	typ<3% 5% max
Response time (7) - voltage output	10ns	10ns	10ns	10ns
Cosine error 4	3%	3%	3%	3%
Azimuth error (5)	<1%	<1%	<1%	<1%
Temperature Co-efficient	$\pm 0.1\%/^{\circ}\text{C}$	$\pm 0.1\%/^{\circ}\text{C}$	$\pm 0.1\%/^{\circ}\text{C}$	$\pm 0.2\%/^{\circ}\text{C}$
Internal resistance - voltage output	c.650ohms	c.650ohms	c.300ohms	c.180ohms
Longterm stability (6)	$\pm 2\%$	$\pm 2\%$	$\pm 2\%$	$\pm 2\%$
Material	Acetal	Acetal	Acetal	Acetal
Dimensions	34mm diameter 38mm height	34mm diameter 38mm height	34mm diameter 38mm height	34mm diameter 38mm height
Cable	2 core screened 7 - 2 - 2C	2 core screened 7 - 2 - 2C	2 core screened 7 - 2 - 2C	2 core screened 7 - 2 - 2C
Sensor Passband	400 - 700 nm	CIE photopic Curve	400 - 700 nm	350 - 1100 nm
Detector	Silicon photocell	Silicon photocell	Silicon photocell	Silicon photocell
Filters	Glass type and/or metal interference	Glass type and/or metal interference	Glass type and/or metal interference	Glass type and/or metal interference

Wavelength	Pixel/2	Pixel^2	WaveEst	WaveError	Pixel #	
202.55	28.5	812.25	202.45	0.10	57	Zn
206.2	33	1089	206.04	0.16	68	Zn
213.86	43	1849	214.01	-0.15	86	Zn
253.65	93.5	8742.25	253.78	-0.13	187	
302.15	156.5	24492.25	302.28	-0.13	313	
312.56	170	28900	312.51	0.05	340	
365.01	240.5	57840.25	365.01	0.00	481	
404.66	295	87025	404.54	0.12	590	
435.83	339	114921	435.77	0.06	678	
546.07	502	252004	546.21	-0.14	1004	
579.07	553	305809	579.06	0.01	1106	
696.54	747	558009	696.62	-0.08	1494	
706.72	764.5	584460.25	706.64	0.08	1529	
727.29	801	641601	727.25	0.04	1602	
738.40	821	674041	738.36	0.04	1642	
750.39	843	710649	750.44	-0.05	1686	
763.51	867	751689	763.45	0.06	1734	
772.38	883.5	780572.25	772.29	0.09	1767	
794.82	926.5	858402.25	794.92	-0.10	1853	
801.48	939	881721	801.39	0.09	1878	
811.53	959	919681	811.64	-0.11	1918	
826.45	988.5	977132.25	826.54	-0.09	1977	
842.46	1020.5	1041420.25	842.39	0.07	2041	

Wavelength Calibration Coefficients

C1 = 0.808788 dispersion

C2 = -0.000156 2nd order

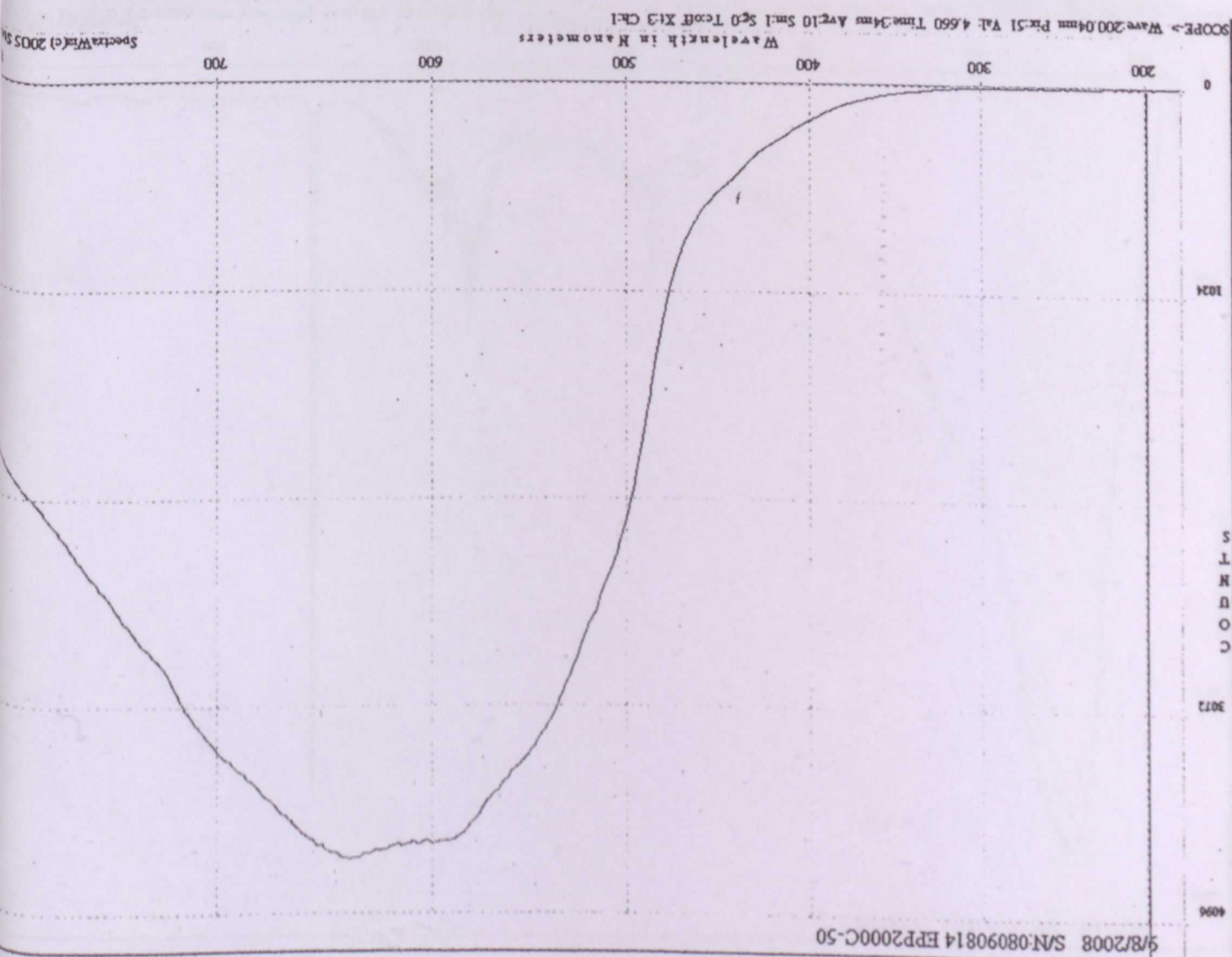
C3 = 179.52 starting wavelength

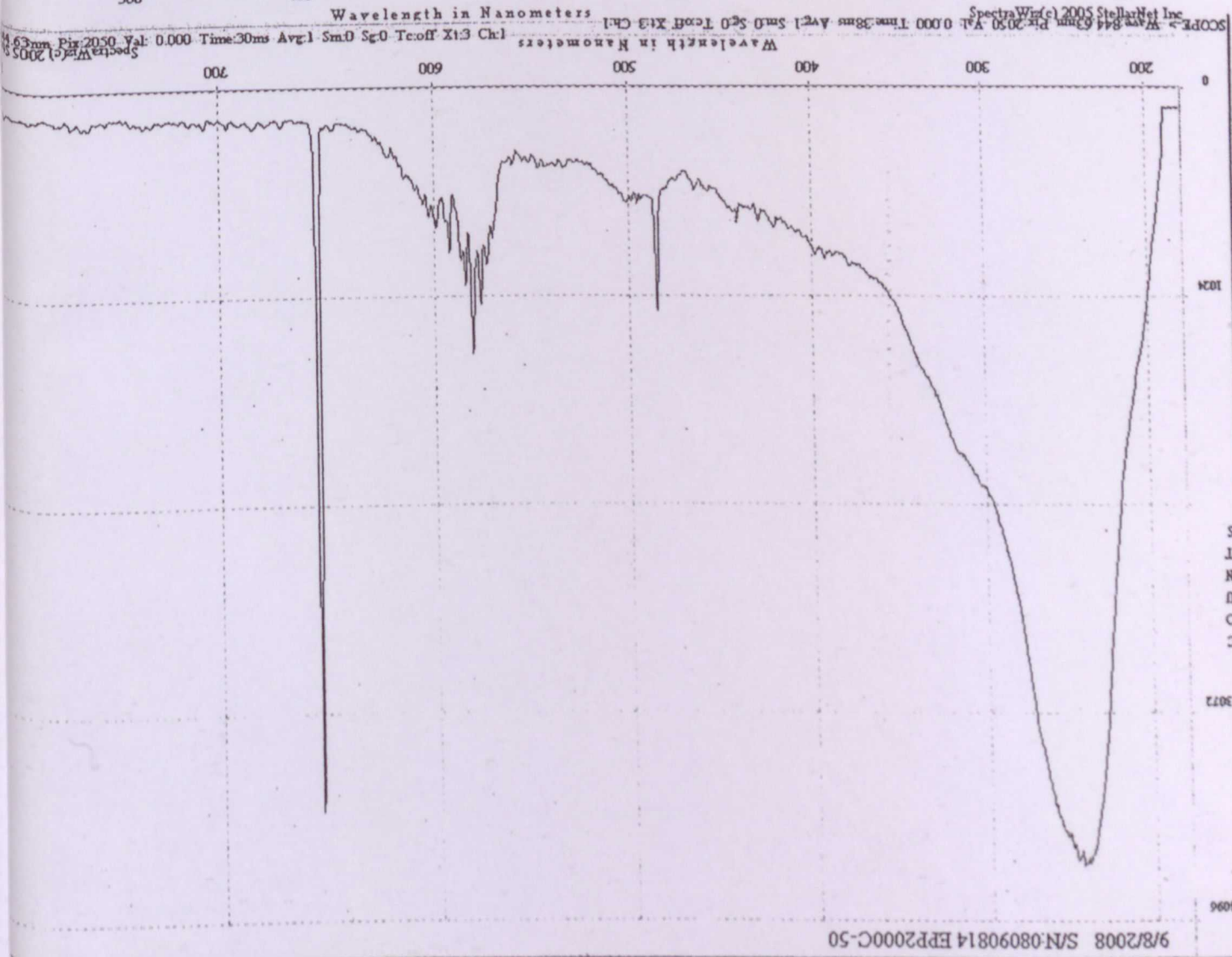
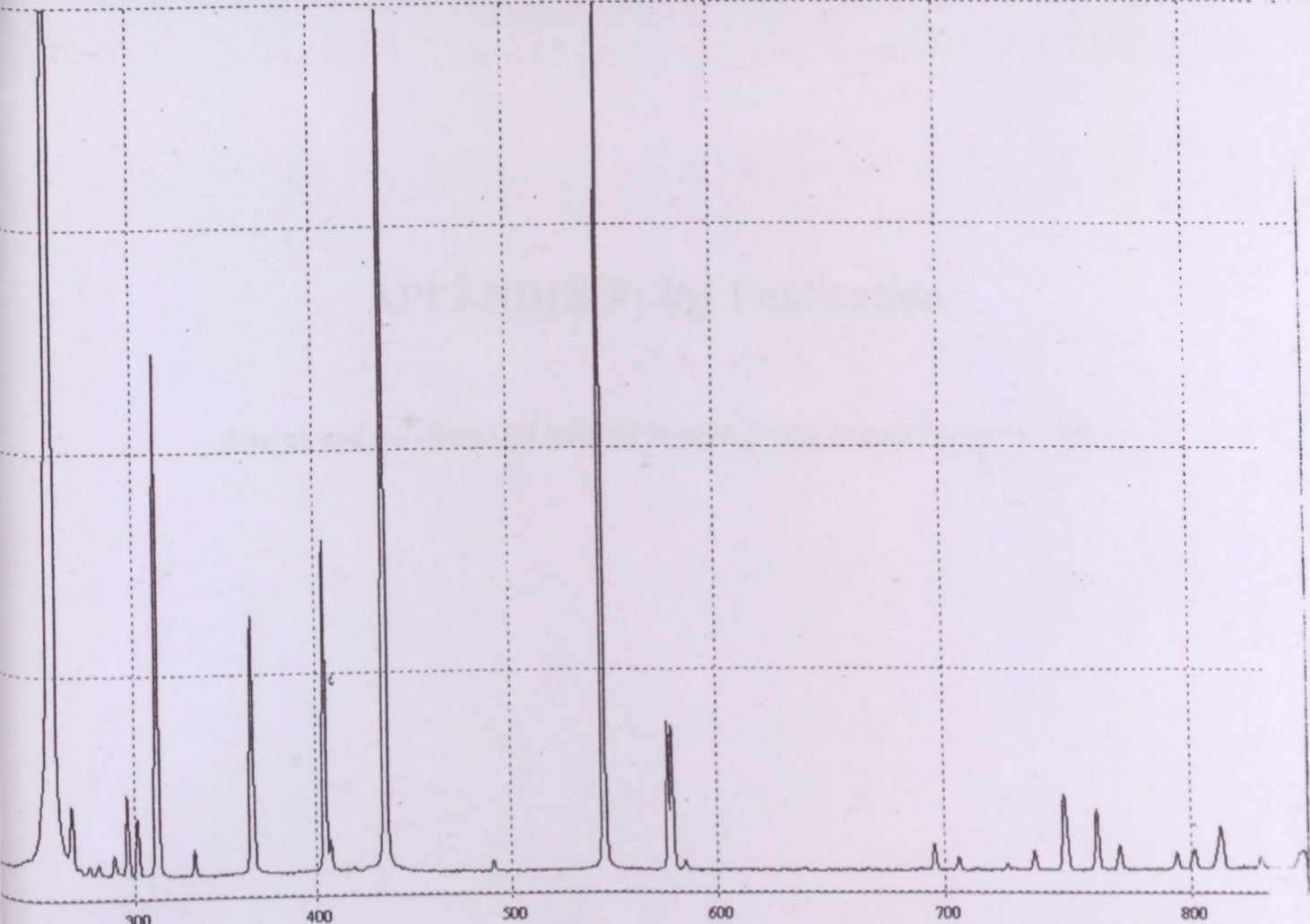
S/N:08090814

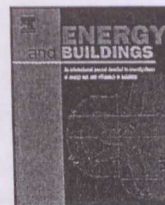
50ums S2

RoHS

e844







Daylighting can be fluorescent: Development of a fiber solar concentrator and test for its indoor illumination

Chen Wang*, H. Abdul-Rahman, S.P. Rao

Center of Project and Facilities Management (PFM), Faculty of Built Environment, University of Malaya, 50603 Kuala Lumpur, Malaysia

ARTICLE INFO

Article history:

Received 23 February 2009
Received in revised form 7 November 2009
Accepted 13 November 2009

Keywords:

Fiber solar concentrator
Remote indoor daylighting
Building integrated
Solar energy

ABSTRACT

Many limitations such as the strict dependence on beam irradiation and difficulties for wiring remain in conventional remote daylighting devices. This paper provides a brief discussion on the working theory and limitations for those conventional devices and presents a new concept developed by the first author for remote indoor daylighting. Based on the developed concept, a new device was designed and fabricated accordingly, which is an optical fiber solar concentrator consisting of a PMMA plate and 150 pieces of three-color 1 m long $\Phi 2$ mm fluorescent fibers. This new device is mounted on a university building roof and the concentrated light is transported to a remote dark room through 10 m long $\Phi 2$ mm clear optical fibers. Outdoor testing and evaluations for remote indoor daylighting and power production have been conducted. A 6-month monitored data from 24th May 2008 to 23rd Nov 2008 has been presented and the results reveal this new device a pleasant potential in remote indoor daylighting for large amount application in building integration.

© 2009 Elsevier B.V. All rights reserved.

Introduction

Besides the rapidly rising price of petroleum, anthropogenic activities, especially the burning of fossil fuels, have released pollutants into the atmosphere increasing global warming and depleting the ozone layer. To improve the situation there needs to be a decrease in energy of which fossil fuel is used. As a result there has been an increased interest in renewable energy systems. Solar energy is made widely available for daylighting, and direct production of electricity [1]. The need for workable energy options is perhaps the greatest single challenge facing the world in the 21st century. The acuteness of the challenge at this point in time results from the “perfect storm” of supply and demand, security, and environmental concerns, namely: (1) a projected doubling of energy use and tripling of electricity demand within a half century, calling for a substantial increase in fossil fuel supplies or dramatic transformation of the fossil fuel-based energy infrastructure; (2) ecological and geopolitical realities concerning the availability of oil and, to some extent, natural gas, specifically the concentration of resources and political instability in the Middle East, underlie major security concerns; and (3) greenhouse gas emissions from fossil fuel combustion are increasingly at the center of decisions about how the global energy system evolves, one that carries on in the “business as usual” overwhelming dependence on fossil fuels

or one that introduces technologies and policies that greatly improve efficiency, dramatically expand use of less carbon-intensive or “carbon free” energy, and implement large-scale carbon dioxide capture and sequestration [1].

Artificial lighting is one of the major sources of electrical energy costs in office buildings, and both directly through lighting energy consumption and indirectly by production of significant heat gain, which increases cooling loads [2]. Electric lighting represents up to 30% of building electricity consumption in commercial and office buildings [3]. Lighting energy used in most buildings can routinely be cut 30–50 percent through a combination of improved technology, automatic controls, and better lighting design [4]. Nevertheless, more than half of existing commercial building floor area still uses old-style, less-efficient systems. Efficient lighting designs are used in only a small minority of spaces, and control systems that maximize the use of daylight are even less common [2,4].

As a solution to the energy issues, solar energy is made widely available for daylighting and direct production of electricity. Various methods have been developed to collect, concentrate, transport, store and convert solar radiation such as the light pipe, optical fibers, optical solar concentrators, and luminescent solar concentrators (LSCs), and so on [5–11].

In the above mentioned conventional remote daylighting devices, many limitations such as strict dependence on beam irradiation and difficulties for wiring still remain to date. In mitigating these limitations, a new concept for remote indoor daylighting is developed and a new device called fluorescent fiber solar concentrator (FFSC) is designed and fabricated accordingly in

* Corresponding author. Tel.: +60 162189875; fax: +60 379675713.
E-mail addresses: derekisleon@gmail.com (C. Wang), arhamzah@um.edu.my (H. Abdul-Rahman), raosp1@gmail.com (S.P. Rao).

000. Such a device has been achieved and the experimental results are in good agreement with the preliminary study.

2. Conventional solar concentrators

Sunlight holds considerable unrealized potential for application in energy efficient room lighting designs. There are currently few existing systems that efficiently utilize sunlight to provide efficient room lighting to remote non-daylit rooms [10,17,18]. Analogous optics can be used for lighting of a room with an immediate daylighting aperture [17,18]. Recently, systems involving concentrating collectors [10], heliostats [19], or mirror light pipes [20] have been developed for illumination of remote rooms. A disadvantage of conventional solar concentrators is while systems using mirrors or lens may be advantageous for large-scale room lighting, they chiefly rely on beam solar irradiation and require tracking mechanisms to avoid astigmatism and other light losses experienced during collection of solar energy so that they lose their functions in cloudy and diffuse conditions [9]. Fig. 2 presents an example of the heliostats solar concentrator and light transmission through optical fibers developed by Kandilli et al. [21].

In order to remove the tracker, a static solar concentrator is proposed by Masato and Toshiro [22] to match the aesthetic features of towns. The concentrator consists of vertical plate solar cells and white/transparent switch-able bottom plate, which is operated with external power. The bottom is switched to be a diffuse reflection white surface when the cell generates electric power, and switched to be a light transmissible transparent surface when the cell does not deliver power. The light collection of this concentrator was analyzed by using multiple total internal reflection model and ray tracing simulation. However, the results are not significantly satisfying for a static solution for solar concentration.

3. Luminescent solar concentrator (LSC)

Luminescent solar concentrators (LSCs) have attracted the attention of a large number of scientists and engineers since the first proposal by Weber and Lambe [23]. The operation of the LSC, which can be considered as a peculiar kind of light guide, is based on the following principles. One or more high quantum yield luminescent species are dissolved in a rigid highly transparent medium of high refractive index. Solar photons entering the plate are absorbed by the luminescent species and reemitted in random directions. Following Snell's law, a large fraction of the emitted photons will be trapped within the plate and transported by total internal

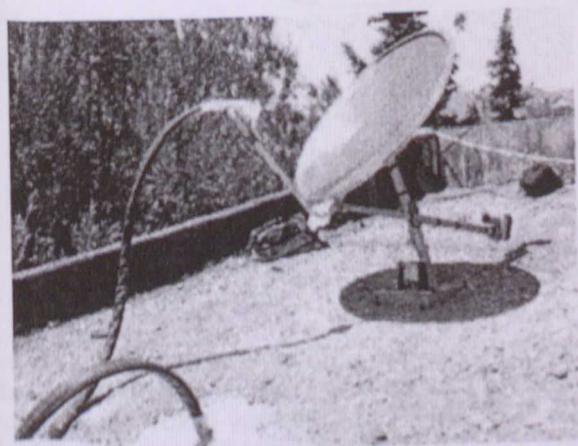


Fig. 2. One example of the heliostats solar concentrator and light transmission through optical fibers.

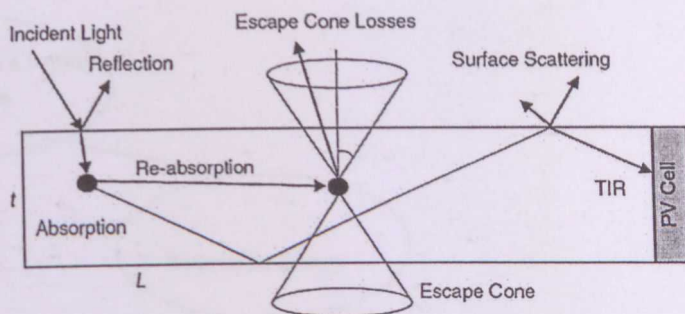


Fig. 3. Example of schematic representation of luminescent solar concentrator (LSC).

reflections to the edge of the plate, as illustrated in Fig. 3, where they will be converted by appropriate photovoltaic cells [24–26]. It has been reported that thin luminescent concentrator films could be implemented in the form of integrated devices or as sensitive elements in the traditional four-detector differential position sensors [27,28].

An LSC daylighting system has been produced by Earp et al. [11], which transports sunlight to remote areas of a building using a stack of pink, green and violet LSCs and clear PMMA light guides. In direct sun of intensity 100,000 lux, prototypes with collector area 1.2 m × 0.135 m deliver 1000 lm of near-white light with a luminous efficacy of 311 lm/W and a light-to-light efficiency of 6%. Surface effects such as excess adhesive and variations in flatness are thought to be causing unnecessary light loss, which can be avoided by careful LSC production. A limitation in the wiring for long distance light transportation has emerged in this LSC system [11].

3. The advantages and necessity of FFSC

In building integration, one of the most important features of remote light transportation is the wiring method and the wiring must be as easy as electrical wires [7,8]. As discussed in Section 2.1.2, only optical fibers are competent for this requirement. However, the light concentrated by Earp et al.'s [11] LSC is transported by polymer sheets instead of optical fibers because the light produced by the LSC is not a pointsource. The polymer sheets have fatal disadvantage in wiring, which therefore makes it impossible for building integration. It is also not energy efficient to further concentrate the sheety light produced by the LSC into a pointsource in order to transport it through optical fibers to a remote place in a building. This problem is expected to be solved in the designed FFSC system. As a summary for Section 2, Fig. 4 illustrates the necessities to design FFSC. In Fig. 4, there are two groups of solutions able to be practiced in the building sector for energy issues, namely: building energy saving and renewable energy applications, which are presented in the left branch and the right branch, respectively.

According to the left branch shown in Fig. 4, as an approach for energy saving, daylighting has a disadvantage that it may not able to reach many areas such as store room, basement, hallway, and it also brings heat gain with the light [13,6]. Light pipes were designed to transfer daylight to unreachable areas. However, the light pipes have their limitation for difficulties in wiring so that daylight transportation through optical fibers is considered as the best approach so far. However, the optical fiber needs a pointsource for it to transport. The FFSC is designed targeting on this requirement.

The right branch in Fig. 4 shows various solar concentrators that were designed using optical approaches such as mirrors or lens as a solution to solar energy applications. Since they are only sensitive

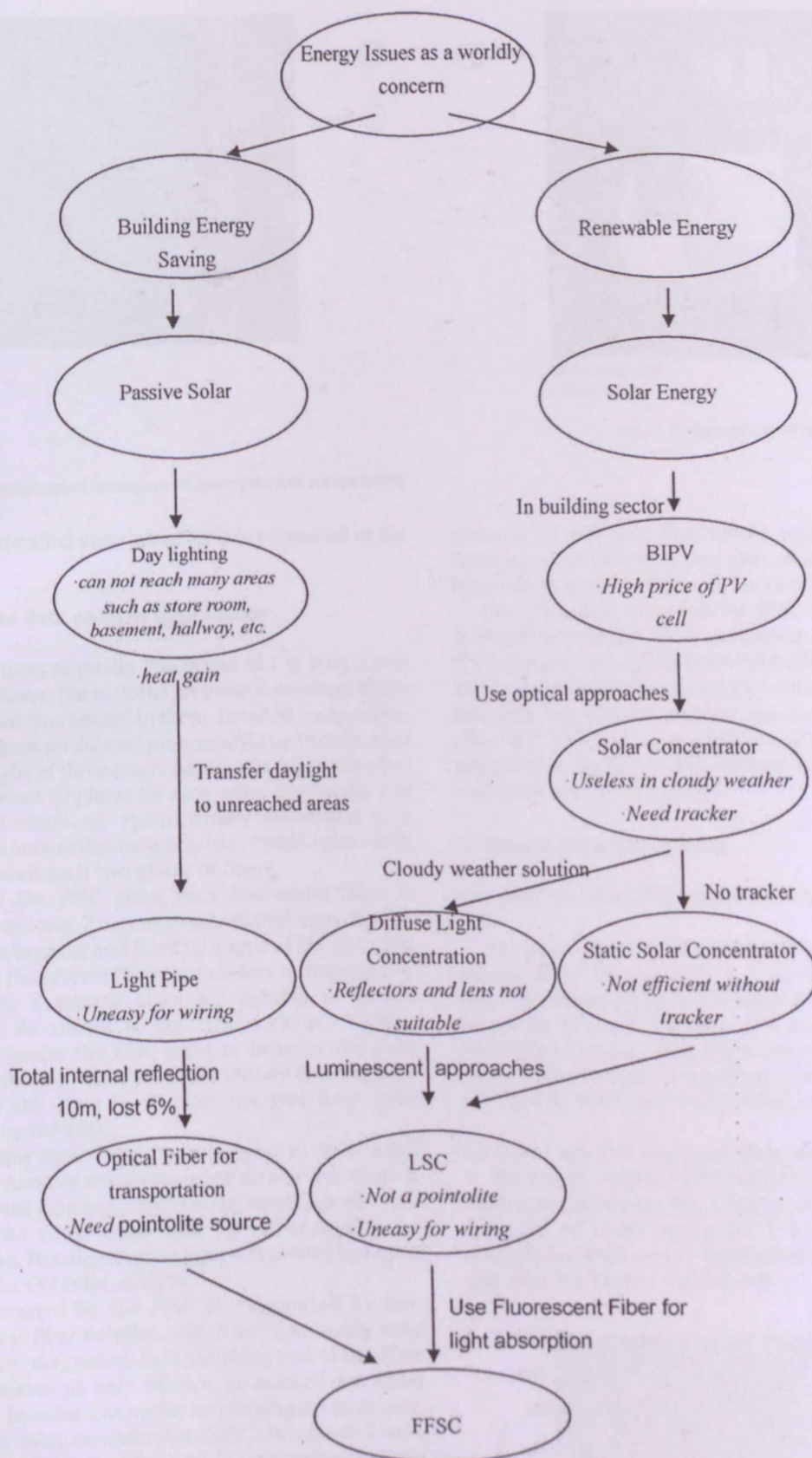
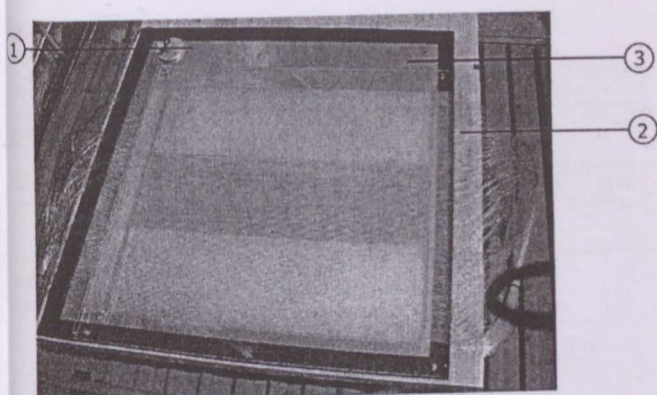


Fig. 4. From energy issue to solar using: the necessity of FFSC (concept developed by the first author, 2008).

beam irradiation, they do not function well in cloudy weather and diffuse conditions and a tracker is always needed. Luminescent solar concentrators (LSCs) and some static solar concentrators are then designed as a diffuse light solution and a static solution, respectively. Static concentrators always come with a poor concentration rate without a tracker and the light concentrated

by normal LSC could not be transported by optical fibers to a remote place since the light produced by LSC is not a pointolite. The developed FFSC system is expected to solve this problem as well.

Both branches in Fig. 4 illustrates that a new solar concentration system is necessary to be designed targeting on the above mentioned problems. Therefore, a device named FFSC is developed



① Pyranometer 1
② FFSC plate
③ Mirror

Fig. 5. FFSC installed on the building roof (concept developed by the first author, 2008).

In this study and the detailed description for it is presented in the next section.

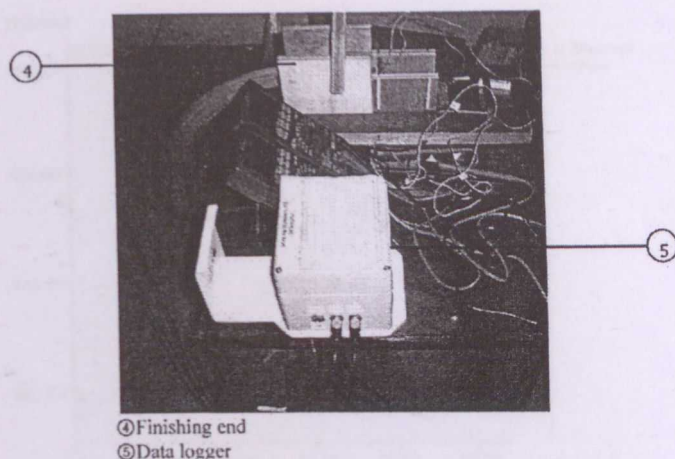
Design of FFSC and data analysis approaches

The FFSC plate consists of totally 150 pieces of 1 m long 2 mm diameter fluorescent fibers. The material for these fluorescent fibers is acrylic with quantum dots seeded in them. Detailed composition and structure of the quantum dots are proprietary. The 150 pieces of fluorescent fibers consist of three colors (green, red, and yellow) as shown in Fig. 5. There are 50 pieces for each color. The totally 150 pieces of fluorescent fibers are symmetrically embedded in a 200 mm × 1200 mm polymethyl methacrylate (PMMA) plate with a space of 2 mm between each two pieces of fibers.

At both edges of the FFSC plate, each fluorescent fiber is connected with a 10 m long, 2 mm diameter PMMA clear optical fiber by an aluminum bushing and fixed by a type of UV glue. The light absorbed by the fluorescent fibers is therefore transported by these clear fibers to a remote place for lighting or power production purpose. As shown in Fig. 5, a 1300 m × 1300 m reflector is installed under the FFSC plate to increase the light absorption. A pyranometer connected with a remote data logger is fixed together with the plate to monitor the real time solar radiation received by the FFSC.

One reason for using three-color fibers is trying to cover a full spectrum band [11]. Another reason for using three-color fibers is because the transported light coming out of the finishing end could considerably mix into white color light by self-scattering for illumination purposes. The mixed white light was proved by naked eye observation and a CIE color analysis.

The light concentrated by the FFSC is transported by two 10 mm diameter clear fiber bundles, which are reasonably easy for wiring in building integration. Each finishing end of the fiber bundles has a diameter of only 30 mm as marked by serial number (4) in Fig. 6. In order to monitor its working performance, the fluorescent fiber solar concentrator (FFSC) is mounted on a building roof and the light concentrated is transported by two 10 m long clear fiber bundles into a remote windowless dark room. One pyranometer, which is coded as Pyranometer 1, is installed with the FFSC plate to measure the solar radiation. The light radiation of one FFSC finishing end is measured by another pyranometer coded as Pyranometer 2. The values measured by the Pyranometer 1 and Pyranometer 2 are denoted as $PY1$ and $PY2$, respectively, which are recorded by a remote data logger at an interval of 10 min for 24 h a day. The unit for $PY1$ and $PY2$ is W/m^2 . Another finishing end is installed upon a Lux sensor with a



④ Finishing end
⑤ Data logger

Fig. 6. Equipments used for testing.

distance of 100 mm. The values read by the Lux sensor are denoted as E_v and they are also recorded by the remote data logger at an interval of 10 min for 24 h a day. The unit for E_v is lux.

The 24-h data recorded for FFSC from 6:00 to 20:00 were selected for each day. Various parameters has been studied for the FFSC system, namely: light-to-light efficiency (η_l), lighting effect, energy-to-energy efficiency (η_e), luminous efficacy ($\eta_e - l$) of the finishing end, and the negative association between light-to-light efficiency (η_l) and solar radiation ($PY1$), and so on, which are discussed in Section 5. The statistic methods such as correlation and linear test are employed.

5. Results from monitoring

5.1. Solar radiation ($PY1$) and FFSC output ($PY2$)

As mentioned in the above section, the solar radiation measured by Pyranometer 1 is denoted as $PY1$, and the light radiation measured by Pyranometer 2 is denoted as $PY2$. The mean values for $PY1$ and $PY2$ in these 6 months are $307.73 W/m^2$ and $17.02 W/m^2$, respectively. The maximum values for $PY1$ and $PY2$ in these 6 months measured both at 13:00 on 14th June 2008, which are $1308.31 W/m^2$ and $64.77 W/m^2$, respectively.

5.1.1. $PY1$ and $PY2$ in one particular day

The hourly values of $PY1$ and $PY2$ on a particular day 24th May 2008 are presented in Fig. 7. The peak values of $PY1$ and $PY2$ both appeared at 13:00, which are $1151.76 W/m^2$ and $60.89 W/m^2$, respectively. Both the $PY1$ and $PY2$ values are negligible before 7:00 and after 19:00 on a normal day.

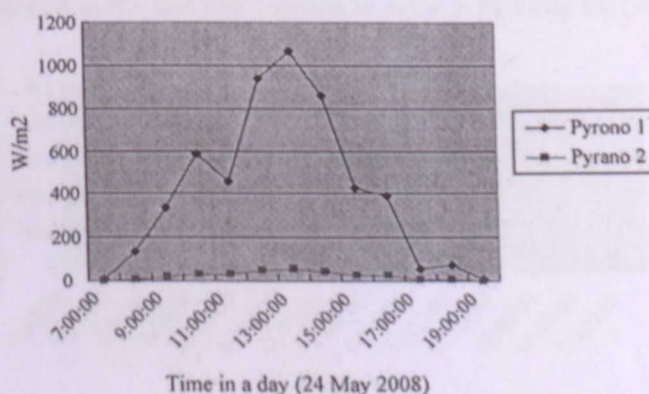


Fig. 7. $PY1$ and $PY2$ in a particular day.

Table 1
Regression of PY1 and PY2.

ANOVA ^b					
Model	Sum of squares	df	Mean square	F	Sig.
Regression	291.779	1	291.779	458.973	.000 ^a
Residual	18.436	29	.636		
Total	310.215	30			

^a Predictors: (constant), Pyranometer1.
^b Dependent variable: Pyranometer2.

2. The linearity between PY1 and PY2

To make it more presentable, the values of $10 \times PY2$ is used here instead of simply using PY2 to compare with the PY1 values since magnifying coefficient 10 is a constant. Fig. 8 shows that the $10 \times PY2$ and $PY1$ have very similar curves, from which it assumes PY1 and PY2 are linear. The assumption is proved by the linear regression as illustrated in Table 1 and Fig. 9.

FFSC light-to-light efficiency (η_l)

System light-to-light efficiency is defined by Eq. (1)

$$\frac{PY2}{PY1} \quad (1)$$

where PY1 is the solar radiation measured by Pyranometer 1, the one installed on the building roof, and PY2 is the light radiation measured by Pyranometer 2, the one installed with the fiber middle finishing end. This section presents the FFSC light-to-light efficiency (η_l) and its stability. In one typical day on 24th May 2008, the maximum value of η_l is 0.079 (17:20) and the minimum value is 0.046 (at 13:40). The mean value of η_l on that day is 0.052 with the standard deviation of 0.0095, which is under a 0.01 level. Therefore, the mean value of 0.052 is significantly representative of that day. Fig. 10 presents the curve of the light-to-light efficiency η_l from 7:30 to 18:30 on 24th May 2008.

Notice that the maximum value of η_l 0.079 appears at 17:20 when the solar irradiation is much weaker than that at 13:40 when the solar irradiation supposes to be around peak value on a day, but the minimum η_l 0.046 appears at 13:40. An assumption has therefore risen that the light-to-light efficiency has a negative correlation with the solar radiation. The discussion on the negative correlation between light-to-light efficiency (η_l) and solar radiation (PY1) are presented in Section 5.6.

The 6-month mean value of η_l is 0.057. Table 2 presents the monthly mean values of light-to-light efficiency in these 6 months from 24th May 2008 to 23rd November 2008. The standard deviation for η_l in the 6-month is 0.0015, which is under a 0.01

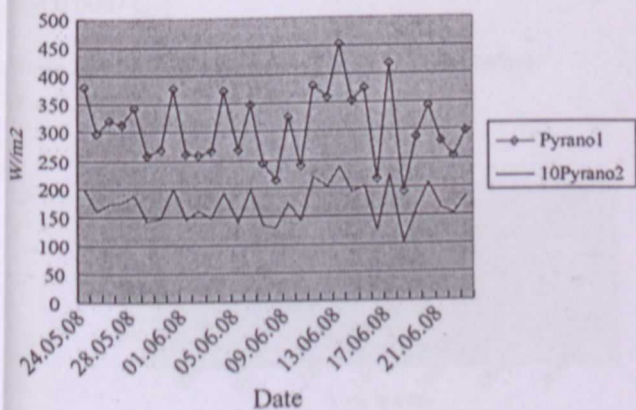


Fig. 8. Daily mean value of PY1 and $10 \times PY2$ for a month.

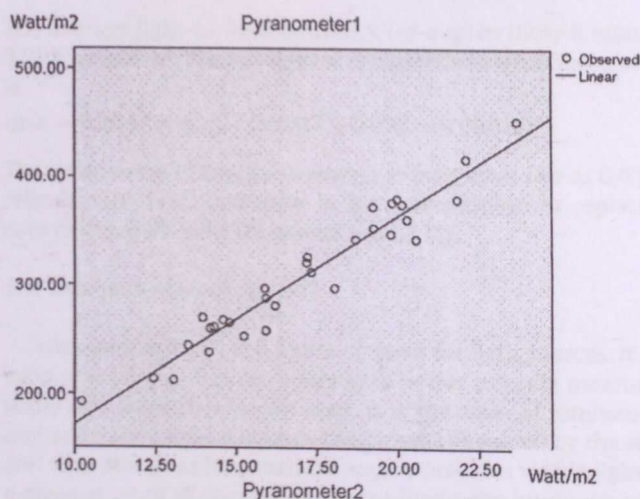


Fig. 9. Linear test of PY1 and PY2.

level, so that the mean value of 0.057 is concluded to be significantly stable and representative for these 6 months.

5.3. System lighting effect

5.3.1. Calculate luminous flux (φ) from illuminance (Ev)

As described by Schiler [29], the illuminance takes into account the area over which the luminous flux is spread. If a light source emits one-candela of luminous intensity uniformly across a solid angle of one steradian, its total luminous flux emitted into that angle is 1 lm. Alternatively, an isotropic one-candela light source emits a total luminous flux of exactly 4π lumens. If the source were partially covered by an ideal absorbing hemisphere, that system would radiate half as much luminous flux, which is only 2π lumens. The luminous intensity would still be one-candela in those directions that are not obscured [29]. The luminous flux (φ) is therefore calculated by Eq. (2):

$$\varphi = Ev \times S \quad (2)$$

where Ev is the illuminance detected by the Lux sensor and the S is the half sphere's surface area radiated by a light source. The distance between the finishing end and the Lux sensor is 0.1 m. So that the radiated half sphere's surface area is calculated as 0.063 m^2 . The luminous flux (φ) from one finishing end is therefore calculated in Eq. (3):

$$\varphi = Ev \times S = 0.063 Ev \quad (3)$$

5.3.2. Comparison of light effect between FFSC and typical incandescent lamps

The luminous flux of typical incandescent lamps [30] is illustrated in the first two columns in Table 3. By using Eq. (3),

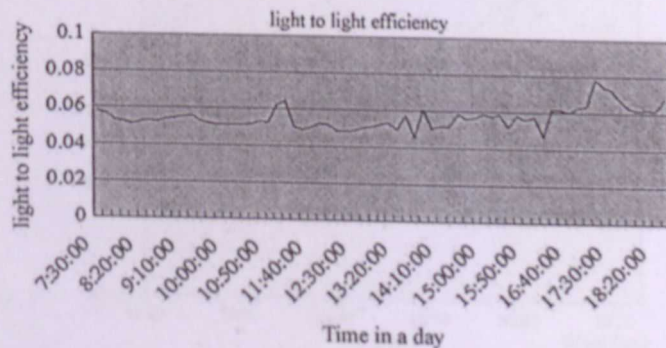


Fig. 10. Daily curve of light-to-light efficiency (η_l) on 24 May 2008.

Table 2
Month monthly mean value of η_l .

June 2008	July 2008	August 2008	September 2008	October 2008	November 2008
0.056	0.058	0.057	0.059	0.055	0.056

Table 3
Converting typical incandescent lamps' lumen to lux.

Watt of lamps	Lumen	Lux
5 W	25	397
15 W	110	1746
25 W	200	3175

The luminous flux of incandescent lamps is converted into illuminance, which is shown in the last column of Table 3. As illustrated in Fig. 11, the lighting effect provided by one of the FFSC finishing end is above 400 lux (equal to a 5 W incandescent lamp with 25 lm) from 8:30 to 16:30, which almost covers the whole office hours on a day. The monitored maximum E_v provided by one FFSC finishing end in these 20 days is 1811 lux, which is at 13:00 on 1st May 2008, when it is even higher than a 15 W incandescent lamp according to Table 3.

4. Energy-to-energy efficiency (η_e)

The energy-to-energy efficiency (η_e) is defined as the ratio of total energy output yielding from both finishing ends divided by the solar energy irradiated on the fluorescent fibers, which is illustrated by Eq. (4):

$$\eta_e = \frac{P_{out}}{P_{sun}} \quad (4)$$

The effective area of the FFSC plate is
 $A = \Phi \times L \times n = 0.002 \times 1 \times 150 = 0.3 \text{ m}^2$

where Φ and L are the diameter and the length of the fluorescent fibers, respectively. The variable n is the number of piece for fluorescent fibers, which is 150. The effective area of one finishing end is

$$S_f = \pi \times R_f \times R_f = 3.14 \times 0.015 \times 0.015 = 0.0007 \text{ m}^2$$

where R_f is the radius of the finishing end. Therefore, the energy-to-energy efficiency η_e is calculated as

$$\eta_e = \frac{P_{out}}{P_{sun}} = 2 \times PY2 \times \frac{S_f}{PY1 \times 50} = \left(2 \times \frac{0.0007}{0.3} \right) \frac{PY2}{PY1} = 0.0047 \frac{PY2}{PY1}$$

where $PY2/PY1 = \eta_l$ as defined in Eq. (1), therefore,
 $\eta_e = 0.0047 \eta_l$

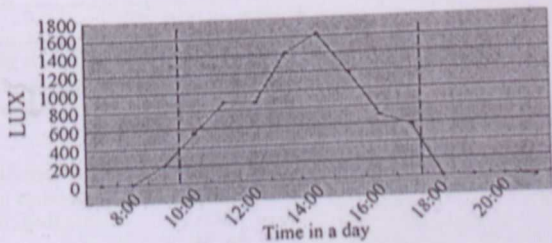


Fig. 11. Lux values in a particular day 24 May 2008.

The average light-to-light efficiency (η_l -avg) in these 6 months is 0.057, so that the average light to energy efficiency in these 31 days is

$$\eta_e - a = 0.0047 \times \eta_l - a = 0.0047 \times 0.056 = 0.000268$$

The mean value of energy-to-energy efficiency as low as 0.000268 reveals that FFSC currently is not yet suitable to replace the conventional PV cells for power producing.

5.5. Luminous efficacy ($\eta_e - l$)

Luminous efficacy is a figure of merit for light sources. It is the ratio of luminous flux (in lumens) to power (usually measured in watts). As most commonly used, it is the ratio of luminous flux emitted from a light source to the power consumed by the source, and thus describes how well the source provides visible light from a given amount of energy [31]. Accordingly, the luminous efficacy ($\eta_e - l$) for FFSC is defined by Eq. (5):

$$\eta_e - l = \frac{2\varphi}{P_{sun}} \quad (5)$$

where φ is the luminous flux produced by one finishing end, and P_{sun} is the solar energy irradiated on the fluorescent fibers. Since there are two finishing ends equally sharing the irradiation from the fluorescent fibers, the coefficient "2" is used here in Eq. (5). Therefore, the luminous efficacy ($\eta_e - l$) is calculated as shown in Eq. (6):

$$\eta_e - l = \frac{2\varphi}{P_{sun}} = 2 \times \left(\frac{0.063E_v}{PY1 \times 50} \right) = 2 \times \left(\frac{0.063E_v}{PY1 \times 0.3} \right) = \frac{0.42E_v}{PY1} \quad (6)$$

A significant value of 0.01 in the linear test conducted for E_v and $PY1$ indicates that the values of E_v and $PY1$ are linear so that $E_v/PY1$ is considered here as a comparatively stable value (Fig. 12). Hence, an average ratio of $E_v/PY1$ could be used in the above equation as a constant in general. From the monitored data, the monthly mean value of $E_v/PY1$ is calculated as 1.53. Therefore, the luminous efficacy ($\eta_e - l$) of the FFSC finishing end is as below:

$$\eta_e - l = 0.42 \times \frac{E_v}{PY1} = 0.42 \times 1.53 = 0.643 \text{ lm/W}$$

5.6. Negative association between light-to-light efficiency (η_l) and solar radiation ($PY1$)

Base on the monitored 10167 sets of effective data in the 6 months with an interval of 10 min, the system light-to-light efficiency (η_l) presents a negative association with the solar radiation $PY1$. As shown in Fig. 13, all these 10167 sets of data are

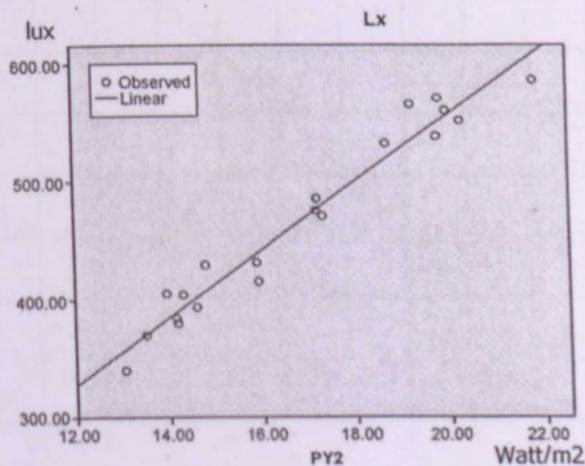


Fig. 12. Linear test of E_v and $PY2$.

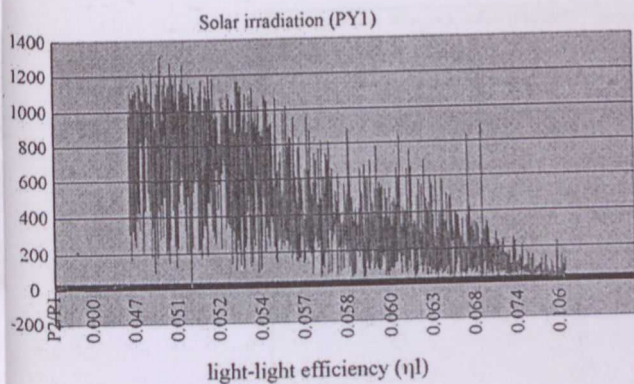


Fig. 13. Negative association between η_l and PY1.

metrically sorted by the light-to-light efficiency (η_l) in an ascending order while the corresponding values of the solar irradiation (PY1) present a descending trend. It is proved in Table 4 that there is a negative correlation coefficient (-0.643) for the association between light-light efficiency and solar irradiation, indicating that the relationship between these two variables is that values of one variable decrease as the other increases.

CIE color analysis and spectral distribution

The CIE (Commission Internationale de l'Eclairage, the International Commission on Color) color analysis and wavelength test of the artificial light produced by FFSC were conducted on a random day 16th Oct 2008 from 9:00 to 15:00. The weather on that day was sunny with a clear sky from 9:00 to 11:00, while from 11:30 to 13:30 it was sunny with little clouds. Since 14:00, it was overcast and raining until the evening. The device used for the CIE color analysis and the wavelength test is the EPP2000 and ISA2000 spectrometer, the responding range for which is from 190 nm to 1100 nm. Since the visible light waveband drops between 400 nm and 700 nm [32], and according to Geoffrey and Earp et al. [32,11], the average wavelength for the white light is around 555 nm, this value is suitable for the test. In order to find out the relationship between the output color and the various sky conditions, a same group of tests was repeated three times on the same day. The first group of tests was conducted at around 10:00 (clear sky condition), the second group of tests was conducted at around 12:30 (sunny with little clouds). The third group of tests was conducted at around 14:30 (overcast condition).

Fig. 14 presents the screen of the CIE color analysis conducted under the irradiant mode at around 12:30 (sunny with little clouds). As indicated in Fig. 14, the solid curve in the right of the diagram is the black body curve. There are two diagonals forming a cross in the central area and the cross point is indicated as "central white point" in the diagram, where $x = 0.333$, $y = 0.333$. Any selected point drops on or near this central white point is considered as white color [31]. The FFSC point in the diagram drops

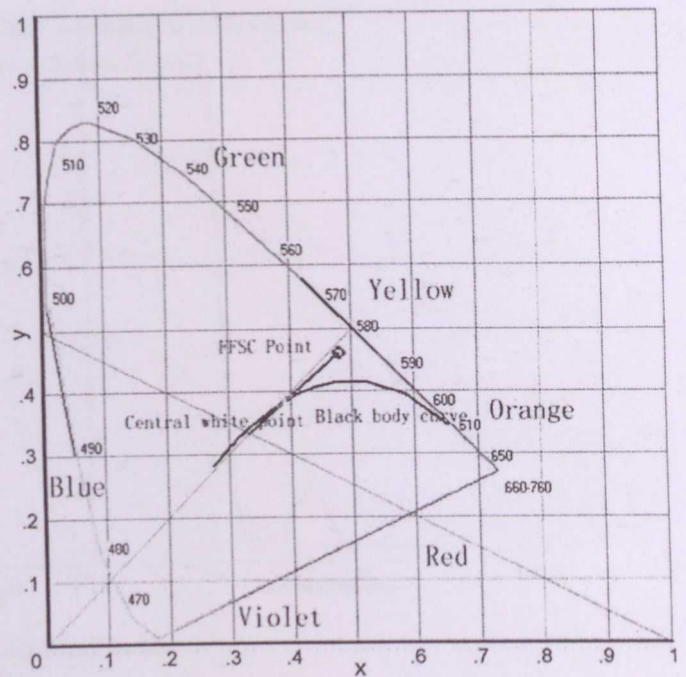


Fig. 14. CIE color analysis for FFSC.

between the central white point and the yellow area, where $x = 0.479$ and $y = 0.460$, indicating that the FFSC light output leans a bit towards the yellow area comparing to the absolutely white light. Referring to the CIE diagram for the direct sunlight ($x = 0.427$, $y = 0.401$) shown in Fig. 15, the FFSC point ($x = 0.479$ and $y = 0.460$) appears a great match to the direct sunlight. Therefore, it concludes that the FFSC light output under a clear sky is a kind of yellow-white color light and its color has a good match to that of the direct sunlight. According to Yoshi [31] and Schiler [29], a yellow-white color light is comforting to human eyes.

The wavelength test was conducted at around 12:30 on the same day on 16th Oct 2008. The sky condition at that time was sunny with little clouds, which was one of the general weather conditions in the tropic zone. Fig. 16 presents a wavelength screen in the scope mode at 12:23, from which it indicates on the top of

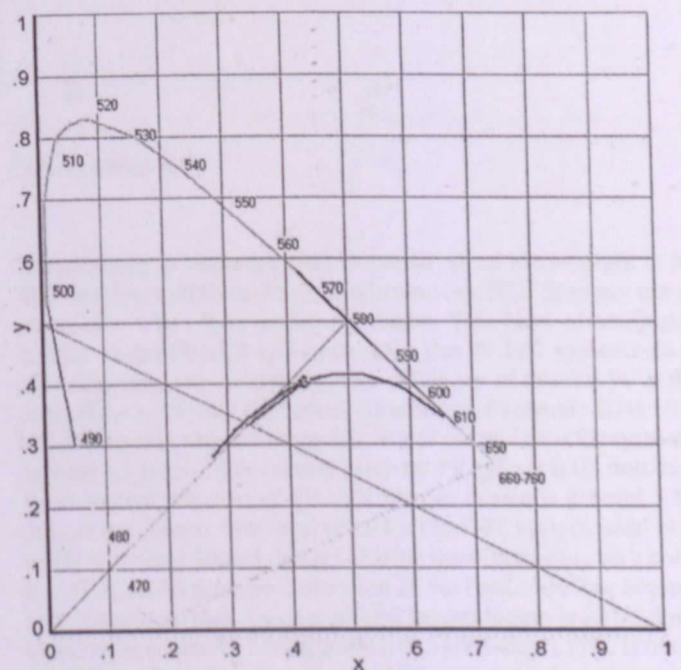


Fig. 15. CIE color analysis for direct sunlight.

Table 4
Correlation of η_l and PY1.

	Light-light efficiency	Solar irradiation
Light-light efficiency	1.000	-.643**
Pearson correlation		.000
Sig. (2-tailed)		
N	10167	10167
Solar irradiation	-.643**	1.000
Pearson correlation		
Sig. (2-tailed)	.000	
N	10167	10167

Correlation is significant at the 0.01 level (2-tailed).

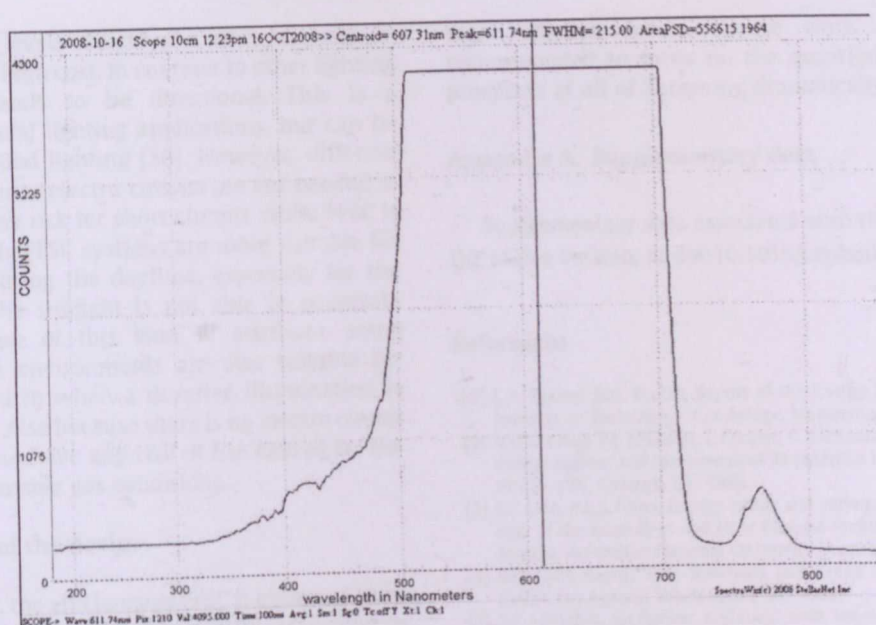


Fig. 16. Wavelength scope mode for FFSC.

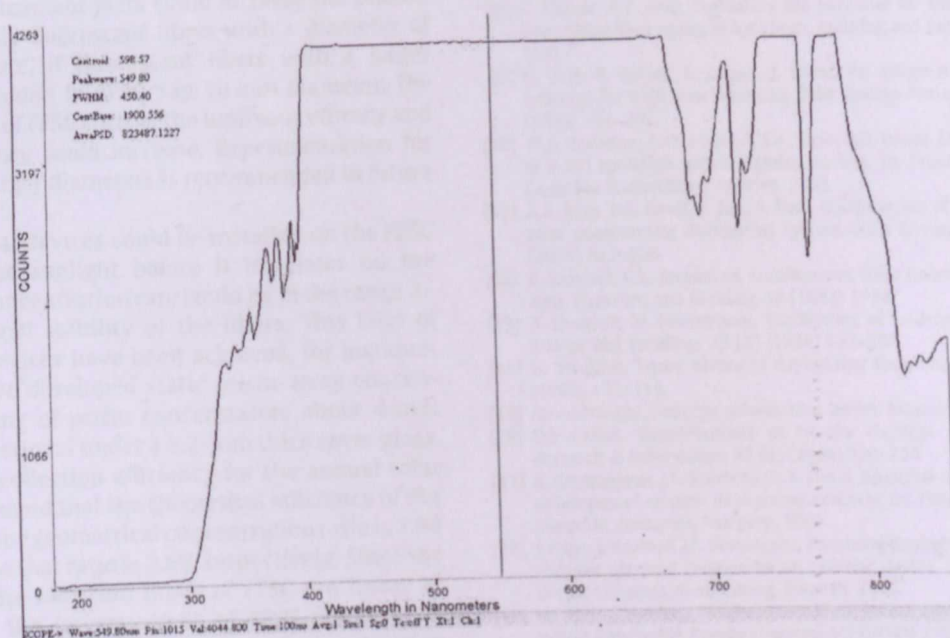


Fig. 17. Wavelength scope mode for natural light.

the screen that the centroid is 607.31 nm. The wave band at 607.31 nm is close to the average band for the white light, which is 555 nm. Comparing to the wavelength centroid of 598.57 nm measured for the natural daylight under the clear sky condition as shown in Fig. 17, the wavelength results reveal a great match between the FFSC light output and the natural daylight.

8. Discussions on economics

The value of FFSC luminous efficacy at 0.643 lm/W is much lower than that of the natural daylight at around 110 lm/W [33]. When compared to standard artificial light sources such as incandescent light bulbs at 16–40 lm/W, fluorescent lamps at 50–80 lm/W and light-emitting diode (LED) at 10 lm/W [33], the FFSC luminous efficacy as 0.643 lm/W is considered low, but it is higher than the luminous efficacy of a combusting candle at 0.3 lm/W

W according to Wapedia [34]. However, since the sunlight is free, different from all the electrical light sources, FFSC does not use any electricity when it is under operation. This kind of attribute is similar as the PV-LED approach since the PV-LED systems do not also consume any electricity. The efficiency of normal PV cells is around 0.11 [35] and the luminous efficacy of normal LED is 10 lm/W [33], so that the luminous efficacy of normal PV-LED systems is around 1.1 lm/W. The normal price for PV cells is 6 US dollars per Watt so that the cost of PV cells for per lumen is around 5.5 US dollars per lumen. The total price for the FFSC system used in this study is around 500 US dollars. During the office hours on a normal day FFSC could provide more than 25 lm luminous flux according to this study so that the cost of FFSC for per lumen is 20 US dollars. Comparing to the PV-LED approach (5.5 US dollars), FFSC is not cost effective. Actually, even the PV-LED approach is not currently economical to produce high levels of lighting. Current LED screw-in

bulbs offer either low levels of light at a moderate cost, or moderate levels of light at a high cost. In contrast to other lighting technologies, LED light tends to be directional. This is a disadvantage for most general lighting applications, but can be an advantage for spot or flood lighting [36]. However, different from the PV-LED systems, since electro circuits are not needed in FFSC systems, there is no any risk for short circuits while FFSC is operating. Hence, potentially FFSC systems are more suitable for aqueous illumination during the daytime, especially for the underwater areas where the sunlight is not able to penetrate through effectively. Because of this kind of attribute, some extremely moist operation environments are also suitable for FFSC systems to be applied in when a durative illumination is needed during the daytime. Also because there is no electro circuit needed, FFSC systems do not have any risk of fire caused by the electrical current in inflammable gas conditions.

Future improvements of the device

For future improvement, the efficiency of FFSC is expected to be increased by the following two approaches. Firstly, according to Richards [24], Reisfeld [25], and Batchelder et al. [26], the size and form of the cross-section could impact on the proportion of photons trapped by the LSC plate and the reduction of the cross-sectional area of the luminescent plate could increase the photon loss. In this research, only fluorescent fibers with a diameter of 1 mm are used. Therefore, if fluorescent fibers with a larger diameter could be embedded in FFSC, say 10 mm diameter, the performance parameters of FFSC such as the luminous efficacy and light-to-light efficiency could increase. Experimentation for fluorescent fibers with larger diameters is recommended in future study.

Secondly, some optical devices could be installed on the FFSC plate to concentrate the sunlight before it irradiates on the fluorescent fibers. The concentration rate could be in the range 2–3 considering the thermal stability of the fibers. This kind of optical concentration devices have been achieved, for instance, Matsui et al. [37] have developed static prism-array concentrator modules consisting of prism concentrators about 4-mm thick assembled unidirectional under a 3.2-mm thick cover glass. Calculating the optical collection efficiency for the annual solar radiation in Tokyo, it found that the theoretical efficiency of the modules is 94.4% when the geometrical concentration ratio is 1.88 and that it is 89.1% when that ratio is 2.66, respectively. Since the radiation output and the radiation input of FFSC are linear as proved by this study, the improvement of FFSC efficiency is expected to be in the range of 2–3 if proper optical concentration devices are installed.

Conclusions

Outdoor testing and evaluations for remote indoor daylighting and power production have been conducted for the developed new device named FFSC from 24th May 2008 to 23rd November 2008. The negative association between light-to-light efficiency (η_l) and solar irradiation is detected and analyzed for the first time. The low energy-to-energy efficiency value of 0.000268 proves that FFSC is not practical yet to replace the conventional BIPV approach for power producing. However, the reasonable light-to-light efficiency with a mean value of 0.057 and the lighting effect up to 110 lm/m² reveal FFSC a pleasant potential in remote indoor daylighting for large amount application in building integration. Moreover, comparing to the conventional artificial lighting powered by PV cells which is converting light to electricity and then back to light again which lost a lot of efficiency in multi converting, the idea of FFSC as a shortcut light–light conversion is considered to have a

more efficient future. Future work on this technology is recommended to focus on the question of whether it has any prospects at all of becoming dramatically more efficient.

Appendix A. Supplementary data

Supplementary data associated with this article can be found, in the online version, at doi:10.1016/j.enbuild.2009.11.011.

References

- [1] C.A. Robert, J.M. Ernest, Report of the Energy Research Council, Massachusetts Institute of Technology, Cambridge, Massachusetts, 2006.
- [2] V.H.C. Crisp, P.J. Littlefair, I. Cooper, G. McKennan, Daylighting as a passive solar energy option: and assessment of its potential in non-domestic buildings, Report BR129, BRE, Garston, UK, 1988.
- [3] J.C. Lam, A.L.S. Chan, Energy audits and surveys of air-conditioning, in: Proceedings of the Australian and New Zealand Architectural Science Association Conference, Australian National University, Australia, (1995), p. 49.
- [4] EPA, EPA Energy Star Buildings and Green Lights Snapshot, Environmental Protection Agency, Washington, DC, 1999.
- [5] P.J. Littlefair, Designing Buildings with Innovative Daylighting, Construction Research Communications Ltd., 1996.
- [6] L. Shao, S.B. Riffat, I. Yohannes, A.A. Elmualim, Measurement and modelling of light pipe for energy efficient lighting, CIBSE National Lighting Conference (1988).
- [7] J.M. Cariou, J. Dugas, L. Martin, Transport of solar energy with optical fibers, Solar Energy 29 (5) (1982) 397–406.
- [8] G. Eneid, A.T. John, Evaluating the potential for energy savings on lighting by integrating fibre optics in buildings, Building and Environment 41 (2006) 1611–1621.
- [9] H. Ries, R. Zaibel, E. Dagan, J. Karni, An astigmatic corrected target-aligned heliostat for high concentration, Solar Energy Materials and Solar Cells 37 (2) (1995) 191–202.
- [10] W.A. Beckman, G.O. Schlegel, S.A. Klein, B.D. Wood, J.D.M. Muhs, A TRNSYS model of a full spectrum hybrid lighting system, in: Proceedings of ISES Solar World Congress, Gothenburg, Sweden, 2003.
- [11] A.A. Earp, B.S. Geoff, F. Jim, S. Paul, Optimisation of a three-colour luminescent solar concentrator daylighting system, Solar Energy Materials & Solar Cells 84 (2004) 411–426.
- [12] R. Reisfeld, C.K. Jorgensen, Luminescent Solar Concentrators for energy conversion, Structure and Bonding 49 (1982) 1–36.
- [13] B. Bouchet, M. Fontoyant, Daylighting of underground spaces: design rules, Energy and Buildings 23 (3) (1996) 293–298.
- [14] G. Sweitzer, Three advanced daylighting technologies for offices, Energy 8 (2) (1993) 107–114.
- [15] Monodraught, Sunpipe information leaflet, Monodraught Ltd., 2008.
- [16] D.J. Carter, Developments in tubular daylight guidance systems, Building Research & Information 32 (3) (2004) 220–234.
- [17] R. Compagnon, J.L. Scartezini, B. Paule, Application of nonimaging optics to the development of new daylighting systems, in: Proceedings of ISES Solar World Congress, Budapest, Hungary, 1993.
- [18] J. Page, J. Kaempf, J.L. Scartezini, Assessing daylighting performances of electrochromic glazings coupled to an anidolic device, in: Proceedings of ISES Solar World Congress, Gothenburg, Sweden, 2003.
- [19] W. Pohl, C. Anslem, Natural room illumination using sunlight, in: Proceedings of World Renewable Energy Congress VII (WREC 2002), Cologne, Germany, 2002.
- [20] V. Garcia-Hansen, I. Edmonds, Natural illumination of deep-plan office buildings: light pipe strategies, in: Proceedings of ISES Solar World Congress, Gothenburg, Sweden, 2003.
- [21] C. Kandilli, K. Ulgen, A. Hepbasli, Exergetic assessment of transmission concentrated solar energy systems via optical fibres for building applications, Energy and Buildings 40 (8) (2008) 1505–1512.
- [22] M. Masato, M. Toshiro, Static solar concentrator with vertical flat plate photo-voltaic cells and switchable white/transparent bottom plate, Solar Energy Materials & Solar Cells 87 (2005) 299–309.
- [23] W.H. Weber, J. Lambe, Luminescent greenhouse collector for solar radiation, Applied Optics 15 (1976) 2299–2300.
- [24] B.S. Richards, Enhancing the performance of silicon solar cells via the application of passive luminescence conversion layers, Solar Energy Materials & Solar Cells 90 (2006) 2329–2337.
- [25] R. Reisfeld, Prospects of sol-gel technology towards luminescent materials, Optic Materials 16 (2001) 1–7.
- [26] J.S. Batchelder, A.H. Zewail, T. Cole, Luminescent solar concentrators: Theory of operation and techniques for performance evaluation, Applied Optics 18 (1979) 3090–3110.
- [27] S.A. Evenson, A.H. Rawicz, Thin-film luminescent concentrators for position-sensitive devices: a cookbook, Applied Optics 34 (1995) 7302–7306.
- [28] I.S. Melnik, A.H. Rawicz, Thin-film luminescent concentrators for position-sensitive devices, Applied Optics 36 (1997) 9025–9033.
- [29] M. Schiller, Simplified Design of Building Lighting, John Wiley, 1992.
- [30] D.M. Egami, Concepts in Architectural Lighting, McGraw Hill, 1983.

- [31] O. Yoshi, Color rendering and luminous efficacy of white LED spectra, Proc. of SPIE (Fourth International Conference on Solid State Lighting), 5530, SPIE, Bellingham, WA (2004), doi:10.1117/12.565757.
- [32] B.S. Geoffrey, Materials and systems for efficient lighting and delivery of daylight, Solar Energy Materials & Solar Cells 84 (2004) 395–409.
- [33] J.C. Lam, D.H.W. Li, Energy Conversion and Management 37 (12) (1996) 1703–1711.
- [34] Wapedia (2009). Online on the World Wide Web: http://wapedia.mobi/en/Luminous_efficacy.
- [35] W. Peter, Physics of Solar Cells: From Principles to New Concepts, Wiley-VCH, Weinheim, 2009.
- [36] I. Moreno, L.M. Molinar, Color uniformity of the light distribution from several cluster configurations of multicolor LEDs, Fifth International Conference on Solid State Lighting Proceedings of the SPIE 5941 (2005) 359–365.
- [37] T. Uematsu, Y. Yazawa, Y. Miyamura, S. Muramatsu, H. Ohtsuka, K. Tsutsui, T. Warabisako, Static concentrator photovoltaic module with prism array, Solar Energy Materials & Solar Cells 67 (2001) 415–423.